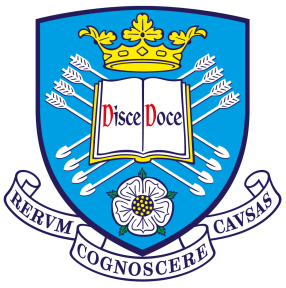

The University Of Sheffield.

High-Throughput Platform Development for Chinese Hamster Ovary (CHO) Cell Culture Performance Enhancement Using Small Molecules

Devika Kalsi

A thesis submitted in partial fulfilment of the requirements for the degree of Doctor of Philosophy

The University of Sheffield

Faculty of Engineering

Department of Chemical and Biological Engineering

September 2018

Declaration

I, Devika Kalsi, hereby declare that this thesis was written solely by myself. All the work presented in this thesis is my own. It has clearly been stated where this was not the case. I confirm that this work has not been submitted for any other degrees.

The work presented in Chapter 6 forms the basis of the following patent application:

A method for improving product titer in a cell and a cell media for improving the same (EP18162761.3) (20th March 2018)

Abstract

While g L^{-1} quantities of recombinant protein are common in Chinese Hamster Ovary (CHO) cell factories, the rise of more complex products presents novel upstream manufacturing challenges. Bioactive small molecule enhancers (SMEs) present opportunities for targeted CHO culture performance improvements. Here we present the development of a high-throughput (HT) screening technology for the identification of SMEs and their combinations for improved bioprocess.

Firstly, we describe the development of the HT screening platform. A miniaturised, shaking culture methodology was developed, enabling rapid assessment of 96 cultures simultaneously. Growth and production performance was similar to shake flask cultures, demonstrating scalability. HT growth, viability and titer measurement technologies were established.

Secondly, a large suite of SMEs was evaluated for the purposes of CHO cell biopharmaceutical production. 43 SMEs were assessed rapidly using the HT culturing and analytical platforms. Molecules that improved cellular growth or production in a stable production format were used to inform combinatorial designs to determine interactions for amplifying culture performance. This work would form the foundation of a commercial screening tool, wherein a deep well plate product pre-coated with selected enhancer concentrations and combinations would be available for testing with cell lines and products of choice. The product along with statistical modelling tools like Design of Experiments methodologies would advise chemical supplementation strategies to create bespoke media for enhanced bioprocess.

Finally, we demonstrate another use of the HT screening tool for the discovery of novel molecules for biotherapeutic production. Molecules were selected based on structural similarity to established titer enhancing SMEs and evaluated using the HT platform. A novel molecule and associated parent molecule maintained production improvements when scaled-up to shake flasks. Various mechanistic analyses revealed that the molecule acted epigenetically, resulting in higher transcription of the product.

Given the age of biosimilars/biobetters, having a competitive edge in terms of speed and cost is crucial. The HT screening tool developed utilises the potential of SMEs as quick, simple and cost-effective methods for improvements in upstream bioprocessing.

Acknowledgements

The research presented in this thesis would not have been possible without the financial support provided by the Engineering and Physical Sciences Research Council and Valitacell Ltd. Thank you for your support in funding my studies.

A huge thanks to Professor David James for providing me the opportunity to work in his laboratory at The University of Sheffield. Your guidance and support were extremely instrumental in making this thesis a reality. Your wisdom, encouragement and optimism have helped make this journey a fantastic and fulfilling learning experience. Many thanks to my industrial supervisor, Dr. Jerry Clifford, for your encouragement, positivity and belief. Much gratitude to Dr. Ben Thompson for your patience, guidance and mentorship.

I would especially like to thank Eleanor Hanson, Yash Patel and Nicholas Barber for being there from the first day and for undertaking and completing each tribulation and milestone together. Thank you to all the laboratory group members (present and past) of the David James' group at Sheffield for making it a supportive, friendly and fun environment to work in. Special thanks to Claire Arnall and Katie Syddall for always being there for me; for your advice, support, guidance, encouragement and even just talking over lunch (or cake). Thanks to Alejandro Fernandez-Martell, Adam Brown, Joe Cartwright and Joanne Noble-Longster for your constant guidance. Much gratitude to the all the members of the Valitacell team, for providing an ever-supportive environment to work in.

Thanks to all my friends who have supported me through this journey. To Harry He, for our many food adventures across Sheffield and for patiently listening to my ramblings about F1 and cricket. To Cara-Jane Colgan, for always being there for support whenever needed. To An-Wen Kung and Beata Florczak for our numerous dinner outings to talk about the most random things.

The biggest thanks goes to my family. To Ma, Pa and my brother Ani—you all have been my pillars of strength. You have supported me through every step in this journey and I do not have enough words to thank you. I love you, and will always remain indebted to you for all the love and support you constantly provide me. Whenever I needed someone to lend an ear (during the day or late at night), you were always there to support me. To Ma, thank you for your ever-lasting patience. To Pa, thank you for your guidance and inspiration. To Ani, thank you for putting up

with my quirky self, and for bringing calmness when most needed. I could not have done this without each of you.

Table of Contents

List of Figures

List of Tables

List of Abbreviations

7-AAD	7-amino-actinomycin D
2-AB	2-aminobenzamide
ABC	Ammonium bicarbonate
ac	Acetylation
ACG	Automatic gain control
ACN	Acetonitrile
ANOVA	Analysis of variance
Anti-HER2	Anti-human epidermal growth receptor 2
ATF6	Activating transcription factor 6
BHK	Baby Hamster Kidney
BiP	Binding immunoglobulin protein
cDNA	Complementary DNA
CHO	Chinese Hamster Ovary
CMV	Cytomegalovirus
Ct	Cycle Threshold
CypB	Cyclophilin B
DHFR	Dihydrofolate reductase
DIA	Data Independent Acquisation
DMSO	Dimethyl Sulfoxide
DOE	Design of Experiments
DTE	Difficult-to-express
DTT	Dithiothreitol
DWP	Deep well plate
E. coli	*Escherichia coli*
ELISA	Enzyme-linked immunosorbent assay
ER	Endoplasmic reticulum
EZH2	Enhancer of zeste homolog 2
FACS	Fluorescence-activated cell sorting
FAS	Fatty acid synthase
Fc	Fragment crystallisable
G1	Gap 1 phase of cell cycle
G2	Gap 2 phase of cell cycle
GlcNAc	N-acetyl-D-glucosamine
GP	Glycan peak
GS	Glutamine synthetase
HDAC	Histone Deacetylase
HEK	Human Embryonic Kidney
HexNAc	N-acetylhexosamine
HILIC	Hydrophilic interaction liquid chromatography
HPLC	High Performance Liquid Chromatography
HT	High-Throughput
IgG	Immunoglobulin G
IVCD	Integral of Viable Cell Density
M	Mitosis phase of cell cycle
mAb	Monoclonal Antibody
MCS	Maximum common substructure

me	Methylation
mRNA	Messenger ribonucleic acid
MS	Mass spectrometry
Neu5Gc	N-glycolylneuraminic acid
OFAT	One factor at a time
PAGE	Polyacrylamide gel electrophoresis
PBS	Phosphate buffered saline
PDI	Protein disulphide isomerase
PE	Phycoerythrin
PFA	Paraformaldehyde
PI	Propidium iodide
PLK1	Polo-like kinase 1
RFU	Relative fluorescence units
RSM	Response Surface Methodologies
S	Synthesis phase of cell cycle
SDS	Sodium dodecyl sulphate
SEAP	Secreted embryonic alkaline phosphatase
SEM	Standard error of the mean
SME	Small Molecule Enhancer
SREBP	Sterol regulatory element-binding proteins
qP	Cell specific productivity
qPCR	Real-time quantitative PCR
OFAT	One-factor-at-a-time
TCA	Tricarboxylic acid cycle
TFA	Trifluoroacetic acid
UDP	Uridine 5-diphosphate
UPLC	Ultra-High Performance Liquid Chromatography
UPR	Unfolded protein response
VCD	Viable Cell Density
XBP1	X-box Binding Protein 1

List of Small Molecule Enhancer Abbreviations

Cu	Copper(II) Sulphate Pentahydrate
DCA	Sodium Dichloroacetate
DMSO	Dimethyl Sulfoxide
FAC	Ferric Ammonium Citrate
Ge	Germanium(IV) oxide
HCA	Hydrocinnamic Acid
Li	Lithium Chloride
Mn	Manganese(II) Chloride Tetrahydrate
NaBu	Sodium Butyrate
4PBA	4-Phenylbutyric Acid
6PHA	6-Phenylhexanoic Acid
PVA	5-Phenylvaleric Acid
2TAA	2-Thiopheneacetic Acid
3TAA	3-Thiopheneacetic Acid
TBA	2-Thiophenebutyric Acid
2TCA	2-Thiophenecarboxylic Acid
TMAO	Trimethylamine N-oxide
TPA	2-Thiophenepropionic Acid
TSA	Trichostatin A
TUDCA	Tauroursodeoxycholic Acid, sodium salt
V	Sodium Orthovanadate
VPA	Sodium Valproate
Zn	Zinc Sulphate Heptahydrate

Chapter 1

Introduction

This chapter reviews and summarises recombinant protein production in mammalian cell factories. Emphasis is given to host cell factory selection and upstream processing leading to the final protein product ready for downstream processing. The significance of high-throughput technologies coupled with statistical modelling for process development is discussed. The potential of culture media engineering as a vital tool for improving cellular production performance is explored.

1.1. Biopharmaceuticals

Biopharmaceuticals refer to pharmaceuticals that are produced using biotechnological techniques. They (also referred to as biologics) mostly encompass recombinant proteins that are mainly used as therapeutic drugs to treat cancer and autoimmune diseases; with a small number being employed in diagnostics (Carter, 2011). Biologics are generally derived from “host” cells that are engineered genetically to produce these therapeutics as part of their protein production machinery. Protein-based biopharmaceuticals dominate the biopharmaceutical industry. Monoclonal antibodies (mAbs) (a protein therapeutic) form the largest selling sub group of biopharmaceuticals (Aggarwal, 2014; Zhang, 2010) and also dominate approval rates (Walsh, 2014). Other biologic types include recombinant hormones, blood factors, growth factors, coagulation factors, interferons, vaccines, fusion proteins and enzymes (Walsh, 2014; Zhang, 2010).

Biopharmaceutical sales have always witnessed steady increases over the years with global sales reaching $163 billion in 2016 (Kesik-Brodacka, 2018). mAb product sales usually account for a large percentage of this figure ($107 billion; 2016) (Kesik-Brodacka, 2018). In 2016, 6 of the top 10 selling drugs were antibody based products (Strohl, 2018). The market is growing at a rapid rate, with 12 biologics being approved in 2017 and 2 being approved in the first quarter of 2018 alone (Defrancesco, 2018; De La Torre and Albericio, 2018).

The advent and steady increase in approvals of biosimilars and biobetters, indicates stiff competition amongst biologics manufacturers. The expiry of patent protection for several large revenue yielding biologics is imminent (Deloitte, 2016; Kesik-Brodacka, 2018), presenting opportunities for biosimilar and biobetter development to further expand.

Walsh (2014) indicates that there is a large degree of innovation in the mAb sector. Fc fusions, antibody fragment, antibody drug conjugates and bispecifics are just some of the antibody derived products (Kesik-Brodacka, 2018; Walsh, 2014). The development and engineering of these next generation biologics can sometimes prove to be more difficult-to-express (DTE) than natural protein products (Johari et al., 2015). Thus, the diversification of protein product

formats along with stiff industrial competition, translates to an ever-increasing need for quick and cost-effective optimisation and innovation in recombinant protein production processes.

1.2. Expression Systems

The first step to creating a biotherapeutic involves selecting a host cell system, a cell type that can be genetically engineered to produce the product (usually a protein) as part of their gene expression machinery. Proteins requiring specific attachment of sugar residues for efficacious biological activity (commonly termed glycosylated proteins or glycoproteins) form 70% of all protein therapeutics (Jaffe et al., 2014). Correct protein glycosylation is essential for desired pharmokinetics and product safety (Jaffe et al., 2014). Production cell factories have a profound effect on determining product quality and thus remain at the heart of the biomanufacturing process (Le et al., 2015).

A plethora of host cell systems are available for recombinant protein production. The first approved recombinant product, recombinant insulin was manufactured using an *Escherichia coli* (*E. coli*) cell factory (Huang et al., 2012). *E. coli* is an easy organism to work with due to its economical nature and quick culturing times. However, they struggle with complex post-translational modifications, particularly glycosylation (Huang et al., 2012). Innovative efforts have focused on engineering the periplasmic secretory pathway along with adding glycosylation machinery in *E. coli* (Berlec and Štrukelj, 2013; Huang et al., 2012; Jaffe et al., 2014). *E. coli* expression systems are the second most employed cell production factory (only behind mammalian cell systems) accounting for nearly 20% of approvals since 1982 (Brown et al., 2017; Walsh, 2014). Other host cell systems employed include yeast and insect expression systems. Both these systems are mainly utilised for protein vaccine production (Walsh, 2014). A summary of the frequency of use of different host cell factories is displayed in **Figure 1.1**.

The major limitation of the host cell systems mentioned above is the inability to produce correct protein folding and post-translational modifications. Bacterial

production systems, as already mentioned, inherently lack efficient glycosylation machinery. Yeast systems are known to produce proteins with high mannosylation epitopes and these glycoforms can elicit human immune responses (Celik and Calık, 2012). Insect systems, on the other hand struggle with correct protein folding, resulting in intracellular aggregates and low production titer outputs. (Demain and Vaishnav, 2009; Drugmand et al., 2012).

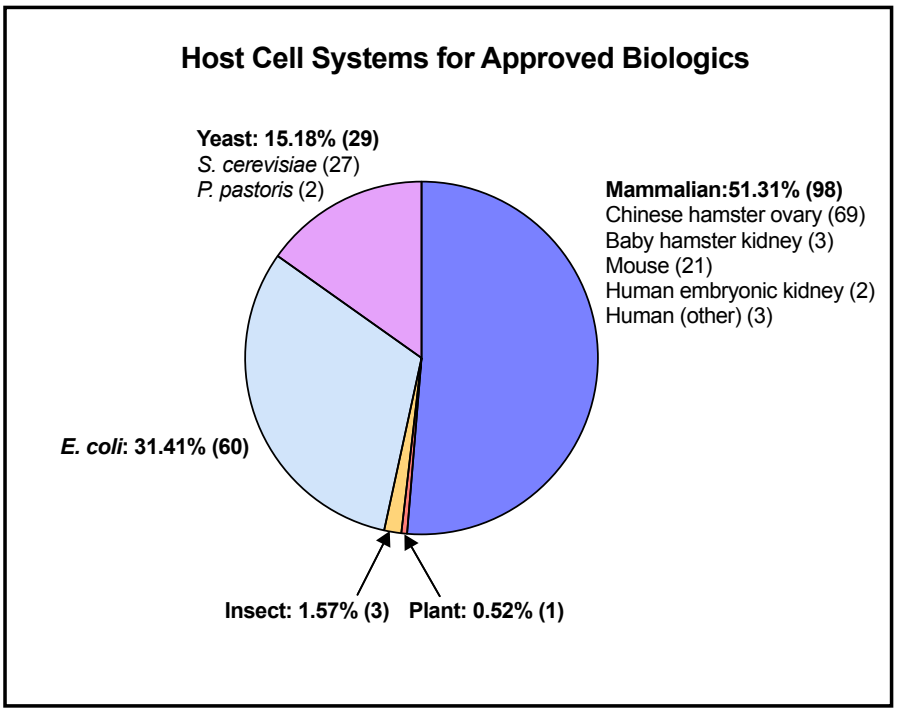

Figure 1.1 A summary of the host cells employed for approved biopharmaceuticals marketed in USA and Europe as of July 2014. Information gathered from: (Walsh, 2014). Host cell information for 191 approved products is displayed. Percentage of total for each host cell type is shown. Actual product numbers per host cell type and subtype displayed in brackets.

1.3. Chinese Hamster Ovary (CHO) Cells

The appeal and utilisation of mammalian cell hosts was significantly boosted by the approval of tissue plasminogen activator as the first biologic produced in Chinese Hamster Ovary (CHO) systems in 1986 (Collen et al., 1984; Collen and Lijnen, 2004; Wurm, 2004). Since then, mammalian cell systems, specifically CHO cells have remained the predominant vehicle for biopharmaceutical production (Jayapal et al., 2007; Zhang, 2010; Zhu, 2012). Mammalian host

utilisation allows for the manufacture of complex proteins like mAbs with more "human like" glycosylation (Zhang, 2010), making them attractive for use in comparison to the non-mammalian hosts discussed above. CHO cells have a remarkable proven safety and approval records making them frontrunners for biopharmaceutical production (Jayapal et al., 2007). 5 of the top 10 selling biopharmaceuticals in 2014 were manufactured in CHO cells, providing evidence of their proven track record (Sanchez-Garcia et al., 2016).

CHO cells were first isolated in 1957 from *Cricetulus griseus* (Chinese hamster) (Tjio and Puck, 1958). These cells were then subjected to multiple genetic engineering and adaptation processes resulting in the creation of distinct CHO lineages (Wurm, 2013). CHO-DG44, CHO-K1, CHO-S, DUKX-B11 and CHO-K1SV are just some of the different CHO cell types available currently (Brown et al., 2017; Derouazi et al., 2006; Estes and Melville, 2014; Wurm, 2013).

The ability to easily manipulate CHO cell function caused by their inherent genetic instability is a crucial factor in its meteoric rise as a model recombinant production host (Brown et al., 2017; Davies et al., 2013). CHO cells have been readily adapted for suspension culture and efforts have been made to push cellular biomass accumulation and production capabilities (Kim et al., 2012). Adaption to serum free and chemical defined media is another factor is the adoption of CHO cells as common protein product production hosts (Lai et al., 2013). Serum containing media is non-ideal due to its animal source and undefined nature (Butler, 2005). CHO cells have been readily adapted to large bioreactor cultures, wherein g L^{-1} quantities of product are commonplace (Lai et al., 2013). CHO cells are non-human in source and thus any human pathogen proliferation (including herpes, measles and human immunodeficiency virus) is kept at bay (Bandaranayake and Almo, 2014; Jayapal et al., 2007; Lai et al., 2013; Rita Costa et al., 2010; Zhang, 2010). This parameter alone distinguishes CHO cells from other able human cell hosts.

Glycosylation, a post-translational modification, is often a crucial parameter for determining efficacy and safety of the protein product. Galα1,3-Gal and N-glycolylneuraminic acid (Neu5Gc) residues are often considered immunogenic (Butler and Spearman, 2014). CHO cells tend to express lower levels of these epitopes in comparison to other mammalian hosts (for example murine cells)

(Butler and Spearman, 2014). Thus, CHO cells are often favourable to employ based on this aspect.

CHO cell host systems are not without their flaws. The same genetic instability that contributes towards ease of genetic manipulation, can exacerbate phenomena like genetic drift. This creates heterogeneity in cell populations which can result in unpredictable production performance and loss in productivity (Davies et al., 2013). Generally, CHO cells have lower proliferation rates in comparison to bacterial and yeast counterparts (Fischer et al., 2015). Additional, it has been brought to attention that CHO host cell proteins can present downstream processing challenges and have the potential to be immunogenic (Yuk et al., 2015a).

Nevertheless, the sheer volume of research that has gone into CHO cell bioprocess, cements their position as the leading biologics production chassis. High titers have been recorded using both transient and stable production formats (Daramola et al., 2014; Fischer et al., 2015). CHO cell dominance remains set to continue in light of the multiple engineering strategies that have been implemented to improve the CHO bioprocess (Fischer et al., 2015).

1.4. Alternative Mammalian Cell Factories

Other mammalian cellular hosts can also be employed for biotherapeutic production. These include mouse myeloma cells (NS0, Sp2/0-Ag14) and baby hamster kidney (BHK) cells. Alternatively, human cells can also be employed. Human cell lines include human embryonic kidney cells (HEK293) and Per.C6, a human retina derived cell line (Berlec and Štrukelj, 2013; Kim et al., 2012). BHK cells are employed mainly for anti-coagulant production (Butler and Spearman, 2014). 10 products that are produced in mouse myeloma cells have been approved for therapeutic use (Walsh, 2014). This cell type has been shown to produce higher levels of two potentially immunogenic epitopes Galα1,3-Gal and Neu5Gc (Butler and Spearman, 2014). Human cell types are logically capable of producing proteins with most suited human-like glycosylation patterns (Dumont et al., 2015). However, human cell types (apart

from HEK293) are comparatively in the nascent stage for biopharmaceutical production purposes. HEK293, perhaps the most rigorously tested of human cell types, has been shown to have an advantage over CHO cells for the manufacture of a particular protein, producing the required carboxylation modifications (Swiech et al., 2012). Additionally, PER.C6, CAP and HKB-11 are attractive to employ from a human-like glycosylation perspective (Brown et al., 2017; Swiech et al., 2012).

1.5. Upstream Production Process For Biopharmaceuticals

The section below details and discusses the iterative approach undertaken in industry and academic circles to produce a protein product through recombinant protein expression **in CHO cells**. Upstream technologies are described beginning from cell factory, expression plasmid selection and optimisation through to process optimisation and bioreactor scale up.

Biologics manufacturing processes originate with cell factory selection. The previous section described the different cell types available for production purposes. Within CHO bioprocessing, there are a number of options of cell lines stemming from different CHO lineages (Wurm, 2013). Even with the established cell lines, multiple engineering strategies, such as anti-apoptosis engineering (Templeton et al., 2014) and glyco-engineering (Hossler et al., 2009) are sometimes necessary for creating a cell line most suited for the required production process. Engineering of the glycosylation pathway is particular rewarding in terms of enhancing pharmacokinetics and product safety (Rita Costa et al., 2014). Monoclonal antibodies lacking a core fucose epitope have higher resultant antibody-dependent cellular cytotoxicity (Fischer et al., 2015). A complete knockdown of the *fut8* gene in CHO cells, an enzyme involved in core fucosylation, results in the product lacking core fucosylation (Yamane-Ohnuki et al., 2004). Similarly, more human-like terminal sialic acid content can be produced by the upregulation of α-2,6-sialyltransferase (ST6GAL) gene (Fischer et al., 2015; Lee et al., 1989).

To surmise, there are a multitude of options available for CHO cell line factory selection. Industrial companies spend a lot of time and resources towards optimising their parental cell lines towards the 'ideal' host cell candidate.

1.5.1. Expression Plasmid

Recombinant protein expression in CHO cells is usually driven by plasmid vector expression. Expression vectors act as carriers of the product gene of interest into the CHO cell host. There are various elements of an effective plasmid vector. A strong promoter that guides transcription along with regulatory elements such as polyA tails is essential (Rita Costa et al., 2010). Selectable marker sequences are also routinely included for stable production modes.

Stable integration into the host genome is a random event, integration into a transcriptionally inactive region can result in little or no product gene expression (Wurm, 2004). Selection markers are included to allow for the isolation of cells that been successfully transfected (Wurm, 2004) . Selection marker genes are co-transfected along with the gene of interest and selective environments are created that only allows cells that have successfully integrated the plasmid (product gene and selectable marker gene) to survive. The two most common selection marker genes employed are dihydrofolate reductase (DHFR) and glutamine synthetase (GS) (Rita Costa et al., 2010). Selection occurs by culturing cells in specific nutrient deficient media. Only cells with the DHFR enzyme would be able to proliferate in hypoxanthine and thymidine deficient media. Likewise, only cells with the GS enzyme would be able to proliferate in glutamine deficient media (Rita Costa et al., 2010). A second stage is employed for the isolation of hosts overexpressing the selection maker (and thus the protein product gene) by subjecting the cells to increasing concentrations of specific enzyme inhibitors; methotrexate for DHFR and methionine sulfoximine for GS. Herein, cell survival is determined by the overexpression of the selection marker gene, leading to co-amplification of the product gene.

Sophisticated strategies such as targeted integration into transcriptionally active regions of the chromosome (Dahodwala and Sharfstein, 2014; Kwaks and Otte,

2006) and epigenetic regulatory elements such ubiquitously acting chromatin opening elements (UCOEs) are increasingly employed for improving protein productivity (Lalonde and Durocher, 2017).

1.5.2. Transfection

The choices available for the mode of insertion of the expression plasmid into CHO cells are diverse. Transfection technologies can vary from being chemical based (lipofection, calcium-phosphate precipitation, polyethylenimine) to physical based (electroporation) (Rita Costa et al., 2010). Extensive efforts have been made to optimise the methods mentioned above with the cell line of choice to achieve high transfection efficiency and titers in both stable and transient modes (Baldi et al., 2007; Thompson et al., 2012). Transient transfection presents a quick approach to generating cell populations expressing the recombinant protein product. Herein, the cells do not stably integrate the gene of interest and thus the expression window is short. No selection and amplification steps are necessary resulting in a shortened development process. Transient expression can prove invaluable to assess general productivity trends, assess gene overexpression strategies, and evaluate protein product characteristics (Baldi et al., 2007; Hansen et al., 2015; Rita Costa et al., 2010). Stably transfected cells provide for a more production relevant setup where large quantities of protein can be manufactured and production capabilities are maintained for a longer period. Development of stable lines is a time consuming and laborious process, however with their ability to achieve production demands, it is the industrial standard for large-scale therapeutic protein production (Rita Costa et al., 2010).

1.5.3. Cloning, Screening and Selection

The initial selection and amplification strategies (through the use of selection markers detailed in **Section 1.5.1**) still result in a largely heterogeneous population in terms of growth rate and productivity. This can lead to inconsistent

production performance. Thus, isolating a single cell clone that exhibits the desired characteristic is crucial (Li et al., 2010). Traditional methods like limiting dilution cloning are time consuming, laborious and relatively low-throughput and can take up to 8 months to complete (Noh et al., 2013; Priola et al., 2016). It is thus unsurprising that there is an active shift toward high-throughput (HT) and more sophisticated clone selection technologies in industrial cell line development.

Flow cytometry based fluorescence-activated cell sorting (FACS) and the ClonePix™system (Kim et al., 2012) present some of the more HT screening options. FACS sorting is based on linking cell productivity with fluorescence and thus allows for isolation based on productivity. In ClonePix™, fluorescently tagged antibodies specific to the protein product are employed. Single cell colonies are formed in semi solid media, wherein the cells secrete the protein product into the matrix. The fluorescent antibody detects the secreted product, which assists in cell sorting based on productivity (Lai et al., 2013).

A further push in industry has instigated the development of a second generation of HT, automated methodologies for single cell cloning. The single-cell printer™ based on microfluidics to ensure monoclonality has been developed (Cytena GmbH, (Gross et al., 2015)). The Beacon platform based on nanofluidics and optoelectro positioning also demonstrates successful automated single cell cloning (Le et al., 2018).

Key attributes such as growth rate and productivity are constantly evaluated during selection stages to narrow the number of clones. When selected clones are brought down to around 10 to 25 in number, mini-bioreactor studies can be used to further evaluate growth, production and product quality characteristics and determine growth media and feeding regimes. The top 4 to 6 clones are further evaluated wherein the final production clone and backup clone decisions are made (Li et al., 2010).

1.5.4. Process Development

The cell line development process culminates in a final production clone that would be scaled up for therapeutic protein production in stirred tank bioreactors. Not every cell clone is created equal and will react differently to media/feed addition and bioreactor conditions. Thus, the process development arm of the upstream production process involves creating the most suitable environmental conditions for biotherapeutic manufacture in CHO production clones. Process development is based on the optimisation of two main factors: (i) culture media and feeds (ii) bioreactor operating conditions. The biopharmaceutical production process involves reviving the banked cell clone, setting up seed and inoculum trains to gather enough biomass to seed production bioreactors ranging from 5,000 to 25,000 L (Kelley, 2009).

Production titers using CHO cells have risen over 20 fold (and well into the g L^{-1} quantities) since their inception as a biopharmaceutical production host (De Jesus and Wurm, 2011). This major improvement is mainly attributed to culture media development (Huang et al., 2010; De Jesus and Wurm, 2011; Kim et al., 2012; Zhu, 2012). Culture media is a vital component of the production process, since it caters to the cell's nutritional requirements and thus impacts cell proliferation, productivity and even product quality (Rouiller et al., 2013). The 1950s and 1960s witnessed the use of serum containing culture media (Landauer, 2014; Yamamoto and Niwa, 1993) for culturing cells *in vitro*. While serum provides cells with the nutrients and proteins essential for cell proliferation, the undefined composition renders itself to lot-to-lot inconsistency (Butler, 2005). Additionally, the animal sourcing of serum increases potential for pathogenic agent proliferation (Li et al., 2010; Zhang, 2010). Thus, serum-free and chemically defined media development was prioritised to abolish these issues.

Animal component free, chemically defined media is a complex entity. Chemically defined media contains a carbon source, amino acids, inorganic salts, vitamins and lipids as a minimum (Landauer, 2014; Sandadi et al., 2006), with individual companies performing optimisation and supplementation studies in-house to cater to their cell lines and products. Culture media components not

only impact cell growth but also affect cellular productivity (Reinhart et al., 2015; Rodrigues et al., 2012), gene expression (Yuk et al., 2014), product quality (Hong et al., 2010) and toxic metabolic by-product accumulation (Ha and Lee, 2014; Luo et al., 2012).

There are a plethora of options at a user's disposal for optimising media for a bioproduction process. The simplest "one factor at a time" (OFAT) screening allows for testing a singular factor effectively but discounts any interactions between components (Parampalli et al., 2007; Rouiller et al., 2013). Thus, multivariate statistical analytical methodologies such as Design of Experiments (DOE) are often employed (Parampalli et al., 2007; Sandadi et al., 2006). Additionally, media blending techniques wherein a number of media component blends (at different ratios) are created and analysed in a HT manner to determine optimal concentrations of components (Rouiller et al., 2013). Spent medium analysis and metabolomics often play a role in media development as well (Li et al., 2010; Liu et al., 2015b). Rational supplementation of production and growth enhancers to the basal medium also returns improvements in protein production (Allen et al., 2008; Kim and Park, 2016; Yuk et al., 2015b). Overall, there are multiple techniques available to create media environments most suited to a user's production process.

Bioreactor conditions also have been shown to have a profound impact on culture performance. Bioreactor culture operating parameters such as operating temperature, gas flow rate, impeller speed, pH and dissolved oxygen can impact production processes and require constant maintenance and optimisation (Li et al., 2010; Shukla and Thömmes, 2010).. Bench top and small-scale bioreactors often assist in the optimisation studies to develop bioreactor operating protocols for a fed-batch production run for a particular cell line and product.

1.6. High-Throughput Technologies for Upstream Process Development

Briefly touched upon in the previous sections, HT technologies form a vital part of upstream processes. The need for HT technologies is extremely high in the

present scenario, given the surge of biosimilars and biobetters stimulated by parent proteins losing patent protection. The rise in demand for more complex proteins like fusion proteins and bispecifics also plays a role in the increasing demand for HT techniques. Simply put, companies need to make large amounts of complex protein products, rapidly and cost-effectively. This section mainly focuses on HT culturing technologies for process development. HT techniques are based on three principles: (i) miniaturisation (ii) parallelisation and (iii) automation (Bhambure et al., 2011).

HT culturing techniques mainly accelerate process development however also aid in clone selection. Miniaturised bioreactors can come in two variants: shaken cultures or stirred impeller cultures (Hemmerich et al., 2018). Stirred impeller mini-bioreactors have the obvious benefit of having the same mixing technique as scaled-up stirred tank bioreactors. The most notable product in the stirred variant is the ambr 15 system (TAP Biosystems (part of Sartorius Stedium Biotech, Hertfordshire, UK). Here, 24 to 48 cultures with 10 to 15 mL culture volumes can proceed in parallel (Hsu et al., 2012). Dissolved oxygen and pH can be monitored in each mini-bioreactor, allowing for sophisticated control (Hemmerich et al., 2018; Rameez et al., 2014). The bioreactors can be linked up to automated liquid handling systems for automated feed addition and sampling (Hemmerich et al., 2018). Similar growth and production profiles were observed with 7L bioreactors demonstrating good scalability (Lewis et al., 2010). However, non-invasive optic based parameter measurements are not possible (Hemmerich et al., 2018) and the instrument is relatively costly and requires high maintenance. Another HT stirred culture system alternative is the bioREACTOR (2mag AG, München, Germany). Similar to the ambr 15, it is mainly employed for microbial cultivation (Hemmerich et al., 2018).

On the other hand, shaken technologies present multiple options for HT culturing. Herein, multi-well plate variants are the most common culture vessel. The level of control and monitoring varies with the different options available. The BioLector (m2p-labs GmbH, Baesweiler, Germany) allows for 48 parallel fermentations, wherein pH, dissolved oxygen can be monitored along with biomass build-up using optical density, fluorescence and backscatter

(Hemmerich et al., 2018). A similar 24 multi-well plate technology is the micro-Matrix (Applicon Biotechnology, Delft, The Netherlands).

Perhaps, the simplest and cheapest culturing technique is the use of general commercial multi-well plates. Containing from 6 to 384 wells, the amount of throughput offered can be decided by the user. Shallow well plates are limited to lower culture volumes (around 150 µL for a 96 well plate) and are more suited for static setup, though shaking is possible (Hermann et al., 2003). Suspension cell lines (like CHO cell lines used in industry today) would logically be better suited to shaking cultures. Thus, many multi-well plate shaking technologies have been developed (Duetz, 2007). These generally employ deep well plates (DWPs), which allow for higher culture volume resulting in multiple invasive culture attribute sampling from the same well (Chaturvedi et al., 2014). Clamps developed by Enzyscreen BV (Heemstede, Netherlands) (Duetz, 2007) are most commonly employed for 24 and 96 DWP culturing (detailed in **Chapter 4**). Herein, the plates are secured in place using a clamp system ("System Duetz"). 16 clamps (1 clamp per plate) fit inside a standard sized incubator, thus 1,536 cultures can be evaluated in parallel (for a 96 well plate) (Enzyscreen BV,). Thus, this system can provide higher throughput than other technologies such as the ambr 15. Culture aeration and mass transfer is dependent upon shaking speed, orbital diameter, well geometry and cultivation volume (Hemmerich et al., 2018). Thus, optimisations are necessary to obtain similar growth and production profiles of a larger scale (such as shake flasks). Due to the simplicity of the system, non-invasive monitoring of pH, dissolved oxygen and biomass content is generally not available (Long et al., 2014). Plate closure systems provided by Enzyscreen BV also help in minimising evaporation while maintaining adequate gas transfer (Chaturvedi et al., 2014) through plate closure systems. This is usually a sandwich cover comprising a stainless steel lid (with holes) with layers of filter and silicone; the cover seals the plate and prevents contamination as well (Chaturvedi et al., 2014; Duetz, 2007). Other closure systems like self-adhesive plate seals were rendered inadequate in providing optimum gas transfer and minimising evaporation rates simultaneously (Chaturvedi et al., 2014).

These HT cultivation systems are invaluable in accelerating process development and optimisation. The addition of multivariate statistical analysis in tandem with these systems, allows for testing multiple parameters and components in conjunction. The most common methodology employed is DOE methodology. This statistical modelling method is based on multiple linear regression (Mandenius and Brundin, 2008). The technique allows for maximising information of factor impact while minimising the number of experimentations required (Franceschini and Macchietto, 2008). This in turn reduces cost, time and resources involved. There are many different types of DOE approaches available, however the most common approaches taken are factorial designs and response surface methodologies (RSM). Factorial designs are extremely useful when the design space is large, allowing for quick screens to identify significant factors and interactions and eliminate non-significant ones. RSM is more suited as a second approach to adopt after factorial designs. The design space is comparatively smaller and is intended to optimise the process and return best factor settings based on the predictive model (Anderson and Whitcomb, 2016; Mandenius and Brundin, 2008).

One of the most common uses of DOE is for media development (Brühlmann et al., 2017b; González-Leal et al., 2011; Grainger and James, 2013; Parampalli et al., 2007; Sandadi et al., 2006). DOE can also be used for other processes in the biopharmaceutical industry such as optimisation of bioreactor operation parameters (Legmann et al., 2009). Despite the power of DOE as a prediction and optimisation tool, many biologists are wary of adopting it in their optimisation experiments. This hesitation stems for a poor understanding of the tool and notion of it being illogical for biological recommendations (Comley, 2009). Nevertheless, there is a real push to employ these strategies for biopharmaceutical production optimisation.

Chapter 2

Small Molecule Enhancer (SME) directed Process Development Approaches to enhance Biopharmaceutical Production

This chapter presents a focused discussion and review on the potential of small molecule enhancer (SME) supplementation as a facile strategy for improvement in protein production. The discussion will aim to highlight the rationale underpinning this research project. The study aims to develop a HT screening platform to rapidly assess SMEs and rational combinations of SMEs. Further, potential utility scenarios will be discussed that would emphasise the opportunities of this research study to facilitate the design of a commercial screening tool to inform a user of a bespoke media environment tailored to their production process. Finally, a thesis overview and outline is provided.

2.1. Introduction: Engineering Culture Media

Every step of the biopharmaceutical upstream process pathway presents opportunities for improvement. There are 3 main strategies to overcome production constraints in CHO cell based manufacturing: engineering the (i) cell, (ii) media and (iii) process conditions. Cellular engineering strategies are often comparatively longer and more tedious to employ (Brühlmann et al., 2017b). Additionally, alternative cell engineering approaches such as the use of a directed evolutionary pressure have extremely long timelines to yield results. Process conditions such as hypothermic temperature shift to create biphasic culture conditions, could be relatively low-throughput, i.e. sequestering a whole incubator for culturing at a different temperature. Media development has been shown to be the major contributor towards improving biotherapeutic production rates in the past 25 to 30 years (Huang et al., 2010; De Jesus and Wurm, 2011). Culture media is always in a state of optimisation, and improvement using strategic supplementation of different chemical additives is an attractive opportunity. These small molecule enhancers (SMEs) could already form part of the growth media (for example: copper (Yuk et al., 2015b) and zinc (Kim and Park, 2016)) as cell line and base media specific optimisations are often required. Such small molecules could also inform feed design. Additionally, media component substitutes could be beneficial: for example, substituting glutamine with other molecules such as glutamate (Hong et al., 2010) or α ketoglutarate (Ha and Lee, 2014) can lower ammonia levels in culture and improve production. Alternatively, some bioactive small molecules that would normally not form part of growth media could be used to strategically enhance the culture process. A notable example is sodium butyrate (Backliwal et al., 2008; Palermo et al., 1991) that has been employed in multiple studies to improve cellular production levels by promoting an actively transcribing chromatin structure. Cell cycle inhibitors (for example lithium (Ha et al., 2014)) can be employed strategically to allow for repression of growth while enhancing cellular productivity (qP). Chemical chaperones can be utilised to promote production, correct protein folding and diminish aggregation in DTE proteins (Johari et al., 2015). Hence, it is visible that chemical supplementation strategies can be used to modify and enhance cell culture media, in turn

manipulating cell culture performance to reach its desired potential. Chemical supplementation guided media engineering strategies are comparatively cheap, facile and quick to execute than their cell engineering counterparts (Brühlmann et al., 2017b; Ha et al., 2014; Park et al., 2016), making it an attractive option to employ for rapid results. Supplementation strategies can be easily varied: concentration, timing of addition, combinatorial supplementation can all impact level of efficacy. This strategy is further discussed in this chapter wherein examples of successful small molecule supplementation approaches are discussed from an enhancement of cell and process function viewpoint. Followed after, the need of a HT screening platform for media additives is discussed through the use of potential utility scenarios. A thesis layout is presented to conclude this chapter.

2.2. SMEs for Bioprocess Improvement and Optimisation

2.2.1. Efficient Metabolic Processing and Control

Inefficient cell metabolic cycling can put strains on production culture performance. Accumulation of toxic by-products such as lactate and ammonia is a common occurrence in CHO cell culture (Dean and Reddy, 2013). This is especially true for fed-batch bioreactor production culture where pH needs to be controlled due to excessive acidification (Luo et al., 2012). Base addition increases osmolarity, which can arrest cell proliferation (Templeton et al., 2013). The major metabolic determinant of the toxic product build-up is the Warburg effect (Warburg, 1956). CHO cells exhibit similar phenotype to cancer cells, wherein they employ aerobic glycolysis for their short-term energy needs (Buchsteiner et al., 2018). This pathway ends in lactate formation and its subsequent build-up in the culture media. To combat this, various metabolic angles within the cells have been investigated. Copper sulphate supplementation has proven effective in modulating lactate metabolism (Luo et al., 2012; Qian et al., 2011; Yuk et al., 2014; Yuk et al., 2015b). Copper plays a role in the electron transport chain and maintaining a specific level of copper can assist in improving respiratory capacity (Luo et al., 2012). Lower reliance on

aerobic glycolysis decreases lactate output. The studies mentioned above all reported an increased in cell proliferation that translated into higher production yields.

Sodium dichloroacetate, a pyruvate dehydrogenase kinase inhibitor, indirectly increases pyruvate dehydrogenase activity and promotes tricarboxylic acid (TCA) cycle entry (Buchsteiner et al., 2018). Similar to copper, Warburg effect and the resulting lactate production are downregulated. Studies have reported on the ability of dichloroacetate to elongate culture durations due to mitigating frequent base additions to maintain pH (Buchsteiner et al., 2018; Skelton et al., 2010). Another detrimental by-product of cellular metabolism is ammonia (Yang and Butler, 2000). Substitution of the carbon source by other agents such as glutamate (Hong et al., 2010) and α ketoglutaric acid (Ha and Lee, 2014) have provided moderate success in improving culture performance by dampening ammonia formation.

De novo lipid synthesis has been shown to play a role in cancer cell proliferation and tumorigenesis (Mukherjee et al., 2012). For instance, fatty acid synthase (FAS) expression (a marker for lipid synthesis) is heightened in cancer cells (Santos and Schulze, 2012). This is understandable since tumour cells depend on lipid biosynthesis to meet their proliferation and energy needs (Mukherjee et al., 2012). 17β-estradiol, a FAS upregulator has been shown to increase cell proliferation in MCF-7 cells (Lu and Archer, 2010). Other molecules have been discovered that have been shown to activate FAS expression (Kim et al., 2004; Mukherjee et al., 2012). Applying the same rationale, these lipid synthesis enhancers can be applied to CHO cell factories to assist in their growth and proliferation.

Basal media itself is another major determinant of cell culture performance. The shift in industry towards chemically defined medium (due to the infection risk and poor reproducibility of serum media) (Jerums and Yang, 2005; Kishishita et al., 2015) has led to the creation of a vast media design space. The ability to plug and play different components is vital to improving CHO production performance. It is obvious that one basal media will not produce optimal culture performance across all cell lines and products. Different commercially available chemically defined media for CHO cells produce varied growth, production and

metabolic responses when applied to the same cell line (Reinhart et al., 2015; Velugula-Yellela et al., 2017). Thus, it is important to find the right balance for the production system at hand. Metal ions form a vital part of base media and modulations of their levels have proven to improve production performance. For instance, zinc supplementation in CHO cultures cultivated in different culture media yielded various degrees of improvement (Kim and Park, 2016). Zinc has insulin mimetic properties that render it a good component in chemically defined media (as a replacement for insulin) (Wong et al., 2004; Zhang et al., 2006). Various iron sources and carriers to replace bovine transferrin have also produced positive impacts on growth and titer upon supplementation (see: selenium, ferric citrate and ferric ammonium citrate in **Table 2.1**). Overall studies investigating singular supplementation of metal ion compounds have shown improvements to the CHO production process, supporting the notion that base media formulations need to be optimised for maximising performance.

Another component that forms part of cell culture media is amino acids. Strategic feeding of a combination of certain amino acids demonstrated production yield enhancements in a study by Kishishita et al. (2015).

Other Strategies for Metabolic Control:

While singular chemical supplementation or optimisation of media components can yield reward, industries and research also employ metabolic flux analysis to fully understand their production system, and use it to inform them of rational media design (Xing et al., 2011). Alternatively, genetic engineering strategies can also be employed for sophisticated metabolic control. To reduce ammonia build-up, urea cycle genes can be overexpressed that promote conversion of ammonia to citrulline; leading to increased cell proliferation (Park et al., 2000). Other overexpression strategies also exist for the improvement of CHO metabolism for enhanced culture longevity and product yields (Chong et al., 2010; Fischer et al., 2015; Gupta et al., 2017; Tabuchi and Sugiyama, 2013). Gene knockdown can also modulate processes that are detrimental towards sustained cell proliferation. Most knockdowns (usually interfering RNA mediated) target the lactate production pathways to tackle the increased media

acidification (Fischer et al., 2015; Jeong et al., 2001; Kim and Lee, 2007; Zhou et al., 2011).

Table 2.1 Literature survey of chemical supplementation/substitution driven metabolic control for improved culture performance. Abbreviations: Viable cell density (VCD), Integral of Viable cell density (IVCD): a measure of culture growth performance (explained in **Chapter 3**), IgG: immunoglobulin G.

Small Molecule Enhancer	Effect	Host	Recombinant Product	Expression System	Additional Information	Reference
Copper (copper sulphate)	2 fold increase in peak VCD 3.7 fold increase in Titer (Cell line 4: in bioreactor)	CHO	mAb: IgG1	Stable	4 CHO lines tested across various production scales. Increase in basic charge variants across all lines. Hypothesises that a minimum level of copper is required to switch to lactate consumption, level varies between cell lines.	(Yuk et al., 2015b)
	1.4 fold increase in IVCD 2.5 fold increase in titer	CHO	Fusion protein	Stable	Decreased lactate accumulation	(Qian et al., 2011)
	1.3 fold increase in peak VCD 1.6 fold increase in titer	CHO	mAb	Stable	Decreased lactate accumulation	(Luo et al., 2012)
Vanadium (sodium orthovanadate)	1.2 fold increase in IVCD	CHO	Interferon Ɣ	Stable		(Wong et al., 2004)
	1.4 fold increase in IVCD	CHO	Fusion protein	Stable		(McGrew, 2005)
Zinc (zinc sulphate)	Culture extended by 4 days 6.5 fold improvement in titer	CHO	mAb	Stable		(Kim and Park, 2016)
	Up to 1.3 fold increase in titer	Hybridoma	mAb	-		(Wong et al., 2004)
	1.6 to 1.7 fold increase in IVCD	Mouse myeloma	-	-		(Wong et al., 2004)
	1.3 fold increase in IVCD	CHO	Interferon Ɣ	Stable		(Wong et al., 2004)
Nickel (nickel chloride)	1.2 fold increase in IVCD	CHO	Interferon Ɣ	Stable		(Wong et al., 2004)
Selenium (sodium selenite)	1.35 fold increase in peak VCD	CHO	mAb	Stable	Iron carrrier	(Zhang et al., 2006)

Ferric citrate	1.22 fold increase in peak VCD	CHO	mAb	Stable	Combined with selenite to efficiently transport iron	(Zhang et al., 2006)
Ferric ammonium citrate	Up to 1.2 fold increase in titer (over other iron compounds)	CHO	mAb	Stable	Increase in titer in comparison to ferrous sulphate Citrate group critical for enhanced titer	(Bai et al., 2010)
Sodium citrate	1.4 fold increase in titer	CHO	mAb	Stable		(Bai et al., 2010)
α ketoglutaric acid	1.6 fold increase in titer	CHO	Fc-fusion protein	Stable	Performed better than culture supplemented with glutamine or glutamic acid	(Ha and Lee, 2014)
Glutamate	Culture extended by 3 days 1.6 fold increase in titer	CHO	mAb	Stable	Decreased ammonia accumulation	(Hong et al., 2010)
Sodium dichloroacetate	Culture extended by 3 days 1.5 fold increase in peak VCD 2 fold increase in titer	CHO	mAb:IgG1	Stable	Lower accumulation of lactate No effect on product quality	(Buchsteiner et al., 2018)
	3 fold increase in titer	CHO	Thy1-GFP fusion protein	Stable	Lower lactate accumulation	(Skelton et al., 2010)
17β-estradiol	1.6 fold increase in cell proliferation	MCF-7 (cancer cell line)	-	-	Increase expression of fatty acid synthase	(Lu and Archer, 2010)
Free fatty acid supplementation: oleic acid,linoleic acid,oleic+linoleic mix	Up to 2 fold increase in peak VCD	Hybridoma	mAb	-		(Butler and Huzel, 1995)

2.2.2. Transcriptional Enhancement

Transgene transcriptional activity and expression stability can be influenced by a multitude of epigenetic and environmental factors. Firstly, the site of integration can impact expression of the product gene (Kwaks and Otte, 2006; Yang et al., 2010). For instance, random integration into the functionally repressive and structurally condense heterochromatin region can lead to transgene silencing. Secondly, changes around the site of integration such as epigenetic modifications on the histone tail (i.e. acetylation, methylation, phosphorylation and ubiquitination of mainly residues on the N-terminus) influence gene activation or repression (Dahodwala and Sharfstein, 2014; Kwaks and Otte, 2006; Nishihara et al., 2017; Zhang and Reinberg, 2001). Thirdly, hypermethylation of the DNA molecule itself, especially at the promoter region can lead to gene silencing (Yang et al., 2010).

In general, two histone modifications play a major role in transgene expression stability: acetylation and methylation along with methylation of DNA molecule itself (Kwaks and Otte, 2006). Several bioactive small molecules can target the aforementioned epigenetic regulatory pathways to restore gene transcription. The most widely employed epigenetic modifiers for biopharmaceutical production are histone deacetylase (HDAC) inhibitors. Histone deacetylases remove acetyl groups on lysine residues on the histone tail, promoting interactions between histone and DNA (Ropero and Esteller, 2007). This results in a more compact chromatin structure obstructing transcription machinery access to DNA (Bora-Tatar et al., 2009; Ropero and Esteller, 2007). HDAC inhibitors regulate global acetylation and promote transcription and gene activation. The most widely employed HDAC inhibitor sodium butyrate has been used extensively to augment product yields in both transient and stable production formats (Jiang and Sharfstein, 2008). While volumetric yield gains from employing this molecule are large, off-target effects such as induction of apoptosis and reactive oxygen species (Backliwal et al., 2008; Lee and Lee, 2012; Malhotra et al., 2008) hamper its appeal.

Interestingly, sodium butyrate has been shown to reduce levels of a potentially immunogenic glycan epitope, Neu5Gc (Borys et al., 2010). However, sodium

butyrate does alter glycosylation profiles undesirably by having a negative impact on galactosylation (Hong et al., 2014) and sialic acid content (Sung et al., 2004). Other HDAC inhibitors such as valproic acid have been applied in biopharmaceutical research with a great degree of success (Backliwal et al., 2008; Wulhfard et al., 2010; Yang et al., 2014). Molecules like trichostatin A and MS 275 have also been employed to with some success in biotherapeutic production setup (Backliwal et al., 2008; Nan et al., 2004) (see **Table 2.2** for summary on other HDAC inhibitors).

Multiple other HDAC inhibitors are been approved for clinical use as cancer therapeutics (Biswas and Rao, 2017). These molecules present opportunities for employment in the bioprocess arena as boosters for recombinant protein transcription. However, since they are used as apoptosis inducers for chemotherapeutic treatments, it is feared that they would impart the same functionality in the bioprocess arena. Thus, a degree of caution needs to be undertaken while employing these molecules. Other avenues such as computational modelling and docking studies have been able to isolate novel HDAC inhibitors based on structural analysis (Bora-Tatar et al., 2009). Most HDAC inhibitors fall under broad structural classes: hydroxamates, carboxylic acids, cyclic tetrapeptides, benzamides and electrophilic ketones (Bora-Tatar et al., 2009). Computational structural modelling could potentiate the identification of novel bioactive small molecules that are more suited to bioprocess production scenarios. Obviously, this would require rigorous testing to validate, especially evaluating apoptosis induction upon addition of the chemical.

Another histone modification that can impact gene activation and repression is histone methylation. Histone methylation occurs on lysine and arginine residues (Zhang and Reinberg, 2001). Methyltransferases confer methyl groups on the histone tail, resulting in gene repression or activation (Curry et al., 2015). Applying the same rationale as with HDAC inhibitors, histone methyltransferase inhibitors are applied in cancer research to target tumours that have characteristic high levels of methyltransferase activity (Curry et al., 2015). Their application as inducers of recombinant protein production is rare, with it being necessary to determine specific inhibitors for transcription repressive marks. A study by Christensen (2016) is the sole documented research study on the use

of histone methyltransferase inhibitors for CHO cell recombinant protein production. The study identified various histone methyltransferase inhibitors that enhanced transient gene expression in CHO cells expressing a luciferase reporter. The exact mechanism of action of the successful molecules remains unknown. While gaining prominence in chemotherapy circles, these molecules are under researched for the purposes of recombinant protein expression and more studies are required to critically assess their efficacy.

Methylation can also occur on the DNA molecule itself. Promoter methylation is a major cause for loss in productivity in mammalian recombinant DNA expression (Yang et al., 2010). This study demonstrated that heavy methylation on the cytomegalovirus (CMV) promoter contributed towards loss in production stability over time. Addition of a DNA methyltransferase inhibitor, 5-aza-2′-deoxycytidine (decitabine), helped recover some of the production capability in their CHO clones (Yang et al., 2010). Similarly, 5-azacytidine has proven useful in rescuing recombinant gene expression in other studies (Backliwal et al., 2008; Escher et al., 2005; Tanigawa et al., 1993). However, 5-azacytidine, decitabine and other nucleoside analogs can cause DNA breaks and apoptosis since they are incorporated into the DNA molecule (Lyko and Brown, 2005; Yang et al., 2010). Thus, different non-nucleoside analogs that do not act in a cytotoxic manner need to be discovered for the purposes of biologics production. A summary on DNA methyltransferase inhibitors that have been previously employed to improve recombinant product yields is displayed in **Table 2.3**.

In conclusion, these molecules are powerful tools for transgene expression enhancements due to their ability to promote transcription. The major drawback of these molecules is that they can present cytotoxicity risks. Thus, it is imperative to titrate the molecules effectively i.e. effective dose is selected based on a balance between expression enhancement and cell viability detriment.

Other Strategies for Transcriptional Control and Enhancement:

Engineering vector elements to maintain and enhance recombinant gene transcription are increasingly being utilised. Scaffold/matric attachment regions present the ability to create favourable conditions for transcription, i.e. opening and maintaining an open chromatin structure (Dahodwala and Sharfstein, 2014). They are also known to recruit histone acetyltransferases and generally promote transcription (Girod et al., 2007). Other vector elements that can promote transgene expression include UCOE and insulator elements (Kwaks and Otte, 2006). Another strategy is hot-spot targeting that aims to guide transgene integration at a transcriptionally active site (Dahodwala and Sharfstein, 2014; Kwaks and Otte, 2006). Synthetic promoters also present opportunities for sophisticated transcriptional control, based on rationally driven promoter designs (for example assemblies based on transcription factor regulatory elements) (Brown et al., 2014).

Table 2.2 Literature summary of the application of HDAC inhibitors as enhancers of recombinant gene expression. Additional reference for table: (Kim and Bae, 2011).

Small Molecule Inhibitor	Effect	Host	Recombinant Product	Expression System	Additional Information	Target HDACs	Reference
Sodium butyrate	2 fold increase in titer	CHO	mAb	Stable		Class I and IIa HDACs	(Jiang and Sharfstein, 2008)
	2 fold increase in titer	CHO	Erythropoietin	Stable			(Lee and Lee, 2012)
	1.7 fold increase in titer	CHO	mAb	Stable	Coupled with a temperature shift to 30°C Decrease in Neu5Gc levels		(Chen et al., 2011)
	1.5 fold increase in titer	CHO	mAb	Transient			(Backliwal et al., 2008)
	4.5 fold increase in titer	HEK293E	mAb	Transient			(Backliwal et al., 2008)
	3.4 fold increase in titer	CHO	mAb	Stable			(Backliwal et al., 2008)
	3.3 fold increase in titer	CHO	Thrombopoietin	Stable	Decreased acidic isoforms and sialic acid content		(Sung et al., 2004)
	4 fold increase in titer	CHO	Therapeutic antibody	Stable			(Hong et al., 2011)
Valproic acid	1.8 fold increase in titer	CHO	mAb	Transient		Class I and IIa HDACs	(Backliwal et al., 2008)
	5.3 fold increase in titer	HEK293E	mAb	Transient			(Backliwal et al., 2008)
	3.2 fold increase in titer	CHO	mAb	Stable			(Backliwal et al., 2008)
	1.2 fold increase in titer	CHO	mAb	Stable	Fed-batch process		(Yang et al., 2014)
	3 fold increase in titer	CHO	mAb	Transient			(Wulhfard et al., 2010)
	1.96 fold increase in titer	CHO	mAb	Stable			(Park et al., 2016)

Trichostatin A	8.5 fold increase in expression	CHO	GFP	Transient		Pan-HDAC inhibitor	(Nan et al., 2004)
	4.3 fold increase in titer	HEK293E	mAb	Transient			(Backliwal et al., 2008)
	1.6 fold increase in titer	CHO	mAb	Transient			(Backliwal et al., 2008)
MS 275	5.1 fold increase in titer	HEK293E	mAb	Transient		HDAC 1,2,3 inhibitor	(Backliwal et al., 2008)
	1.5 fold increase in titer	CHO	mAb	Transient			(Backliwal et al., 2008)
Suberanilohydroxamic acid	5 fold increase in titer	Plant: *Medicago truncatula*	lipocalin-type prostaglandin D2 synthase	Stable		Pan-HDAC inhibitor	(Santos et al., 2017)

Table 2.3 Summary of literature survey on the use of DNA methyltransferase inhibitors to enhance recombinant gene expression. Additional reference for table: (Biswas and Rao, 2017).

Small Molecule Inhibitor	Effect	Host	Recombinant Product	Expression System	Additional Information	Type	Reference
5-Azacytidine	1.7 fold increase in titer	CHO	mAb	Transient	Combined with HDAC inhibitors for further improvement	Nucleoside analogue	(Backliwal et al., 2008)
	1.6 fold increase in titer	HEK293E	mAb	Transient			(Backliwal et al., 2008)
	1.9 fold increase in titer	CHO	mAb	Stable			(Backliwal et al., 2008)
	2 fold increase in titer	CHO	β galactosidase	Stable			(Tanigawa et al., 1993)
	1.5 fold increase in titer	Mouse myeloma	β galactosidase	Stable			(Tanigawa et al., 1993)
	3.2 fold improvement in transfection efficiency	Murine macrophage cells	β galactosidase	Transient			(Escher et al., 2005)
Decitabine (5-aza-2'-deoxycytidine)	Up to 2 fold improvement in qP	CHO	Interferon Ɣ	Transient	Decreased methylation levels on the CMV promoter	Nucleoside analogue	(Yang et al., 2010)
Procainamide	1.2 fold increase in titer	CHO	mAb	Transient		Non-nucleoside analogue	(Backliwal et al., 2008)
	1.3 fold increase in titer	HEK293E	mAb	Transient			(Backliwal et al., 2008)
Hydralazine	1.4 fold increase in titer	CHO	mAb	Transient		Non-nucleoside analogue	(Backliwal et al., 2008)
	1.1 fold increase in titer	HEK293E	mAb	Transient			(Backliwal et al., 2008)
RG108	1.8 fold increase in titer	CHO	mAb	Transient	Combined with HDAC inhibitors for further improvement	Non-nucleoside analogue	(Backliwal et al., 2008)
	1.8 fold increase in titer	HEK293E	mAb	Transient			(Backliwal et al., 2008)
	1.8 fold increase in titer	CHO	mAb	Stable			(Backliwal et al., 2008)

2.2.3. Proliferation Control to Enhance Cell Production Resources

Maintaining a high growth rate is considered vital for good production performance using mammalian cell factories. However, uncontrolled proliferation can sometimes yield the opposite of the performance expected. Nutrient depletion and accumulation of toxic by-products can shorten culture duration, deteriorate the product and complicate downstream processing (Du et al., 2015; Mazur et al., 1998).

Additionally, there is an emphasis on focusing resources completely towards protein production and improving specific cellular productivity. It has been reported that a cell cycle arrest at the G1 phase bolsters qP (Du et al., 2015; Dutton et al., 2006; Ha et al., 2014; Kumar et al., 2007; Mazur et al., 1998; Sunley and Butler, 2010). The definite mechanism that causes this boost in qP is unknown, however many theories have been put forward to partially explain this gain. The cells are generally more metabolically active and bigger in size (Carvalhal et al., 2003). There is also evidence that ribosome synthesis is heightened at the G1 phase (Dez and Tollervey, 2004). Many small molecule inhibitors of the G1 phase of the cell cycle are proven boosters of cellular qP. The most notable ones are sodium butyrate, sodium phenylbutyrate and valproic acid (Ha et al., 2014; Kumar et al., 2007; Park et al., 2016). These molecules mostly act as histone deacetylase inhibitors inhibiting HDAC1, which indirectly restrains entry into S phase. It can be considered that their epigenetic regulation plays a larger role in their ability to boost qP and titer. However, a specific CDK4/6 inhibitor arresting cell cycle in the G1 phase (Du et al., 2015) has also been shown to improve cellular productivity, indicating cell cycle block at G1 has the ability to improve cellular production capabilities. Also, reducing culture temperature has served as a popular technique to improve cell specific yield (discussed briefly in **Other Approaches for Controlled Proliferation and Cell Cycle Arrest**). This also relies on a cell cycle block at G1, adding to the evidence of G1 arrest being an effective strategy to improve productivity.

There has also been interest surrounding inducing a cell cycle block at the G2/M phase. A study by Yokota and Tanji (2008), reported that maximum production of a tissue plasminogen activator analogue occurred in the G2/M

phase in CHO cells. Lithium chloride, a G2/M inhibitor was easily titrated into both stable and transient producing cultures and was able to bolster cell qP (Ha et al., 2014; Kim et al., 2016a). Already employed in clinical setting as an anti-depressant, regulatory concerns for using this molecule in cell culture are comparatively low (Ha et al., 2014). Other bioprocess G2/M phase arrest strategies through chemical deployment are highlighted in **Table 2.4**. G2/M arresting small molecules (mostly kinase inhibitors) find use in cancer research due to their ability to stop malignant cells from proliferating, followed by the onset of apoptosis. In the bioprocess arena this is not ideal, since cells need to remain viable to continue with protein production. There were some candidates highlighted in literature that sustained cell viability. D,L sulforaphane, a naturally occurring molecule, when trialled in human ovarian cancer cells did not induce apoptotic pathways (Chang et al., 2013). Some G2/M inhibitors in bioprocessing circles have proved effective in increasing transient gene expression (Galbraith et al.,; Kim et al., 2016a; Tait et al., 2004). It is suggested that these molecules aid in gene delivery by (a) increasing nuclear membrane permeability and (b) increasing available cell surface area due to bigger cell size (Christensen, 2016; Kim et al., 2016a). Additionally, obstruction of cell proliferation prevents the transfected DNA from getting diluted too quickly, retaining enough copies in each cell, thus increasing qP (Kim et al., 2016a). With regards to stable production modes, due to the growth arrested cells being considerably larger and containing double recombinant DNA content, an increase in cellular productivity is not entirely unexpected (Tait et al., 2004). Lloyd et al. (2000) also noted that recombinant protein productivity was highest when CHO cells were in the G2/M phase. However, they concluded that cell size was the predominant determinant of qP (Lloyd et al., 2000; Tait et al., 2004).

Other Approaches for Controlled Proliferation and Cell Cycle Arrest:

While the use of bioactive small molecule inhibitors of cell cycle is extremely easy to implement and cost-effective, off-target effects such as apoptosis can yield undesired effects. Perhaps, the most common alternative for cell cycle arrest is hypothermic shock. Cells cultured at 32°C have a lower growth rate,

are bigger in size and have a higher qP (Coronel et al., 2016; Kumar et al., 2007; Sunley and Butler, 2010). Similar to the chemical cell cycle arrest using sodium butyrate and valproate, these cells are arrested in G1. Another approach is through genetic manipulation. Inducible overexpression of Gadd45, a protein involved in the G2/M checkpoint, improved transgene expression in CHO cells (Kim et al., 2014). Genes involved in CDK inhibition can be targeted for overexpression and upregulation, often arresting cells in G1 phase to improve productivity (Kumar et al., 2007; Sunley and Butler, 2010). Overexpression of an anti-apoptotic gene, Bcl2 also causes cell cycle arrest but viability is maintained, co-expression with other cell cycle arrest inducers can improve transgene expression (Du et al., 2015; Fussenegger et al., 1998; Kumar et al., 2007).

Table 2.4 Previous examples of the use of cell cycle inhibitors in mammalian cell bioprocessing as a means for productivity enhancement. Note: For sodium butyrate and valporic acid, only studies that confirmed G1 arrest are shown. More examples in **Table 2.2**.

Small Molecule Inhibitor	Effect	Host	Recombinant Product	Expression System	Additional Information	Reference
Valeric acid	1.4 fold increase in titer	CHO	Therapeutic protein	Stable	Combined with hypothermia	(Coronel et al., 2016)
	2.8 fold increase in titer	CHO	mAb	Stable	G1 phase blocker Improved galactosylation	(Park et al., 2016)
Nocodazole	1.9 fold increase in titer	CHO	secreted embryonic alkaline phosphatase (SEAP)	Transient	G2/M phase blocker	(Tait et al., 2004)
	2.3 fold increase in titer	CHO	Luciferase reporter	Transient	G2/M phase blocker	(Tait et al., 2004)
Valproic acid	1.96 fold increase in titer	CHO	mAb	Stable	G1 phase inhibitor	(Park et al., 2016)
Lithium	3.8 fold improvement in titer	HEK293E	mAb	Transient	Also assisted in gene delivery	(Kim et al., 2016a)
	4.4 fold improvement in titer	CHO	mAb	Transient	Also assisted in gene delivery	(Kim et al., 2016a)
	2.3 fold increase in titer	CHO	Fc-fusion protein	Stable	Reduced sialylation	(Ha et al., 2014)
	1.3 fold increase in titer	CHO	mAb	Stable	G2/M phase blocker	(Park et al., 2016)
Sodium butyrate	1.7 fold increase in titer	CHO	mAb	Stable	G1 arrest Coupled with a temperature shift to 30°C Decrease in Neu5Gc levels	(Chen et al., 2011)
	3.3 fold increase in titer	CHO	Thrombopoietin	Stable	Decreased acidic isoforms and sialic acid content Increase in sub G1 (debris/apoptosis)	(Sung et al., 2004)
Hydroxyurea	2.8 fold increase in titer	CHO	Luciferase reporter	Transient	G1 phase inhibitor	(Tait et al., 2004)

CDK4/6 Inhibitor	2 fold increase in qP	CHO	mAb	Stable	G1 phase inhibitor	(Du et al., 2015)
BI 2536	6 fold increase in titer	Human prostate cancer cells	Luciferase reporter	Transient	G2/M phase blocker	(Christensen, 2016)
Germanium	2.2 fold increase in qP	CHO	mAb: IgG4	Stable	G2/M phase inhibitor: CDK1 inhibitor	(Galbraith et al.,)
	1.6 fold increase in titer	CHO	mAb: IgG4	Transient		(Galbraith et al.,)

2.2.4. Aggregation and Protein Secretion Control

Diseases caused by protein misfolding are a common occurrence: Alzheimer's, Parkinson's and Prion disease to name a few (Cortez and Sim, 2014). Chemical chaperones are effector small molecules that have demonstrated success in attenuating protein misfolding and aggregation in the aforementioned disease models. The exact mechanism of this set of molecules remains poorly understood, however the general consensus remains that they act by promoting correct protein folding, mitigating aggregation and generally enhancing protein production. Additionally, some chemical chaperones have been shown to be effective in assisting molecular chaperone function (De Almeida et al., 2007). Applying the same rationale as in misfolding diseases, these molecules have been applied in biopharmaceutical production scenarios. With industry focus shifting towards the production of more complex and DTE proteins, efficient cellular production machinery and correct protein folding becomes critical. Thus, chemical chaperones would have a higher sense of utility in these scenarios.

Most chemical chaperones that are used to improve recombinant protein production are osmotically active. These include amino acids and their derivatives such as proline, glycine taurine; methylamines like betaine, trimethylamine N-oxide and polyols like glycerol, sucrose (Cortez and Sim, 2014; Welch and Brown, 1996). These molecules are mostly involved in the stabilisation of protein structure by sequestering water molecules to promote correct protein folding (Cortez and Sim, 2014). The other class of chemical chaperones are termed hydrophobic chaperones. These interact with hydrophobic regions of the protein that are susceptible to aggregation (Cortez and Sim, 2014). The most noteworthy chaperones in this category are 4 phenylbutyric acid and tauroursodeoxycholic acid.

A summary of published research on the use of chemical chaperones in the biopharmaceutical production design space is shown in **Table 2.5**. While the chaperones that have been tested mainly play a role in upregulating protein expression and secretion and/or attenuating aggregation, some chaperones were also shown to improve cellular growth. This could be explained by their

indirect impact on the unfolded protein response (UPR) and alleviation of ER stress, thus promoting cell survival. This is expanded upon below.

While chemical chaperones directly modulate protein structure, these molecules have been shown to indirectly crosstalk with cellular mechanisms that deal with protein secretion and unfolded protein responses. 4 phenylbutyric acid and tauroursodeoxycholic acid were shown to affect expression of unfolded protein response activators, binding immunoglobulin protein (BiP) and glucose-regulated protein 94 (GRP94) (De Almeida et al., 2007; Kolb et al., 2015; Mimori et al., 2013). 4 phenylbutyric acid is also known to induce transcription of other heat shock proteins (De Almeida et al., 2007; Mimori et al., 2012). Additionally, tauroursodeoxycholic acid demonstrated cytoprotective effects in sepsis models in mice (Doerflinger et al., 2016; Uppala et al., 2017). Betaine has been shown to facilitate correct protein transport from the endoplasmic reticulum (ER) to the Golgi (Roth et al., 2012). Some chaperones are also known to impact the oxidative status of the cell. Glycine betaine (Rabbani and Choi, 2018) , trehalose (Patel et al., 2017) and proline (Krishnan et al., 2008) are all known to reduce reactive oxygen species in the cell and promote cell viability.

The most comprehensive study on the use of chemical chaperones in CHO cells is by Johari et al. (2015). The authors of this study utilised a DTE protein product, transient CHO system and attempted to improve production and diminish aggregation through chemical chaperone use. There were several positive results using singular chemical chaperones (as shown in **Table 2.5**). It was interesting to note that combining 4 phenylbutyric acid and glycerol treatment with molecular chaperone cyclophilin B (cypB) overexpression in a biphasic culture process, recorded a 5.9 fold improvement in overall titer. While this study did not conclusively reveal crosstalk mechanism between chemical and molecular chaperones, it did demonstrate the advantages of a combined strategy of gene overexpression and chemical treatment. However, if time, money and resources are limited, chemical chaperones are an attractive prospect for improving recombinant production performance over gene overexpression.

Other Approaches for Aggregation and Secretion Control:

In contrast with chemical approaches, genetic engineering approaches can be applied to tackle DTE protein secretion and reduce aggregation. Optimising expression vectors with signal peptide engineering (Le Fourn et al., 2014; Zhou et al., 2018) assist with efficient polypeptide translocation to the ER. Overexpression of various ER chaperones such as protein disulphide isomerase (PDI), BiP and calnexin (Chung et al., 2004; Johari et al., 2015; Zhou et al., 2018) has also shown varying degrees of success. Other strategies include UPR engineering (X-box binding protein 1 (XBP1), activating transcription factor 6 (ATF6) overexpression) (Pybus et al., 2014; Zhou et al., 2018) and decrease in culture temperature to alleviate aggregation (Johari et al., 2015).

Table 2.5 Studies that employed chemical chaperone supplementation for improved recombinant protein production.

Small Molecule Enhancer	Effect	Host	Recombinant product	Expression system	Additional information	Reference
Dimethyl Sulfoxide	2.1 fold increase in qP	CHO	Human β-interferon	Stable	Reduced sialylation	(Rodriguez et al., 2005)
	2 fold increase in titer	Hybridoma	mAb	-		(Ling et al., 2003)
	1.8 fold titer increase 3.6 fold qP increase	CHO	Flag-tagged COMP-Ang1	Stable		(Hwang et al., 2011)
	1.5 fold titer increase	CHO	Sp35Fc	Transient	Reduced aggregation	(Johari et al., 2015)
Ectoine	1.25 fold increase in titer	CHO	Recombinant factor VIII	Stable		(Roth et al., 2012)
Betaine	1.4 fold IVCD improvement 1.3 fold titer improvement	CHO	Sp35Fc	Transient	Reduced aggregation	(Johari et al., 2015)
	1.5 to 1.8 fold increase in titer	CHO	Recombinant factor VIII	Stable	Promotes correct folding, ER to golgi transport	(Roth et al., 2012)
4 Phenylbutyric acid	1.6 improvement in titer	CHO	Sp35Fc	Transient	Reduced aggregation	(Johari et al., 2015)
	2.6 fold reduction in aggregation	HEK293T	HFE C282Y	Transient		(De Almeida et al., 2007)
	4 fold increase in titer	CHO	PC_{A267T}	Stable		(Chollet et al., 2015)
	1.2 fold titer increase 3 fold qP increase	CHO	Flag-tagged COMP-Ang1	Stable		(Hwang et al., 2011)
Proline	2.6 fold titer increase 4.6 qP increase	CHO	Flag-tagged COMP-Ang1	Stable		(Hwang et al., 2011)
Trehalose	2.5 fold increase in titer	CHO	Fusion protein	Stable	Bioreactor cultures	(Onitsuka et al., 2014)
Taurour-sodeoxycholic acid	Improved protein stability Reduced ER stress response	HEK293T	HFE C282Y	Transient		(De Almeida et al., 2007)
Trimethylamine N-oxide	1.5 fold increase in IVCD	CHO	Sp35Fc	Transient	Reduced aggregation	(Johari et al., 2015)

Glycerol	2 fold titer increase 2.8 qP increase	CHO	Flag-tagged COMP-Ang1	Stable		(Hwang et al., 2011)
	1.4 fold increase in titer	CHO	Sp35Fc	Transient	Reduced aggregation	(Johari et al., 2015)
	1.4 fold increase in titer	CHO	Macrophage-colony stimulating factor	Stable		(Liu and Chen, 2007)

2.2.5. Glycosylation Processing

Protein product glycosylation is a major factor in determining biotherapeutic efficacy, potency and safety (Brühlmann et al., 2015). Control of protein glycosylation to prevent any immunogenic epitopes is especially important. Additionally, there has been a meteoric rise in the number of biosimilar molecules in the bioprocess arena. Maintaining the same glycoprofile as the parent biosimilar is imperative. Thus, modulation to achieve the desired glycoform is an important requisite in upstream processing. Chemical supplementation approaches are simple and effective tools to achieve this objective. Nucleotide sugar precursor supplementation can affect final N-linked glycosylation through their role in increasing intracellular pools of glycosylation substrates, nucleotide sugars (Blondeel et al., 2015) (see **Table 2.6**). Manganese is co-factor for galactosyltransferases (Lee et al., 2017) and has been shown to play a unique role in combination with galactose and uridine in promoting galactosylation (Grainger and James, 2013; Gramer et al., 2011). Conversely, manganese in the absence or limitation of glucose has been shown to increase high mannose profiles (Surve and Gadgil, 2015). Other modulators such as raffinose and kifunensine (Brühlmann et al., 2017b) can be used to tune the glycoprofile towards its optimum, a trait that is especially vital in the creation of biosimilars. The major advantage in using small molecules to control protein glycosylation is the ease of use: the molecules can be titrated, combined and applied at any stage of production to achieve the desired profile. This is in contrast to some of the alternative strategies discussed below.

Other Strategies for Glycosylation Control:

Genetic overexpression and/or knockout account for most of the glycosylation modulation approaches undertaken in the biotherapeutic industry. For example, overexpression of st6gal-I concomitant with a knockout of st3gal resulted in increased α-2,6 sialylation levels relative to α-2,3 sialylation levels (Chung et al., 2017). This was beneficial in creating more human-like glycoforms (Fischer et al., 2015). Overexpression of galactosylation genes can also help increase

sialic acid content (Tejwani et al., 2018). Core fucose residues in glycoproteins can negatively impact effector function of monoclonal antibodies (Tejwani et al., 2018). Knock out of the FUT8 gene (a gene that controls α-6-fucosylation) resulted in antibodies devoid of core fucose with enhanced antibody dependent cell mediated cytotoxicity (Fischer et al., 2015; Malphettes et al., 2010).

Table 2.6 Summary of chemical supplementation approaches to improve galactosylation and sialylation in mammalian cell bioprocessing. Adapted from:(Blondeel and Aucoin, 2018). Abbreviations: Uridine 5-diphosphate (UDP), N-acetylhexosamine (HexNAc).

Small molecule Modulator	Effect	Host	Recombinant product	Expression system	Additional information	Reference
N-acetyl-D-glucosamine (GlcNAc)	Favoured G0 and FG0 glycoforms Up to 2 fold increase in UDP-GlcNAc pools	CHO	mAb	Stable	Less than 5% reduction in growth rate	(Blondeel et al., 2015)
	Favoured G0 and FG0 glycoforms Reduced galactosylation	CHO	mAb	Stable		(Kildegaard et al., 2015)
Glucosamine	Favoured G0 and FG0 glycoforms	CHO	mAb	Stable	50% growth rate reduction	(Blondeel et al., 2015)
	Increase in UDP-GlcNAc pools Decrease in tetrasialylation	CHO	Erythropoietin	Stable		(Yang and Butler, 2002)
	Increase in UDP HexNAc pools Decrease in galactosylation	NS0	mAb	Stable	Reduced growth	(Hills et al., 2001)
Galactose	1.12 fold increase in galactosylation	CHO	mAb	Stable	No reduction in growth or titer	(Kildegaard et al., 2015)
	1.2 fold increase in galactosylation 1.14 fold increase in sialylation	CHO	Fc fusion protein	Stable	No reduction in growth	(Liu et al., 2015a)
	1.26 fold increase in sialylation	CHO	Recombinant human Factor II	Stable		(Lee et al., 2017)
Manganese	Improved galactosylation and sialylation	CHO	Erythropoietin	Stable		(Crowell et al., 2007)
	1.3 fold increase in sialylation	CHO	Recombinant human Factor II	Stable		(Lee et al., 2017)
Galactose+manganese+uridine	1.2 to 1.24 fold increase in galacotsylation	CHO	mAb	Stable		(Gramer et al., 2011)
	Up to 2 fold improvement in galactosylation	CHO	mAb	Stable		(Grainger and James, 2013)
N-acetyl- D-mannosamine	1.2 fold increase in sialylation	CHO	Recombinant human Factor II	Stable		(Lee et al., 2017)

2.2.6. High-Throughput Bespoke Media Development could de-bottleneck Upstream Biomanufacturing Processing

With speed to market being vital, quick process optimisation to maximise benefit is crucial. Host cell and process engineering are central to maximising product output at the upstream level. Engineering these elements can be achieved mainly by optimising genetic elements (vector engineering, host gene overexpression/knockdown), evolving cells, media/feeds optimisation and bioreactor environment control. Bioactive small molecules present an attractive opportunity for the improvement of biologics production in both transient and stable formats. There has been a steady rise in use of bioactive small molecules in bioprocess. The precision and control can vary greatly depending on the process they target, however they are quite effective in increasing proliferation, titer or modulating protein quality.

We envisage that the use of small molecules as media additives can effectively fine tune therapeutic protein production processes. Small molecule additives have the following advantages: (i) quick and easy to titrate, (ii) cheap and (iii) ease of deployment at different stages of culture. **We propose a closed box testing kit comprising a suite of SME molecules targeting various cell processes, coated on a multi well plate.** Rational and HT screening of these molecules can inform the creation of bespoke media environments tailored to a user's upstream protein production process. There is no universal media environment suitable for every cell line and product: media has to be optimised for every process, strengthening the need for HT media optimisation approaches.

To expand upon the possible utility and demonstrate the need for such a product, various industrial production scenarios are discussed. Depending on the situation at hand, informed and educated SME screening can be used to provide potential solutions to the various scenarios discussed below.

2.2.6.1. Scenario 1: Undesirable Proliferation Phenotype

Most biopharmaceutical companies have a panel of host CHO cell lines that are employed for biopharmaceutical production. When a new product is needed for production, vector engineering is normally the first route to improve production capabilities. Multiple clones are generated and cell proliferation and production capabilities are monitored to select the best proliferating and producing CHO host. Even after strenuous rounds of cloning and selection, depending on the complexity of the product and host system, the user might have a sub-optimal production set up, due to slow cell proliferation. Manufacturing process development (including media optimisation) plays a huge role in countering this. A focused screening plate with growth enhancer molecules **(metal ions, metabolic modulators)** could help speed up media and feed development. A proposed deployment of the plate would be after the best performing clone is selected. The "best" clone is normally selected based on production performance in fed-batch mini bioreactor studies. However, it is probable that proliferation performance has not reached full potential. The SME enhancer plate profile would prove beneficial in identifying which supplements would be useful in improving cell growth and proliferation, in turn helping optimise the basal media and feed compositions.

2.2.6.2. Scenario 2: DTE Product Molecule

Development of novel complex proteins such as bispecifics and fusion proteins has been rising steadily (Walsh, 2014). However, expression of these proteins and some mAbs in cellular hosts can prove difficult and return low titers (Johari et al., 2015). There is an increase in time and cost associated with these DTE proteins wherein efforts need to made to meet their production demands (Pybus et al., 2014). Some proteins have a tendency to aggregate whereas others have folding, assembly and secretion issues. The burden of improper folding can result in the initiation of unfolded protein responses, which downregulates protein secretion and can result in apoptosis (Zhou et al., 2018). Multiple

studies have reported on post-transcriptional bottlenecks causing low protein titers (Johari et al., 2015; Ku et al., 2008; Pybus et al., 2014).

A suite of SMEs specifically known to counter these production issues would have a high impact when employed. Specifically, **chemical chaperones** have a variety of mechanisms by which they can target aggregation and/or folding, assembly and secretion abnormalities. These have been shown to be highly effective in comparison to genetic engineering approaches (Johari et al., 2015). The functional pathways targeted and the modulation of the surrounding protein structure can be exceptionally versatile. Based on the bottleneck, various chemical candidates can be rationally tested and selected to restore correct protein production and folding. Simple, easy to deploy and cost-effective, SMEs or combinatorial SME deployment could prove attractive to battle production incapability in transient and stable production modes.

2.2.6.3. Scenario 3: Isolating the Best Performing Clone

Clone selection is an important step in the bioproduction process. Clones are usually tested in standard conditions (i.e. same media and process conditions) and the best producing clone is taken forward for production runs. It has been stated that “dynamic” ranking of clones (performed by testing clones in their best performing condition) could provide a more accurate representation of the true best clone (Legmann et al., 2011). This study showed that clone ranking changes significantly in different media and process conditions. Clones can respond differently to various media conditions. Applying the same rationale, a media supplementation testing plate could be beneficial if incorporated into clone selection pathways. The plate would show which supplements elevate production performance and give a more educated view on the diversity in clone performance. Once a clone is picked based on this new strategy, the plate outputs for that particular clone can be used to make informed media optimisation and supplementation decisions.

2.2.6.4. Scenario 4: Biosimilar Product Quality

The advancement of biosimilars in the biopharmaceutical market has resulted in stringent rules being applied to confirm biosimilarity. This is especially crucial for glycosylation patterns since they can determine molecule efficacy and safety. Cell lines and processes can impose variations in glycoform profiles for the same protein molecule. Thus, complete replication of glycoprofiles can require some intervention. Bioactive small molecule modulators of glycosylation present simple and cost effective strategies. Depending on the glyocoform that needs enriching, specific molecules can be used to target glycoprofiles of interest and increase molecular fingerprint similarity to the parent molecule (Brühlmann et al., 2017a). Since speed-to-market is important to fend off other biosimilar competition, a focused HT plate based screening method to identify glycosylation modulators that heighten biosimilarity would prove especially useful.

2.2.6.5. Scenario 5: Biphasic Culture Modality

The concept of biphasic cultures is not novel. Biphasic cultures are characterised by a cell proliferation phase followed by a protein production phase. The most common strategy employed to achieve this is hypothermic culture shock. Cells are cultivated at 37°C for a stipulated time period and then shifted to 30-32°C. The lower temperatures stagnate growth while maintaining cell viability and cellular resources are prioritised for recombinant protein production (Sunley and Butler, 2010). Similar rationale applied, chemical arrest/solely qP enhancement strategies can be applied to create a biphasic culture modality. **G1 and G2/M cycle inhibitors and/or epigenetic inhibitors** can prove useful to this effect. The ease of manipulation and opportunity for combination for an enhanced effect make chemical use attractive. The ability to screen different chemicals for this purpose in a HT manner is important. Thus, having a coated plate with cell cycle inhibitors and qP enhancers allows for multiple biphasic culture trialling. The cells can be cultivated on an uncoated plate for a certain time period followed by addition of the re-solubilised

chemicals from the coated plate to create a HT biphasic culture testing modality.

2.3. Thesis Aims and Overview

The previous section highlighted the need and potential utility of HT bioactive small molecule testing to accompany bioprocess development. This project focuses on the development of simple and quick HT testing technologies to harness the potential of bioactive small molecules as enhancers for CHO based bioprocessing. This research study has 4 aims. Firstly, to investigate the development of a HT screening platform. The envisioned screening platform is standardised and easy to use, allowing for the screening of multiple effectors concurrently. Secondly, to assess the efficacy of a suite of SME molecules in a model production system. Efficacious molecules are defined as those that improve one or more culture attribute (growth, volumetric titer or qP). Thirdly, to investigate the potential of chemical combinatorial strategies as tools to further amplify cell growth or production. Both singular and combinations of successful enhancers will form part of the envisioned media additive screening tool. An embedded screening design would allow the user to concurrently assess media additives and their selected combinations in their production system. Finally, to use the developed HT screening tool to investigate potential novel enhancers for CHO bioprocess. These could be enhancers that have never been tested in CHO production systems specifically or enhancers that have never been employed in bioproduction scenarios at all previously.

The research findings of this project are presented across 3 results chapters. Each chapter contains a brief introduction and experimental approach taken to tackle the research aim. Investigation of the development of a HT screening platform is displayed in **Chapter 4**. HT, miniaturised culturing methodologies were investigated and optimised. Additionally, analytical technologies to assess cellular growth and titer were and optimised for HT use. Timing of chemical addition and culture attribute sampling was investigated.

Chapter 5 depicts the chemical screens undertaken using the HT platform to inform the media supplement screening tool design. The envisioned product design is based on SME coated multi-well plate technologies for easy screening of culture performance enhancers. Potential SMEs were selected based on literature surveys and past experience. 43 SME (across 8 functional categories) screens were performed in a stable producer CHO cell line, wherein singular chemical addition was assessed at different concentrations. Chemicals were mostly added at the start of culture with additional screens performed for a small subset of molecules deployed at mid-exponential phase. Growth and production assessments were performed at a single time point in culture. Rational combinations of efficacious chemicals were investigated to identify any positive interactions between SMEs that elevated growth and/or production performance. This was performed using factorial design based DOEs. Finally, the chapter depicts the scale-up performance (in shake flasks) of a recommended chemical deployment strategy for a model CHO stable producer line.

Chapter 6 demonstrates the use of the HT culturing methodology to test for novel SME molecules. A parent molecule was selected based on initial screening. Structural similarity testing tools were employed to identify novel structural analogues of the parent molecule and test them using the HT platform. Multiple analogues were shown to boost qP and/or product titer. While the parent molecule has been shown to improve volumetric titer in a previous publication, there is no published description of its mechanistic role in cellular production pathways. Thus, culture performances of the parent molecule and one effective analogue were mechanistically deconstructed using a series of functional analyses. It was shown that both molecules acted epigenetically. Further, product quality was confirmed to be fairly similar to that of the control cultures, demonstrating the potential of these molecules as specific production enhancers in CHO cells.

Chapter 3

Materials and Methods

This chapter provides an overview of the materials and methods employed throughout the research described in this thesis.

3.1. Mammalian Cell Culture

3.1.1. Cell Line and Routine Sub Culture

The cell line employed in all experiments in this thesis was the Cobra 38 suspension cell line (Cobra Biologics, Södertälje, Sweden). The line is a CHO-S transfectant stably producing an anti-human epidermal growth receptor 2 (anti-HER2) like IgG1 antibody. Cells were cultured in CD CHO medium (Thermo Fisher Scientific, Paisley, UK), supplemented with 8 mM L-glutamine, 1% hypoxanthine and thymidine supplement and 12.5 μg mL^{-1} puromycin selection marker (all from Thermo Fisher Scientific). The cells were sub-cultured every 3 to 4 days in vented Erlenmeyer shake flasks (Corning, Amsterdam, The Netherlands) maintained at 140 rpm, 37°C and 5% CO_2. Cells were typically seeded at 0.2×10^6 cells mL^{-1}. Routine sampling of cell growth and viability (Viable Cell Density (VCD)) was performed using a Vi-CELL XR cell viability analyser (Beckman Coulter, High Wycombe, UK) based on trypan blue exclusion.

3.1.2. Cell Cryopreservation and Revival

Master and working cell banks for the Cobra 38 clone were prepared and stored at −196°C (in liquid nitrogen) for the purposes of this project. Cells were harvested in mid-exponential phase and pelleted at 200×g. Cells were resuspended in freezing media: CD CHO media containing 10% v/v dimethyl sulfoxide (Sigma-Aldrich, Dorset, UK) at a concentration of 1×10^7 cells mL^{-1}. Aliquots of 1.5 mL were transferred to cryovials (Sigma-Aldrich) and frozen down in a rate-controlled manner in a Mr. Frosty container (Thermo Fisher Scientific) at −80°C. Vials were transferred into liquid nitrogen after 24 hours.

For experimentation purposes, a vial was thawed out from liquid nitrogen and sub-cultured for around 20 passages. Upon removal from −196°C, the vial was thawed at 37°C for 2 to 3 minutes. Vial contents were transferred to a tube containing 8.5 mL pre-warmed CD CHO. The mixture was centrifuged at 1000 rpm for 3 minutes. The pellet was re-suspended in 10 mL of CD CHO media

containing all supplements (as mentioned in **Section 3.1.1**). Cell density was measured and cells were accordingly sub-cultured into a 30 mL culture at 0.2×10^6 cells mL^{-1}.

3.2. Fed-Batch Culture

Fed-batch experimentation was performed over a 12 day time period in shaking Erlenmeyer flasks (E125). Cells were seeded at 0.2×10^6 cells mL^{-1} in a 25 mL culture volume and incubated at 140 rpm, 37°C and 5% CO_2. CHO CD EfficientFeed™B (Thermo Fisher Scientific) was added at 10% of the initial culture volume. The culture was fed on days 2, 4, 6 and 8.

3.3. High-Throughput Cell Culture

For HT experimentation, cells were cultivated in 96 deep well plates (square well, v-bottomed) (MasterBlock®; Greiner Bio-One, Gloucestershire, United Kingdom). Cells grown in these plates were incubated at 320 rpm (25 mm throw), 37°C, 5% CO_2 and 85% humidity (unless specified otherwise). The plates were covered with vented lids and secured using clamps (“System Duetz”; Enzyscreen B.V., Heemstede, Netherlands). Cells were seeded at 0.2×10^6 cells mL^{-1} with a seeding volume of 450 µL (unless specified otherwise). Cells were cultured for 5 days before culture attributes were recorded, unless otherwise stated.

3.4. Alternative Culture Formats

Cultures were generally performed in shake flasks or DWPs. For some experimentation (stated where so), culture methodology was varied. Some experiments was performed in TubeSpin® Bioreactor 50 (TPP, Trasadingen, Switzerland). The working volume was 10 mL and cultures were maintained at 170 rpm (50 mm throw), 37°C and 5% CO_2. Experimentation was also performed in 96 well shallow microplates (round well, flat-bottomed, clear)

(NUNC™; Thermo Fisher Scientific). Cultures were incubated in static, humidified conditions at 37°C and 5% CO_2. The working volume was 90 µL per well.

3.5. High-Throughput Measurement of Cell Growth Performance

3.5.1. Viable Cell Population: PrestoBlue Assay

The viable cell population in each well in a 96 DWP was measured using the PrestoBlue™ Cell Viability Reagent (Thermo Fisher Scientific). PrestoBlue™ is a cell permeable, blue, resazurin based solution that is virtually non-fluorescent. When added to wells containing viable cells, the solution is converted to a highly fluorescent, red coloured compound (known as resorufin), due to the reducing environment of a living cell. The fluorescence intensity is a direct indication of the viable cell population in the well.

45 µL of culture sample was taken from each well of a DWP and transferred to a 96 well clear flat-bottomed microplate (Nunc™, Thermo Fisher Scientific) containing 45 µL of cell culture media (1:1) dilution (unless otherwise stated). Typically, 3 media-only samples (blanks) were included on each assay plate to account for background fluorescence. PrestoBlue™ was diluted 1:1 in cell culture media to make a fresh stock of PrestoBlue mix. 20 µL of the PrestoBlue mix was added to each sample containing well. Plate mixing was performed using orbital shaking at 700 rpm for 20 seconds before being incubated in the dark at 37°C for 30 minutes. Post incubation, the fluorescence intensity of each well was measured using the PHERAstar *Plus* (BMG Labtech, Ortenberg, Germany) (excitation: 540 nm; emission: 590 nm). Raw values were converted to final normalised readings (expressed in relative fluorescence units (RFU)) using the equation below:

$$final\ fluorescence = \frac{sample\ fluorescence}{blank\ fluorescence} - 1$$

Equation 3.1

3.5.2. Viable Cell Population and Culture Viability: Iprasense Norma

In instances where absolute viable cell numbers and a measure of cell viability were required, the Iprasense Norma (HT version) (Iprasense, Clapiers, France) was employed. The instrument is based on lens-free microscopy (Allier et al., 2017; Allier et al., 2018). Samples are loaded onto slides (each containing 48 fluidic chambers) and a point source illuminates each sample. The cells diffract light to create distinct holograms and a sensor captures the hologram intensity of the sample from the selected field of view (usually set at 29.4 mm^2). A holographic reconstruction algorithm is then employed for phase and module retrieval of each cell. Dead and live cells have distinct holographic signatures (derived from the longitudinal and Z profiles) allowing for calculation of culture viability.

For total cell densities between 0.2 and 7×10^6 cells mL^{-1}, a slide thickness of 100 µm was employed with a loading volume of 10 µL. For total cell densities between 1.8 and 40×10^6 cells mL^{-1}, a slide thickness of 20 µm was employed with a loading volume of 3 µL. Hologram reconstruction for cell number and viability determination was performed using the HORUS software (Iprasense).

3.6. Recombinant Protein Quantification

IgG titer was measured using the Valita™TITER assay (Valitacell, Dublin, Ireland). The assay can quantify any Fc-containing recombinant protein molecule in solution. Sample containing the IgG of interest is loaded onto a well (containing a fluorescently labelled peptide) in the 96 well Valita™TITER plate. The interaction of the IgG molecule with the fluorescent probe alters the polarisation state of the well. The amount of IgG present in the sample is directly proportional to the polarisation of the well.

Supernatant containing the recombinant protein was diluted accordingly in cell culture medium (Valita™TITER assay range: 2.5-80 mg L^{-1}). 60 µL of Valita™MAb Buffer (Valitacell) was added to black, pre-coated antibody binding plates followed by the addition of 60 µL of diluted sample. After mixing with a

multichannel pipette, the plate was incubated in the dark for 30 minutes. Post incubation, the fluorescence polarisation of the plate was recorded using the PHERAstar *Plus* (BMG Labtech) (excitation: 485 nm; emission (parallel and perpendicular): 520 nm). The polarisation value (in mP) was calculated using the MARS data analysis software (BMG Labtech). Sample polarisation values were normalised against the media-only blank controls by subtraction. Standard curves (using IgG1 kappa standard (Sigma-Aldrich)) spanning the assay range were generated to interpolate recombinant protein concentration.

3.7. Equations to Quantify Cell Culture Parameters

3.7.1. Integral of Viable Cell Density

The integral of viable cell density (IVCD; 10^6 cell day mL^{-1} or RFU day) between 2 time points was calculated as follows:

$$IVCD = \left(\frac{N_1 + N_2}{2}\right) \times \Delta t$$

Equation 3.2

where N_1 and N_2 are the viable cell densities (10^6 cells mL^{-1} or RFU) at the first and second time points and t is the time (days) between the time points.

3.7.2. Specific Productivity

Specific productivity, also known as qP (pg $cell^{-1}$ day^{-1} or mg L^{-1} RFU^{-1} day^{-1}) was calculated using the following equation:

$$qP = \frac{T_2 - T_1}{\left(\frac{N_1 + N_2}{2}\right) \times \Delta t}$$

Equation 3.3

where T_1 and T_2 are the protein titer levels (mg L^{-1}) at the first and second time points. N_1 and N_2 are the viable cell densities (10^6 cells mL^{-1} or RFU) at the two time points. t is time (days).

3.8. Small Molecule Enhancer Preparation

The SME molecules employed in this study were ordered from commercial suppliers in powder or solubilised forms (Suppliers detailed in **Table 5.1**). Powder SMEs were solubilised in the solvent of choice (deionised water, dimethyl sulfoxide or ethanol; in accordance with powder manufacturer recommendations) to create stock solutions. Each stock in deionised water was filter sterilised using 0.2 µm filters (Corning). Stocks were stored at 4°C for short-term storage and at −20°C for long-term storage.

3.9. Flow Cytometry

3.9.1. Cell Cycle Analysis

Cells were fixed for cell cycle analysis using 4% paraformaldehyde (PFA; Alfa Aesar, Lancashire,UK).

1×10^6 cells were harvested from culture and spun at 200×g for 3 minutes. After medium removal, the cells were washed with warm 1×phosphate-buffered saline (PBS) (Thermo Fisher Scientific) and centrifuged again. The cells were then incubated in cold 4% PFA at a concentration of 1×10^7 cells mL^{-1} for 15 minutes at 4°C. After incubation, the PFA solution was removed. Cells were re-suspended in cold PBS and stored at 4°C for further analysis.

Flow cytometric analysis was carried out on the Attune Acoustic Focusing Cytometer (Thermo Fisher Scientific). FxCycle™ PI/RNase Staining Solution (Thermo Fisher Scientific) was employed for cell cycle analysis. The staining solution contains propidium iodide (PI), a nucleic acid binding fluorescent dye and RNase to ensure that the dye does not bind to RNA and only DNA content is measured. Measuring DNA content allows for differentiation of cells into various phases of the cell cycle (Gap 1 (G1), Synthesis (S) and Gap 2(G2)).

The cells were centrifuged to remove the PBS storage solution. The cell pellet was re-suspended in 0.5 mL of FxCycle™ PI/RNase Staining Solution. The cells were incubated for ~30 minutes in the dark. Samples were analysed on

the flow cytometer using a 488 nm excitation laser and the emitted fluorescence captured using a 574/26 bandpass filter (BL2). At least 10,000 cell events were recorded. Data was analysed using the Attune Cytometric Software (version 2) (Thermo Fisher Scientific).

3.9.2. Apoptosis Analysis

The apoptotic state of the cell (early apoptosis, dead) was assessed using the PE Annexin V Apoptosis Detection Kit I (BD Biosciences, Berkshire, UK) according to the manufacturer's instructions. The apoptosis indicator Annexin V is supplied as a complex with phycoerythrin (PE), a fluorophore.

An aliquot of 1×10^6 total cells was taken from culture and pelleted at 200×g for 3 minutes. Cells were washed twice in cold PBS. Cells were then pelleted and re-suspended in 1×binding buffer (as provided in the kit) to a concentration of 1×10^6 cells mL^{-1}. 100 µL of the solution was transferred to a new eppendorf and 5 µL each of Annexin V (apoptosis indicator) and 7-amino-actinomycin D (7-AAD) (a dead cell indicator) was added to the solution. The cells were gently vortexed and incubated for ~15 minutes in the dark. 400 µL of 1×binding buffer was added prior to analysis on the Attune Acoustic Focusing Cytometer (Thermo Fisher Scientific). ~10,00 total events were analysed for each sample. Unstained samples and samples containing either 7AAD or Annexin V were used as controls for compensation. Samples were excited by the 488 nm laser and emitted fluorescence captured using a 574/26 bandpass filter (BL2: PE) and a 690/50 bandpass filter (BL3: 7-AAD). Data was analysed using the Attune Cytometric Software (version 2) (Thermo Fisher Scientific).

3.10. Measurement of Cellular mRNA

Real-time quantitative PCR (qPCR) was employed to quantify mRNA levels of the production antibody heavy and light chain.

3.10.1. RNA Extraction

Total RNA was extracted from cells using the RNeasy® Mini Kit (Qiagen, Crawley, UK) according to the manufacturer's instructions. 1×10^6 cells were harvested from culture. The cells were disrupted using Buffer RLT and homogenised using a QIAshredder spin column (Qiagen). Samples were then applied to RNeasy spin columns. Total RNA bound to the membrane and contaminants were washed away. RNA was eluted in nuclease free water (Qiagen). Purity was confirmed using 260:230 nm and 260:280 nm absorbance ratio measurements on the NanoDrop spectrophotometer (Thermo Fisher Scientific). RNA samples were stored at −20°C until further use.

3.10.2. Reverse Transcription

800 ng of extracted RNA was reverse transcribed into cDNA using the QuantiTect® Reverse Transcription kit (Qiagen) according to the manufacturer's instructions. The procedure comprised 2 main steps: Elimination of genomic DNA and cDNA synthesis. Quantiscript Reverse Transcriptase was used to convert RNA into cDNA. For each RNA sample, an extra reverse transcription reaction was performed in the absence of reverse transcriptase. These served as negative controls for qPCR reactions, to establish the presence of genomic DNA post the elimination step.

3.10.3. Real-Time Quantitative PCR (qPCR)

cDNA was diluted 1 in 1000 in nuclease free water (Qiagen) before performing qPCR reactions on a 7500 Fast Real-Time PCR system (Applied Biosystems, Cheshire, UK). Reaction mixtures (25 µL) contained the following components: 12.5 µL of 2×QuantiFast SYBR Green PCR Master Mix, 2.5 µL primer mix (final concentration of 200 nM per primer), 2 µL cDNA and 8 µL of nuclease free water. These mixtures were set up in MicroAmp Fast Optical 96-well plates (Applied Biosystems). The thermal cycle conditions were as follows: 50°C for 2

minutes 95°C for 15 minutes, 40 cycles at 94°C for 15 seconds and 60°C for 60 seconds. Each plate contained negative controls as follows: reactions containing no template and reactions containing product in the absence of reverse transcriptase (as mentioned in **Section 3.10.2**). Each sample was run in triplicate and mean cycle threshold (Ct) values were recorded.

Primers for cDNA corresponding to the recombinant antibody heavy and light chain mRNA were employed. Internal reference controls used were: Mmadhc and Fkbp1a (Brown et al., 2018). All primer sequences are shown in **Table 3.1**. Primer efficiencies were tested by melting curve analysis using a 10-fold serial dilution standard curve of sample cDNA (performed from 60°C-95°C post amplification steps).

Table 3.1 Primer sequences for genes employed in the qPCR study.

Gene	Primer sequence
IgG1 Light chain	CAGCAAGGACAGCACCTACA GACTTCGCAGGCGTAGACTT
IgG1 Heavy chain	ACCAAGAACCAGGTCAGCCT TGAGAAGACGTTCCCCTGCT
Fkbp1a	CTCTCGGGACAGAAACAAGC GACCTACACTCATCTGGGCTAC
Mmadhc	TGTCACCTCAATGGGACTGC CAGGTGCATCACTACTCTGAAAC

Efficiency was calculated using:

$$E = \left(-1 + 10^{\left(\frac{-1}{slope}\right)}\right) \times 100$$

Equation 3.4

All primer efficiencies were between 98 to 101% (see **Appendix A**).

Heavy and light chain mRNA levels were quantified using the $2^{-\Delta\Delta\ Ct}$ method (Livak and Schmittgen, 2001).

3.11. Mass Spectrometry: Histone Modification Analysis

10×10^6 cells were pelleted by centrifugation at 200×g for 5 minutes. Pellets were stored at −20°C till further analysis. Histones were extracted from the cells as described below and fragmented into peptides that were analysed by mass spectrometry, different charge states were analysed and histone modifications identified. Acetylation and methylation were the identified modifications and relative abundance was calculated for each unique modification in the peptide analysed.

Histone preparation, mass spectrometry and data analysis was performed by PhD student Eleanor Hanson at The University of Sheffield.

Histones were extracted using acid extraction detailed in Shechter et al. (2007). The extracted histones were washed twice in ice cold acetone and dissolved in 100 µL HPLC grade water. Chemical derivatisation of histone proteins was performed with propionic anhydride as detailed in Garcia et al. (2007). Propionylation was performed twice. Trypsin digestion was performed on the derivatised histones. These methods are explained in more detail in **Appendix A**.

Propionylated histone samples were re-suspended in 30 µL of 0.1% trifluoroacetic acid (TFA). HyperSep™ Hypercarb tips (Thermo Fisher Scientific) were primed for use with five 20 µL washes using elution buffer (90% acetonitrile (ACN), 0.1% TFA) followed by 5×20 µL washes using binding buffer (0.1%TFA). Peptides were bound on the tips by ~100 aspirations in volumes of 20 µL. The tip was washed twice with 20 µL of binding buffer. The peptides were eluted into fresh eppendorfs using 200 µL of elution buffer in increments of 20 µL. 80 µL of binding buffer was added to the tube prior to drying down using the SpeedVac (Thermo Fisher Scientific).

Samples were re-suspended in 0.1% TFA prior to being run on the QE-HF Orbitrap mass spectrometer (Thermo Fisher Scientific) coupled to an UltiMate 3000 HPLC (Dionex; Thermo Fisher Scientific). A PepMap300 c18 trapping column was used along with a 50 cm×75 um EASY-Spray PepMap c18 analytical column (both Thermo Fisher Scientific). Flow rate was set at 300

nL/min and column temperature maintained at 40°C. Buffers employed were as follows:

Buffer A: 0.1% Formic acid, 3% ACN

Buffer B: 0.1% Formic acid, 80% ACN

Loading buffer: 0.1% TFA, 3% ACN

Samples were injected into the trapping column and washed with Buffer A for a minute. This was followed by elution onto the analytical column, with Buffer B applied at a gradient rising from 3% to 25% over 55 minutes and then from 25% to 60% over 26 minutes (see **Appendix A**).

Data was collected using Data Independent Acquisation (DIA). MS1 and MS2 resolution detailed in **Appendix A**. Sample data was analysed using Skyline (MacLean et al., 2010). A spectral library using data dependent analysis of CHO histones *(created by Eleanor Hanson)* was employed. Modifications to the N-terminus were set up as separate modifications. Histones H3 and H4 were analysed with each modified peptide entered as a separate entity into Skyline. MS2 data was employed to manually identify the correct peak. The area under the peak was extracted from the MS1 scan using the MStats package. Relative abundance was calculated as follows:

$$relative\ abundance = \frac{area\ under\ peak\ intensity\ of\ proteoform}{sum\ of\ all\ proteoform\ intensities\ for\ the\ peptide}$$

Equation 3.5

where a proteoform is a unique modified version of the peptide.

3.12. Glycoform Analytics

3.12.1. Protein A Purification of IgG1

On day 6 of batch culture, all available culture volume (30-50 mL) was centrifuged at 200×g, supernatant collected and stored at −80°C till further use. HiTrap™ MabSelect SuRe™ 1 mL protein A prepacked columns (GE

Healthcare Life Sciences, Buckinghamshire, UK) were utilised for antibody purification. These columns have high specificity for the Fc region of IgG molecules and can bind up to 30 mg of human IgG mL^{-1} of medium (GE Healthcare, 2014). Buffers were prepared as follows:

Binding buffer: 20 mM sodium phosphate, 0.15 M NaCl, pH 7.2

Elution buffer: 0.1 M sodium citrate, pH 3.5

Neutralisation buffer: 1 M Tris-HCl, pH 9.0 (~250 µL per 1 mL fraction)

Cleaning-in-place wash buffer: 0.5 M NaOH

Supernatant was filtered through a 0.2 µm filter (Corning) before application to the column. Sample and buffers were applied to the column using a 50 mL syringe (BD Biosciences) driven by a syringe driver at flow rates in accordance with manufacturer instructions. Eluted antibody was collected in fractions of 5 for each condition. Cleaning-in-place was performed immediately after elution to prepare the column for the next purification.

Purity (A260/230: 0.5-0.6) and concentration of each fraction of the eluted antibody was determined using the NanoDrop spectrophotometer (Extinction coefficient 15.00) (Thermo Fisher Scientific). Fractions were collated accordingly. Samples were run on an SDS-PAGE gel to confirm presence of IgG molecule and any degradation.

3.12.2. SDS-PAGE

SDS-PAGE was run under reducing and non-reducing conditions to confirm presence of IgG antibody after purification and to detect any degradation. Pre-cast NuPAGE™ 4-12% Bis-Tris gels (Thermo Fisher Scientific) were employed. 2 µg of protein was prepared for each well along 2.5 µL of NuPAGE™ LDS Sample Buffer (4×), 1 µL NuPAGE™ Reducing Agent (10×) (both Thermo Fisher Scientific), and deionised water to make up a total of 10 µL. The reducing agent was omitted for the non-reducing condition. Reducing sample mixes were heated at 70°C for 10 minutes.

Samples were loaded appropriately on the pre-cast gels contained in a XCell SureLock™ Mini-Cell gel running tank (Thermo Fisher Scientific). A protein standard (Chameleon™ Duo, LI-COR UK, Cambridge, UK) was included on each gel. 1×NuPAGE™ MOPS SDS running buffer (Thermo Fisher Scientific) was added to the chamber and the gel run for 50 minutes at 200 V. The gel was removed from the cassette, washed and stained using Coomassie Blue staining (Thermo Fisher Scientific).

3.12.3. *N*-Glycan Analytics

Purified protein samples were provided to the NIBRT Glycoscience group in Dublin for glycosylation analysis. *Analysis was performed by Dr Roisin O'Flaherty and Dr Karen P. Coss.* 2-aminobenzamide (2-AB) derivatised *N*-Glycans were analysed by Ultra-High Performance Liquid Chromatography (UPLC).

Briefly, glycoprotein denaturation and glycan release was performed as follows: 55 µL of denaturation buffer (100 mM ammonium bicarbonate (ABC), 12 mM dithiothreitol (DTT)) was added to each sample containing well (5 µL) in a 96 well v bottom microplate (Greiner Bio-One). The mix was incubated at 65°C, 700 rpm for 30 minutes. After cooling, 10 µL of 120 mM iodoacetamide solution was added, and the mix was incubated at room temperature, 700 rpm for 30 minutes. 10 µL of trypsin (40,000 U/mL) solution was added and the mix incubated at 37°C, 700 rpm, 120 minutes. Next, temperature was increased to 105°C for 10 minutes. The plate was then cooled to room temperature and 10 µL PNGase F (New England Biolabs® (0.13 mU in 1 M ABC, pH 8.0)) added to each well and the plate incubated at 40°C, 700 rpm for 120 minutes. Hydrazide-assisted glycan clean-up and glycan labelling and solid phase extraction was performed as previously described (Stöckmann et al., 2015). 2-AB derivatised *N*-glycans were separated by UPLC with fluorescence detection on a Waters Acquity UPLC H-Class instrument (Waters, Milford, MA, USA). The hydrophilic interaction liquid chromatography (HILIC) separations were performed using a Waters Ethylene Bridged Hybrid Glycan column (Waters), with 50 mM ammonium formate, pH 4.4, as solvent A and ACN as solvent B. Gradient: 70-

53% ACN at 0.56 mL/min in 30 min. Samples in 70% v/v ACN were injected (19 µL) at 40°C. Fluorescence excitation: 330 nm; emission: 420 nm. A dextran ladder described previously (Royle et al., 2008) was used to assign glucose unit values based on retention times.

3.13. Design of Experiments Methodology

Experiments to test for interactions between SMEs were designed and analysed using the Design-Expert®10 modelling software (Stat-Ease, Minneapolis, USA). Full factorial designs were employed for all combinatorial experimentation. Each chemical enhancer (termed "factor") was coded at 2 levels:−1 and +1. The −1 level was set at 0 i.e. no addition of the factor. +1 level concentrations were based on previous experimentation. Experimental runs were randomised. Each design was replicated thrice to improve model precision.

After experimentation, the culture attribute results (IVCD, Titer and qP) were entered back into Design-Expert®10 for model creation. The following steps summarise the analytical approach undertaken by Design-Expert®10 to model the combinatorial data:

1. For each factor and combination, an effect was calculated for a culture attribute as follows:

$$\frac{\Sigma \mathrm{Y}_{+}}{n_{+}} - \frac{\Sigma \mathrm{Y}_{-}}{n_{-}}$$

Equation 3.6

   Where Y is the attribute output and n is the number of runs at a particular level.

2. The effects were plotted on a half normal plot. A line was fit through the residual points. Any points that deviated from this line were selected as model terms.

3. An analysis of variance (ANOVA) table was created to provide results on model and factor/combination significance. Lack of fit was tested for the model.

4. Normality of residuals was tested to validate statistical assumptions and test for outliers. Any outliers were removed and power transforms conducted where necessary.
5. A predictive linear equation model was created based on the effects of the significant singular and combinatorial factors. Non-significant singular parent factors of significant combinations were included to maintain hierarchy.
6. Interesting interactions were investigated based on interaction plots.

Chapter 4

High-Throughput Platform Development for SME Screening

ABSTRACT: In the present competitive biopharmaceutical arena, high-throughput technologies have gained prominence. To rapidly assess multiple small molecule enhancers for CHO cell bioprocess, a high-throughput culturing and analytical platform was crucial. We tested and optimised high-throughput cell growth, viability and product titer measurement technologies. To accurately determine viable cell growth, we employed the PrestoBlue assay. The assay, based on the metabolic activity of a living cell, had a large dynamic counting range (0.22 to 7×10^6 cells mL^{-1}) and compared favourably with the Vi-CELL XR. Additionally, we investigated and calibrated the use of the Iprasense Norma for high-throughput cell counting and viability determination. The Norma consistently yielded lower cell densities than the Vi-CELL XR, prompting the inclusion of a correction factor for comparative analysis. The Valita™TITER assay was employed for product titer quantification; the dynamic range was found to be 1.25 to 80 mg L^{-1}. To develop microscale culturing methodologies, we explored the use of shaking deep well plates using the Duetz platform, which allowed plates to be clamped in place with covers that minimised evaporation. Interestingly, plate well type and material had an impact upon viable cell growth. Only 1 plate type was able to support high viable cell growth. Speeds of 320 rpm with a shaking diameter of 25 mm were deemed the best conditions for cell growth and productivity. Further optimisation revealed the optimum seeding density and fill volume as 0.2×10^6 cells mL^{-1} and 450 µL respectively. Cell growth and protein production performance was highly similar to that of shake flasks at the aforementioned conditions, with cultures lasting 7 days. Lastly, we evaluated the best timing of addition for qP enhancers. Some well-known qP enhancers were utilised in the study. Day 3 addition of the chemical generally yielded higher increases in product yield with titers reaching up to 3 fold higher than the control cultures at the day 5 analysis point. The culturing and analytical methodologies amalgamated to form an easy-to-use screening platform that could be utilised to quickly test multiple culture conditions concurrently.

Chapter Acknowledgements

The development of the HT culturing platform was undertaken in collaboration with Dr. Joe Cartwright and Dr. Alejandro Fernandez-Martell at The University of Sheffield.

4.1. Introduction

Before embarking on the development of a HT media additive screening tool, it was imperative to design a standardised testing platform. Shake flask experimentation is laborious in nature, wherein large numbers of parallelised flask experimentation are tedious (Amanullah et al., 2010). Thus, the shift towards HT technologies to accelerate biopharmaceutical manufacturing processes is understandable. The biopharmaceutical industry has a large repertoire of HT screening technologies, most of which are employed in cell line development, clone selection and process development (Hansen et al., 2015; Rouiller et al., 2013; Rouiller et al., 2016). HT miniaturised culturing technologies like the ambr 15 (Sartorius Stedium biotech,) and Biolector (m2p-labs GmbH, 2018) present added benefits of sophisticated in-line monitoring of process parameters like pH and dissolved oxygen for multiple cultures (Long et al., 2014) (as discussed in **Section 1.6**). However, the capital cost incurred by the utilisation of these technologies is high, resulting in low adoption rates in small and medium sized enterprises. Additionally, these technologies (especially the ambr 15) lack flexibility towards the incorporation of closed box media additive screening technologies that the commercial product is envisioned to be. Shallow microplate and deep well plate culturing technologies present low cost, facile technologies for miniaturised parallel HT experimentation (Long et al., 2014). The ability of these technologies to be adapted for shaking culturing allows for a suitable miniaturisation of shake flasks and stirred tank bioreactors. The “System Duetz”, initially developed for microbial culturing, has been readily adapted for CHO cell culturing and allows for multi-well plate culturing at high speeds that promote efficient culture mixing and gas exchange (Barrett et al., 2010). The Duetz system is based on enabling shaken plate culture modes with an emphasis on closure systems to

prevent evaporation and contamination (detailed explanation in **Section 4.3.5**) (Chaturvedi et al., 2014; Duetz, 2007). The platform is cost-effective, however, does not offer online monitoring as the other systems mentioned above (Long et al., 2014). The platform is readily adaptable to different plate types, culture volumes and shaking speeds. Traditional media and feed optimisation require intense component and mixture screening (Chaturvedi et al., 2014). Media optimisation techniques such as media blending, along with bioactive small molecule screens have employed DWP culturing along with "System Duetz" in previous industry studies (Brühlmann et al., 2017b; Rouiller et al., 2013). This indicates the successful application of this technology in industry. DOE technologies allow for testing for component interactions and can be readily tested in a multi-well plate based screening platform as evidenced in previous literature (Brühlmann et al., 2017b).

We have to consider the potential commercialisation of the HT media additive screening platform that we aim to develop. It would not be ideal to develop a product that would have rigid requirements (such as having the sophisticated ambr 15 platform with in-line monitoring of pH). We would want a platform that can be easily adapted to the company's already available culturing technologies. Microplate and DWP culturing present simple, standard solutions that would enable easy adoption into the available incubator technologies in industry. Thus, these technologies were mainly focused upon for the development of the media additive screening tool. While literature is available on culturing methodologies using microplates and shaken DWP cultures (Allen et al., 2008; Brühlmann et al., 2017b; Hansen et al., 2015; Rouiller et al., 2013), a multitude of factors influence the culturing efficacy in this miniaturised platform (Duetz, 2007; Duetz and Witholt, 2004). Thus, our studies focused upon optimisation of the multi-well plate culturing modalities.

Another component of the HT screening platform would be the implementation of HT analytics. Growth and production titer were focused upon as the most crucial attributes that were required to evaluate SME efficacy. This chapter delves into the evaluation of available assays and instrumentation for the determination of cell growth, viability and titer.

Overall, this chapter describes the experimentation involved in the development of the HT screening platform. Two aspects of the platform are focused upon: HT culturing and HT analytics for growth and titer. Additional analytics (such as product quality) or implementation of fed-batch culturing at small scale can be thought of as future prospects to consider to further enhance the HT platform described in this chapter.

4.2. Experimental Approach

A systematic approach was adopted for the development of the HT screening platform. The ideal HT culturing platform would be one that (i) contained multiple parallel culturing (for example 96 wells) (ii) followed the same growth and production profile as a higher scale platform (for example shake flasks), (iii) was able to support long term cultures (for example a 7 to 8 day batch culture), (iv) was flexible (for example addition of feeds for fed-batch production culturing) and (v) had ample culture volume to allow for multiple analytics from the same culture well. All experimentation was performed using the Cobra 38 CHO cell line. Firstly, the most simplistic HT platform readily available in the laboratory was evaluated: static microplate culturing. Analysis of that platform revealed it to be non-ideal for our purposes. Due to this, a survey of potential alternative culturing platforms was performed and 96 deep well plate culturing was evaluated as a HT platform for SME screening. Initial experimental evaluation was followed by optimisation and characterisation. In parallel, HT analytical technologies were evaluated for the culture attributes of interest: cell growth, viability and production titer. Herein, the criteria for selecting an ideal analytical assay would be based on (i) cost, (ii) throughput, (iii) assay time and (iv) ease of use. After the finalisation of the culturing and analytical platforms, different days of addition were evaluated to understand the impact of timing of addition of the SME on culture performance. Finally, chemical solubilisation vehicles were tested to account for and minimise any impact on cell culture performance by the solubilisation vehicle controls.

4.3. Results

4.3.1. Evaluation of Cell Growth Measurement Technologies

The ability to screen multiple SMEs in parallel required high-throughput analytics. Cell growth analytics formed a vital part of our HT platform, since it is important to determine cytotoxicity, growth suppression or growth improvement as a result of the SME addition. There are multiple fluorescence multi-well plate based assays commercially available to determine viable cell populations. We chose to employ the PrestoBlue assay (using the PrestoBlue™ Cell Viability Reagent (Thermo Fisher Scientific)) primarily due to its ease of use. Incubation times are quicker compared to similar cell viability assays (minimum 10 minutes vs. minimum 1 hour (alamarBlue) (Thermo Fisher Scientific,). It is highly sensitive in comparison to other metabolic cell viability assays, such as alamarBlue and MTT assay (Thermo Fisher Scientific, 2012), and can detect as low as 10 viable mammalian cells per well.

Since a high variation in viable cell number was expected in one experimental setup, i.e. high control cell numbers vs. extremely low viable cell population due to small molecule toxicity vs. SMEs that improve cell growth, it was vital that our growth performance assessment methodology was sensitive across a larger cell concentration range. We tested a standard curve of cell concentrations ranging from 0.22 to 28×10^6 cells mL^{-1}. Each concentration in the dilution series was double that of the previous one. The cell concentrations were also measured on the Vi-CELL XR (Beckman Coulter) (based on trypan blue exclusion), which served as the cell counting standard in this case. The standard curve is displayed in **Figure 4.1**.

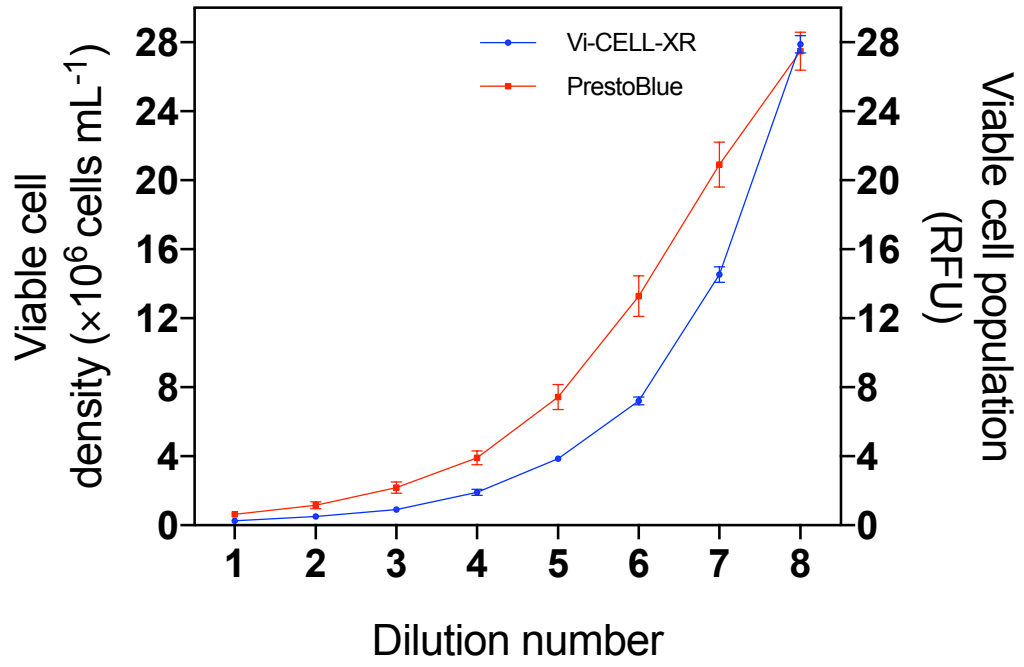

Figure 4.1 Standard curve profile of increasing cell populations using PrestoBlue assay in comparison to Vi-CELL XR. A viable cell concentration standard curve was created from 0.22 to 28×10^6 cells mL^{-1}. 90 µL of sample for each cell concentration was transferred to 3 wells on a 96 well microplate. 20 µL of the PrestoBlue mix (PrestoBlue™ reagent to CD CHO media 1:1) was added to each well and the plate was incubated for 30 minutes at 37°C, away from light. 3 control wells containing CD CHO media were also included to account for background fluorescence. The sample fluorescence values were normalised to the media-only fluorescence. Samples were also run on the Vi-CELL XR for comparative purposes. PrestoBlue data is plotted on the right y-axis while the Vi-CELL XR data is plotted on the left y-axis. Presto blue data is represented as the mean and standard error of three experimental replicates, each with three technical repeats. The Vi-CELL data is represented as the mean and standard error of three experimental replicates.

The PrestoBlue readings displayed consistent doubling in fluorescence values until the 7×10^6 cells mL^{-1} (Concentration 6). Post that cell concentration, there was saturation in fluorescence values observed. Conversely, the Vi-CELL XR displayed accurate doubling in cell concentration across all points tested. It would be possible to curb any inaccuracies in PrestoBlue readings above 7×10^6 cells mL^{-1} using 3 possible actions: lowering incubation time, adding more PrestoBlue reagent or diluting the cells to be within the linear dynamic range of the PrestoBlue assay. Application of the first action point could lead to ambiguity and might require further optimisation of the ideal incubation time. It

could also translate to lower sensitivity at the lower end of the cell concentration curve due to the lower incubation time. Application of the second action point would result in an increased cost and would require further optimisation. Thus, for simplicity, the third approach was employed where necessary.

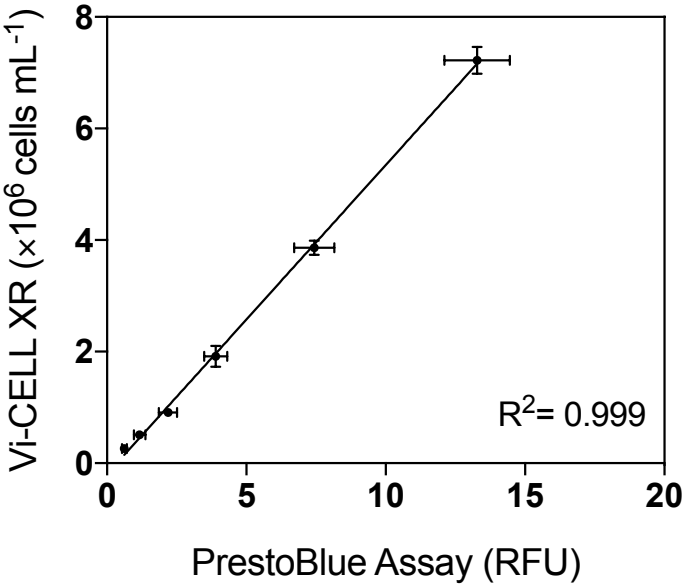

Figure 4.2 Correlation of PrestoBlue Assay and Vi-CELL XR. The fluorescence values within the accurate dynamic range of the PrestoBlue assay as tested in **Figure 4.1** (between 0.22 and 7×10^6 cells mL^{-1}) were plotted against the values recorded on the Vi-CELL XR. Linear regression line was fitted and R^2 calculated. Mean values plotted for both measurement techniques with error bars representing standard error of three experimental replicates.

From **Figure 4.2**, it was evident that within its accurate range, the PrestoBlue assay yielded a strong linear correlation with the Vi-CELL XR. The PrestoBlue assay is based on the **metabolic activity of a living cell**. The active reagent is a cell permeant, non-fluorescent dye, resazurin, which when comes in contact with the reducing environment of a living cell is converted to resorufin, a highly fluorescent compound that is red in colour (Thermo Fisher Scientific, 2012). The conversion to the reduced form is initiated mainly by mitochondrial enzyme activity, with resazurin accepting electrons from NADH, NAPDH and FADH (Xu et al., 2015). Thus, only viable cell population is measured that is directly proportional to the fluorescence intensity of the sample. In contrast, the Vi-CELL XR is based on the membrane integrity of cells. Here, the active

ingredient, trypan blue can only enter cells with compromised membranes, i.e. dead cells. Thus, it is based on the **exclusion of trypan blue** and directly labels dead cells. Images are captured using a camera and cells that have visibly not taken up the dye are classed as living. It is evident that there is a huge mechanistic contrast between the two techniques. However, they were highly comparable. With the cost of assaying one well being 3.5 pence (Thermo Fisher Scientific,), PrestoBlue was selected as the main assay for growth performance assessment based on low cost, high sensitivity and quick turnaround.

The major limitation of PrestoBlue is the inability to quantify viability percentage of the cell population tested. It was deemed that viability determination was not required for concentrations of chemicals that were ineffective in enhancing cell growth or titer. However, it was vital to determine if, at the effective dose (one that produced an improvement in growth or titer), there was detriment to viability. For small sample sizes, the Vi-CELL XR was employed, however, for a large set of samples, the Iprasense Norma (Iprasense) was utilised. The Norma works on the principle of **light diffraction**. Viable and dead cells have different light diffraction profiles. Samples are loaded on a flat slide with 48 chambers for increased throughput. Automated analysis is performed by illuminating each chamber, with a sensor recording the hologram intensity. A hologram reconstruction algorithm is employed to retrieve and reconstruct the hologram profile of each cell, which is then marked as live or dead based on the similarity to the standard live and dead profiles. This allows for the determination of viable cell densities, total cell densities and percentage viability per sample.

A cost (56 pence per sample) and resource restraint prevented the Norma from being adopted for every screening experiment. However, it still served as a useful tool for selected experiments wherein absolute cell numbers were required and where viability of large numbers of cultures needed to be determined. As with the PrestoBlue assay, the cell number determination accuracy was compared with the Vi-CELL XR. Two slide thickness modes are available, 100 µm thickness slides that are more ideal for low cell numbers and the 20 µm thickness slides that are suited for higher cell numbers.

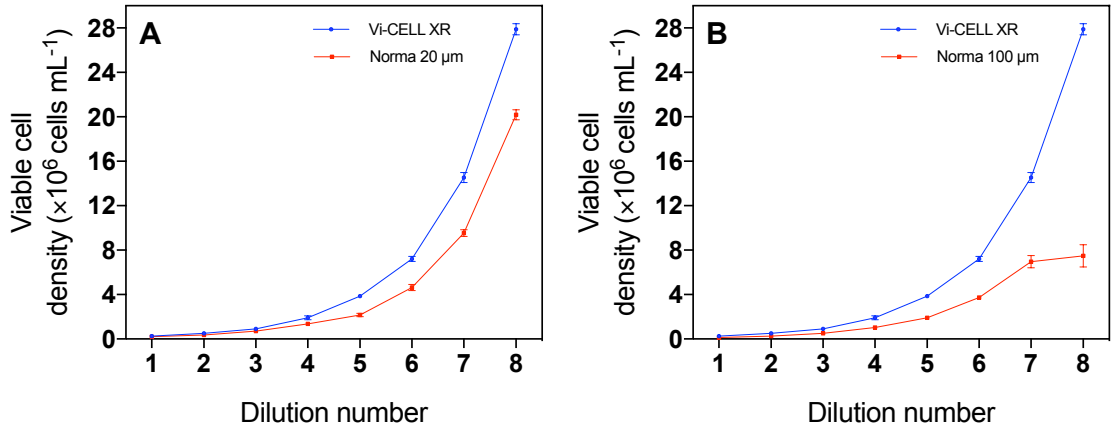

Figure 4.3 Standard curve profile for the Iprasense Norma in comparison to the Vi-CELL XR. A standard curve ranging from 0.22 to 28×10^6 cells mL^{-1} (99% viability on the Vi-CELL XR) was tested on **(A)** 20 µm and **(B)** 100 µm slide thickness. Each concentration in the series is double the previous one. For the 20 µm thickness slides, 3 µL of sample was loaded into each chamber. For the 100 µm thickness slides, 10 µL was loaded into each chamber. The slides were placed in the Norma reader and cell concentration and viability was computed using the HORUS software. The data for Norma readings is represented by the mean and standard error of three experimental replicates, each with three technical repeats. The Vi-CELL XR data is the mean and standard error of three experimental replicates.

Figure 4.3 summarised the cell counting performance on both the slide thickness modes on the Norma and compared performance against the Vi-CELL XR. It was evident that the Norma typically counted less cells in comparison to the Vi-CELL XR, irrespective of the plate thickness used. The 2 different plate thickness modes are suggested for accurate reading across a large concentration range. The 20 µm thickness represents a slide chamber that is comparatively thinner than its counterpart and can only hold a 3 µL volume. A higher cell density can be loaded using these slides. Our data revealed that while the curve was linear and showed doubling for each concentration point across the range tested, viability readings were heavily skewed towards a total lower viability at the lower concentration range (dilutions 1, 2 and 3) (data not attached). This indicated that the extremely low sample volume had a negative impact on the accurate differentiation of live and dead diffraction profiles at low cell concentrations. In addition, there was extremely poor distinction at the lowest 2 standard curve points. Thus, it was decided that

the accurate counting range for the 20 µm slides was from around 1.8×10^6 cells mL^{-1} (Concentration 4) onwards. A linear regression line was drawn for this range and an equation generated to show the linear relationship with the Vi-CELL XR readings (**Figure 4.4A**). Like with PrestoBlue, there was a good linear correlation with the Vi-CELL XR, however, the values generated by the Norma were consistently lower. Interestingly, the size bounds for classification of a cell were highly similar. To compare readings across both methods, a correction factor of ×1.4 was taken into account for the Norma 20 µm slides (**Figure 4.4A**). The correction factor was stable across the concentration range and confirmed with experimentation performed by other laboratory group personnel.

The 100 µm slides have a comparatively larger slide chamber and thus can hold a larger sample volume of 10 µL. This allows for a lower cell concentration to be determined accurately. This was evident from **Figure 4.3B**, wherein an accurate doubling in concentration was observed up to 7×10^6 cells mL^{-1} (Concentration 6). Post this concentration, a plateauing of cell number and variable viability readings were observed. Like with the 20 µm slides, a linear regression plot was constructed to quantify the linear relationship with the Vi-CELL XR (**Figure 4.4B)**.

It was observed that for the 100 µm slides, the Vi-CELL XR recorded double the cell density. This was consistent across the concentrations tested that fell within the accurate counting range. Thus, for any comparative analysis between the two measurement techniques, a correction factor of ×2 was adopted for the 100 µm slides.

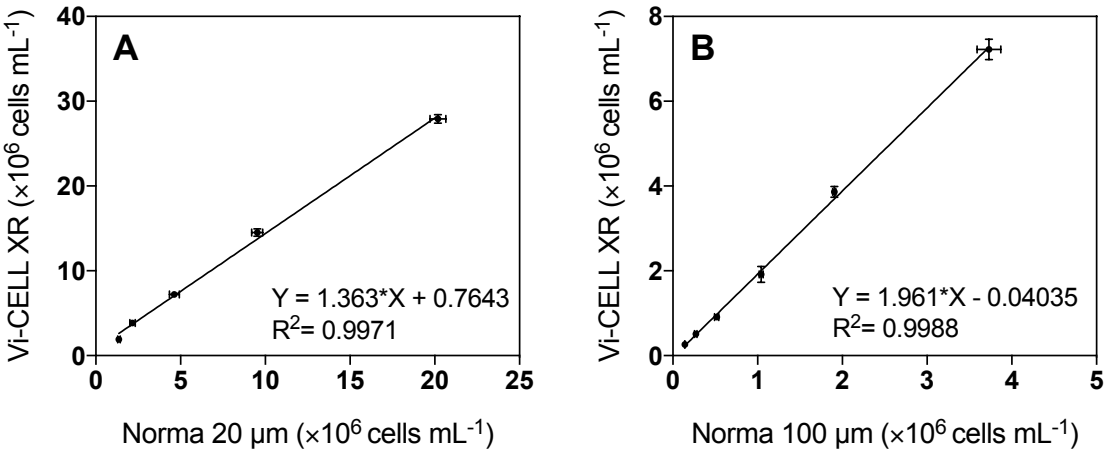

Figure 4.4 Linear regression analysis to investigate Norma and Vi-CELL XR count correlation. (A) represents the 20 µm thickness slides that had an accurate counting range from 1.8×10^6 cells mL^{-1} onwards. **(B)** shows the 100 µm thickness slides that had an accurate reading range from 0.22 to 7×10^6 cells mL^{-1}. The viable cell densities recorded on the Norma (x-axis) were plotted against the Vi-CELL XR value (y-axis). Linear regression was fitted and R^2 calculated (>0.99 in both cases). Mean values plotted for both measurement techniques with error bars representing standard error of three experimental replicates.

4.3.2. Evaluation Of Cell Viability Measurement Technologies

As shown in the previous section, the Iprasense Norma can be employed to determine viable cell numbers in a high-throughput manner. While the PrestoBlue assay is available for viable cell population determination, its major drawback stems from its inability to evaluate culture viability as a whole. The Norma, though considerably more expensive than the PrestoBlue assay (56 pence vs. 3.5 pence), overcomes this drawback. Thus, in cases where viability needed determination, the Norma was employed.

A series of culture viabilities were trialled in both the slide sizes available and compared against the Vi-CELL XR (**Figure 4.5**). Both slides showed a strong linear correlation with the Vi-CELL XR. The trends followed were the same across all the methodologies tested, with each technique able to distinguish between high and low viable cultures. The 100 µm thickness slides (**Figure 4.5B**) were relatively more sensitive at detecting extremely low viabilities than

the 20 µm slides. Overall, both the slides were competent in differentiating between high and low viable culture populations.

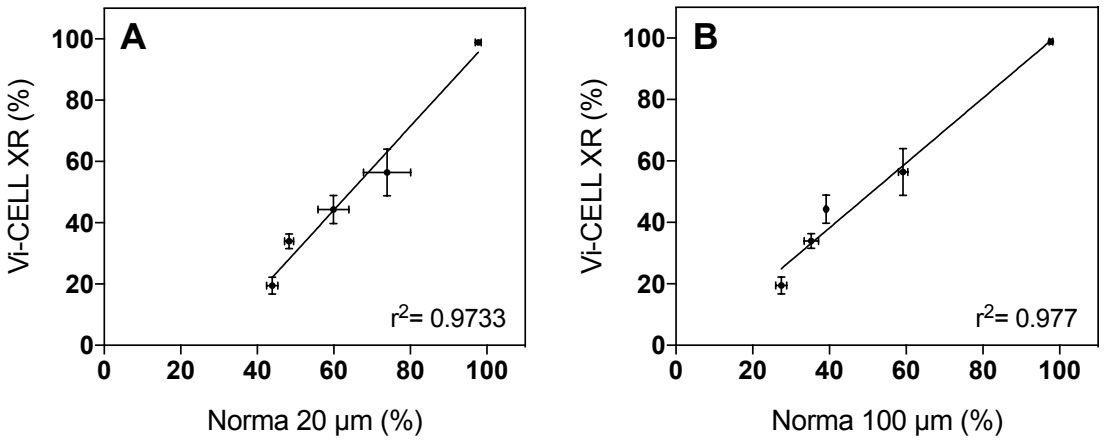

Figure 4.5 Viability comparison of the Iprasense Norma and the Vi-CELL XR. A series of differing viability samples beginning at about 100% viability and going down to 20% (according to the Vi-CELL XR) were tested on the 20 and 100 µm slides on the Iprasense Norma. 3 µL of sample was added to the 20 µm thickness slides. 10 µL of sample was added to the 100 µm thickness slides. Viability was determined based on the light diffraction profile for each cell. Readings were taken on the Vi-CELL XR for comparison purposes. Viability on the Vi-CELL XR was determined using the trypan blue exclusion method. The data is represented as the mean and standard error of three experimental replicates.

4.3.3. Evaluation of Titer Measurement Technologies

To enable screening of large numbers of singular and combinatorial SME deployment strategies for increased titer, HT methodologies for antibody titer measurement were necessary. We adopted the Valita™TITER assay (Valitacell) to quantify the antibody titer levels in our screens. The assay presents a quick, HT and cost-effective measuring methodology that spans a large dynamic range (1.25 to 80 mg L^{-1}). Currently available titer measurement technologies are either low-throughput (Protein A high-performance liquid chromatography (HPLC)), have narrow dynamic ranges (Enzyme-linked immunosorbent assay (ELISAs)) or incur large costs (Biolayer interferometry) (Thompson et al., 2017). The Valita™TITER assay negates the aforementioned drawbacks and was thus perfectly suited for our purposes. The assay is

presented in a multi-well microplate format allowing for a larger throughput. The assay is based on fluorescence polarisation. A protein G based fluorescent probe displaying high specificity for the Fc region of mAbs is employed. The fluorescent probe (also termed fluorophore) is excited by polarised light. The fluorophore emits light depolarised to a degree that is proportional to the rate of molecular rotation (Moerke, 2009). To elaborate, attachment of the protein of interest to the fluorophore would lower the rate of molecular rotation, and result in less depolarisation of light in comparison to the free fluorophore. Thus, the extent of polarisation is directly proportional to the amount of protein of interest in solution. A standard curve was plotted to confirm linearity between 1.25 and 80 mg L^{-1} (**Figure 4.6**). The curve was stable across different plates. A comparison against HPLC and biolayer interferometry presented in Thompson et al. (2017) confirmed a good correlation (R^2 >0.99) for both measurement techniques. Thus, the assay was employed for titer measurements in our HT platform.

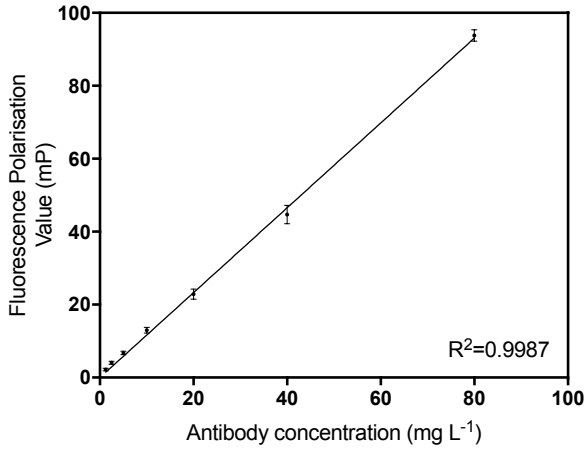

Figure 4.6 Linearity of the Valita™TITER assay across the 1.25 to 80 mg L^{-1} antibody concentration range. A serial dilution series of known antibody concentrations of an IgG1 protein standard were run on the Valita™TITER assay. Culture media (CD CHO) only wells were included to account for background fluorescence. The media polarisation values were subtracted from sample polarisation values. The data represented is the mean and standard error of three experimental replicates with two technical replicates.

4.3.4. Microplate Culture

The culture cultivation vessel is a crucial factor that influences cell growth (Duetz and Witholt, 2004). High-throughput culturing methodologies are essential to be able to screen multiple media components and supplements. Shake flask cultures can be classed as low-throughput and cost ineffective, while sophisticated mini-bioreactors (such as the ambr 15) can be expensive and difficult to operate manually. Since cost, resource and automation abilities were limited, 96 microplates presented the most straightforward approach for culturing cells in a HT manner. This was the first approach deployed to develop a scale down culture model to rapidly test small molecule culture enhancers. Plates would be cultivated in static conditions, lowering the number of factors to optimise since shaking speed and throw optimisations were negated. Culture volumes were limited to 90 µL of a 400 µL total fill volume in the 96 well plates to allow for headspace (based on personal communication on previous work performed in the David James' laboratory at The University of Sheffield). Comparative 8-day batch culture experimentation (using the Cobra 38 cell line) was performed; with 30 mL shake flask cultures serving as a benchmark. Growth and production profiles are depicted in **Figure 4.7**.

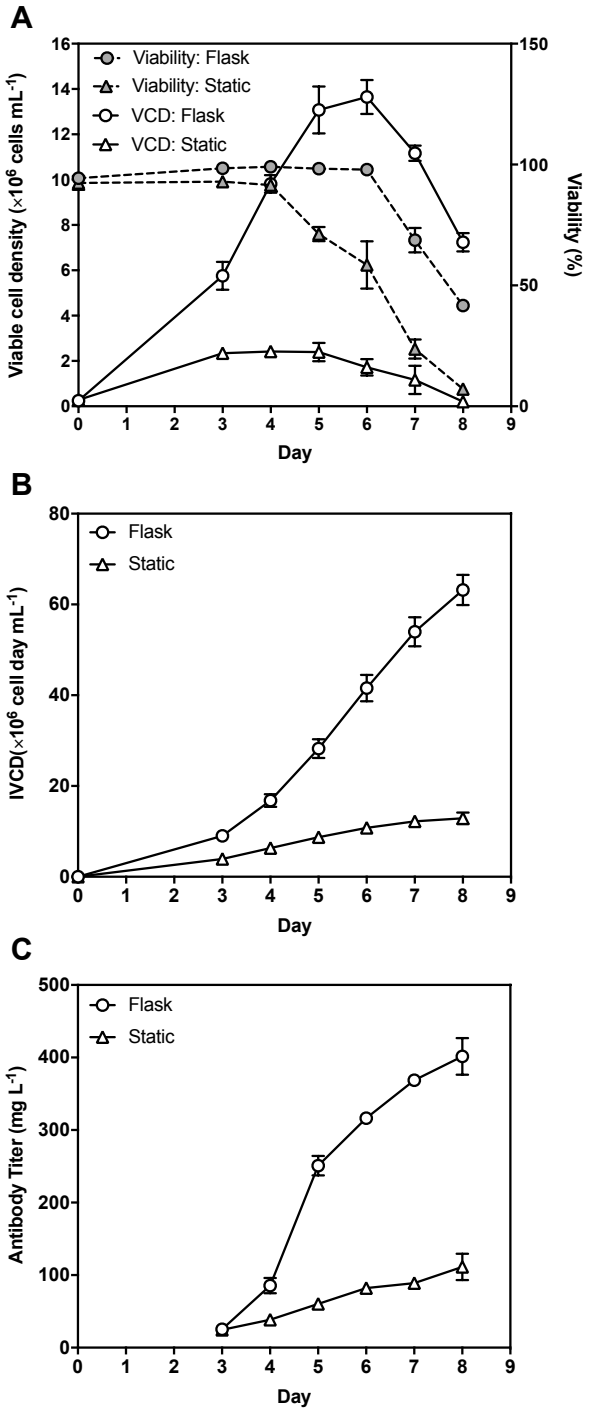

Figure 4.7 Static 96 well microplate culture performance evaluated against 30 mL shake flask cultures. Cobra 38 cells were seeded at 0.2×10^6 cells mL^{-1}. Cells were cultivated in 96 well microplates (90 µL) and 30 mL shake flask cultures in parallel to investigate microplate growth and production phenotype. Growth and production were monitored on multiple days as shown. Cell growth and viability were monitored using the Iprasense Norma and IgG1 titer measured using the Valita™TITER assay. Data represented is the mean and standard error of the mean (SEM) of three experimental replicates each with three technical repeats.

There were multiple observations based on the results shown in **Figure 4.7**. Firstly, static microplates were unable to support long-term cultures. This was evidenced by the drop in culture viabilities day 5 onwards while Erlenmeyer shake flask cultures dropped in viability only on day 7. Since cultures were static, there was no proper cycling of nutrients or gases, with cells settling at the bottom of the well (Jordan and Stettler, 2014) thus failing to provide cells a hospitable environment for growth and proliferation. Secondly, culture IVCD and titer were drastically lower than shake flasks across all measured time points. This was expected post the early drop in viability. However, biomass accumulation during the first 4 days where cell viability remained high, was still considerably poor in comparison to shake flask cultures. This proved that viable cell proliferation was limited. Again, this could be attributed to a multitude of factors such as lack of oxygen transfer, inefficient mixing of nutrients, settling of cells and potential contact inhibition. To directly compare, the final IVCD recorded on day 8 was 4.9 fold lower than the shake flask cultures. From production perspective, titer recorded was 3.6 fold lower in microplates than shake flask cultures that recorded titers in the range of 400 mg L^{-1} at the end of culture. SMEs like copper and sodium dichloroacetate have been proven to be late stage culture modulators (Buchsteiner et al., 2018; Yuk et al., 2015b). Thus, microplate culturing, which was unable to sustain long-term cultures, would be ineffective in isolating such late stage modulators. Additionally, edge effect is a well documented feature in microplate culture (Lundholt et al., 2003; Wagener and Plennevaux, 2014). This effect is characterised by differences in cell growth between the edge wells and the rest of the plate wells. This phenomenon occurs mainly due to thermal gradients leading to increased evaporation at the edges (Lundholt et al., 2003). This discrepancy is undesirable and can result in a lower throughput if edge wells are to be negated. These shortcomings coupled with the major deviation from larger scale culture growth and production phenotype eliminated shallow 96 well static microplates as a viable culturing option for the identification of bioactive small molecule enhancers of growth and titer.

4.3.5. Deep Well Plate Culture Optimisation

It was evident that 96 well microplates presented an unsuitable culturing methodology for SME screening. The major limitation was the short culturing time in comparison to shake flasks. The disparity would be further exacerbated when compared to higher scale platforms such as stirred tank bioreactors. This would directly impact the scalable predictive capabilities of the platform. It was hypothesised that shifting plate incubation from static to shaking mode could alleviate some of the cellular growth bottlenecks. Shaking plate cultures are slowly becoming the norm in industry to support HT clone screening and process optimisation (Amanullah et al., 2010; Long et al., 2014). A shaking deep well plate approach ("System Duetz") developed by Duetz et al. (2000) was initially developed for microbial cultures but has since been widely adopted into mammalian cell bioprocessing (Barrett et al., 2010; Hansen et al., 2015; Rouiller et al., 2013). The shift to shaking microwell cultures allowed for an improved oxygen transfer rate (Barrett et al., 2010; Duetz and Witholt, 2004). We applied and optimised the Duetz system in-house to improve growth profiles at the microscale level. The Duetz system we employed consisted of 2 components: A clamp system to keep the DWP secured during shaking conditions, and a sandwich cover (stainless steel lid (with holes) with layers of filter and silicone) that allowed for (i) efficient gas exchange (ii) controlled evaporation (no edge effects observed) and (iii) prevention of cross contamination (Chaturvedi et al., 2014; Duetz, 2007; Jordan and Stettler, 2014). The type of plate and orbital shaking speeds employed can be varied, and thus these factors were focused upon for optimisation experiments.

4.3.5.1. Speed, Throw and Plate Type

Incubator shaking speed, orbital diameter (or throw) and plate geometry have all been shown to impact cell growth performance in previous studies (Barrett et al., 2010; Duetz and Witholt, 2004; Long et al., 2014; Zhang et al., 2008). These factors mainly impact oxygen transfer rates and nutrient mixing. We aimed to

optimise culture conditions in DWPs so that growth profiles were comparable to shake flask cultures.

There are 2 major 96 deep well plate types based on well shape: round or square. We initially trialled a number of commercially available square and round 96 DWPs (data not attached), however, there were a number of plates that could not support viable cell growth (this is likely due to leachables promoting cytotoxicity (Hill et al., 2018)). Our initial screens showed that only 1 plate type was not cytotoxic or completely suppressing cell growth. These were the MasterBlock® Plates (square well, v bottom) (Greiner Bio-One). These plates were taken forward for more extensive optimisation experiments. The results of varying speeds and throw while utilising the MasterBlock® square plates are displayed below in **Figure 4.8**. The speeds were selected based on previous literature sources and personal communication (Duetz, 2007; Duetz and Witholt, 2004; Hansen et al., 2015; Rouiller et al., 2013; Rouiller et al., 2016). 4 different seeding volumes and 2 seeding densities were employed to give a larger design space to evaluate and inform future experimentation to optimise seeding densities and working volumes. All readings were taken 3 days post-seeding (no detriment to viability was observed across all conditions). Growth readings were only taken on a singular day so as to rapidly evaluate a number of conditions. The worst performing condition was the 350 rpm and 50 mm throw combination (**Figure 4.8D**), wherein the best performing sub-condition (i.e. culture volume and seeding density combination) only reached 58% of the control flask culture growth. It was speculated that the high speeds combined with a larger orbital radius was too harsh on the cells; as high shear stress can stagnate mammalian cell proliferation (Jordan and Stettler, 2014). In contrast, the best performing condition was the 320 rpm and 25 mm throw combination (**Figure 4.8A**). Herein, the 0.2×10^6 seeded cells mL^{-1} across all volumes grew between 60 and 72% of the flask controls. Conversely, cultures seeded at 0.3×10^6 cells mL^{-1} (450 and 500 µL) matched the viable cell densities in flask cultures seeded at 0.2×10^6 cells mL^{-1}. While those cultures did not match their flask counterparts that were also seeded at 0.3×10^6 cells mL^{-1}, this was the first indication that growth performance in DWPs could match those of shake flasks. This combination (Speed: 320 rpm, Throw: 25 mm and Plate well

type: square) certainly seemed promising. However, it remained to be seen how these DWP cultures would fare against shake flask cultures in a full batch culture setup, with readings taken daily.

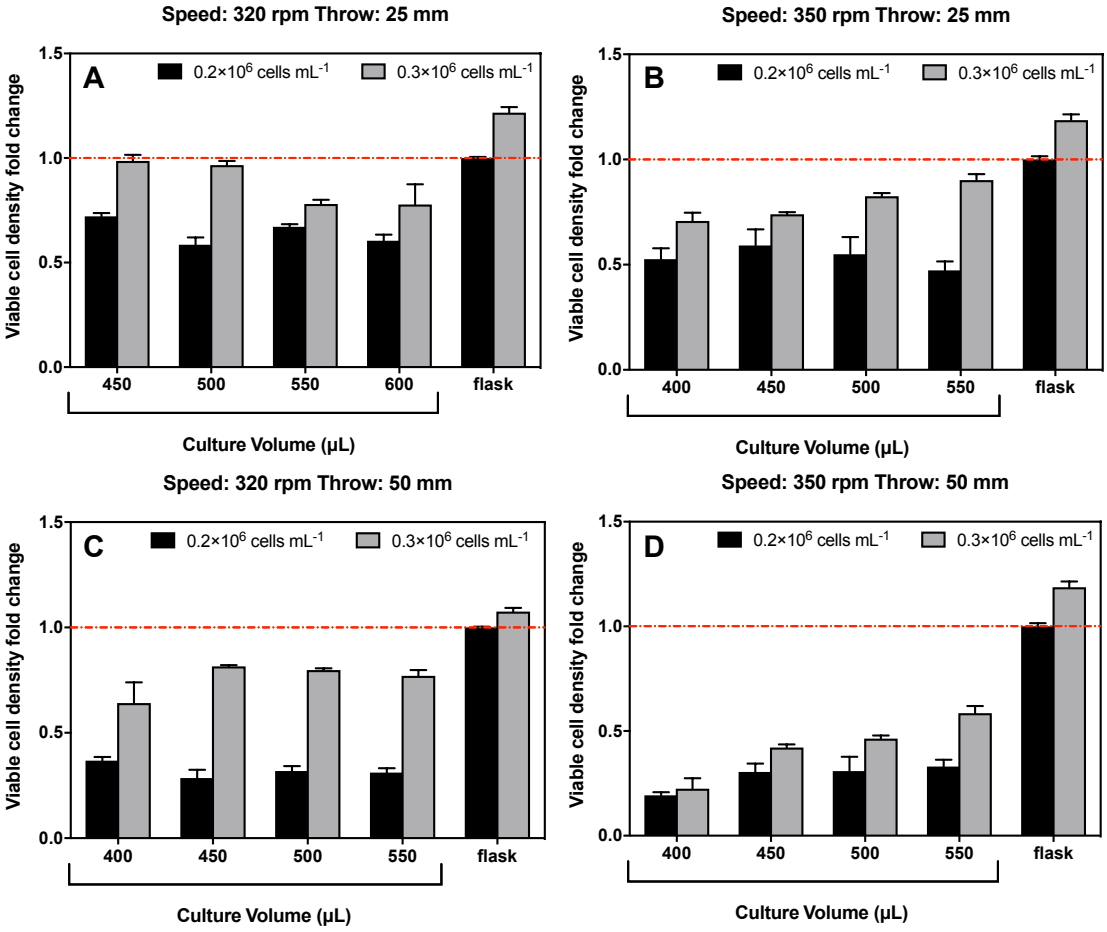

Figure 4.8 Cell growth performance in MasterBlock® 96 square DWPs varied for shaking speed and orbital diameter (throw). 4 combinations of speed and throw were assessed. Cobra 38 cells were seeded at 0.2 or 0.3×10^6 cells mL^{-1} and cultured in the specified culture conditions for 3 days before cell growth was evaluated. Cell growth and viability was recorded using the Vi-CELL-XR. A 30 mL batch culture in an E125 flask was included as a control to compare performance. All cell densities presented as a fold change to the 30 mL flask control. The plates were cultured at their indicated speed and throw at 37°C, 5% CO_2 and 85% humidity. The control flask cultures were incubated at 37°C, 5% CO_2 and 85% humidity, with a speed and throw of 140 rpm and 25 mm respectively. Red dotted line indicates the level of performance in 0.2×10^6 cells mL^{-1} seeded shake flask cultures (which was set to 1 to base fold change calculations). Data shown is the mean and standard error of three technical replicates.

4.3.5.2. Seeding Density and Volume

Having determined the plate type, speed and throw conditions for the DWP platform, it was imperative to determine if seeding densities and volumes could be further optimised to achieve culture profiles similar to shake flasks. Additionally, since previous optimisation efforts focused only on day 3 culture sampling, it was vital to observe culture performance profiles over a longer time course. Thus, we assessed 2 seeding densities (0.2 and 0.3×10^6 cells mL^{-1}) and 4 culture volumes (400 to 550 µL). The experimentation was performed at a shaking speed of 320 rpm and a throw of 25 mm using the Greiner MasterBlock® DWPs as recommended in the previous section. The cell growth performance when cells were seeded at 0.2×10^6 cells mL^{-1} at various culture volumes is depicted in **Figure 4.9**. The cells in the DWPs had a slower growth rate in comparison to shake flasks during the exponential culture phase. This was in agreement with our 3 day screens that indicated a slight reduction in growth in DWPs. However, moving from late exponential into stationary phase, DWP cultures (especially 450 µL) witnessed a highly similar cell density to shake flask cultures. However, IVCD was still lower throughout the culture duration period with all culture volumes recording around 90% IVCD of the control cultures on day 7. Interestingly, DWP cultures witnessed a slightly less drastic drop in culture viability on day 7 (450 µL: 83% viable, shake flask: 66% viable, **Appendix B**). This possibly had a bearing on the titer performance on day 7 (**Figure 4.9C**). While the flask cultures plateaued with regards to production on day 7, DWP production rates were still high resulting in identical titer values on day 7 for shake flasks and DWPs. Otherwise, across the other days tested (days 4-6), the DWP cultures recorded titers ranging from 65% to 80% of the flask control titer values (**Figure 4.9C**).

The growth and production trajectories followed by the different culture volumes were highly similar and it was concluded that any volume between 400 and 550 µL would be acceptable to employ.

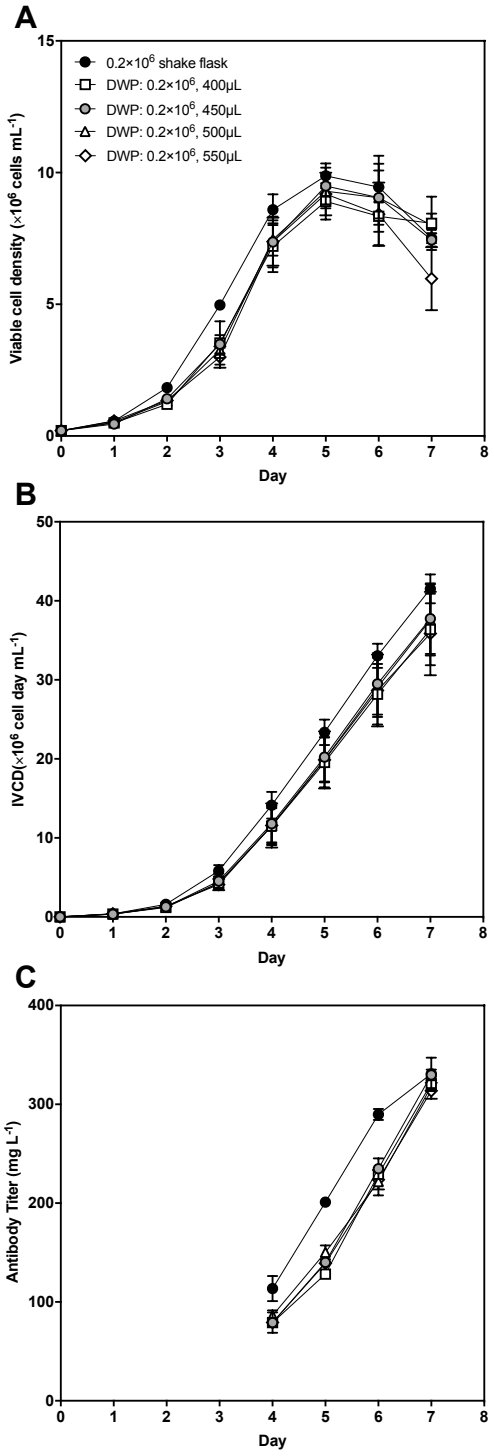

Figure 4.9 Batch culture performance of cells seeded at 0.2×10^6 cells mL^{-1} in MasterBlock® 96 DWPs with varying seeding volumes. 4 culture volumes: 400 µL ( ), 450 µL ( ), 500 µL ( ) and 550 µL ( ) were assessed and compared against 0.2×10^6 cells mL^{-1} seeded shake flasks ( ). **(A)** Viable cell density was measured using the Vi-CELL XR. **(B)** shows the progression of IVCD across the culture period **(C)** depicts the antibody titer calculated using the Valita™TITER assay. The data depicted is the mean and standard error of three experimental replicates each with three technical repeats. Day 7 IVCD and Titer not significantly different for any condition compared to the 0.2×10^6 cells mL^{-1} shake flask (one-way ANOVA, Dunnett's multiple comparisons test).

We also investigated if increasing the seeding density allowed the culture profile to reach the same level as the 0.2×10^6 cells mL^{-1} seeded shake flasks. Our earlier studies to optimise speed and throws revealed that at certain seeding volumes, 0.3×10^6 cells mL^{-1} seeded cells matched the viable cell concentrations of the 0.2×10^6 cells mL^{-1} seeded flasks on day 3 (**Figure 4.8**). While this was promising, we were wary of exceeding the growth performance of shake flasks across the batch culture period. Keeping the same experimentatal model as with previous experimentation, we trialled 4 different culture volumes seeded at 0.3×10^6 cells mL^{-1} across a 7-day batch culture using the IgG producing Cobra 38 cells. The resultant growth and product profiles are displayed in **Figure 4.10**.

The target profile was the 0.2×10^6 cells mL^{-1} seeded shake flasks (shown with black circles), however a 0.3×10^6 cells mL^{-1} shake flask profile (shown with grey circles) was also included for comparison. While the 0.3×10^6 cells mL^{-1} seeded DWP cultures could not match the 0.3×10^6 cells mL^{-1} flask profiles, they were able to replicate the 0.2×10^6 cells mL^{-1} flask trajectory (**Figure 4.10A**). Interestingly, on days 4 and 5, the 400 µL cultures (white square symbol) surpassed the cell densities observed in the 0.2×10^6 cells mL^{-1} flask cultures. This resulted in total IVCD for the 400 µL cultures surpassing that of the 0.2×10^6 cells mL^{-1} shake flasks (**Figure 4.10B**). The other cultures recorded a similar IVCD to that of the 0.2×10^6 cells mL^{-1} seeded shake flasks. Surprisingly, the production profiles indicated that all DWPs produced slightly lower titers than the target 0.2×10^6 cells mL^{-1} flasks from days 4 to 6. This resulted in lower qP on those days.

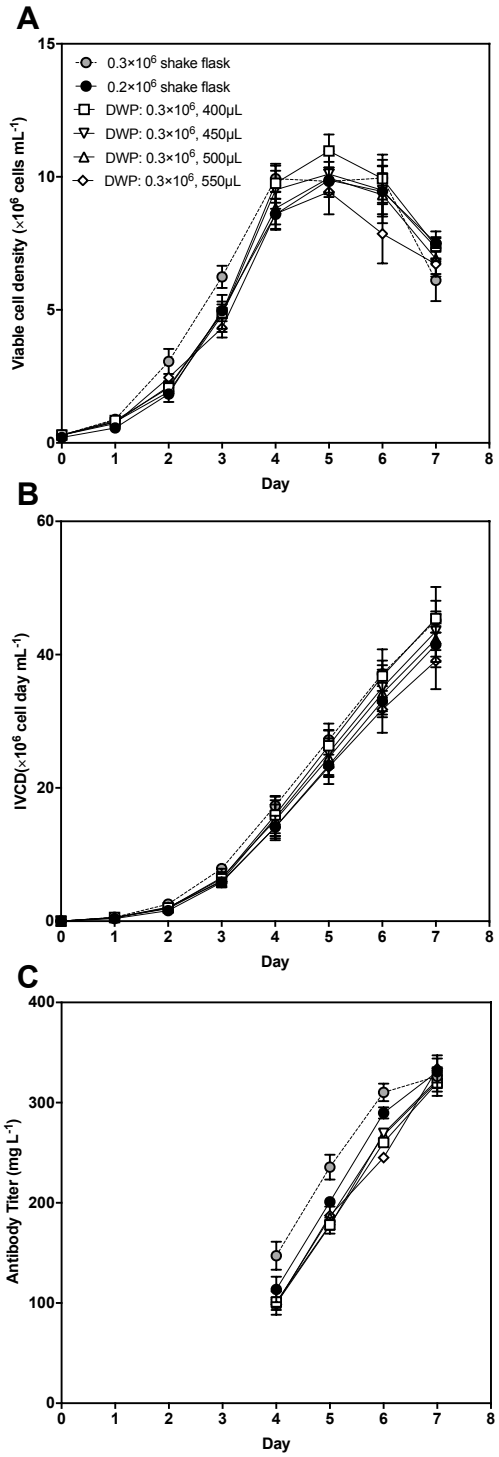

Figure 4.10 Batch culture performance of cells seeded at 0.3×10^6 cells mL^{-1} in MasterBlock® 96 DWPs with varying seeding volumes. 4 culture volumes: 400 µL (□), 450 µL (▽), 500 µL (△) and 550 µL (◇) were assessed and compared against 0.2×10^6 cells mL^{-1} (●) and 0.3×10^6 cells mL^{-1} (○) seeded shake flasks. **(A)** Viable cell density was measured using the Vi-CELL XR. **(B)** shows the progression of IVCD across the culture period **(C)** depicts the antibody titer calculated using the Valita™TITER assay. The data depicted is the mean and standard error of three experimental replicates each with three technical repeats. Day 7 IVCD and Titer not significantly different for any condition compared to the 0.2×10^6 cells mL^{-1} shake flask (one-way ANOVA, Dunnett's multiple comparisons test).

qP analysis on day 5 (**Figure 4.11**) indicated that the high speed shaking DWP conditions did not particularly exert stress on the recombinant protein production pathways. qP values across all conditions were highly similar to the 0.2×10^6 cells mL^{-1} seeded shake flasks (qP was not significantly different for any condition, one-way ANOVA, Dunnett's test). From the experimentation results explained above, seeding density and volume were not vital factors that impacted cell growth and productivity in DWPs. In this case, it could be argued that any of the 4 volumes and 2 seeding density combination could depict a valid representation of shake flask culture and thus be employed for screening experiments to isolate SMEs. We decided to employ a **450 µL seeding volume and 0.2×10^6 cells mL^{-1} seeding density.** This would allow us the flexibility to modify the setup if required, for example the addition of feeds increasing culture volume and cell growth rates. Day 5 was chosen as the point in culture for the collection of growth and productivity data for our SME screens.

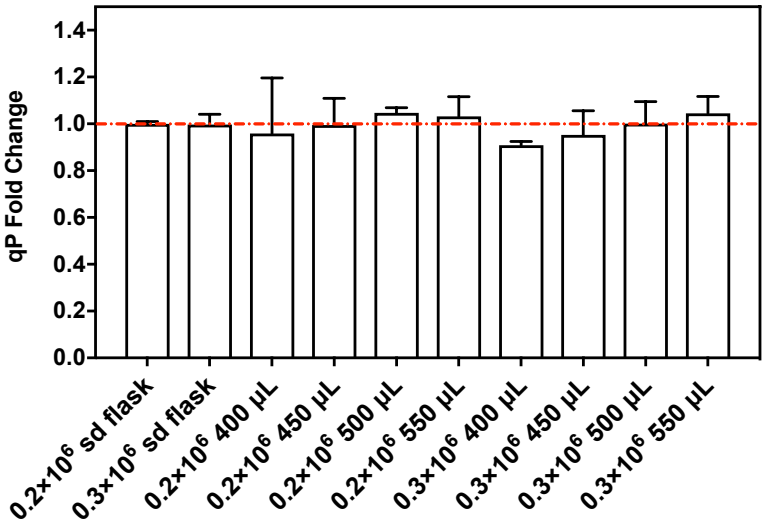

Figure 4.11 Specific productivity of all DWP cultures tested relative to 0.2×10^6 cells mL^{-1} seeded shake flasks. Specific productivity was calculated at the day 5 time point of the batch cultures depicted in **Figure 4.9** and **4.10**. qP is expressed as a fold change to the 0.2×10^6 cells mL^{-1} seeded shake flask control (indicated by the red dotted line). Data represented is the mean and standard error of two experimental and three technical repeats.

4.3.6. Delayed SME Addition Strategies

The optimisation of the DWP platform allowed us to create a scale-down culturing modality that was validated against shake flask cultures. Another factor that can affect SME identification is the timing of addition of the small molecule. The most straightforward approach of adding the chemical at day 0 was adopted for all initial screening. However, some chemicals have been shown to improve titer at the expense of growth. When these types of chemicals are added on day 0, a massive inflation in qP is observed, however, titer normally does not surpass control values. Since the overarching aim of this project is to enhance growth and/or titer over the no addition controls, it can be argued that later SME addition might serve as a better strategy for these qP enhancing molecules. This type of "biphasic" strategy is quite common in the biopharmaceutical industry (for example, hypothermic culture shifts) and often results in a bigger boost in titer compared to implementing the strategy at day 0 (Yoon et al., 2006). Not stifling cells' ability to proliferate in the early stages of culture, results in a larger biomass capable of producing the product of interest. When the chemical is added at the late stage, there are more cells that can be manipulated by the SME to improve their production capacity.

Applying this rationale to our HT system, we investigated different days of addition for qP enhancing molecules. We chose to test chemical addition on day 3 and day 4 (mid to late exponential stage) and compare against the growth and titer achieved by chemical addition on day 0. The chemicals employed for this trial were well known qP enhancers that have been shown to improve qP in mammalian cells previously. The chemicals chosen were sodium butyrate (NaBu) (Chen et al., 2011), Trichostatin A (TSA) (Backliwal et al., 2008), MS 275 (Backliwal et al., 2008), sodium phenylbutyrate (4PBA) (Johari et al., 2015) and 2 Thiopheneacetic acid (2TAA) (Allen et al., 2008). Most of these were histone deacetylase inhibitors wherein their mode of titer enhancement is indirectly linked to growth suppression (Bora-Tatar et al., 2009; Park et al., 2016; Sung et al., 2004). As stated earlier, we had decided to record culture attributes on day 5 of a 7-day batch culture process in DWPs. With delaying the addition of chemical, we also had to check if day 5 was too early in the culture

process to quantify the benefit of the addition of the chemical. Thus, we also recorded culture attributes on day 6 to see if we witnessed larger gains at this time point, having the cells incubating with the chemical for an extra day. The results from this experimentation are displayed in **Figure 4.12**.

Figure 4.12A depicts day 5 titer performance of the Cobra 38 cells incubated with various concentrations of different singular SMEs added on days 0, 3 or 4. There was a wide spread of titer improvements across all concentrations and days of addition tested. Unsurprisingly, day 4 addition of the chemical yielded the lowest titer gains on day 5 since incubation with the chemical was only a single day. Interestingly though, the highest concentrations of NaBu and 2TAA still yielded titer gains of 1.8 to 1.9 fold even though they were present in culture for only one day. Generally, day 3 addition returned higher improvements in titer performance over day 0 addition. For example, the highest absolute titer yielding TSA concentration at day 0 addition (0.35 μM) still generated titer 20% lower than the control culture titers. However, adding the chemical on day 3, yielded a titer boost of 45% for the best concentration (1 μM). Both concentrations of 4PBA returned 70% titer increase when added on day 3 compared to non-increase when added on day 0. Similarly, the best performing 2TAA concentration (0.4 mM) at the day 0 addition stage returned a titer yield of 1.6 fold over the control, however the best titer boost using the day 3 addition strategy was a 3.2 fold increase (2 mM). NaBu addition on day 0 recorded that best titer increase of 2.2 fold (0.25 mM) while day 3 addition yielded a 2.6 fold increase (1 mM). Interestingly, there was no real benefit of adding MS 275 on day 3 over day 0 addition.

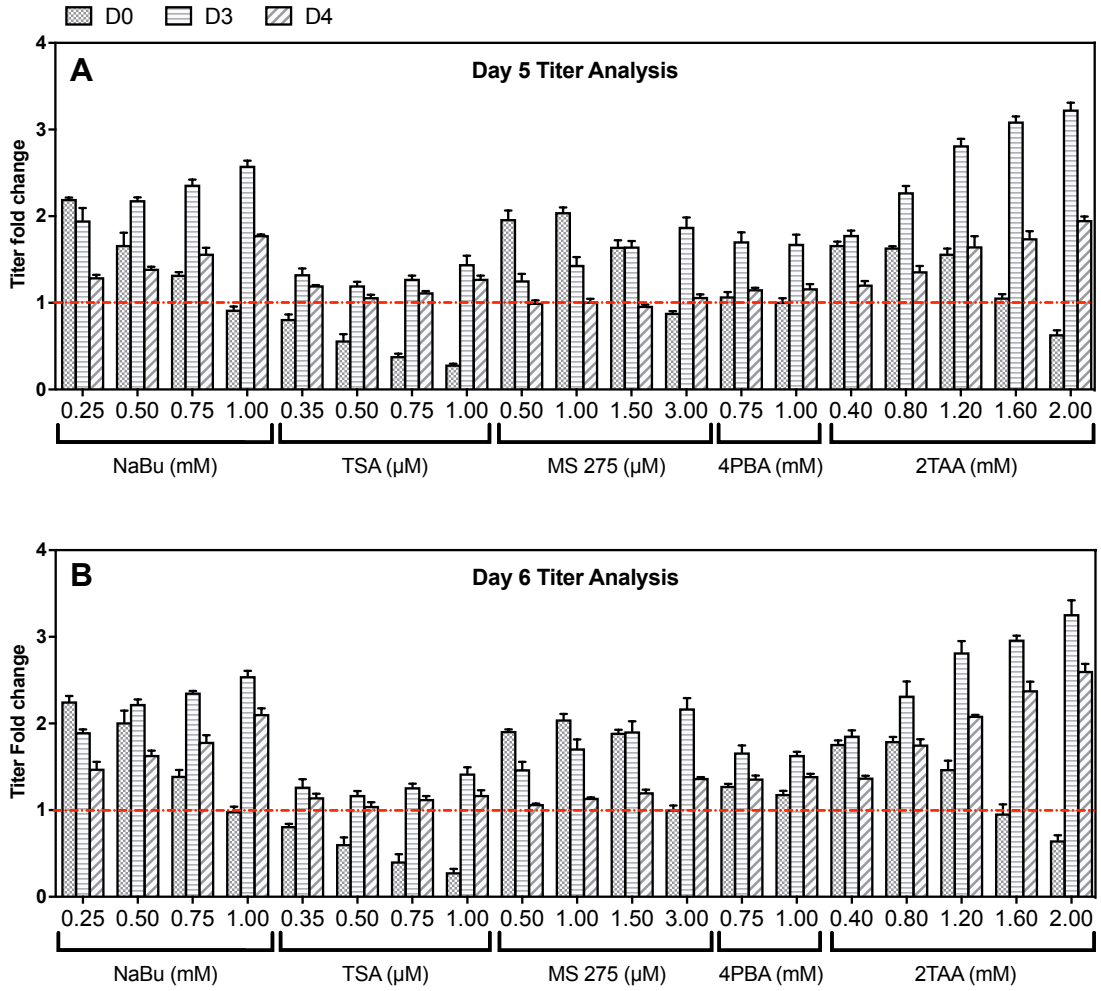

Figure 4.12 Titer output summary for the delayed SME addition strategies tested. Cobra 38 cells were seeded at 0.2×10^6 cells mL^{-1} in 96 DWPs with a total culture volume of 450 µL. The 5 SMEs (at various concentrations) were added to culture on days 0, 3 or 4 (as indicated). Antibody titer was measured using the Valita™TITER assay. **(A)** depicts the antibody yields on day 5 in DWP cultures while **(B)** displays titer recorded on day 6. The data is represented as the mean and standard error of three experimental replicates with three technical replicates.

The same experiment was repeated with the cultures incubated with the different chemicals for an extra day with titer being assayed on day 6 (**Figure 4.12B**). While the absolute titer values did increase, the change in titer relative to the controls mostly remained constant for the day 0 and day 3 additions when compared to their fold changes on day 5. Day 4 addition of the chemical yielded larger benefit when assayed on day 6 in comparison to day 5, due to the obvious longer duration. However, generally the [day 4 addition/day 6 assay] titer fold change could not surpass the [day 3 addition/day 5 assay] fold

change. For example, [day 3 addition/day 5 assay] for 2TAA yielded a maximum of 3.2 fold increase in titer. Conversely, a [day 4 addition/day 6 assay] yielded a 2.6 fold increase in titer for 2TAA. Similarly, for NaBu, [day 3 addition/day 5 assay] yielded a larger titer boost than [day 4 addition/day 6 assay] (2.6 vs 2.1 fold). From this data, we were able to conclude that there was lower merit of adding the SME in culture on day 4 in comparison to day 3. Day 3 addition improved titers over the day 0 addition for most chemicals and this was evident on day 5. Thus, we decided to proceed with a two-tiered screening strategy. Chemicals that were shown to improve qP in the day 0 screens would be taken forward for delayed SME screening. For the delayed addition screening, the chemical would be added on day 3 with culture attributes assayed on day 5.

4.3.7. Appropriate Solubilisation Vehicle Concentration Determination

A general literature survey of chemical enhancers revealed that some chemicals require a vehicle for solubilisation (Backliwal et al., 2008). Dimethyl sulfoxide (DMSO) and ethanol are general choices for help solubilise otherwise poorly water soluble chemical candidates to form a solution. With especially high concentrations of the solubilising vehicles impacting cell viability and functional pathways (Galvao et al., 2014), it was important to evaluate what concentrations can negatively impact CHO cell growth, viability and titer. This would give us a better indication of what volume percentage to employ in our SME candidate studies and minimise any functional impact of the vehicles on our screening outputs.

Our selected chemicals that were not water soluble, were either soluble in DMSO or ethanol. We tested various concentrations of both solubilisation chemicals to test which concentrations did not impact culture attributes of interest i.e. IVCD, qP and/or titer. The chemicals were added on day 0 of batch culture in 96 DWPs and performance attributes were recorded on day 5. The results are displayed in **Figure 4.13**. DMSO had a higher impact on titer than on cell growth (**Figure 4.13A**). Cell growth remained unaffected until 0.3% v/v. qP

and consequently titer fell below 80% of the control cultures from 0.25% v/v onwards. Thus, the maximum acceptable DMSO concentration as a solubilisation vehicle was kept at 0.2% v/v, where no significant change in culture attributes was observed. The use of ethanol in culture (**Figure 4.13B**) did not impact cell growth till 0.5% v/v. Similar to DMSO, titer was more severely impacted by the use of ethanol. Titer dropped to about 80% of the control cultures at 0.3% v/v. Thus, the maximum ethanol percentage in SME cultures (that used ethanol as a vehicle control) was limited to 0.2% v/v where no significant change in growth or titer was observed.

This experimentation model served to investigate the appropriate concentration in culture of 2 vehicle controls. A SME screen, where the SME being evaluated was solubilised using a vehicle other than water, would include a vehicle control.

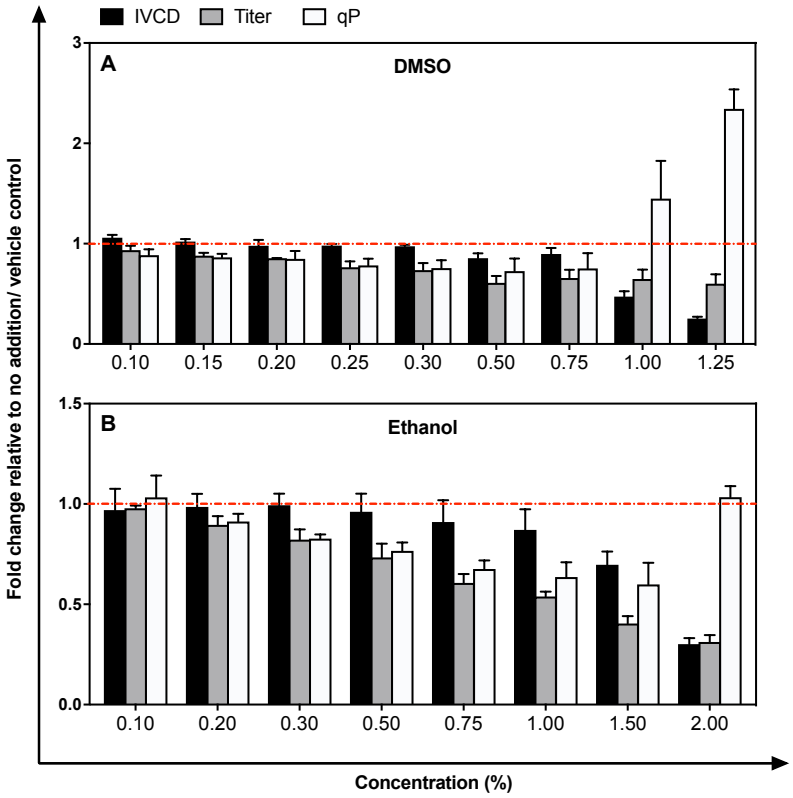

Figure 4.13 Impact of chemical solubilisation vehicle on DWP culture performance. Increasing concentrations of **(A)** DMSO and **(B)** Ethanol were added on day 0 of a 5-day batch culture in 96 deep well plates. Plates were seeded at 0.2×10^6 cells mL^{-1} with a culture volume of 450 µL. Cell growth was established using the PrestoBlue assay and volumetric titer determined using the Valita™TITER assay. The data represented is the mean and standard error of three experimental replicates with three technical repeats.

4.4. Discussion

This research chapter investigated the development of a HT screening platform to assess potential SMEs for improved CHO bioprocess. The screening platform would form the basis of a SME screening commercial tool, wherein singular enhancers and their rational combinations can be rapidly evaluated in a HT manner. All optimisation experiments were performed using the Cobra38 cell line, the model cell line used for the SME screens in the following chapter. The HT platform development experiments were focused on 2 main aspects: (i) analytics and (ii) culturing methodology.

From an analytics point of view, we were mainly concerned with measurements of 3 culture attributes: cell growth, viability and production titer. We evaluated the PrestoBlue assay and the Iprasense Norma as the two main HT growth analytical tools. Each analytical approach was compared against the Vi-CELL XR, the industry cell counting standard. Both PrestoBlue and Norma produced large accurate dynamic ranges. The PrestoBlue assay is based on reduction of the active ingredient to a highly fluorescent molecule in the presence of a viable cellular reducing environment. The assay is based on the output fluorescence being proportional to viable cell number and does not return absolute cell number or culture viability. This can be viewed as a disadvantage. However, we were mainly concerned with evaluating SME performance relative to a control, so absolute cell numbers were not necessary. The setup employed for the PrestoBlue assay reached VCD determination saturation post 7×10^6 cells mL^{-1}, thus prompting dilutions with CD CHO (1:1) when concentrations approached those levels. Other fluorescent dyes based on membrane integrity (for example TO-PRO-3 (Bradford and Buller, 2009)) can be analysed using flow cytometry techniques and provide a measure of cell viability. However, flow cytometry is usually cost and time intensive, thus ruling out regular use of this approach.

At the other end of the spectrum, a relatively new equipment, the Iprasense Norma determines cell viability based on light diffraction. We assessed the cell counting and viability determination capabilities of a series of samples and a strong positive correlation was observed against the Vi-CELL XR. Sample setup is similar to that of a microscope slide, with Norma slides containing 48

individual chambers for HT capabilities. An even distribution of sample is pipetted into each chamber, which in turn is analysed by light diffraction, creating holograms for each cell. Hologram patterns are unique for live and dead cells allowing for identification. It was impressive that accurate doubling of concentrations was observed on the standard curve series with sample volumes as low as 3 µL (20 µm plate thickness). However, cell numbers were consistently lower than the Vi-CELL XR. It could be postulated that the low sample volume played a role in the lower cell count. Surprisingly, when the sample volume was increased (10 µL; 100 µm plate thickness), the numbers recorded were consistently half that of the Vi-CELL XR. It could be possible that the increased slide thickness led to uneven distributions of cells resulting in lower cell counts. For consistency purposes with the Vi-CELL XR, we implemented correction factors for both slide types (20 µm: ×1.4, 100 µm: ×2).

In terms of viability, the Vi-CELL XR and the Norma were evenly matched. The Norma would serve an ideal HT cell counter and viability analyser, however its high operating cost and late availability in our laboratory impeded its use as a sole HT cell growth analyser. In future projects the Norma could prove useful for daily culture monitoring (such as in fed-batch cultures), since the extremely low sample volumes would allow for multiple readings to be taken from the same well. In contrast, the PrestoBlue assay is more suited as an end-point assay where readings are only taken upon culture termination (like in the case of our platform). The simple, robust and cost-effective nature of the PrestoBlue assay made it attractive to employ for our purposes. To conclude, we employed the PrestoBlue assay as the main assay for cell growth analysis, with the Norma and the Vi-CELL XR employed in support whenever cell numbers and viability determination were deemed necessary.

Volumetric titer was perhaps the most vital culture attribute that needed determination for our SME screens. We employed the Valita™TITER assay that was developed in-house to quantify Fc domain containing proteins in solution. Comparative analysis performed against the HPLC and biolayer interferometry showed a correlation R^2 >0.99 (Thompson et al., 2017), with readings being stable across different plates. The large dynamic range coupled with quick assaying times gave it an edge over the other HT titer assay commonly

employed, ELISAs. Overall the assay was fit for purpose for our HT screens that utilised the Cobra 38 cell line, an IgG1 producer.

Having evaluated and optimised the analytical methodologies for growth and titer, we focused our attention towards the development of a HT culturing platform. The main aim here was to be able to reproduce shake flask batch culture performance at a scaled down HT level. Initial analysis of 96 microplate static culturing technology revealed that cell proliferation was extremely limited with cultures stagnating at 2×10^6 cell mL^{-1}. Viability also dropped prematurely in comparison to shake flasks indicating that long culture periods could not be supported. Oxygen transfer rates have been shown to be extremely limited in static plate cultures in comparison to shaking plates (Duetz and Witholt, 2004). This improper cycling of gases and nutrients could explain the poor culture performance in 96 static microplates. Culture volume was also limited to 90-100 µL, which resulted in culture growth and titer performance often being assayed from different technical replicate wells. A different rate of evaporation between the plate centre and edges was also an impactful factor that could influence erroneous results. Thus, this culture mode was discounted as a potential HT culturing methodology.

Shaking DWP culturing is slowly becoming the norm in bioprocess circles. Development of this culturing methodology had the potential to nullify 2 main problems of static shallow well culturing: poor cell growth and low culture volumes. Multiple studies have referenced the use of DWPs for different screening purposes; including for transient transfection (Hansen et al., 2015), recombinant cell line screening and selection (Rouiller et al., 2016), media blending experiments (Rouiller et al., 2013) and assessment of product quality modulators (Brühlmann et al., 2017b). These aforementioned studies formed the basis of our optimisation experiments. The availability of only a single incubator with varying speed and throws translated to an iterative approach and a smaller design space for speed and throw optimisation. Shaking speed, orbital diameter and plate geometry influence hydrodynamic behaviour in miniaturised shaking cultures (Barrett et al., 2010; Duetz, 2007; Duetz and Witholt, 2001; Duetz and Witholt, 2004). It is said that square well DWPs often have twice the oxygen transfer rate of round well DWPs (Duetz, 2007) at the

same fill volume. This is often attributed to the turbulent flow pattern caused by the square well shape (Duetz, 2007). It could be argued that this flow pattern could also enhance nutrient mixing and keep cells in suspension. All these factors could be influential in presenting conditions for better cell growth. Our studies conformed to these observations made in past literature, with Greiner MasterBlock® 96 square well DWPs outperforming other plates (notably round well plates: see **Appendix B**). The "System Duetz" was employed to secure plates with vented lid covers, minimising evaporation and edge effect, while allowing for sufficient gas exchange. Shaking speeds and orbital diameter were also varied to estimate the conditions most suited for cell proliferation in the square DWPs. A speed of 320 rpm and orbital diameter of 25 mm was best suited for cell proliferation at various seeding densities and culture volumes. This initial optimisation experimentation already recorded culture densities higher than static culture plates, thus the benefits of shaking on cell growth were obvious. Additionally, shaking DWP cultures allowed for larger culture volumes; multiple attribute sampling from a single well was made possible.

The next line of optimisation efforts was focused on seeding volume and seeding density. Fill volume influences headspace availability and networks with speed, throw and plate geometry in influencing gas transfer (Duetz, 2007). Interestingly, fill volume did not majorly influence cell growth in our studies. Admittedly, a narrow range of fill volumes was only tested (based on previous literature guidance (Jordan and Stettler, 2014; Rouiller et al., 2016)) and thus impact of largely different culture volumes was not visible. 2 seeding densities were tested based on the results shown in **Figure 4.8A**, which indicated 0.3×10^6 cells mL^{-1} DWP cultures could match 0.2×10^6 cells mL^{-1} seeded flasks. Interestingly, evaluation over the 7 day batch culture period showed that 0.2×10^6 cells mL^{-1} seeded DWPs were not far removed from 0.2×10^6 cells mL^{-1} seeded shake flasks in terms of growth, IVCD and titer. Cellular qP was consistent with shake flasks when analysed on day 5 of culture. The 0.3×10^6 cells mL^{-1} seeded DWPs matched 0.2×10^6 cells mL^{-1} seeded shake flasks over the 7 day batch culture period, with the 400 µL cultures slightly surpassing shake flask growth performance. Interestingly, titer was slightly lower, leading to slight reduction in qP as well. It could be debated whether seeding higher,

resulting in a larger biomass in the small well space, could negatively regulate antibody production pathways. More experimentation would be needed to accurately determine the impact.

Seeding cells at 0.2×10^6 cells mL^{-1} in a culture volume of 450 µL was decided upon for all future screening experiments. This would allow for increase in culture volume (until 550 µL) by feed addition, for example. Seeding lower (0.2 instead of 0.3×10^6 cells mL^{-1}) would not limit the improvement capabilities in cell numbers over a longer culture period due to the addition of a chemical additive or feeds.

The last variable in finalising the culture platform was the timing of addition of the SME. While day 0 addition was the most practically simple approach, any molecules that repressed cell growth concomitant with an increase in qP would be better suited for a delayed addition approach to amplify titer. This would allow for an initial biomass accumulation phase followed by a maximal production phase (Johari et al., 2015). Day 3 and day 4 additions were investigated with analytics performed on day 5 and day 6. It was evident that day 3 addition majorly improved titer performance (on days 5 and 6) for most qP enhancers. Functionality of molecules could have a bearing on the best timing of addition. Thus, it was important to have some degree of flexibility within the HT system to allow for the isolation of enhancers with differing timing of additions best suited to their mode of action. Thus, day 0 addition testing followed by a small subset being evaluated using a day 3 addition strategy was deemed a suitable addition to the HT platform. Both culture supplementation strategies would still be evaluated on day 5 since extending the culture by a day did not yield any new information (**Figure 4.12**).

A visual summary of the final HT screening platform is displayed in **Figure 4.14**. Future studies could embed feed addition leading to longer culture duration. Addition of HT product quality analytics could also further enhance prediction capabilities at the microscale level (Yang et al., 2016). Additionally, the platform displays versatility in terms of applicability, the platform could be adapted for transient transfection and cell clone screening similar to those recorded in previous literature (Brühlmann et al., 2015; Brühlmann et al., 2017b; Hansen et al., 2015; Rouiller et al., 2013; Rouiller et al., 2016).

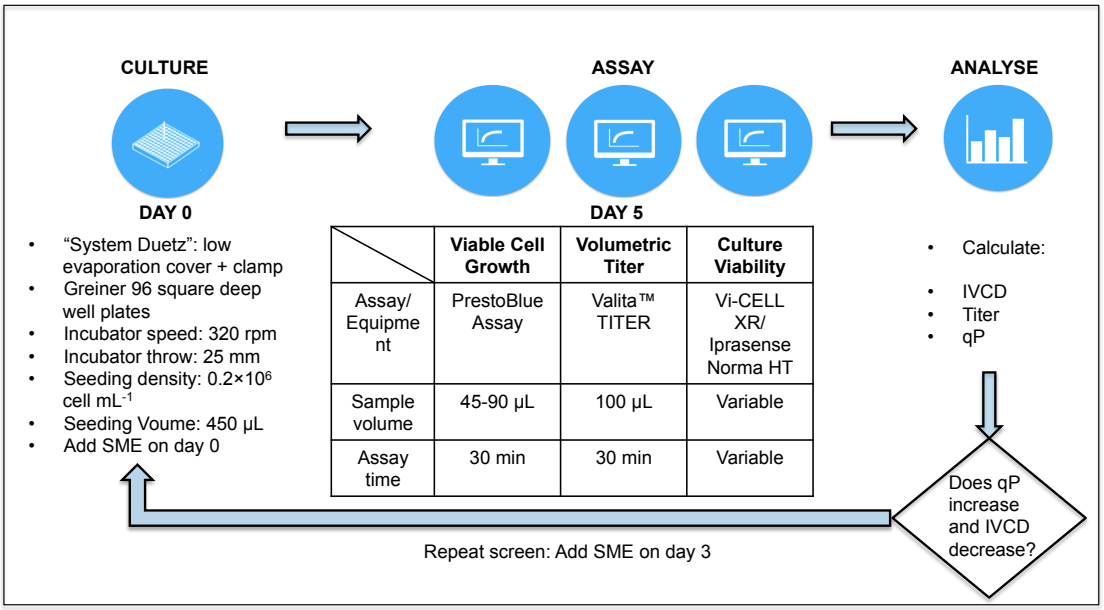

Figure 4.14 Developed HT screening platform for the isolation of small molecule enhancers for improved CHO bioprocess. The developed platform consists of two components: HT Culturing technology and HT Analytics.

Chapter 5

High-Throughput Assessment Of Small Molecule Enhancers

ABSTRACT: In this chapter, we describe the implementation of the developed high-throughput screening platform described in Chapter 4 to rapidly screen and titrate various small molecule enhancers of growth, titer and qP. 8 functional categories (metal ions, metabolic modulators, fatty acids, chemical chaperones, HDAC inhibitors, DNA/histone methyltransferase inhibitors, cell cycle inhibitors and carboxylic acids) were evaluated, with molecules being selected based on prior art and likelihood of efficacy based on function. Each chemical was tested at a wide range of concentrations in a CHO cell line stably producing a mAb. The chemical was added on day 0 of a 5-day deep well plate batch culture. Metal ions (maximum IVCD fold change: 1.6) were particularly efficacious in improving cell growth, while histone deacetylase inhibitors (maximum titer fold change: 1.9) were responsible for large increases in volumetric titer. A sub-set of enhancers that actively suppressed growth, concomitant with an increase in cellular productivity were re-evaluated using a delayed addition strategy. 2TAA recorded the highest improvement in titer (3.2 fold) when added on day 3. A collection of successful enhancers was used to inform combinatorial strategies based on the Design of Experiments Methodology. The best combination of growth enhancers (2.1 fold IVCD enhancement) and the best combination of titer enhancers (4.3 fold titer enhancement) outweighed their best performing singular counterparts. Finally, selected combinations were tested in scaled-up fed-batch cultures to provide insight into the predictive capabilities of microscale batch cultures. The best performing combination yielded a product titer of 2.9 g L^{-1} which was 60% higher than control cultures. It was evident that some of the improvements were lost due to feed addition; however, the trends observed were in agreement with deep well plate data. The data presented in this chapter can be used to inform the design of commercial screening tools for chemical enhancer testing. Such a product would find use in diverse CHO cell host production scenarios, informing the creation of bespoke media environments catered to the user's cell line, product and base media.

5.1. Introduction

While g L^{-1} protein titers are commonplace in the CHO host cell factory arena (Pybus et al., 2014), there is always an impetus to enhance upstream production outputs further. This need is further exacerbated due to the demand of novel complex molecules and the rise of biosimilars and biobetters (Walsh, 2014). In short, high-throughput methodologies need to take centre-stage. In the previous chapter, we described the development of a high-throughput screening platform comprising HT culture techniques and analytics.

There has been a steady increase in the use of SME entities in cell culture to boost protein production and cell growth. Functionally diverse, easy to titrate and comparatively cheap, these molecules present attractive utility opportunities. The use of these molecules is not entirely novel, with sodium butyrate being used as a protein production inducer since the 1990's (Palermo et al., 1991). Since then, the repertoire of molecules available to modulate CHO function has only increased (Backliwal et al., 2008; Du et al., 2015; Ha et al., 2014; Park et al., 2016). However, there is a lack of resources available to rapidly test these molecules in parallel to underpin their utility in CHO production environments. It cannot be denied that there are small molecule chemical libraries commercially available, however, these are majorly concerned with drug discovery and phenotypic profiling (Biolog, 2013; Selleck Chemicals, 2013; Sigma-Aldrich, 2018). These libraries are also not configured for optimal combinatorial screening. The lack of high throughput platform based focused libraries available for CHO cell bioprocessing presents a commercial opportunity.

There are few previous studies that have undertaken large chemical library screening in recombinant protein producing CHO hosts. The first one by Allen et al. (2008) was able to identify novel enhancers for stable production in CHO cells. In this study, effects of 192 compounds on CHO cells (cultured in 96 well microplates (100 µL) for 4 days) were examined. Static, shallow well plate culturing implied that late stage culture performance could not be ascertained. Additionally, predictive capabilities when scaled from shallow plates to shake flask culture were not ideal, however the ability to identify enhancers was good.

Our static microplate (90 µL) studies suggested that growth in this culture modality deviated from shake flask profiles (short culture period with low cell densities and volumetric yield) (**Section 4.3.4**). So poor scalability in this study was not unexpected. Chemicals in this study were selected based on their structure, for example, carboxylates, acetamides and hydroxamic acids. Many well known HDAC inhibitors exhibit similar structure to these compounds. Additionally, no combinations of chemicals were trialled, missing an opportunity to elevate performance.

Another study by Meyer et al. (2017) screened 31,000 potential SMEs as enhancers for transient protein expression in HEK293 cells. 16 compounds were taken forward for further testing. Due to the vast number of compounds tested, only 1 concentration could be tested per chemical, presenting high probabilities of missing effective dose and eliminating promising candidates. Also, studies were performed using the transient expression mode, thus performance in stable production mode (routinely employed for large-scale production purposes) could not be established.

Perhaps, another relevant study of chemical modulators in CHO cells would be one by Brühlmann et al. (2017b). Herein, 17 chemical modulators of glycosylation were assessed using DWP culturing technology. The main aim of their experimentation was to develop culture feeding strategies to maintain biosimilar product quality to the reference medicinal product. Multiple DOEs were performed in parallel, each with a subset of chemical modulators. Scale-up predictive capabilities were assessed using TubeSpin shaking tubes. Interestingly, cellular growth and productivity were assayed for but data was not displayed. Only 2 concentrations were tested per chemical, although it was mentioned that prior studies were performed on some of the chemicals. Cross-functional interactions between factors were ignored and no focus was given to the identification of novel modifiers. The number of compounds tested was comparatively small, and given that HT culturing and analytical technologies were employed, the design space could have easily been widened.

The aforementioned screening studies depicted moderate success in isolating enhancers. However, many of them (especially the first 2) were practically not viable to implement as standard within a cell line and process development

process. We stipulate that a more function and mode of action led SME screen could yield greater benefit in various production scenarios. Instead of extremely large (>100 factors) SME screens, testing a more focused small number of chemicals would also mean more concentrations could be tested per chemical. Bearing these design criteria in mind, we chose 8 functional categories to rigorously evaluate. A total of 43 molecules were tested across all categories. This chapter details and discusses the chemical screens performed that would guide the creation of a commercial screening tool to assess the efficacy of small molecule enhancers in a high-throughput manner for CHO cell bioprocessing. Cell growth, titer and qP were chosen as important culture attributes to target. The HT culture and assessment techniques employed for this study are detailed in **Chapter 4**. This chapter also delves into combinatorial treatment strategies to observe if higher degree of improvement can be achieved through rational combinations of compounds. The addition of combinations of enhancers to the proposed screening tool can be viewed as advantageous, since no commercial HT screens at this scale investigate combinations. Of course, the various combinations would need to be tested across different cell lines and products to confirm validity as an additive to the screening tool (unfortunately this was beyond the time and resource window for this project). Small scale-up studies followed to investigate the validity of the HT study predictions.

As mentioned earlier, this chapter would inform the design of a commercial screening tool to employ in the biopharmaceutical industry. Given that optimal concentrations and combinations are likely to be process dependent (cell line, product, base media) we aimed to develop a simple screening platform and process to enable bespoke media supplementation strategies as potential “out of the box” solutions. The product platform would be based on the HT platform described in **Chapter 4**. **A 96 DWP coated with enhancers or combinations of enhancers in each well would be available for a user to test with their production system.** The analytical data gathered from the screens and DOEs would help create novel media supplementation strategies that are completely bespoke to a user’s production system.

5.2. Experimental Approach

Before embarking on an extensive screening exercise to identify SMEs, it was imperative to devise a hierarchical approach to maximise information and probability of success. This approach is highlighted in **Figure 5.1** and expanded upon in **Figure 5.2**. Firstly, we undertook a vast literature survey to identify prior successful SME deployment strategies and functions of the cell to target. Studies in mammalian cells (especially CHO) were prioritised and any previous work performed in the David James' laboratory at The University of Sheffield was also taken into account. Functional targets were chosen based on their ability to improve cell growth and production processes. This amalgamated into the creation of a screening library wherein SMEs were grouped based on their broad function.

SME screens were performed in a simple setup, with the chemical added on day 0 of a 5-day batch HT process. Minimum of 6 concentrations were tested per chemical. A one-factor-at-a-time (OFAT) approach was employed. HT measurements of growth and titer were recorded on day 5. Data from these screens informed which chemicals improve cellular productivity at the expense of growth. These chemicals would be better suited for a delayed addition strategy (as detailed in **Section 4.3.6**). A biphasic culture modality would thus be created allowing cells to proliferate (allowing sufficient biomass accumulation) before switching to protein production phase stimulated by the addition of the chemical. A small subset of chemicals was taken forward for delayed addition testing with the SME added to culture on day 3.

Having completed the rigorous screening phase, we were able to elucidate clear enhancers of growth and titer/qP in our model cell line. With the aim of maximising these benefits, combinatorial designs were investigated to test for positive interactions (synergistic, additive or enhancing). 2 separate full factorial designs were employed to test for combinations while trying to maximise growth and qP respectively. A third combinatorial design with both enhancer groups aimed to display DOE designs as an informatic resource to manipulate culture performance for a desirable output.

Having performed all experimentation in 96 DWP batch conditions, we were interested to observe how selected chemicals and combinations performed in a more industrially relevant setting. Shaking Erlenmeyer fed-batch studies were performed over 12 days to ascertain scalability. Given time constraints, extra optimisation (for example: trialling different feed days, addition of SME at different stages of cell growth) was not performed to extract the best fed-batch performance. Thus, this part of the study should only be viewed as an exemplar case study and does not indicate best performing fed-batch conditions.

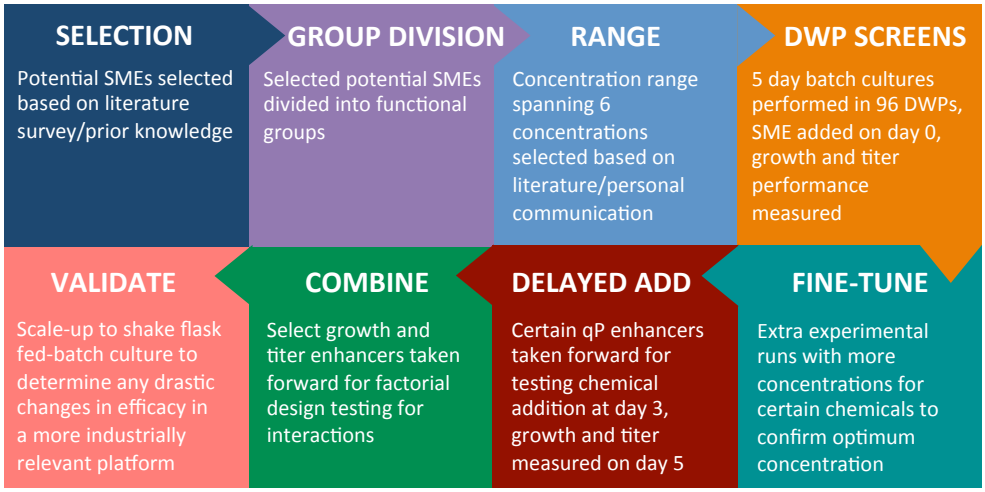

Figure 5.1 Iterative approach taken to identify and test SMEs and their combinations. Decision-making approaches for each molecule are highlighted in subsequent sections. All experimentation performed in 96 DWP micro-scale cultures. The final experimentation approach involved scale-up to shake flask fed-batch culture to validate micro-scale observations. Figure concept from:(Brühlmann et al., 2017b)

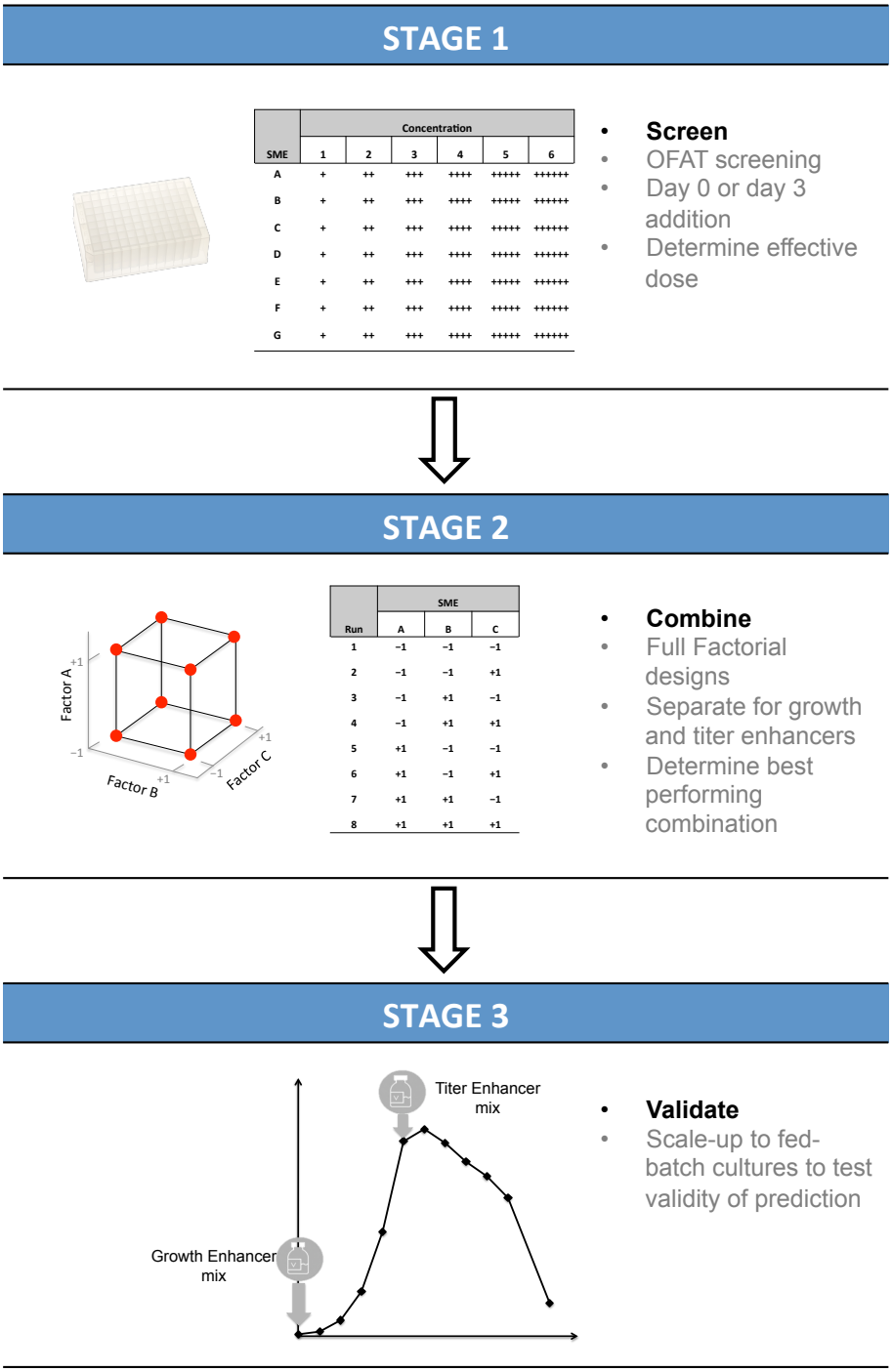

Figure 5.2 Enhancer screening strategy for recombinant protein production. A summary of the experimental approach undertaken to determine bespoke media environments for enhanced growth and/or protein production performance of a biopharmaceutical production host. Stage 1: One-factor-at-a-time screening of various factors of interest that were selected from previous literature. Day 0 addition or exponential phase addition were trialled at multiple concentrations to determine best concentration and timing of addition. Stage 2: Selected growth and qP/titer enhancers taken forward for DOE based combinatorial designs. 1 effective concentation per chemical. Stage 3: Validation of the deep well plate predictions at a larger scale. Fed-batch shaking flask mode was selected to observe how additional nutrient feeds impact enhancer performance.

5.3. Results

5.3.1. Informed Selection of Potential SMEs

Detailed selection criteria were designed to inform the selection of SMEs from experimental data in literature sources and *a priori* knowledge. An effective SME is a molecule that:

(i.) Has been trialled in mammalian cell types.

(ii.) Is not toxic to CHO cells at its effective concentration i.e. cells remain viable (≥ 85%) for the duration of incubation.

(iii.) Produces a titer or growth boost of at least 1.2 fold in prior literature (or is significance tested) or is predicted to produce a titer/growth enhancement based on function.

(iv.) Is soluble in a solvent of choice. Ideally the solvent is water. If the molecule is insoluble in water, the solvent selected must not majorly impact cell culture performance negatively at its final volume percentage (v/v%). Suitable vehicles and their working volume percentage are as described in **Section 4.3.7**.

(v.) Do not have any major regulatory concerns known. Some small molecules are being trialled for therapeutic use; any regulatory concerns raised during testing would have to be considered in a biopharmaceutical production scenario as well.

(vi.) Generally safe to handle in a laboratory premise.

(vii.) Potential for performance elevating interaction with other SMEs, i.e. act in conjunction with other SMEs to produce a growth or titer boost greater than that of the singular SME.

Based on these set of rules, a broad literature survey was performed, leading to the development of an effector SME library. The potential effector molecules were divided into 8 distinct functional categories; the categories and rationale behind adoption is shown below. A further summary of all chemicals used in this study is shown in **Table 5.1**.

(i.) Metal ions: Components of media and generally co-factors for various metabolic processes in the cell. Supplementation into basal media has proved successful in prior studies.

(ii.) Metabolic modulators: Chemicals that target various metabolic processes in the cell. Processes targeted include lactate and ammonia metabolism to reduce toxic-product build up. Other processes important to cell growth have also been targeted in mammalian lines with benefit to growth.

(iii.) Fatty acids: Free fatty acids form media components and can assist in cell growth and survival. Fine-tuning their concentrations in media could be beneficial for improved growth/productivity.

(iv.) Chemical chaperones: Employed in misfolding disease models to prevent aggregation and correct protein folding. Recent studies on application in CHO cells to relieve folding, assembly and secretion bottlenecks.

(v.) HDAC inhibitors: Molecules that generally up regulate transcription through HDAC inhibition.

(vi.) DNA/Histone methyltransferase inhibitors: Molecules that can relive transcriptional bottlenecks by inhibiting gene repressive methyltransferases.

(vii.) Cell cycle inhibitors: Chemicals that enhance qP by arresting cells at a certain cell cycle phase while maintaining viability.

(viii.) Carboxylic acids: structurally similar entities to common HDAC inhibitors.

Stock concentrations were created, filter sterilised and stored at 4°C for short-term storage and at −20°C for long-term storage. The subsequent sections highlight the effects of the OFAT SMEs on cellular growth and productivity. All experimentation was performed in 96 DWPs with culture attributes recorded on day 5. Cobra 38, a CHO-S transfectant stably producing an IgG1 molecule was employed for all experimentation.

Table 5.1 Bioactive small molecules tested in this study.

Small Molecule Enhancer (abbreviation)	Chemical Formula	Source	Solvent	Stock Conc.	Range Tested	Delayed Addition: Range	Rationale	Reference
FUNCTIONAL GROUP 1: METAL IONS								
Copper(II) Sulphate Pentahydrate **(Cu)**	$CuSO_4.5H_2O$	Sigma Aldrich	H_2O	5 mM	0.5 to 100 µM		• Assists in metabolic shift from lactate production to consumption; known to improve growth and titer. • Co-factor for many enzymatic processes.	(Yuk et al., 2014; Yuk et al., 2015b)
Zinc Sulphate Heptahydrate **(Zn)**	$ZnSO_4.7H_2O$	Sigma Aldrich	H_2O	2.5 mM	2 to 200 µM		• Protects cells from oxidative damage. • Co-enzymes for reactions in the cell. • Part of zinc finger proteins that regulate transcription. • Insulin mimicking properties.	(Kim and Park, 2016; Sigma-Aldrich,; Wong et al., 2004)
Ferric Ammonium Citrate **(FAC)**	$C_6H_{11}FeNO_7$	Acros Organics	H_2O	200 mM	0.05 to 5 mM		• Iron: an enzyme co-factor. • Citrate: intermediate of TCA cycle; used for generating energy.	(Bai et al., 2010; Sigma-Aldrich,)
Manganese(II) Chloride Tetrahydrate **(Mn)**	$MnCl_2.4H_2O$	Sigma Aldrich	H_2O	0.2 mM	0.05 to 5 µM		• Galactosylation modulator: co-factor for β- 1,4 galactosyltransferase.	(Grainger and James, 2013; Gramer et al., 2011)
Sodium Orthovanadate **(V)**	Na_3VO_4	Sigma Aldrich	H_2O	0.5 mM	0.05 to 50 µM		• Insulino-mimetic.	(McGrew, 2005; Srivastava and Mehdi, 2005)
FUNCTIONAL GROUP 2: METABOLIC MODULATORS								
Citric Acid	$HOC(COOH)(CH_2COOH)_2$	Sigma Aldrich	H_2O	200 mM	0.05 to 5 mM		• Intermediate of TCA cycle; used for generating energy. • Helps in the initiation of lipid synthesis.	(Bai et al., 2010)
Sodium Dichloroacetate **(DCA)**	Cl_2CHCO_2Na	Sigma Aldrich	H_2O	200 mM	0.5 to 20 mM		• Pyruvate dehydrogenase kinase inhibitor. • Promotes entry into Kreb's cycle. • Decreases lactate production.	(Buchsteiner et al., 2018; Skelton et al., 2010)
SB 216763	$C_{19}H_{12}Cl_2N_2O_2$	Abcam	DMSO (0.2% v/v)	50 mM	0.5 to 30 µM		• Activates transcription factor/genes involved in lipogenesis: SREBP1c, FAS.	(Hansmannel et al., 2006; Kim et al., 2004)
T 0901317	$C_{17}H_{12}NSO_3F_9$	Santa Cruz Biotechnology	DMSO (0.2% v/v)	17.5 mM	0.05 to 5 µM		• Activates transcription factor/genes involved in lipogenesis: SREBP1c, FAS.	(Hansmannel et al., 2006)

Small Molecule Enhancer (abbreviation)	Chemical Formula	Source	Solvent	Stock Conc	Range Tested	Delayed Addition: Range	Rationale	Reference
FUNCTIONAL GROUP 3: FATTY ACIDS								
Palmitic Acid	$CH_3(CH_2)_{14}CO_2H$	Acros Organics	Ethanol (0.2% v/v)	140 mM	0.1 to 150 µM		• First fatty acid produced in lipid biosynthesis pathway, precursor for other fatty acids.	(Schmid et al., 1991)
Linoleic Acid	$CH_3(CH_2)_4CH=CHCH_2CH=CH(CH_2)_7CO_2H$	Sigma Aldrich	Ethanol (0.2% v/v)	14 mM	0.1 to 150 µM		• Improved survival of cells in agitated cultures. • Precursor for other fatty acids.	(Butler et al., 1999; Butler and Huzel, 1995; Schmid et al., 1991)
FUNCTIONAL GROUP 4: CHEMICAL CHAPERONES								
Glycerol	$C_3H_8O_3$	Sigma Aldrich	Liquid form	100%	0.1 to 4%		• Stabilises proteins; reduces aggregation.	(Johari et al., 2015; Liu and Chen, 2007; Rodriguez et al., 2005)
Trehalose	$C_{12}H_{22}O_{11} \cdot 2H_2O$	Sigma Aldrich	H_2O	1.25 M	25 to 250 mM		• Suppresses antibody aggregation.	(Onitsuka et al., 2014)
L-Proline	$C_5H_9NO_2$	Sigma Aldrich	H_2O	4 M	12.5 to 300 mM		• Decreases aggregation. • Improves protein production. • Can protect against oxidative stress.	(Hwang et al., 2011; Krishnan et al., 2008)
4-Phenylbutyric Acid **(4PBA)**	$C_{10}H_{11}NaO_2$	Sigma Aldrich	H_2O	100 mM	0.125 to 4 mM	0.75 to 1 mM	• Most well researched chemical chaperone. • Promotes synthesis of molecular chaperones. • Reduces ER stress.	(De Almeida et al., 2007; Cortez and Sim, 2014; Johari et al., 2015)
6-Phenylhexanoic Acid **(6PHA)**	$C_6H_5(CH_2)_5CO_2H$	Sigma Aldrich	DMSO (0.1% v/v)	5 M	25 to 500 µM		• 4PBA analog.	(Mimori et al., 2012; Yam et al., 2007)
Betaine	$(CH_3)_3N^+CH_2COO^-$	Sigma Aldrich	H_2O	2.5 M	10 to 200 mM		• Used in protein misfolding diseases. • Non-cytotoxic in previous studies. • Facilitates ER to Golgi transport.	(Johari et al., 2015; Roth et al., 2012)
Ectoine	$C_6H_{10}N_2O_2$	Sigma Aldrich	H_2O	2.5 M	25 to 300 mM		• Non-toxic. • Alleviates protein misfolding and aggregation.	(Roth et al., 2012)

Small Molecule Enhancer (abbreviation)	Chemical Formula	Source	Solvent	Stock Conc	Range Tested	Delayed Addition: Range	Rationale	Reference
Tauroursodeoxycholic Acid, sodium salt **(TUDCA)**	$C_{26}H_{44}NO_6S.Na$	Merck Millipore	H_2O	200 mM	0.25 to 3 mM	0.25 to 3 mM	• Alleviates protein aggregation. • Cytoprotective: antioxidant and anti-apoptotic. • Mitigates ER stress induced UPR.	(De Almeida et al., 2007; Cortez and Sim, 2014; Uppala et al., 2017)
Trimethylamine N-oxide **(TMAO)**	$(CH_3)_3N(O)$	Sigma Aldrich	H_2O	2.5 M	6.25 to 200 mM		• Stabilises proteins.	(Gawron et al., 2010; Johari et al., 2015; R.S. et al., 2011)
Dimethyl Sulfoxide **(DMSO)**	$(CH_3)_2SO$	Sigma Aldrich	Liquid form	100%	0.5 to 3% (v/v)	1 to 1.5 mM	• Promotes protein folding.	(Cortez and Sim, 2014; Johari et al., 2015)
FUNCTIONAL GROUP 5: HDAC INHIBITORS								
Sodium Butyrate **(NaBu)**	$CH_3CH_2CH_2COONa$	Sigma Aldrich	H_2O	50 mM	0.25 to 2 mM	0.25 to 1 mM	• Class I and IIa histone deacetylase inhibitor. • Improves gene accessibility to a transcription factor. • Frequently employed in CHO cell production studies.	(Backliwal et al., 2008; Jiang and Sharfstein, 2008; Kim and Bae, 2011; Sung et al., 2004)
Sodium Valproate **(VPA)**	$C_8H_{15}NaO_2$	Sigma Aldrich	H_2O	50 mM	0.15 to 2 mM		• Class I and IIa histone deacetylase inhibitor • Considered less cytotoxic compared to NaBu in certain studies.	(Backliwal et al., 2008)
Scriptaid	$C_{18}H_{18}N_2O_4$	Sigma Aldrich	DMSO (0.1% v/v)	4 mM	1.6 to 3.2 µM	1.8 to 2 µM	• HDAC inhibitor. • Does not induce apoptosis.	(Lee et al., 2008; Su et al., 2000; Xu et al., 2013)
Trichostatin A **(TSA)**	$C_{17}H_{22}N_2O_3$	Cayman Chemical	DMSO (0.1% v/v)	10 mM	0.1 to 1.5 µM	0.35 to 1 µM	• Pan HDAC inhibitor, competitive inhibition of HDACs.	(Backliwal et al., 2008; Nan et al., 2004)
MS 275	$C_{21}H_{20}N_4O_3$	Selleckchem	DMSO (0.1% v/v)	7 mM	0.1 to 3 µM	0.5 to 3 µM	• HDAC 1,2,3,4 inhibitor.	(Backliwal et al., 2008)
FUNCTIONAL GROUP 6: METHYLTRANSFERASE INHIBITORS								
WDR5-0103	$C_{21}H_{25}N_3O_4$	Sigma Aldrich	DMSO (0.2% v/v)	150 mM	5 to 100 µM		• Histone methyltransferase inhibitor. • Successful in increasing transgene expression in CHO-K1.	(Christensen, 2016)

Small Molecule Enhancer (abbreviation)	Chemical Formula	Source	Solvent	Stock Conc	Range Tested	Delayed Addition: Range	Rationale	Reference
RSC133	$C_{18}H_{15}N_3O_2$	Sigma Aldrich	DMSO (0.2% v/v)	100 mM	5 to 100 µM		• Dual inhibitor of DNA methyltransferases and HDACs. • Successful in increasing transgene expression in CHO-K1.	(Christensen, 2016)
Procaine Hyrdochloride **(Procaine)**	$H_2NC_6H_4CO_2CH_2CH_2N(C_2H_5)_2{\cdot}HCl$	Sigma Aldrich	H_2O	50 mM	0.05 to 1.5 mM		• DNA methyltransferase inhibitor. • Used in medical circles: no regulatory issue.	(Lyko and Brown, 2005)
UNC1999	$C_{33}H_{43}N_7O_2$	Cayman Chemical	DMSO (0.1% v/v)	50 mM	0.5 to 15 mM		• Histone methyltransferase inhibitor. • Successful in increasing transgene expression in CHO-K1.	(Christensen, 2016)
RG108	$C_{19}H_{14}N_2O_4$	Sigma Aldrich	DMSO (0.2% v/v)	200 mM	20 to 180 µM		• Enzyme blocking DNA methyltransferase inhibitor. • Does not bind to DNA: less cytotoxic.	(Backliwal et al., 2008; Lyko and Brown, 2005)
FUNCTIONAL GROUP 7: CELL CYCLE INHIBITORS								
Germanium(IV) oxide **(Ge)**	GeO_2	Sigma Aldrich	H_2O	50 mM	0.1 to 10 mM		• G2/M phase inhibitor. • Shown to improve specific mAb production in CHO.	(Chiu et al., 2002; Galbraith et al.,)
Lithium Chloride **(Li)**	LiCl	Sigma Aldrich	H_2O	250 mM	0.005 to 20 mM	12.5 to 20 mM	• Causes G2/M phase arrest. • Improves production of various proteins: fc fusion and mAb .	(Ha et al., 2014; Park et al., 2016)
D,L-Sulforaphane	$C_6H_{11}NOS_2$	Sigma Aldrich	DMSO (0.1% v/v)	70 mM	2.5 to 30 µM	15 µM	• Novel G2/M phase inhibitor	(Chang et al., 2013; Park et al., 2016)
BI 2536	$C_{28}H_{39}N_7O_3$	Cayman Chemical	DMSO (0.2% v/v)	0.5 mM	0.005 to 0.15 µM	0.1 µM	• Inhibits polo-like kinase 1 (PLK1), an enzymatic precursor for mitosis. • Improved transient yields (more likely to be involved in gene delivery)	(Christensen, 2016)
RO3306	$C_{18}H_{13}N_3OS_2$	Cayman Chemical	DMSO (0.2% v/v)	25 mM	1 to 20 mM		• G2/M phase inhibitor.	(Vassilev et al., 2006; Vassilev, 2006)

Small Molecule Enhancer (abbreviation)	Chemical Formula	Source	Solvent	Stock Conc	Range Tested	Delayed Addition: Range	Rationale	Reference
FUNCTIONAL GROUP 8: CARBOXYLIC ACIDS								
5-Phenylvaleric Acid **(PVA)**	$C_6H_5CH_2CH_2CH_2CH_2COOH$	Sigma Aldrich	DMSO (0.2% v/v)	2.8 M	0.2 to 2 mM		• Many successful SMEs have an aromatic carboxylate structure. • Hypothesise that generally carboxylates could act as SMEs. • These 3 molecules been trialled in a similarly hypothesised study in CHO.	(Allen et al., 2008; Bora-Tatar et al., 2009; Camire et al., 2017; Liu et al., 2001)
Hydrocinnamic Acid **(HCA)**	$C_6H_5CH_2CH_2COOH$	Sigma Aldrich	Ethanol (0.1% v/v)	4 M	0.2 to 4 mM	1.2 to 3.5 mM		
2-Thiopheneacetic Acid **(2TAA)**	$C_6H_6O_2S$	Sigma Aldrich	DMSO (0.2% v/v)	2.8 M	0.2 to 2 mM	0.4 to 2 mM		
2-Thiophenecarboxylic Acid **(2TCA)**	$C_5H_4O_2S$	Sigma Aldrich	DMSO (0.2% v/v)	2.8 M	0.2 to 4 mM		• 2TAA structural analogues.	PubChem Similarity search (Kim et al., 2016b)
2-Thiophenepropionic Acid **(TPA)**	$C_7H_8O_2S$				0.2 to 4.8 mM	1.6 to 4.8 mM		
2-Thiophenebutyric Acid **(TBA)**	$C_8H_{10}O_2S$				0.2 to 2 mM			
3-Thiopheneacetic Acid **(3TAA)**	$C_6H_6O_2S$				0.2 to 5.6 mM	1.6 to 5.6 mM		

Sections 5.3.2 to 5.3.9 *describe the screens of 43 SME molecules in a stable producing CHO system. SME was added on day 0.*

5.3.2. Metal Ion Supplementation

5 metal ion compounds: copper sulphate (Cu), zinc sulphate (Zn), ferric ammonium citrate (FAC), manganese chloride (Mn) and sodium orthovanadate (V), were selected for supplementation experiments. Since these compounds are already components of general cellular growth media, it was interesting to observe if additional supplementation could fine-tune responses for added benefit. Metal ion supplementation results are shown in **Figure 5.3**. Cu supplementation at even its lowest concentration (0.5 µM) produced a growth stimulation of 1.4 fold over the control. Similar gains were seen at higher concentrations. Increase in total IVCD led to an increase in production titer. These results are consistent with previous studies performed with Cu (Qian et al., 2011; Yuk et al., 2014; Yuk et al., 2015b), wherein a reduction in lactate accumulation was observed concurrently.

Zn and FAC produced concentration specific responses. Zn at 150 µM produced a 20% increase in total IVCD and 30% increase in overall titer. Interestingly, at 200 µM, no growth stimulation but a major titer stimulation was observed. This was interesting to observe since Zn is considered an insulino-mimetic compound and was predicted to preferentially enhance cell growth (Wong et al., 2004). FAC (500 µM) improved IVCD by 1.6 fold and titer by 1.8 fold. Mn supplementation did not produce any noteworthy improvements in growth or titer. This was not unexpected, since Mn is involved in the modulation of galactosylation (Grainger and James, 2013; Gramer et al., 2011), rather than protein production itself. It would be interesting to observe how the molecule impacted galactosylation in our production system, however the lack of HT glycosylation analytics at our disposal hindered this. Various concentrations of V induced slight titer boosts (ranging from 7 to 18%), however no improvements in cell growth were observed.

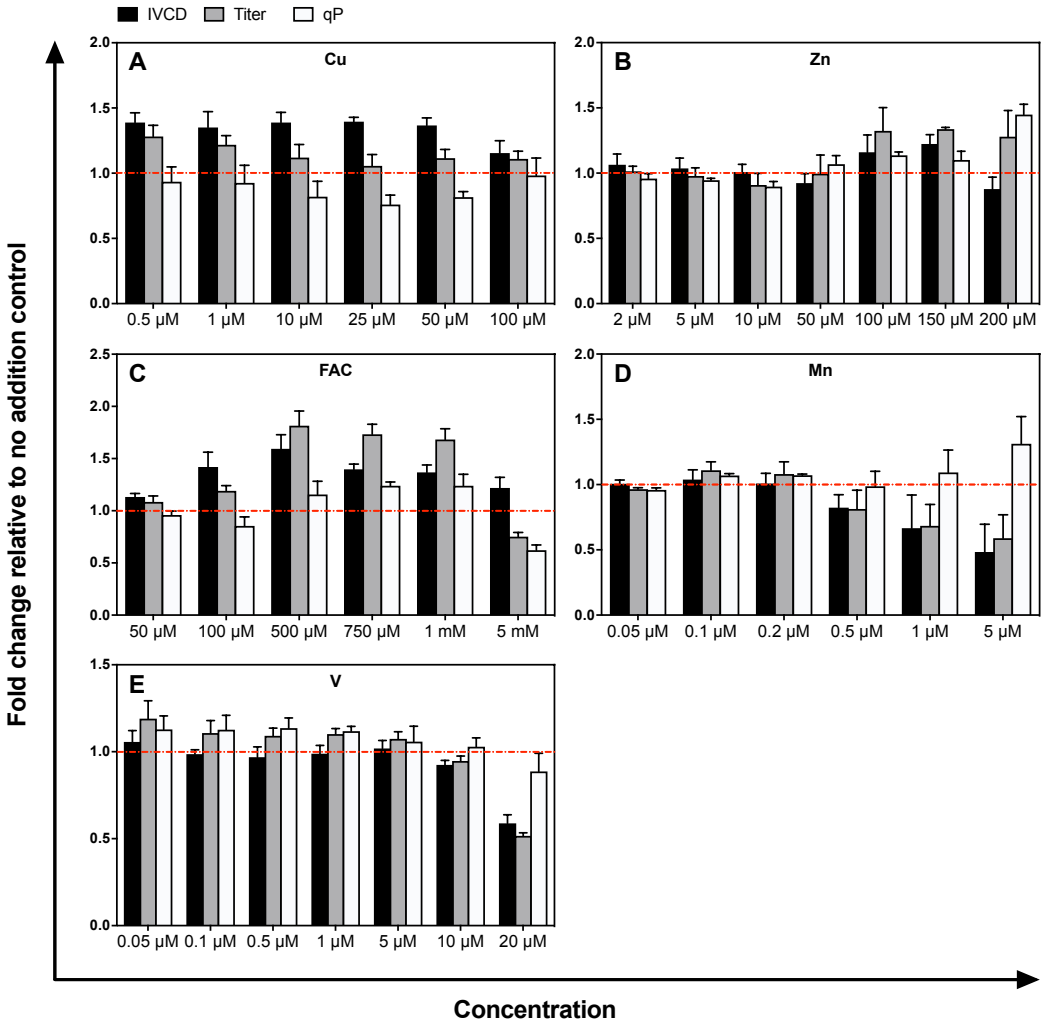

Figure 5.3. Culture responses due to metal ion supplementation. Cobra 38 cells were cultured in the presence of increasing concentrations of different metal ions. Cells were seeded at 0.2×10^6 cells mL^{-1} in a 96 DWP system and cultured for 5 days. Growth was measured using the Vi-CELL XR and/or PrestoBlue assay and titer recorded using the Valita™TITER assay. SMEs: **(A)** Copper Sulphate (Cu), **(B)** Zinc Sulphate (Zn), **(C)** Ferric Ammonium Citrate (FAC), **(D)** Manganese(II) Chloride (Mn) and **(E)** Sodium Orthovanadate (V). Data is shown as a fold change to the no addition control (red dashed line). Data shown is the mean and SEM of three biological replicates (two experimental replicates for Mn) with three technical replicates.

5.3.3. Metabolic Modulator Supplementation

Modulating cell metabolism towards increased viable cell proliferation can yield benefits to the mammalian cell production processes (Altamirano et al., 2001; Kumar et al., 2007). Using small molecule modulators as a tool to achieve this,

we trailed 5 different small molecule modulators. Dichloroacetic acid (DCA) is a well-known inhibitor of pyruvate dehydrogenase kinase, funnelling cellular metabolism towards the TCA cycle (Skelton et al., 2010). This reduces flux towards aerobic glycolysis, which is known to produce lactate, a toxic by-product. We observed mild titer enhancement using DCA as a supplement (**Figure 5.4A**). This could be explained by its indirect effect on histone acetylation, which is known to play a role at the transcription level (Matsuhashi et al., 2015; Moussaieff et al., 2015). Interestingly, no stimulatory effect on cell growth was observed.

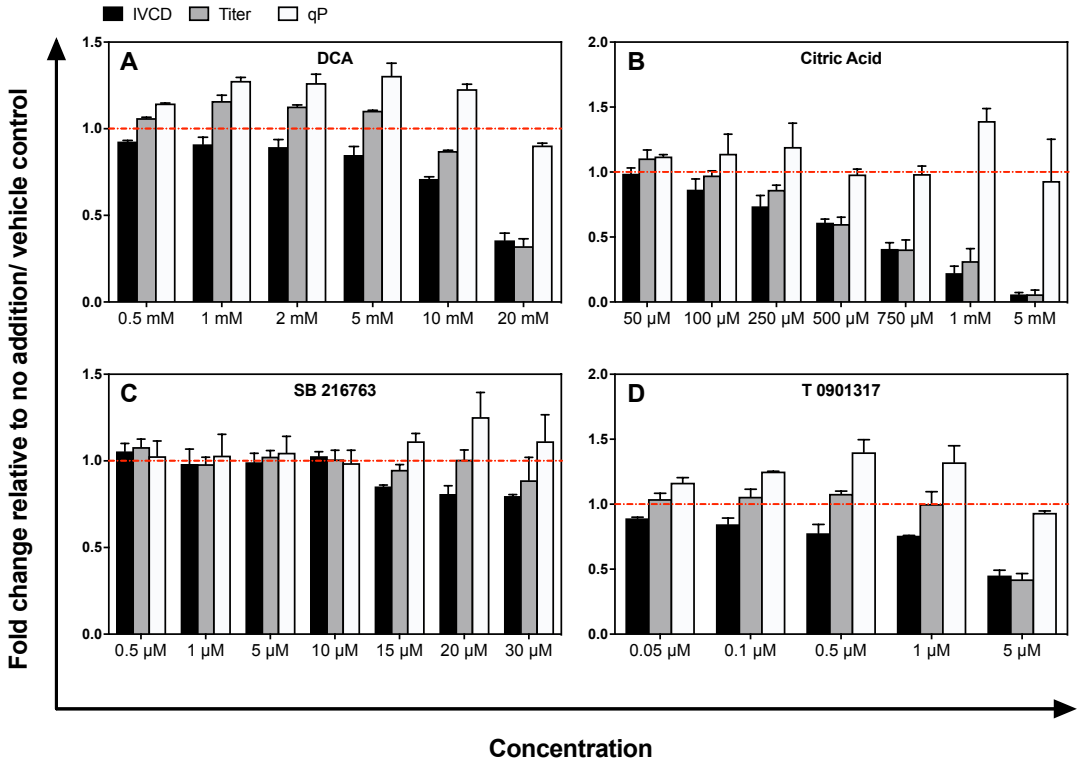

Figure 5.4. Growth and titer responses to metabolic modulator supplementation. Cells were seeded at 0.2×10^6 cells mL^{-1} in a 96 DWP culture system. Growth and titer were measured on day 5. SMEs: **(A)** Dichloroacetic Acid (DCA), **(B)** Citric Acid, **(C)** SB 216763 and **(D)** T0901317. Red dashed line indicates level of no addition/vehicle control. Data represented as a fold change to the control. Mean ±SEM represented of two experimental replicates each with three technical repeats.

We employed citric acid (the first TCA cycle substrate) to attempt to redirect cellular metabolism towards the TCA cycle instead of lactate production. Maximum titer production is associated with increased flux to the TCA cycle

(Templeton et al., 2013). However, we were unable to demonstrate any utility of citric acid in improving cell growth/proliferation or titer. This was interesting since the iron compound of citrate (FAC: **Figure 5.3**) did yield improvements in cell growth and productivity across the same concentration range. This observation revealed that the iron component could play a crucial role towards the improvement in performance and that citrate could be fulfilling the role of an iron carrier and not impacting TCA cycling efficiency. Further experimentation would need to be performed to confirm this. It cannot be discounted that addition of citric acid in media could have deleterious effects on cell culture such as increased acidity and osmolarity masking any benefit to cell metabolism.

Cancer cells are known to depend on lipid biogenesis to meet nutritional requirements while proliferating (Mukherjee et al., 2012). Based on this principle, we tried SB 216763 (**Figure 5.4C**) and T0901317 (**Figure 5.4D**) supplementation. Both molecules facilitate the upregulation of transcription factors (sterol regulatory element-binding proteins (SREBP)) involved in lipogenesis pathways (Hansmannel et al., 2006; Kim et al., 2004). Expression of fatty acid synthase (FAS), a key lipogenic gene was enhanced through the use of these chemicals in previous studies (Hansmannel et al., 2006; Kim et al., 2004). However, only slight improvements in growth, titer or qP were observed in our production system.

5.3.4. Fatty Acid Supplementation

Fatty acid biosynthesis, like previously mentioned, is important for cancer cell proliferation. While we did employ modulators of metabolism to promote TCA cycling to produce precursors for fatty acid synthesis, we were intrigued to investigate free fatty acid supplementation (Schmid et al., 1991). Free fatty acids do form part of commercially available cell culture media, so it was interesting to observe if additional supplementation yielded any benefit. Palmitic and linoleic acids form precursors for more complex fatty acids and we trialled various concentrations of these two molecules (**Figure 5.5A and B**). There were no positive improvements in IVCD with no real improvement in titer either.

It could be that CHO cells relied mostly on *de novo* lipid synthesis or that the levels of fatty acids in media were sufficient. We decided against testing other fatty acid molecules and focused our efforts on other interesting compound groups.

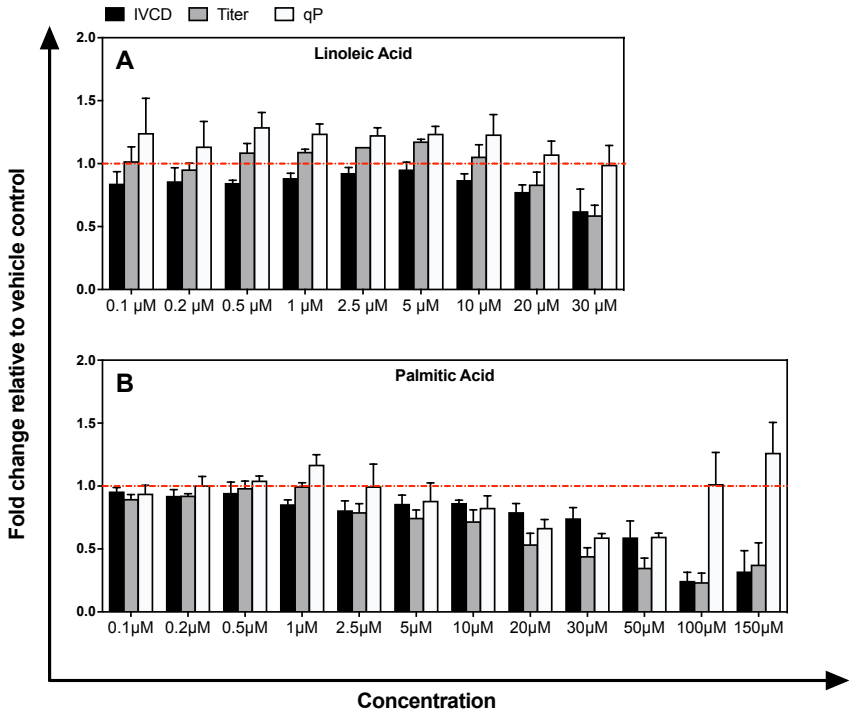

Figure 5.5 Fatty acid supplementation effects on culture attributes. Cells were seeded at 0.2×10^6 cells mL^{-1} in a 96 DWP culture system. Growth and titer were recorded on day 5. Chemicals employed: **(A)** Linoleic Acid and **(B)** Palmitic Acid. Data (IVCD: black bar, Titer: grey bar, qP: white bar) represented as a fold change over the ethanol vehicle (0.2%v/v) control. Data shown is mean ± SEM of two experimental and two technical replicates.

5.3.5. Chemical Chaperone Supplementation

Chemical chaperones are indirectly involved in improvements to protein folding and stabilisation. They are unlike their molecular chaperone counterparts that are directly involved in cellular processes that target protein folding and secretion (Cortez and Sim, 2014). Chemical chaperones have proved extremely effective in cases of DTE protein expression (Johari, 2015; Roth et al., 2012) and various misfolding diseases (Yam et al., 2007). Employing the same

rationale as the studies mentioned above, we trialled chemical chaperone molecules in our CHO-S expression system. Keeping in mind that the molecule expressed in our system is not particularly difficult-to-express (as seen with the high protein titers from our system (**Figure 4.7**)), we hypothesised that any effects seen in our system could be further amplified in a truly DTE protein system. The chemical chaperones tested were categorised into 2 sub-divisions: osmolytes (**Figure 5.6A-G**) and hydrophobic chaperones (**Figure 5.6H-J**). The osmolyte chaperones stabilise the protein molecule and promote folding. L-proline recording a 1.4 fold increase in volumetric titer at 50 mM was the most effective osmolyte. Cell growth remained unaffected at that concentration. Interestingly, all CHO cells in use today require proline for their growth (Wurm, 2013). Thus, it could be debated whether the increase in cellular production was a result of fulfilment of the nutritional requirement of the cell rather than a chaperone based improvement. Testing with different cell lines and different products would help test the validity of this narrative. 0.5% (v/v) Glycerol supplementation displayed a 20% titer increase. All other osmolytes only displayed stimulatory effects to cellular qP, with dimethyl sulfoxide (DMSO) recording the best qP sitmulation of 4.1 fold at 1.5% (v/v) without complete suppression of cell growth. Betaine (Johari et al., 2015; Roth et al., 2012), Trimethylamine N-oxide (TMAO) (Johari et al., 2015) and trehalose (Onitsuka et al., 2014) have previously been shown to improve volumetric titer and/or decrease aggregation, however they were ineffective in our expression system, strengthening the notion that SME efficacy is cell line and product specific.

3 hydrophobic chaperones were also tested in our stable expression system. 4-Phenylbutyric acid (4PBA) is perhaps the best-known chemical chaperone since it is approved for clinical use to treat urea cycle disorders (Kolb et al., 2015). It was not highly effective with our cell line and product, with 1 mM producing a qP increase of 1.68 fold. 2 mM was cytotoxic to cells and thus was not taken into consideration for further testing. 6-Phenylhexanoic acid (6PHA) was reported as an analogue of 4PBA by Mimori et al. (2012), wherein it proved to be more effective than 4PBA in blocking aggregation and protecting against ER stress in human neuroblastoma cells. However, no such positive effects to cell growth and/or titer were observed in our setup. Furthermore, we trialled a

bile acid, Tauroursodeoxycholic acid (TUDCA). Though operating through a similar mechanism as 4PBA, we observed drastically different results in comparison of 4PBA. TUDCA had no cytotoxic effects, improving titer by 1.6 fold at the 2 mM concentration. All concentrations tested provided various ranges of titer improvements, with some degree of growth repression. The polarising effects of both supposedly functionally similar molecules has been reported before (De Almeida et al., 2007; Uppala et al., 2017) indicating that there could be other underlying mechanisms playing a role in TUDCA titer boosting abilities.

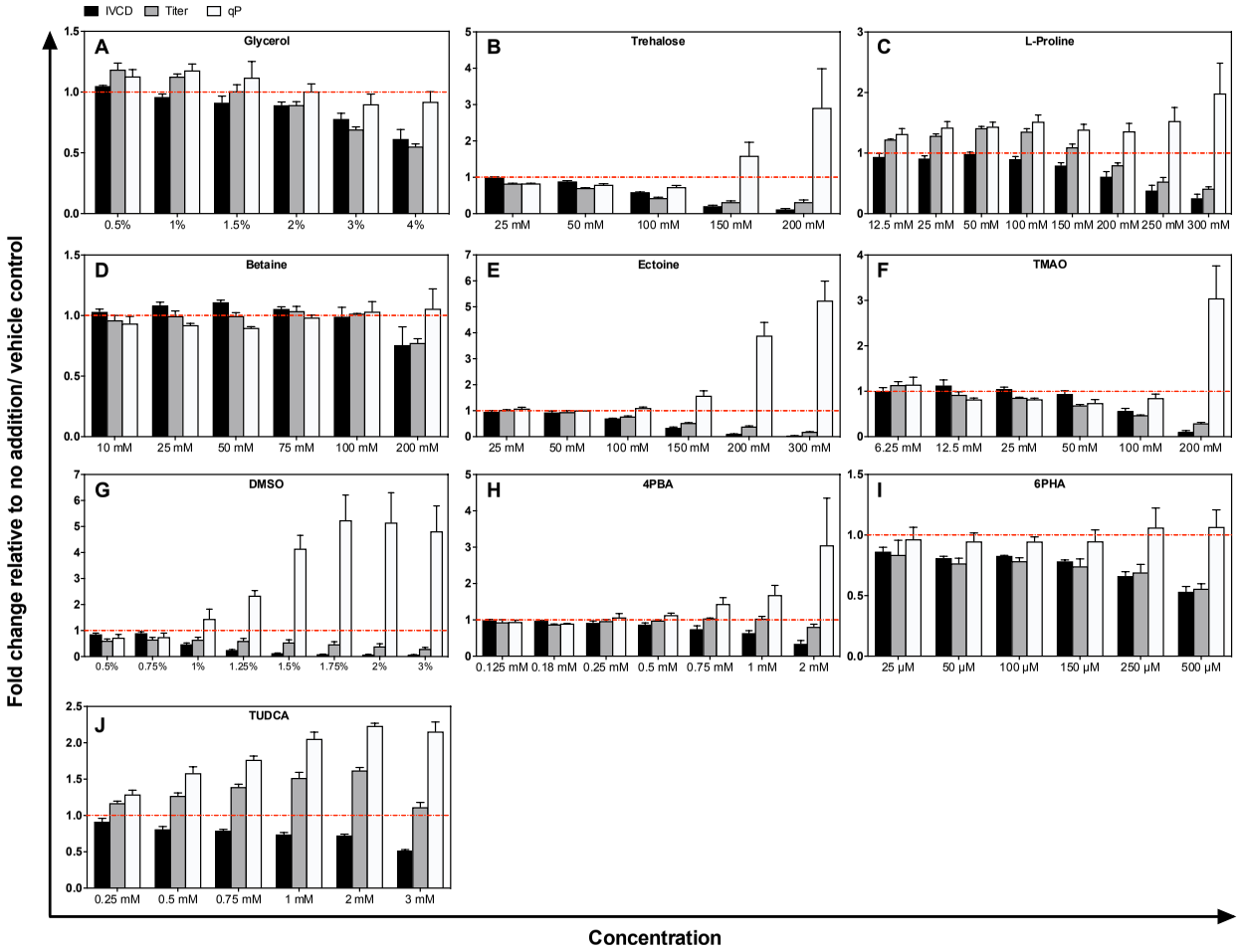

Figure 5.6. High-Throughput screening of chemical chaperone molecules as enhancers of growth and titer. IVCD, titer and qP depicted as a fold change. Growth and titer measurements taken on day 5. SMEs tested: **(A)** Glycerol, **(B)** Trehalose, **(C)** L-Proline, **(D)** Betaine, **(E)** Ectoine, **(F)** Trimethylamine N-oxide, **(G)** Dimethyl sulfoxide (DMSO), **(H)** 4-Phenylbutyric acid (4PBA), **(I)** 6-Phenylhexanoic acid (6PHA) and **(J)** Tauroursodeoxycholic acid (TUDCA). Data represented mean ± SEM of three experimental replicates, with three technical replicates. (6PHA, Trehalose, Betaine, Ectoine and TMAO have two experimental replicates, three technical replicates).

5.3.6. HDAC Inhibitor Supplementation

Epigenetic modification (especially histone acetylation) is heavily associated with antibody production (Backliwal et al., 2008). HDAC inhibitors form the most well researched group of SMEs for the purposes of antibody production stimulation. **Figure 5.7** shows the growth and titer responses to various small molecule HDAC inhibitors. Sodium butyrate (NaBu) is perhaps the most commonly used small molecule HDAC inhibitor. In our system, we observed titer enhancement up to 1.9 fold. Higher concentrations reported a large qP enhancement, with a suppression in growth. Previous studies have shown that NaBu induces apoptosis in cells (Lee and Lee, 2012). In our system, decreased viability was observed from 1.4 mM onwards. Further investigation would be necessary to investigate initiation of any apoptotic pathways. Sodium valproate (VPA) (**Figure 5.7B**) recorded a titer enhancement of 1.27 fold. This is in disagreement with previous literature, which conclude VPA to be a better/on par titer enhancer in comparison to NaBu (Backliwal et al., 2008). Scriptaid was tested as a novel HDAC inhibitor, that has been previously shown to be a general transcriptional enhancer in mammalian cells (Lee et al., 2008; Su et al., 2000; Xu et al., 2013). It only displayed improvements in qP when trialled in our system. Trichostatin A (TSA) is another commonly used HDAC inhibitor. Similar to scriptaid, there were an increase in qP coupled with growth suppression. MS275, an HDAC1 to 4 inhibitor, proved to be an effective titer enhancer (**Figure 5.7E**). At 1 µM, titer was enhanced by 1.7 fold over the vehicle control. Also, growth suppression was not as severe as NaBu.

All chemicals tested in this group improved qP concomitant with growth repression and it was hypothesised that this set of chemicals might yield bigger improvements when deployed at a later stage in the cell culture process. This would mean the cells would be allowed to proliferate for a certain time period before chemical addition, leading to more biomass available for increased qP, resulting in bigger improvements in titer.

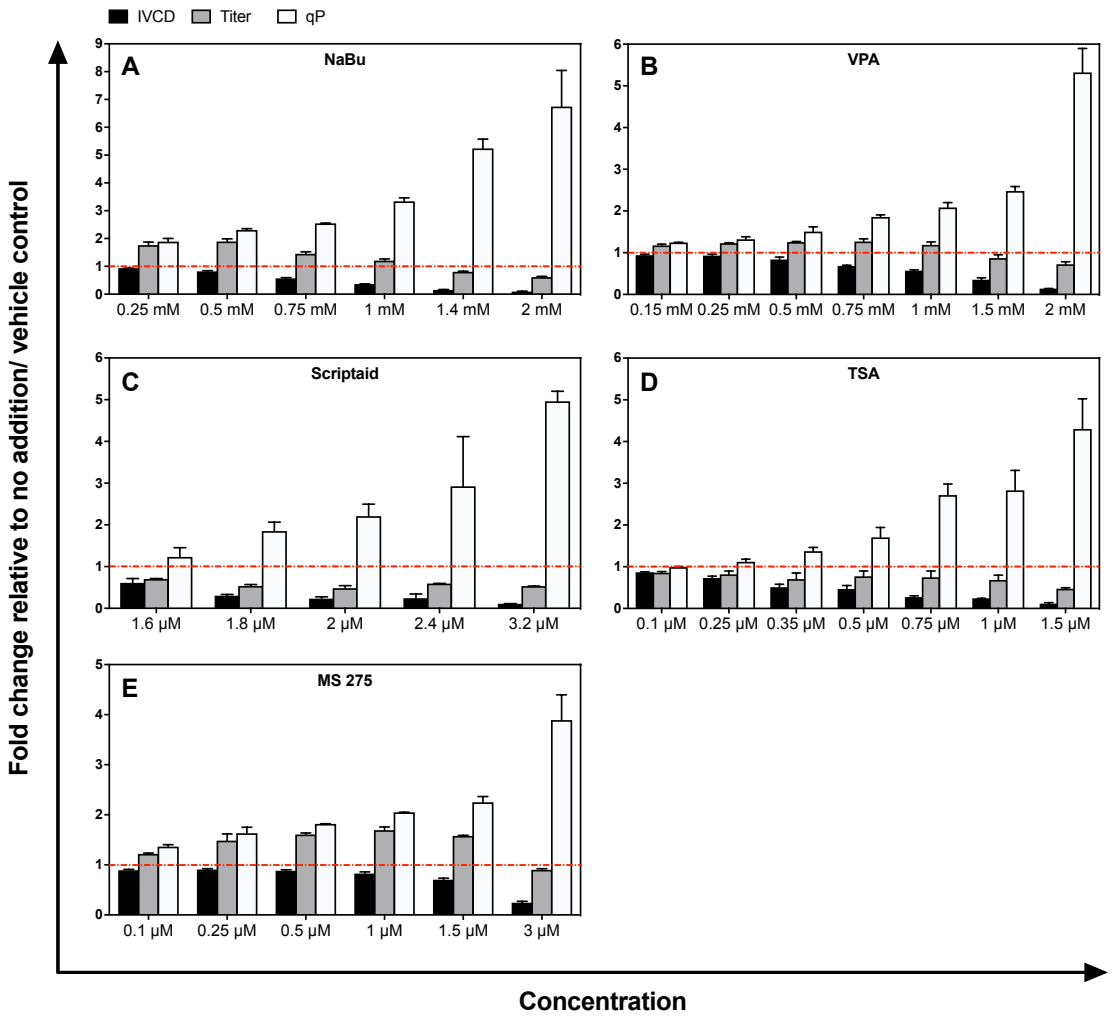

Figure 5.7. HDAC inhibitor supplementation responses over 5 days of DWP batch culture. SME added on day 0 of culture. Growth and titer recorded on day 5. SMEs: **(A)** Sodium butyrate (NaBu), **(B)** Sodium Valproate (VPA), **(C)** Scriptaid, **(D)** Trichostatin A (TSA) and **(E)** MS 275. IVCD, Titer and qP shown as a fold change relative to the no addition/DMSO control (red dashed line). Mean ± standard error represented of two experimental replicates (Scriptaid and TSA: three experimental replicates) with three technical replicates.

5.3.7. DNA/Histone Methyltransferase Inhibitor Supplementation

DNA methylation correlates with a loss in recombinant gene expression in CHO cells (Yang et al., 2010). Few research studies have investigated the use of methyltransferase inhibitors in mammalian cells for improvements in the recombinant protein production process. Backliwal et al. (2008) demonstrated the use of DNA methyltransferase inhibitors in CHO cell production systems; there was substantial benefit of adding these enhancers to culture (up to 1.8

fold improvement over the control) in both transient and stable modes. Using this as a precursor study, we adopted some methyltransferase inhibitors in our HT screens. 2 DNA methyltransferase inhibitors, RG108 (**Figure 5.8E**) and procaine (**Figure 5.8C**) were trialled. There was no substantial stimulation of qP or titer observed with either chemical additive. Procaine produced dose dependent growth repression leading to a qP increase above control level at the highest concentration (1.5 mM). RG108 is generally non-toxic in comparison to other demethylating agents (such as 5-azacytidine), since it does not complex with DNA, preventing strand breaks (Christman, 2002; Xu et al., 2013). While cell growth and viability were largely unaffected across all doses of RG108 trialled in our cell line, no major stimulatory effect on titer was observed. Changing the concentration range could potentially provide more positive results for this molecule.

Apart from DNA methyltransferase inhibitors, we also investigated the use of histone methyltransferase inhibitors. H3K27 (Histone 3, lysine position 27) methylation is associated with gene repression (Wang and Patel, 2013). UNC1999 inhibits enhancer of zeste homolog 2 (EZH2), a catalyst for H3K27 methylation. UNC1999 proved to be an effective transgene expression enhancer (~1.4 fold improvement), in a study performed by Christensen (2016). In our system, there was no titer improvement observed when the molecule was added (**Figure 5.8D**). Similarly, other histone methyltransferases inhibitors tested: WDR5-0103 (**Figure 5.8A**) and RSC133 (**Figure 5.8B**) did not present any major benefit to antibody production, which were previously shown to be beneficial in the study by Christensen (2016).

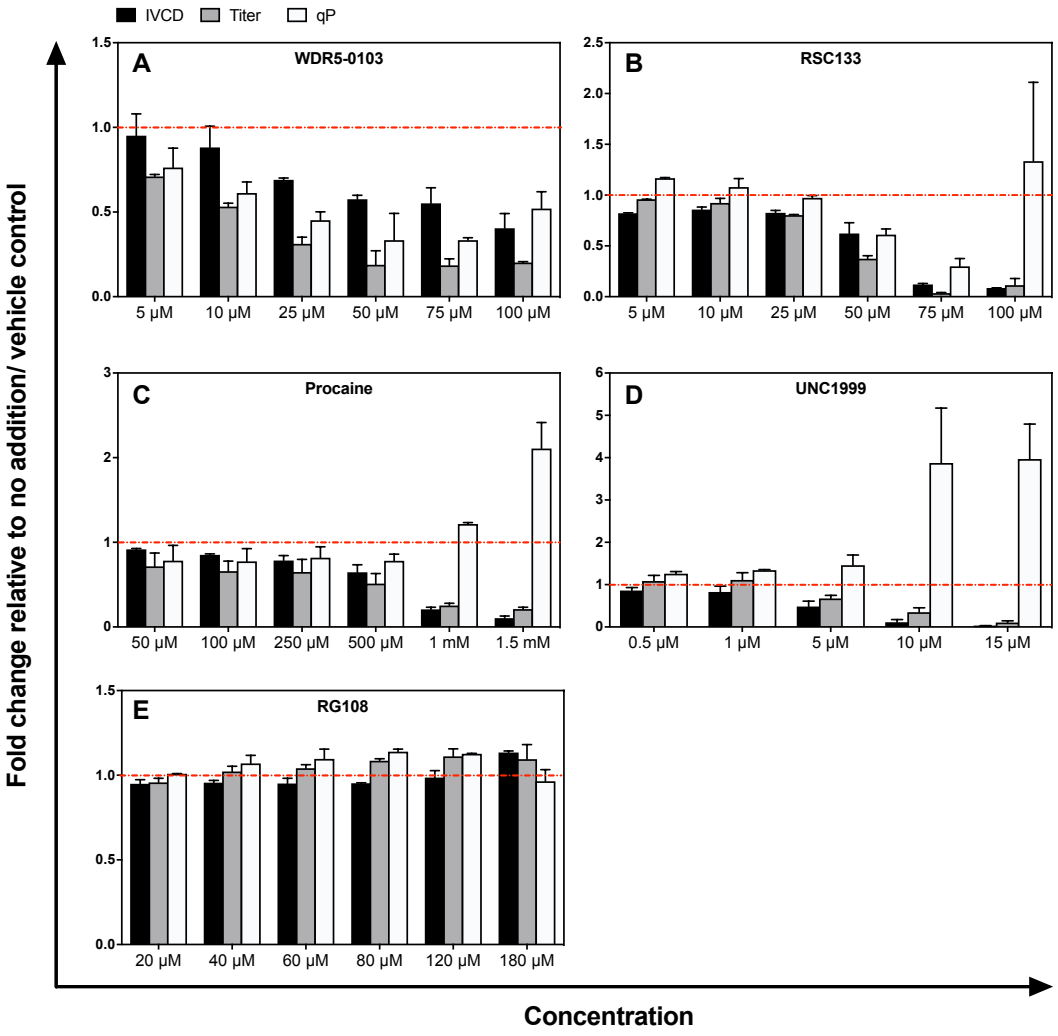

Figure 5.8. Culture responses to the supplementation of various methyltransferase inhibitors. SME added on day 0 of a 5-day batch production process in DWPs. Growth and titer recorded on day 5 and displayed as a normalisation to the control. SMEs used: histone methyltransferase inhibitors: **(A)** WDR5-0103, **(B)** RSC133 and **(D)** UNC1999; DNA methyltransferase inhibitors: **(C)** Procaine and **(E)** RG108. Data displayed as mean ± SEM of two biological replicates with three technical repeats.

5.3.8. Cell Cycle Inhibitor Supplementation

Cell cycle (specifically G2/M) inhibitors were trialled using the DWP systems. It is known that cell cycle phases correlate with specific production of the recombinant protein (Dutton et al., 2006).

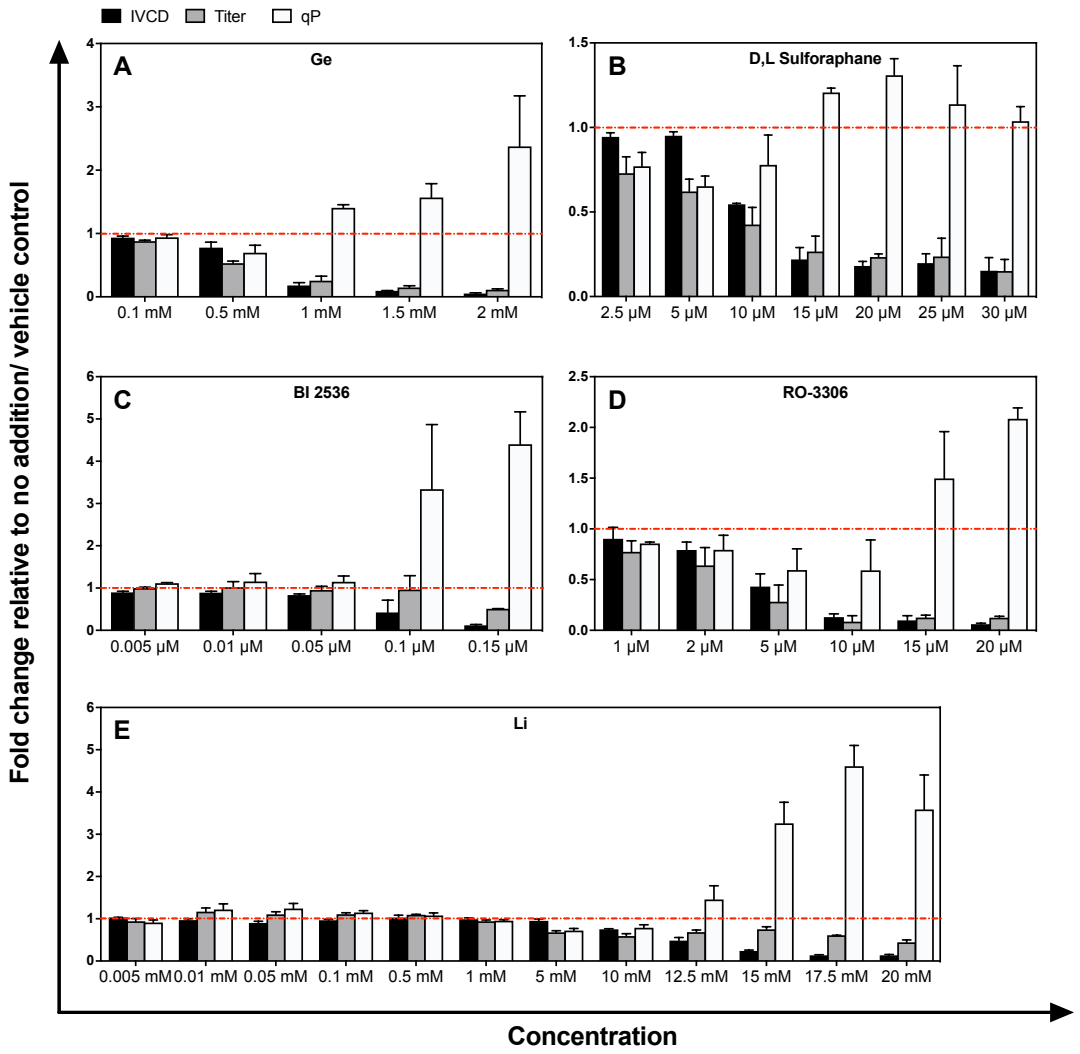

Figure 5.9. Cell cycle inhibitor supplementation responses at various concentrations. G2/M phase inhibitors were added at day 0 of a 5-day screen in DWPs. Cobra 38 cells were seeded at 0.2×10^6 cells mL^{-1}. Dose response curves shown are: **(A)** germanium dioxide (Ge), **(B)** D,L sulforaphane, **(C)** BI 2536, **(D)** RO-3306 and **(E)** Lithium chloride (Li). Date represents mean ± SEM of two experimental replicates (Li represents means ± SEM of four experimental replicates), each with three technical replicates.

Figure 5.9 summarises the dose responses of Cobra 38 cells to the addition of various singular cell cycle inhibitors in an OFAT setup. Growth inhibition was observed in a dose dependent manner, consistent with cell cycle phase inhibition. All cell cycle SMEs tested showed an improvement in qP at particular concentrations. Top concentrations of most cell cycle inhibitors (Germanium dioxide (Ge), BI 2536, Lithium chloride (Li) and RO-3306) majorly reduced cell growth (down to ~10% of the control) and viability. Due to the minimal growth

and titers at these concentrations, noise during data acquisition can lead to an artificial inflation in qP. Thus, these concentrations were ignored for any further testing. Among the SMEs tested, Li ranked the best. Li recorded a 17% titer increase at 0.01 mM (the only cell cycle inhibitor in our screens to give a total volumetric titer boost) and qP improvements of 3.3 and 4.6 fold at concentration of 15 and 17.5 mM respectively.

5.3.9. Carboxylic Acid Supplementation

Allen et al. (2008) reported the use of various carboxylic acids (or carboxylates) for the purposes of improving recombinant protein expression in CHO cells. These molecules were analogous in structure (i.e. contained a carboxyl group) to well-established HDAC inhibitors like sodium butyrate and valproic acid or the chemical chaperone 4PBA. The study elaborated on the use of novel carboxylic acids, including hydrocinnamic acid (HCA), 5-phenylvaleric acid (PVA) and 2-thiopheneacetic acid (2TAA) to improve titer in a recombinant stable mAb reporter system and a stable type II receptor for interleukin 1 production system. Using this study as a precursor, we performed carboxylic acid supplementation studies in our 5-day DWP screens.

Figure 5.10 depicts the cell culture responses when Cobra 38 cells were cultured in the presence of various singular carboxylic acids. PVA and HCA only recorded increases in qP, overall titer was not boosted unlike the study performed by Allen et al. (2008). PVA also severely impacted cell viability at 0.8 mM onwards (data not attached). This indicates that responses to SMEs can be cell line and product dependent. All carboxylic acids recorded dose dependent growth inhibition consistent with well-established carboxylic acid SMEs such as 4 PBA.

2TAA produced a titer boost of 1.6 fold over the DMSO (0.2% v/v) control at 0.8 mM, with increases in qP observed at higher concentrations. With 2TAA being the only SME from the initial screen to yield volumetric titer enhancement, we hypothesised that structural analogues of 2TAA could inform novel enhancer molecules for increasing volumetric titer. **Figure 5.10 D-G** shows culture responses to structural analogues of 2TAA. 4 structural analogues were tested

based on structural similarity tests (Tanimoto similarity score>0.5) performed using the PubChem similarity search (Kim et al., 2016b) (analogue identification process described in more detail in **Section 6.3.1**). 2-Thiophenepropionic acid (TPA), 2-Thiophenebutyric acid (TBA) and 3-Thiopheneacetic acid (3TAA) recorded major enhancement in qP. However, TBA was detrimental to cell viability (data not attached). 3TAA matched the parent analogue efficacy (2TAA), recording a 1.6 titer improvement at 2.5 mM. It was interesting to note that 3TAA had a lower impact on cell growth (75% of the vehicle control) compared to 2TAA (54% of control) at their highest titer yielding concentrations. 3TAA could be titrated to higher concentrations (up to 5.6 mM) without a detriment to cell viability in comparison to 2TAA, which recorded minimal cell growth and decreased viability at 1.6 mM. Another structural analogue tested, TPA proved to be an effective qP enhancer. Titer never fell lower than 75% of the control, while growth was reduced majorly. However, viability was reduced post 3.5 mM, making it imperative to modulate concentration of the chemical to prevent any cytotoxicity.

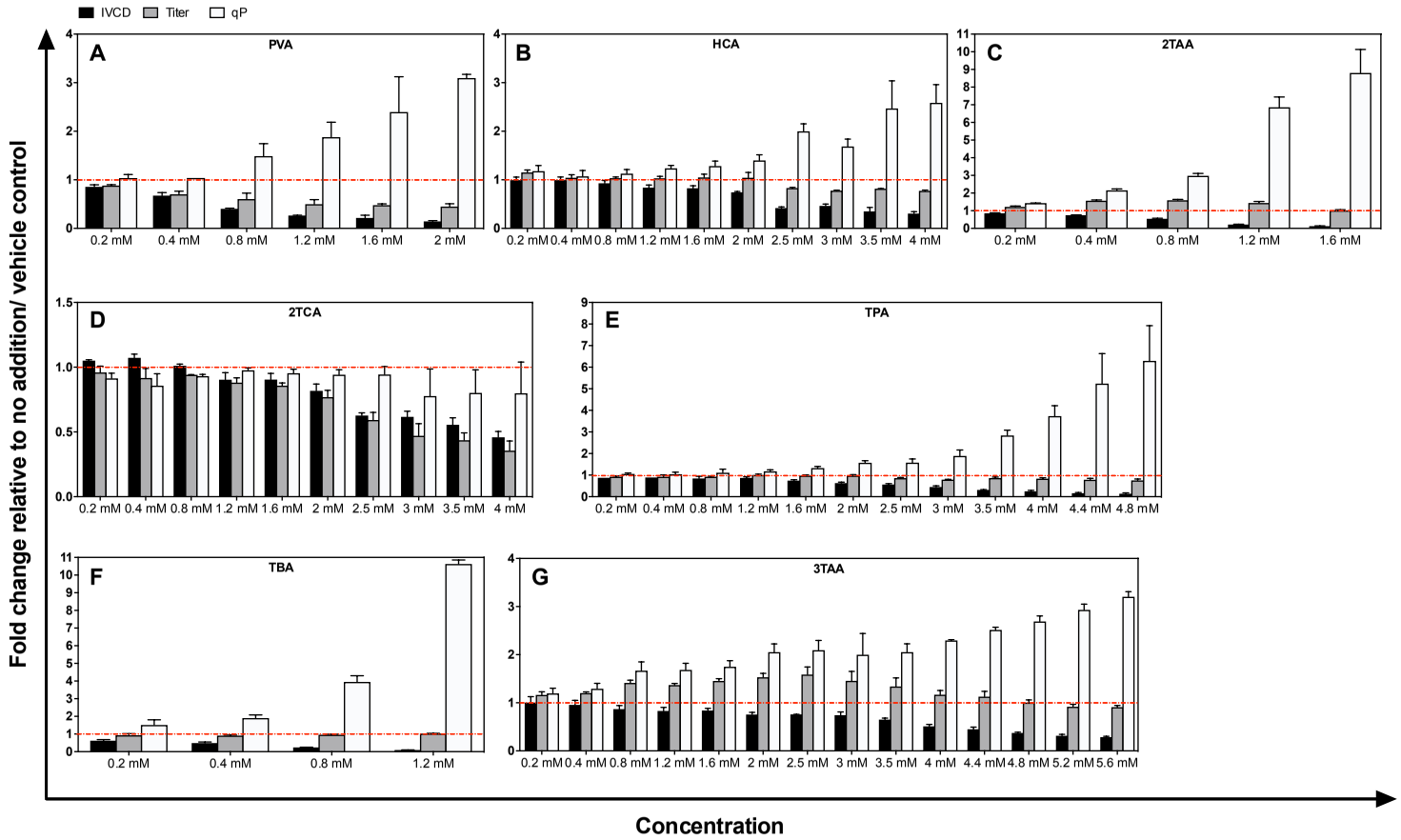

Figure 5.10. A summary of culture responses to the addition of carboxylic acid molecules. SME was added on day 0 of a 5 day batch culture process in 96 DWPs. Titer and cell growth assayed using the Valita™TITER assay and PrestoBlue assay respectively. IVCD (black bar), Titer (grey bar) and qP (white bar) depicted as a fold change compared to the vehicle control. SMEs: **(A)** 5-Phenylvaleric acid (PVA), **(B)** Hydrocinnamic acid (HCA), **(C)** 2-Thiopheneacetic acid (2TAA), **(D)** 2-Thiophenecarboxylic Acid (2TCA), **(E)** 2-Thiophenepropionic acid (TPA), **(F)** 2-Thiophenebutyric acid (TBA) and **(G)** 3-Thiopheneacetic acid (3TAA). Data represents mean ± SEM of at least three experimental replicates with three technical replicates. Data for PVA, 2TCA and TBA represents mean ± SEM of two experimental replicates with three technical replicates.

5.3.10. Delayed Addition of SMEs

Completion of SME testing using day 0 deployment served a dual purpose. Firstly, we were able to elucidate the range of concentrations that produced improvements in IVCD, Titer or qP and thus assess the efficacy of a particular molecule. Secondly, molecules that primarily boosted qP in the day 0 screens helped inform the next line of experimentation for delayed SME addition. Overall volumetric titer is dependent upon cell specific productivity (qP) and cellular biomass (IVCD). Our delayed addition hypothesis was based on the observation that most molecules that enhance qP, concomitantly suppress growth. This is depicted in **Figure 5.11**, wherein a negative correlation was confirmed between qP and IVCD for the enhancers tested in the previous section.

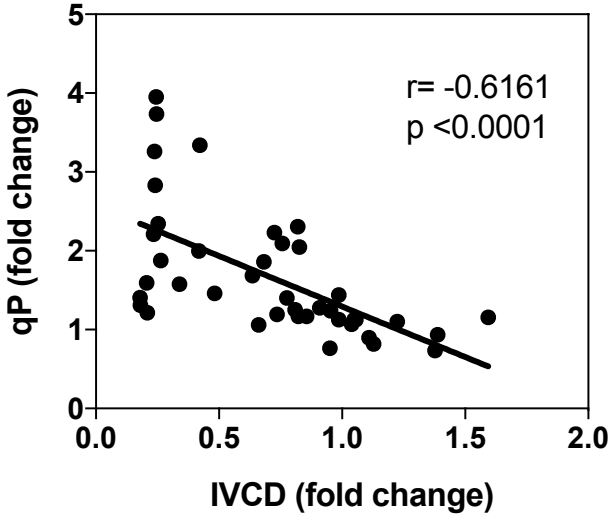

Figure 5.11 Negative correlation between IVCD and qP for small molecule chemical enhancers. A single concentration per chemical enhancer depicted. r: Pearson correlation coefficient.

As a result, there is a severe reduction in biomass that is capable of producing the protein product. To resolve this and maximise titer, we opted for a biphasic culture strategy for qP enhancers (Yoon et al., 2006). Cells would be allowed to proliferate in the absence of the chemical for a certain time period, before the

SME is added to culture. This would result in more biomass being available for production capacity enhancement by the chemical, leading to a bigger gain in volumetric titer. Certain concentrations of SMEs that were on the cusp of titer enhancement using the day 0 addition strategy would produce larger positive shifts in titer at the delayed addition stage. We chose day 3 as the time point for delayed addition of qP enhancers (based on experimentation discussed in **Section 4.3.6**); this time point coincided with mid-exponential stage of culture in DWPs, allowing the cells to proliferate before chemical addition. The chemicals and concentrations taken forward for this stage of screening were selected based on the following criteria, in addition to the obvious criteria of demonstrating a qP increase:

(i.) SME supplementation at day 0 produced a growth reduction of not more than 90% (i.e. cellular IVCD should be at least 10% of the no addition/ vehicle control level).

(ii.) Day 0 addition titer is at least 20% of the vehicle control at the day 5 analysis point.

(iii.) SME would potentially be better suited for later stage addition based its function, for example: cell cycle inhibitor, HDAC inhibitor.

Based on these criteria, selected chemicals from 4 functional compound groups were tested in a day 3 addition setup in 96 DWPs. Selected chemicals are shown in **Table 5.2**. Growth and titer measurements were performed on day 5.

Table 5.2 A summary of SMEs tested using the day 3 addition strategy. Chemicals indicated by their functional groups.

Cell Cycle Inhibitors	Chemical Chaperones	HDAC Inhibitors	Carboxylic Acids
BI 2536 Li D,L Sulforaphane	DMSO TUDCA 4PBA	NaBu Scriptaid TSA MS 275	2TAA 3TAA TPA HCA

Cell cycle inhibitors did not show any major improvements when using the delayed addition setup (**Figure 5.12A**). This could indicate that cell cycle block at the G2/M phase did not improve specific productivity of the protein product. However, the range of concentrations tested at day 3 did not produce growth inhibition in some cases at all, indicating the design space of concentrations for this group was perhaps out of the effective range. We hypothesise a certain degree of growth inhibition would be required to stimulate cellular production.

Chemical chaperones, conversely, achieved varying degrees of benefit using a delayed addition setup. Previously, day 0 addition of 4PBA showed no noteworthy improvements in overall titer, though major increases in qP were observed (**Figure 5.6H**). Day 3 addition of 4PBA (0.75 mM) resulted in a 71% boost in titer (4.2% for a day 0 addition at the same concentration). Though overall titer levels were improved by adding DMSO at day 3 instead of day 0, no concentration was able to surpass control production levels. The largest titer improvements recorded with TUDCA were highly similar to the day 0 addition titers.

Amongst the HDAC inhibitors tested, NaBu performed the best in terms of titer improvement. Adding 1mM of NaBu on day 3 produced a 2.6 fold titer enhancement. In contrast, the best performing NaBu concentration at day 0 addition produced a 1.9 fold improvement in titer (**Figure 5.7A**). TSA (1 µM) also recorded a titer boost of 1.4 fold using a day 3 addition strategy, wherein previously no titer boosts were observed using a day 0 addition strategy. There was no added benefit of a day 3 addition for MS 275 towards protein production compared to a day 0 addition.

Carboxylates (**Figure 5.12D**) recorded the biggest improvement when the day of SME addition was changed for day 0 to day 3. 2TAA had previously recorded maximum titer boost of 1.6 fold (0.8 mM) using day 0 deployment. Using delayed addition propelled the maximum titer enhancement to 3.2 fold using 2 mM. There was no detriment to viability when the molecule was added at day 3 and assayed on day 5. It remains to be seen whether viability would be affected over a longer culture period. 2TAA analogue, 3TAA showed a 2.5 fold improvement in titer at 5.6 mM with no negative effect on viability (data not shown). However, there were diminished returns from 4 to 5.6 mM, suggestive

that the maximum titer enhancement through the use of that molecule had been achieved. TPA showed improvements up to 2.3 fold, however, similar to 3TAA there were only minor increases with increase in concentration from 3.5 to 4.8 mM. This was an enhancement over the TPA day 0 addition strategy wherein no titer boost was observed. HCA recorded improvements ranging from 1.5 to 1.9 fold. Viability remained unaffected while cell growth decreased with dose increase (data not displayed).

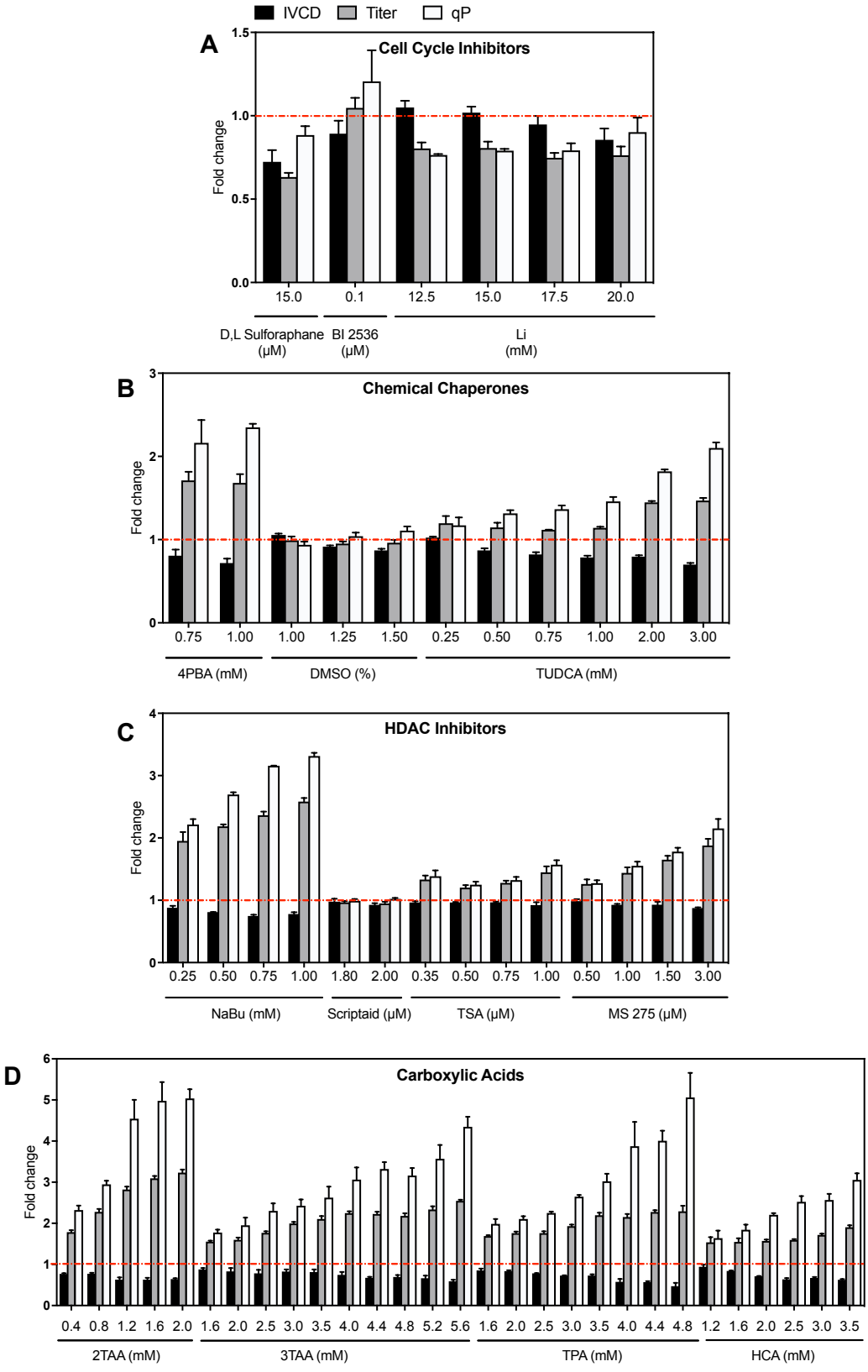

Figure 5.12 Culture attributes in response to supplementation of SMEs on day 3 of a 5-day batch culture in 96 DWPs. IVCD, titer and qP depicted as a fold change to the no addition/vehicle control. 4 sub-categories of chemicals: **(A)** Cell Cycle Inhibitors, **(B)** Chemical Chaperones, **(C)** HDAC Inhibitors and **(D)** Carboxylic Acids were tested. Concentrations used were based on previous experimental results. Data is represented as mean and SEM of three experimental replicates with three technical replicates.

Figure 5.13 displays the maximum titer obtained per chemical (as a fold change over the control) at the 2 different timings of addition. It was evident that majority of qP enhancers had a larger positive impact on total volumetric titer when added during exponential growth phase (day 3) rather than at the start of culture. 2TAA, TPA and HCA witnessed at least a doubling in titer improvement through a shift in timing of deployment to day 3. SMEs (such as Li and MS 275) that did not witness any benefit of delaying deployment did not observe any drop in yield either. Overall, it could be concluded there was a large degree of merit in adding this set of enhancers during the exponential phase of the culture process rather than at the start.

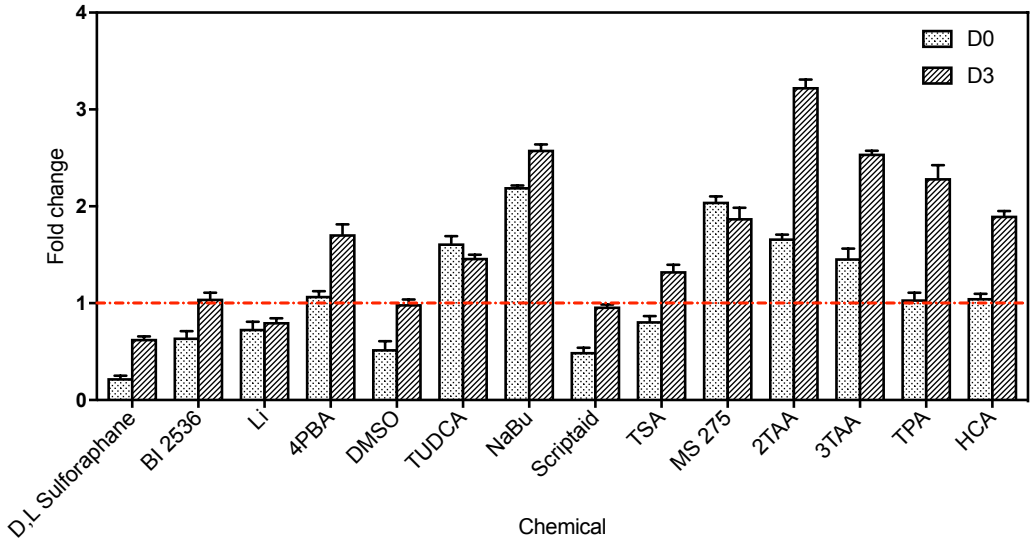

Figure 5.13. Effect of the day of addition of SME on volumetric titer. Addition of SME on 2 days compared: Day 0 (dotted bars) and Day 3 (diagonal striped bars). A single highest volumetric titer observed per chemical on each day of addition is shown. Mean ± standard error of three experimental replicates each with three technical replicates.

5.3.11. Identifying the DOE Design Space

Having established enhancers for growth and titer/qP, the next line of experimentation involved testing for any combinations to boost performance further. For ease of experimentation, we categorised the enhancers into either growth enhancers or qP enhancers. We employed statistical modelling using

DOE full factorial design techniques. Full factorial designs were selected due the lack of aliases for complete determination of significant factors and combinations. This meant only a select number of factors (SMEs) could be tested to ease experimental setup. Also, it is highly unlikely that significant interactions between 4 or more factors occur (Anderson and Whitcomb, 2016), thus testing all positive enhancers for growth/or titer was considered cost, resource and time ineffective.

Stringent criteria were thus designed to determine which SMEs to take forward for combinatorial testing. Design rationale is outlined below:

(i.) To prevent overburdening the cells and raising osmolarity levels beyond cellular tolerance limits (Takagi et al., 2000), it was decided to implement a biphasic DOE approach. Growth enhancer combinations were added on day 0 and titer/qP enhancers on day 3. This also allowed for larger titer effects to be recorded since cells had a proliferation period before switching to protein production stimulated by qP enhancer addition. This narrowed the design space for titer/qP enhancers to the molecules with previous data on day 3 addition available (see section **5.3.10**). Separate DOEs for growth and qP specific enhancers were performed first before combining both.

(ii.) Growth enhancer and effective concentration selection:

- Improve growth (minimum of 20% enhancement over control).
- No detriment to cell viability.
- Maintain or improve titer.

(iii.) qP/Titer enhancer and effective concentration selection (day 3 addition only):

- Improve titer (minimum of 30% improvement).
- No detriment to cell viability.
- Growth repression (maximum of 50% reduction to control).
- Only 1 molecule will be used if there are multiple structurally similar titer enhancers (NaBu and 4PBA).

- Freedom to operate (2TAA is patented).

This narrowed down the design space significantly to the following:

(i.) Growth Enhancers: Cu, Zn, FAC

(ii.) Titer/qP Enhancers: TUDCA, NaBu, MS 275, 3TAA

3 types of **positive** interactions were of interest in the DOE studies (explained below through the use of 2 example arbitrary factors: A and B):

(i.) Synergy: **AB>A+B**; wherein the effect of the combination is more than the sum of each component factor of the combination.

(ii.) Additivity: **AB=A+B**; wherein the effect of the combination is equal to the sum of each component factor effect.

(iii.) Enhancing: **AB>max (A,B)**; wherein the effect of the combination is more than the most effective singular factor.

5.3.12. Combinatorial Design 1: Maximising Growth

A 2-level factorial design was employed to determine interactions of growth enhancers. Cu (Factor A), Zn (Factor B) and FAC (Factor C) were each tested at 2 levels -1 and +1. -1 levels for each factor were set at 0 µM; +1 levels: Cu: 0.5 µM, Zn: 150 µM, FAC: 500 µM. The enhancers were added on day 0 in 96 DWPs. As with previous experimentation, cell culture attributes were recorded on day 5. Cell growth and viability were established using the ViCELL-XR; titer recorded using the Valita™TITER assay.

Results of the combinatorial design are displayed in **Figure 5.14**. All outputs were displayed as separate graphs: **(A)** IVCD, **(B)** Titer, **(C)** qP and **(D)** Viability with the fold change (to the no addition control) of combinations ranked in ascending order. All conditions tested improved growth, indicating no combinations of chemicals had a severe negative interaction leading to complete nullification of each of their positive effects. Conversely, no combination completely outscored their individual component counterparts. Cu+FAC (AC) ranked the highest for IVCD showing a 2.1 fold increase

compared to the no addition control. FAC (C) ranked a close second showing a 1.9 fold improvement.

While this design was concerned with maximising cellular IVCD, titer improvements were observed resulting from the increased biomass. Again, all combinations tested increased total volumetric titer. However, from the qP rankings it was evident that combinations AB, BC and ABC had larger improvements in titer relative to the increase observed in total IVCD. This indicated that there were other mechanisms for improvement in total titer in addition to the increase in viable cell population. Viability remained above 96% for all combinations tested.

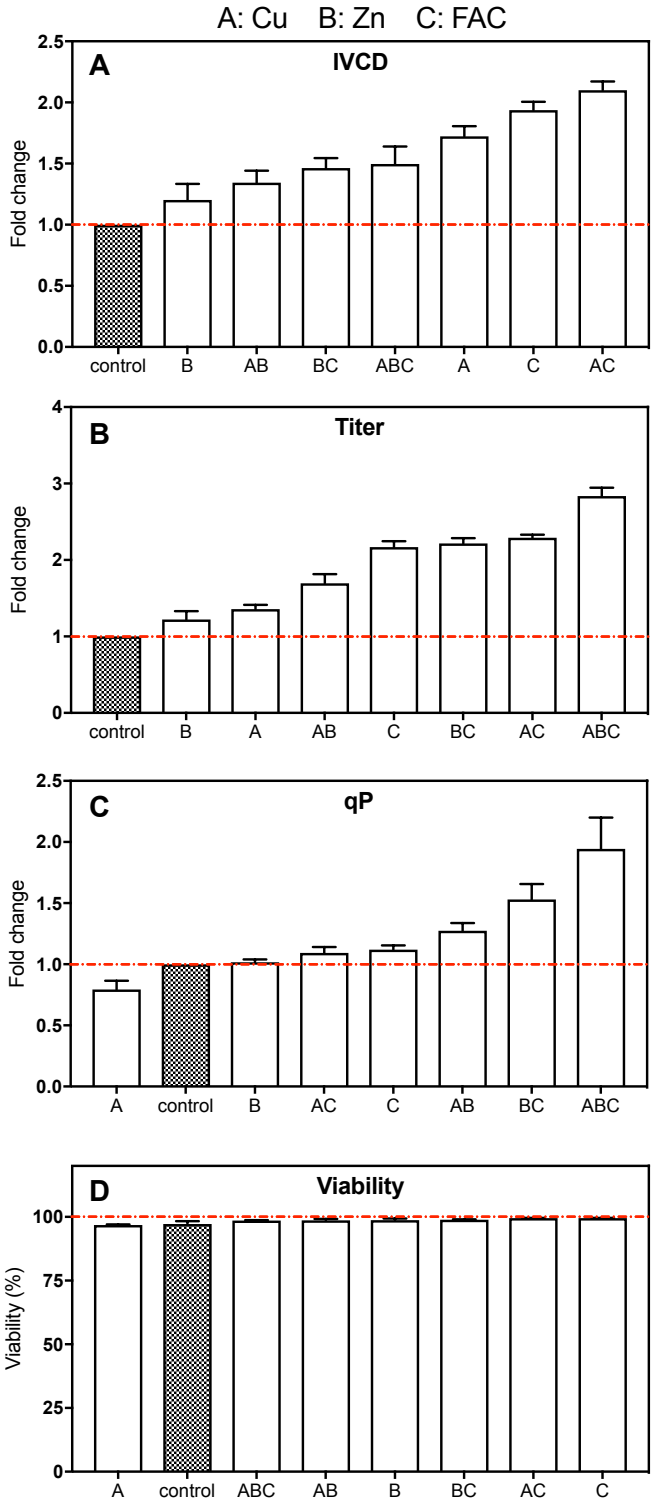

Figure 5.14. Ranked performance for a 3 factor full factorial design. The 3 factors employed were Cu (coded as A), Zn (coded as B) and FAC (coded as C). 8 production runs were randomised. Experimentation was performed in 96 DWPs, cells were seeded at 0.2×10^6 cells mL^{-1} and enhancer (or combination) added on day 0. Each factor or combination of factors was prepared on the day of experimentation to the desired concentration before addition to the plate. Plate was cultured in shaking conditions for 5 days. Cell growth and viability **(D)** were determined using the Vi-CELL XR; titer assayed using the Valita™TITER assay. **(A)** IVCD, **(B)** Titer and **(C)** qP represented as fold improvement over the no addition control. Data represented mean ± SEM of three experimental replicates, with three technical replicates.

The cellular responses to the various combinations were further analysed using the DesignExpert® 10 software. Influential factors (shown in the half-normal plot **Figure 5.15**) that impacted the cellular response were employed to construct a model to predict said cellular response. Linear models were created for IVCD, Titer and qP. No aliasing of terms was observed, strengthening the accuracy of the model and the effect estimates of each term. The predictive models for each response are provided below. The responses are depicted as a fold change over the no addition control.

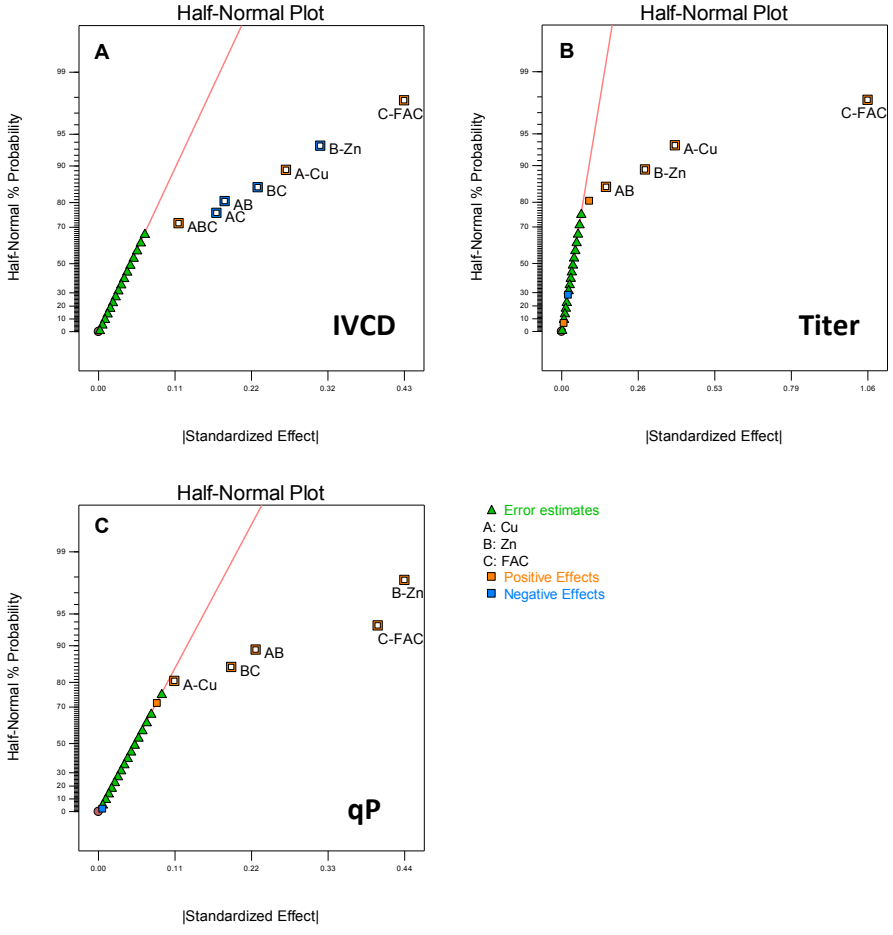

Figure 5.15 Growth DOE: Half-Normal plots to identify significant factors and/or combinations. Effect of each factor calculated mathematically based on all production runs. All factor effects displayed on a half normal plot. A straight line was drawn through residual factors. Any factors deviating from the line were taken forward for significance testing and formed part of the predictive model. Half-Normal plots for **(A)** IVCD **(B)** Titer and **(C)** qP are displayed. Positive effectors are shown in orange whereas negative effectors are shown in blue. Three experimental replicate data was employed in the creation of the half normal plots.

$$IVCD = 1.53 + 0.13A - 0.16B + 0.22C - 0.089AB - 0.083AC - 0.11BC + 0.057ABC$$

Equation 5.1

$$Titer = 1.85 + 0.2A + 0.14B + 0.53C + 0.077AB$$

Equation 5.2

$$qP = 1.22 + 0.055A + 0.22B + 0.20C + 0.11AB + 0.095BC$$

Equation 5.3

All models were significant (based on ANOVA statistics) with non-significant lack of fit. Most terms employed in the model had significant effects (see **Appendix C**). All singular factors were significant. A normality plot of the residuals confirmed that no model transform was required (**Appendix C**). Effect analysis of the factors indicated that the singular factors were most impactful on IVCD, with combinations not having the same level of effect.

5.3.13. Combinatorial Design 2: Maximising qP

To investigate interactions between chemicals that improved qP and/or total titer, we employed a 4 factor full factorial design. Factors were as follows: (A) TUDCA, (B) NaBu, (C) 3TAA and (D) MS 275. The chemicals were tested at 2 levels: -1 and +1. -1 level was set at 0 (mM or µM) for all factors and +1 levels were as follows: TUDCA: 2 mM, NaBu: 1 mM, 3TAA: 4 mM and MS 275: 3 µM. The chemical or cocktail of chemicals was added on day 3 of DWP culture, with culture attributes recorded on day 5. Ranking based fold change analysis is displayed in **Figure 5.16**. While all singular and combinatorial entities repressed cell growth (**Figure 5.16A**), culture population remained viable across all the tested conditions (above 90%, see **Figure 5.16D**).

The rankings of titer (**Figure 5.16B**) indicated that various combinations were of interest. For example, AB in combination (3.5 fold) resulted in a bigger titer boost than the sum of A (1.32 fold) and B (2.45 fold). This indicated that AB was a synergistic interaction. All 4 chemicals in combination produced a titer improvement of 3 fold, outscoring the highest-ranking singular effector (B; NaBu), which produced a 2.45 fold titer improvement. Thus, this would be

termed as an enhancing interaction. The most effective titer enhancer combination was ABD. Adding factor D (2 fold) to AB was able to push the titer fold change from 3.5 (AB) to 4.3 fold (ABD). This again indicated a positive synergistic interaction between factors. It would be logical to conclude that certain combinations of chemical enhancers were able to generate greater titer enhancement when compared to singular molecule addition. Thus, combinatorial experiments provide valuable information that can elevate culture performance over singular additions. Several combinations also enhanced the cellular capacity to generate the protein product. The top performing qP enhancer combination (ABCD; 7.67 fold) improved qP more that twice over its nearest singular counterpart (B; 3.03 fold). A combination of ABD also had a major beneficial impact on qP, echoing its impact on titer. It was evident that there were several positive interactions between factors.

Both the growth and qP/titer DOE experimentation served as a strong proof of concept of combinatorial screening. This gave impetus to include combinatorial screens as part of the design space for the envisioned commercial screening tool.

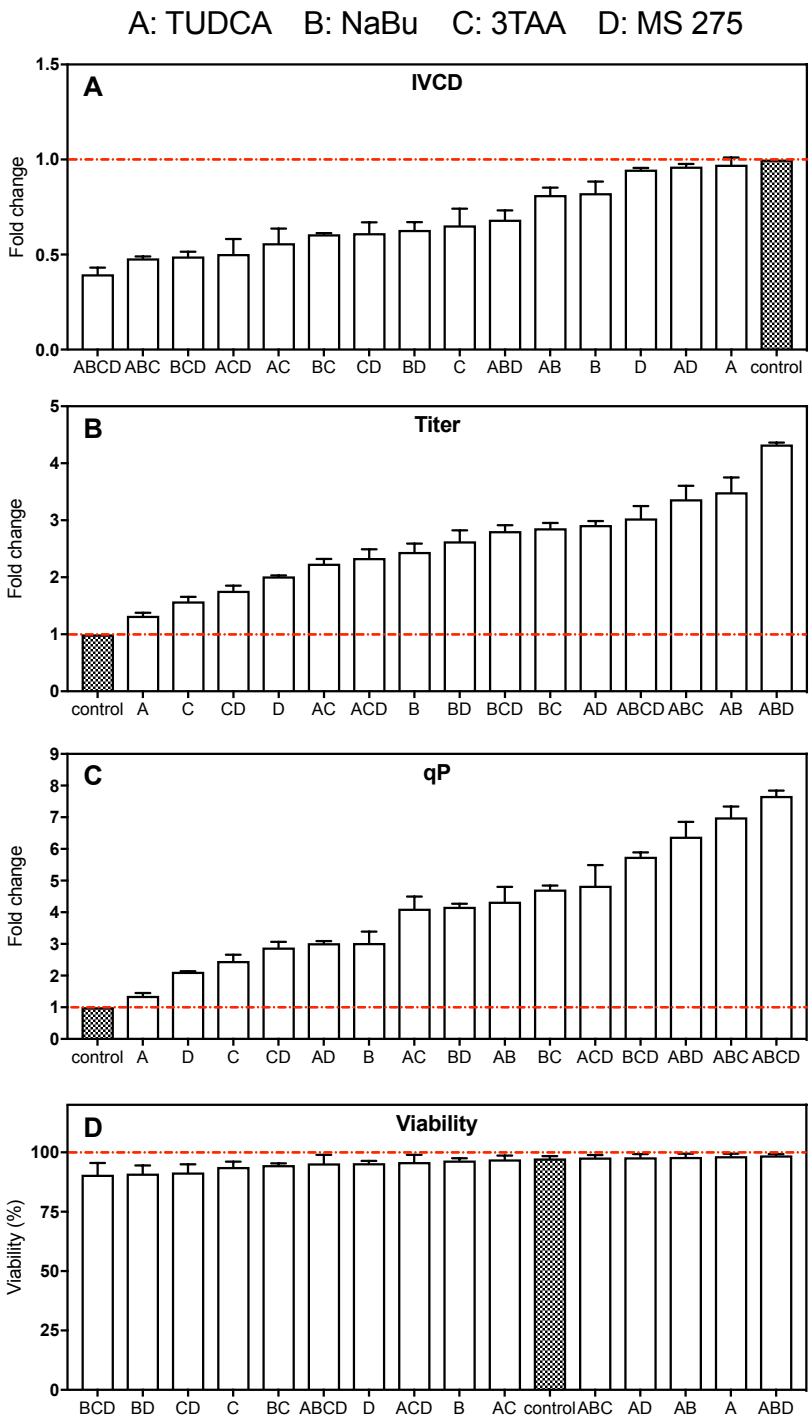

Figure 5.16 Ranked responses for qP/Titer enhancer factorial design. The 4 factors employed were TUDCA (coded as A), NaBu (coded as B), 3TAA (coded as C) and MS 275 (coded as D). 16 randomised production runs were performed. Experimentation was performed in DWPs (cells seeded at 0.2×10^6 cells mL^{-1}) with enhancer added on day 3. Culture attributes were recorded on day 5. Cell growth and viability **(D)** assayed using the Vi-CELL XR/Iprasense Norma; titer was assayed using Valita™TITER. **(A)** IVCD, **(B)** Titer and **(C)** qP represented as fold improvement over the no addition/vehicle control. Data represented mean ± SEM of three experimental replicates, with three technical replicates.

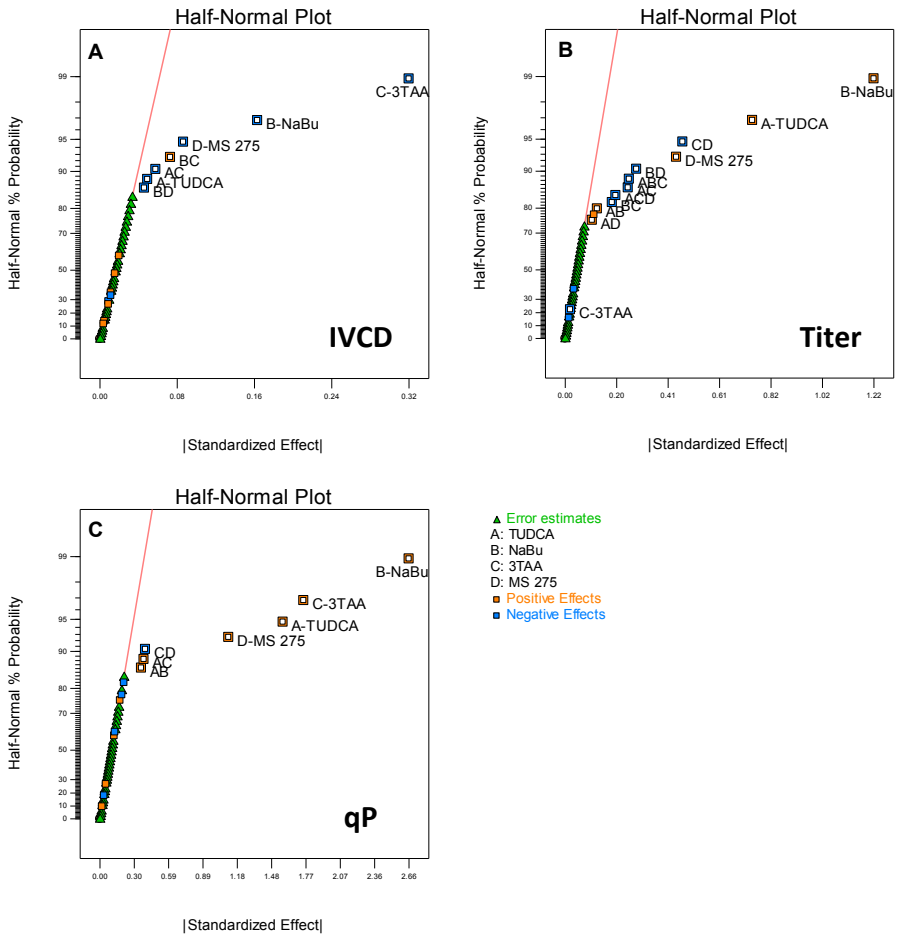

Figure 5.17. qP/Titer DOE: Half-Normal plot depicting factor effects and significance. A straight line was drawn through residual factors. Any factors deviating from the line were taken forward for significance testing and formed part of the predictive model. Half-Normal plots for **(A)** IVCD, **(B)** Titer and **(C)** qP are displayed. Positive effectors are shown in orange whereas negative effectors are shown in blue. Three experimental replicate data was employed in the creation of the half-normal plots.

As performed in the previous DOE, model fitting and analysis was performed in DesignExpert®. Significant effectors and combinations were identified through the half-normal plot with subsequent statistical significance testing (**Figure 5.17** and **Appendix C**) and used to create a linear model to predict IVCD, titer and qP. Viability was not modelled for since all combinations maintained high viability and it was not an attribute that needed improving above the control. Predictive linear models for the 3 attributes are displayed below:

$$IVCD = 0.70 - 0.024A - 0.081B - 0.16C - 0.043D - 0.029AC + 0.036BC - 0.023BD$$

Equation 5.4

$$Titer = 2.51 + 0.37A + 0.61B - 0.01C + 0.22D + 0.064AB - 0.12AC + 0.054AD - 0.093BC - 0.14BD - 0.23CD - 0.13ABC - 0.10ACD$$

Equation 5.5

$$qP = 4.06 + 0.79A + 1.33B + 0.88C + 0.55D + 0.18AB + 0.19AC - 0.20CD$$

Equation 5.6

Significant factors were revealed through ANOVAs and were used to base the model. All models were significant with a non-significant lack-of-fit (**Appendix C**). Normality analysis of residuals confirmed normality and that no transform was required (**Appendix C**). It was evident that most model terms had a negative impact on IVCD. In contrast, most combinations and singular entities had positive effects on titer and qP. The equations can be employed to determine levels of factors to achieve a desired IVCD, titer or qP. All models outputs would be a fold change over the control condition.

5.3.14. Combinatorial Design 3: Maximising Titer

The first 2 factorial designs revealed combinations of interest for the elevation of growth and protein production performance separately. We were interested to determine if testing all the factors together yielded unique positive combinations that could not be predicted from performing the designs separately. Thus, a full factorial design comprising 7 factors was employed (128 unique experimental runs). Experimentation was performed in 96 DWPs as previously. A secondary aim of the design was to investigate the potential of system control. The question to be addressed would be: Can we achieve desired cellular response phenotypes, for example, maximise titer while minimising biomass or maximise growth and titer through the use of chemical combinations? Growth enhancers (Factors E, F and G: Cu, Zn and FAC respectively) were added on day 0. qP enhancers (Factors A, B, C and D:

TUDCA, NaBu, 3TAA and MS 275) were added on day 3. The concentrations were as used previously (i.e. in the separate DOEs).

A scatter plot (displayed in **Figure 5.18**) revealed that a high number of combinations improved IVCD and titer (top right quadrant) or titer specifically (top left quadrant). No extremely detrimental interactions were observed, with each combination maintaining an improvement over the control for titer.

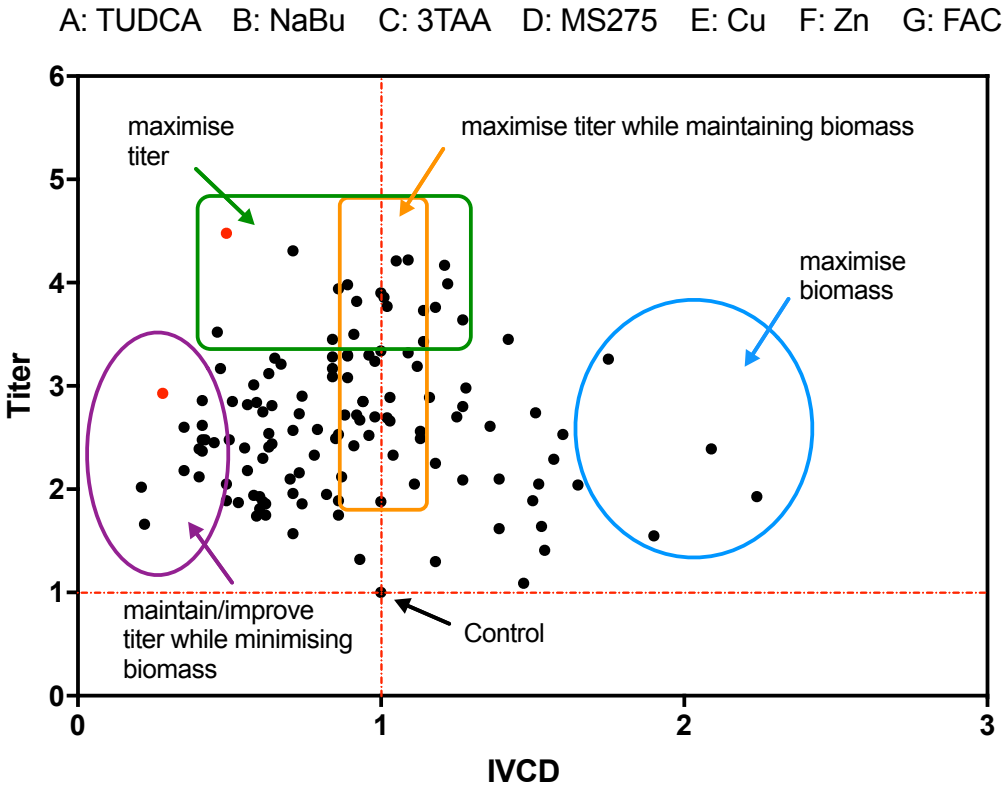

Figure 5.18 Scatter plot for each run of the 7 factor DOE. Each run is a unique factor or combination of factors (128 in total). Culture attributes recorded on day 5. Growth and viability assayed using the Iprasense Norma. Titer assayed using the Valita™TITER assay. Resulting IVCD and titer from each run are displayed. The plot can be divided into four quadrants. Top left: increased titer, decreased IVCD; Top right: increased titer, increased IVCD; Bottom left: decreased titer, decreased IVCD; Bottom right: decreased titer, increased IVCD. Dots marked in red indicate viability below 85%. Data depicted is the mean of two experimental and two technical replicates. Error bars omitted for clarity purposes.

This experimental model mainly served as a snapshot of the flexibility of the design space to suit a user's requirements. For instance, 4 discrete culture phenotypes could be observed on the scatter plot:

(i.) Maximising cellular biomass (blue circle): If the user would like to improve cellular IVCD, various combinations could present potential solutions. All combinations presented improved volumetric titer as well.

(ii.) Maximising titer while maintaining biomass (orange box): If the user desires to exclusively increase titer without disturbance to other cellular processes impacting cell growth.

(iii.) Maximise titer (green box): If the user would like to achieve the largest boost in volumetric titer through the use of various chemical combinations.

(iv.) Maintain/improve titer while minimising biomass (purple oval): If the user would like to minimise downstream processing complexity while still maintaining a titer increase. Herein, cellular biomass would be minimised while cellular productivity improved, resulting in lower cell impurities to purify for downstream processing. These combinations would be valuable in situations where low cell numbers are desirable such as lines susceptible to host cell protein accumulation or to ease downstream processing.

The spread of responses across the spectrum depict the flexibility of modulation. Chemicals would be added in tandem for a desired response, demonstrating the combinatorial power of bioactive small molecules to modulate cell function.

At the top end of the spectrum for titer improvements, there were a number of combinations that improved titer, however with fold changes being extremely tight, there was no standout combination for the maximisation of titer (**Figure 5.19)**. However, this bestows flexibility on the user. For those who are reluctant to change their production system, can be parsimonious in their addition of chemical enhancers. For example, only a small reduction in titer is observed when going from 5 factors (ABCDE: 4.48 fold) to 3 (ABG: 3.76 fold). This factor redundancy is also shown in **Figure 5.20**. Herein, it can be concluded that combining 2 or more factors did have a beneficial impact on the volumetric titer gains in our system, however adding more than 4 factors together yielded diminishing returns. Interestingly, adding all 7 factors together still returned titer improvements over the control, however it was evident that individual

improvement effects of factors were muted. This instates the impetus towards parsimony and reducing complexity, similar titer improvement could be gained through the use of less number of factors (for example 4 vs. 5 in this case), thus reducing system complexity.

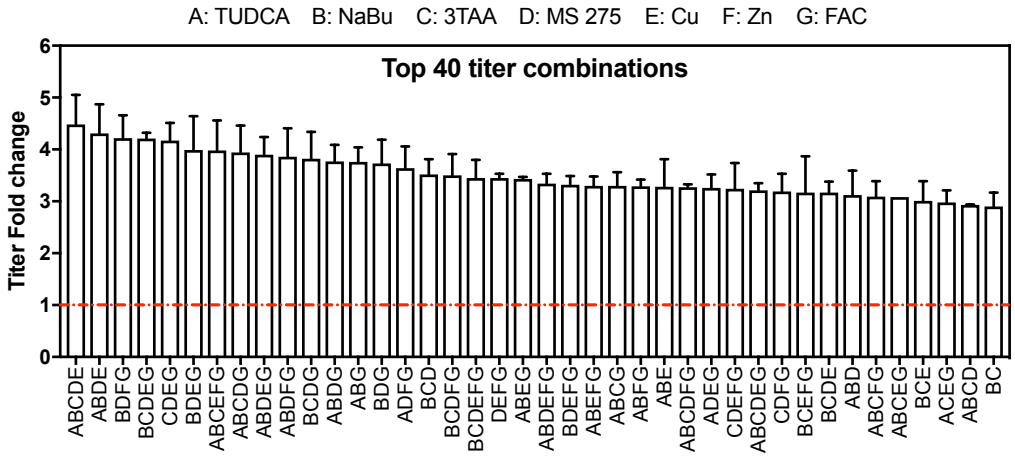

Figure 5.19 Seven factor titer DOE: Top 40 titer boosting combinations. Top 40 of 128 combinations depicted here. Control titer set to 1. All runs depicted as a fold change. Data depicted is the mean and standard error of two experimental and two technical replicates.

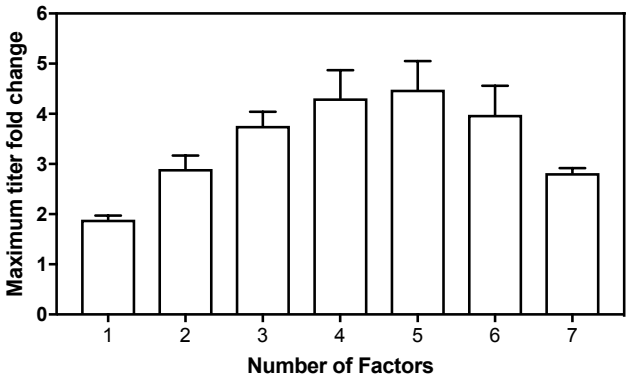

Figure 5.20 Seven factor titer DOE: Impact of the number of factors on titer performance. Largest titer fold change yielding run for each number of factors is displayed. Data represented is the mean and standard error of two experimental replicates each with two technical repeats.

As performed previously, the data was entered into Design-Expert®10 to model the system. Expectedly, multiple factors and combinations were shown to be

significant (**Figure 5.21**) Significant models were created (with non-significant lack of fit). Non-normality of residuals was dealt with recommended power transforms. The predictive linear equation and information on the significance testing performed can be found in **Appendix C**.

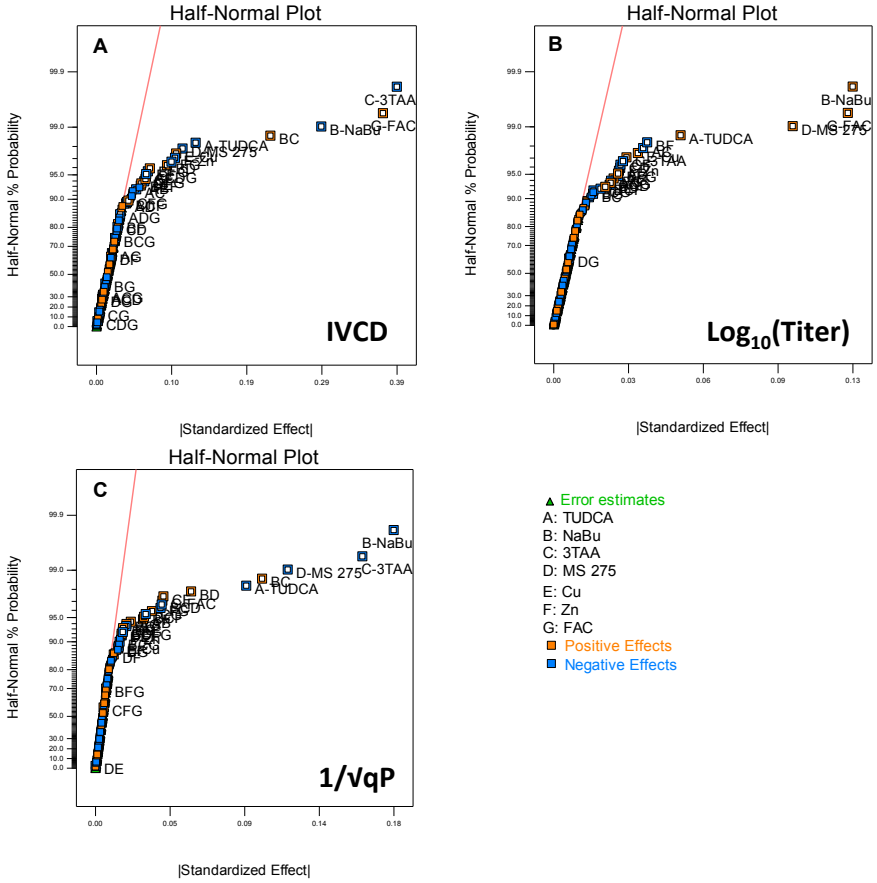

Figure 5.21 Half-Normal plots for the seven factor Titer DOE. Effect of each factor calculated mathematically based on 128 production runs. No aliasing was observed. Standardised effects of each factor and combination plotted on a half-normal plot. A straight line was drawn through residual factors. Any factors deviating from the line were taken forward for significance testing and formed part of the predictive model. Half-Normal plots for **(A)** IVCD **(B)** $\log_{10}$(Titer) and **(C)** $1/\sqrt{qP}$ are displayed. Power transforms were performed for Titer and qP to restore normality. Positive effectors are shown in orange whereas negative effectors are shown in blue. Two experimental replicate data was employed in the creation of the half normal plots.

To summarise, the seven factor DOE design served to provide a glimpse of the power of combinatorial designs to decipher combinations of interest for a variety of situations. However, it has to be noted that, in our case, for maximising titer,

there was no standout combination that provided a massive improvement in comparison to other combinations. Conversely, a large number of combinations ranked higher than singular effectors.

5.3.15. Scale-Up Performance in Fed-Batch Culture

Industrial production processes are often performed in fed-batch culture modes. In order to determine the capabilities of the HT platform to predictably isolate effective combinations of SMEs for scale-up culture, we trialled fed-batch production cultures (25 mL starting culture volume) that utilised a selection of SME combinations. It was hypothesised that correlation between 96 DWPs and shake flask fed-batch cultures in our experimental model would not be perfect. This was due to 3 reasons: (i) The HT screens were performed in batch culture, thus ignoring the effect of feeds on the process. It is highly likely that some enhancers like metal ions would form components of the feed so improvement effects could be muted, (ii) The feeding strategy of the feeds and enhancers was not completely optimised i.e. due to a time bound environment, only a single feeding strategy and single day of qP SME addition was employed and (iii) Since fed-batch processes yield high productivity conditions (due to replenishment of nutrients periodically), it is thought that the margin for improvement in fed-batch processes would be much lower than batch systems.

The fed-batch experimentation can be divided into 3 categories. The first was growth enhancer supplementation. The best performing combination from the HT screens for growth (EG: Cu, FAC) was taken forward for fed-batch testing. The SME combination was added on day 0, with another condition also having an extra feed of the same combination at day 4. We aimed to discern if extra feeding of the growth enhancers is beneficial as the cells approach stationary phase. **Figure 5.22A** depicts the performance of the growth enhancers in fed-batch culture. There were slight improvements in growth rate from day 3 onwards in cultures that were supplemented with growth enhancers. The control and enhancer cultures reached maximum VCD on day 6. From there onwards the enhancer fed cultures were able to sustain the high cell number until day 11. In contrast, the control cultures declined in viable cell numbers post day 6,

with all conditions cultured culminating on day 12. The IVCD calculations also revealed that there was a significant 13% increase in total IVCD (for both day 0 only and day 0,4 fed cultures) on day 12 (**Figure 5.23A**) ($P<0.05$; one-way ANOVA, Dunnett's test). There was no real benefit of adding an extra EG feed on day 4 compared to just the day 0 feed. While the margin of improvement was not similar to the ones shown in the 96 DWP 5 day batch mode, there was still credibility of the plate to predict enhancers of growth. As stated earlier, metal ions are commercial feed components and thus enhancer effects could be dampened. Titer recorded on day 10 (**Figure 5.23B**) showed slight reduction in the enhancer-supplemented cultures over the control (not significant; one-way ANOVA, Dunnett's test), suggesting that the mechanism of titer improvement in 96DWP batch mode did not translate to shake flask fed-batch mode.

Secondly, the best performing titer (ABD: TUDCA, NaBu, MS 275) and qP (ABCD: TUDCA, NaBu, 3TAA, MS 275) enhancers from combinatorial design 2 were tested in fed-batch mode (**Figure 5.22C**). The enhancers were added at mid to late exponential stage (day 5). Post addition, ABCD supplemented cultures had a reduction in growth rate, accompanied by decreasing viability over time (**Figure 5.22D**). This decline in viability was not observed in the 96 DWP screens. We estimate that this was due to viability performance being only measured once at the start of DWP stationary phase, 2 days after the addition of chemicals. Conversely, ABD supplemented cultures followed a more standard viability trajectory. However, ABCD cultures were more productive overall, recording around 60% (**2.9 g L^{-1}**; $p<0.001$, one-way ANOVA, Dunnett's test) titer improvement over the respective control cultures. In comparison, ABD produced a 40% improvement (**2.73 g L^{-1}**; $p<0.01$, one-way ANOVA, Dunnett's test) (**Figure 5.23B**). Again, the cultures did not record the same level of improvement as in the DWPs. It is anticipated that since the shake flask fed-batch control cultures recorded titer levels of around **1.85 to 2 g L^{-1}**, we might be reaching the limits of culture production capabilities and thus margins for improvement are lower. However, these were still major improvements in comparison to the control, syncing with the DWP data that predicted these combinations to be effective in improving titer.

Lastly, we evaluated whether any beneficial effects were observed by adding the IVCD enhancers and titer enhancers together (**Figure 5.22E**). While all conditions displayed a rescue of IVCD in comparison to just the titer enhancer conditions (**Figure 5.23A**), there was no major beneficial impact on titer in comparison to the titer enhancer (ABD and ABCD) only conditions (**Figure 5.23B**).

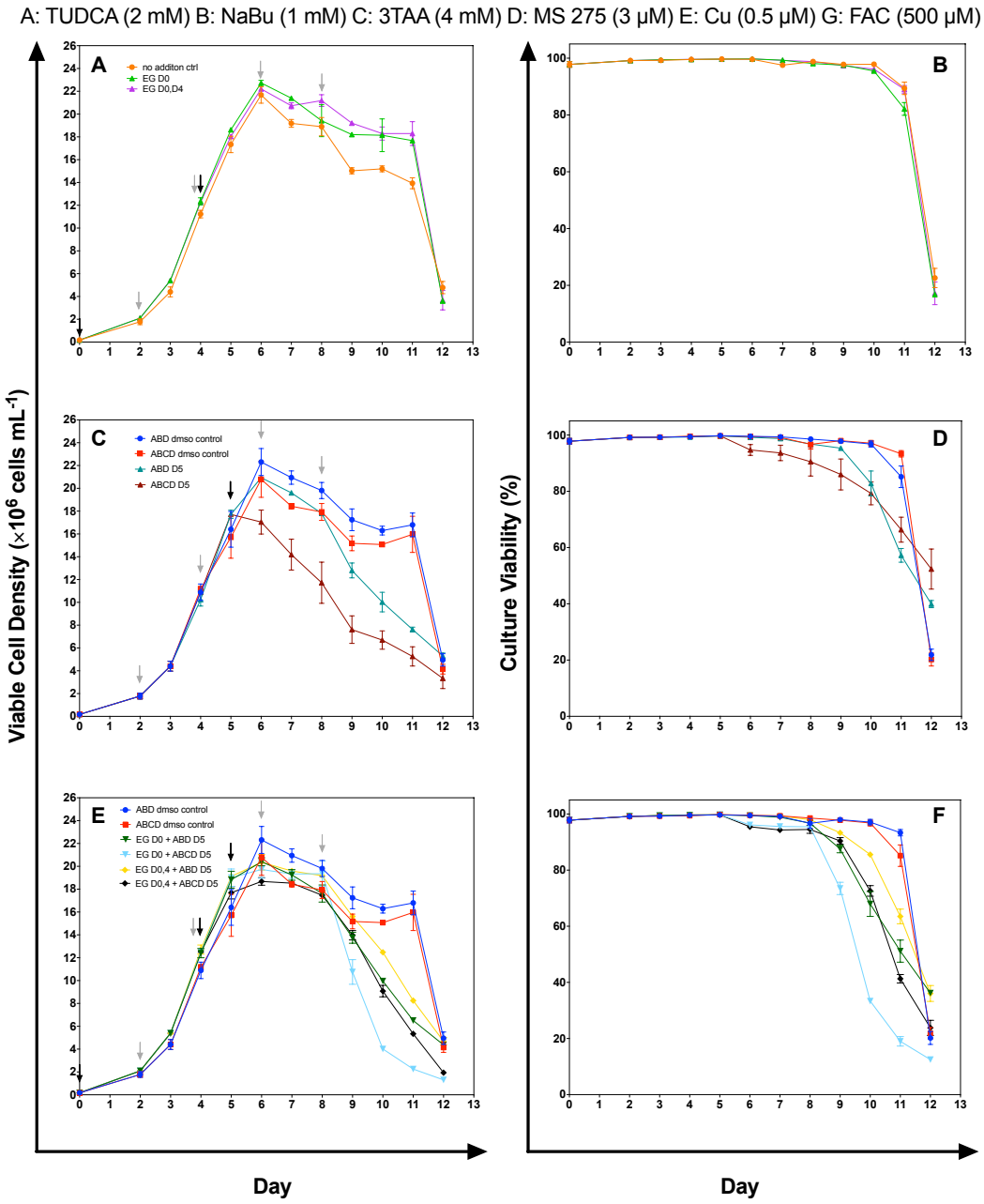

Figure 5.22 Fed-batch growth performance with various enhancer combinatorial strategies. Fed-batch culture studies were performed in shaking Erlenmeyer flasks for 12 days. Cells were seeded at 0.2×10^6 cells mL^{-1}. Samples were taken daily for cell density and viability analysis using the Vi-CELL-XR. **(A)** Cell growth and **(B)** viability performance in the presence of growth enhancers. The growth enhancers EG were added on day 0 (▲) or day 0 and 4 (▲). **(C)** Cell growth and **(D)** viability data for titer/qP enhancer combinations. 2 different combinations were tested ABD (▲) and ABCD (▲). SME added on day 5. **(E)** Growth and **(F)** viability data for IVCD and titer/qP enhancers in combination. Combinations tested were: day 0 addition of EG + day 5 addition of ABD (▼); day 0 addition of EG + day 5 addition of ABCD (▼); day 0 and 4 addition of EG + day 5 addition of ABD (◆); day 0 and 4 addition of EG + day 5 addition of ABCD (◆). Controls used: no addition (●), ABD control (0.2% DMSO v/v) (●) and ABCD control (0.3% DMSO v/v) (■). CHO CD EfficientFeed™B added on days 2, 4, 6 and 8 (light grey arrows). Black arrows indicate chemical enhancer cocktail addition. All data represented is the mean and standard error of two experimental replicates, with two technical replicates.

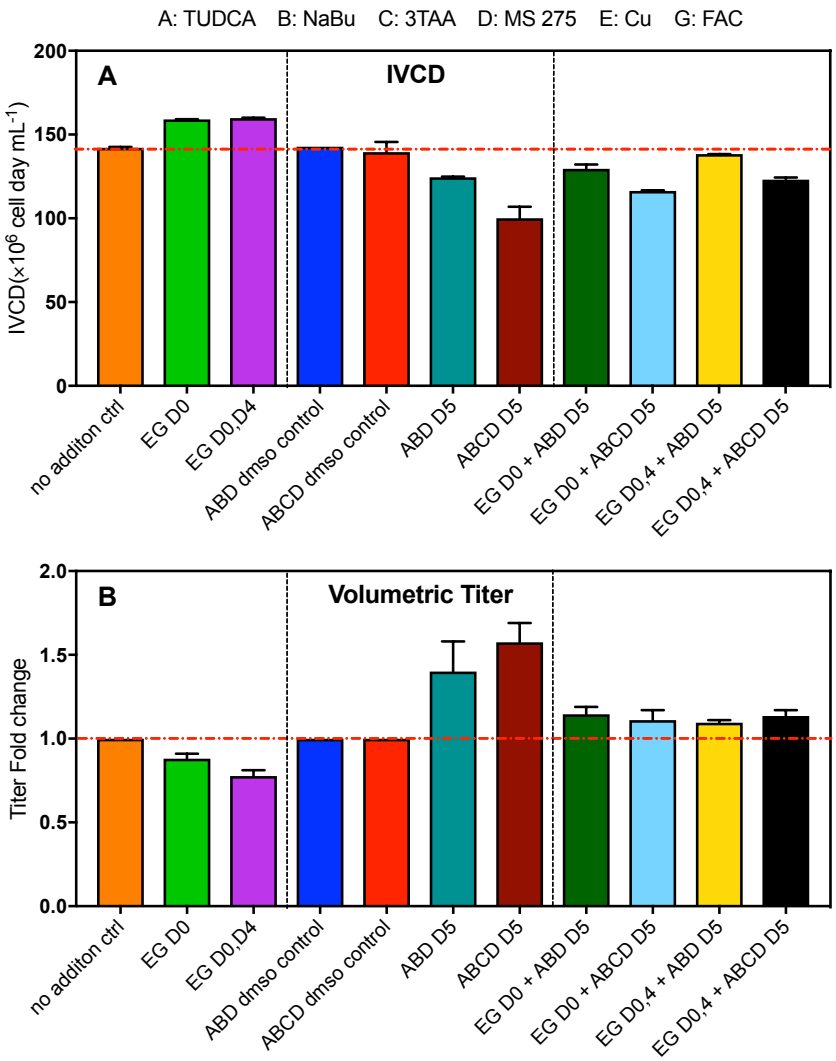

Figure 5.23 IVCD and Titer outputs for all conditions tested in fed-batch production mode. (A) Absolute IVCD data plotted for each condition tested. Enhancers depicted in coded terms. IVCD level of no addition control depicted by the red dotted line. **(B)** Normalised titer values for all conditions tested. Values for each condition depicted as a fold change to their respective control (no addition, ABD control (0.2% DMSO v/v) or ABCD control (0.3% DMSO v/v). Data depicted is the mean ± SEM of two experimental replicates and two technical replicates.

5.4. Discussion

The work depicted in this chapter, firstly served as an exemplar for the utility of the HT screening platform. We were able to identify SME chemicals that were successful in improving 1, 2 or 3 culture attributes (IVCD, titer, qP) in a stable mAb expressing CHO system. The use of the 96 shaking culture platform

bypassed the problems faced in static culture as discussed earlier (Section 4.3.4). This was ideal for testing SMEs since the cells could be incubated for a longer duration with the chemical of interest, to get an amplified signal or detect cytotoxicity.

We were able to rigorously evaluate 8 functional groups of SMEs. Each group recorded varying success rates. We were able to thus present a suite of chemical enhancers that can be employed in cell culture for production performance elevation. The work presented here is envisioned to form the basis of a commercial HT screening tool. Thus, it is important to evaluate the efficacy of these enhancers in other model systems; i.e. different media and cell lines. Due to limitation on cell line and product resource availability, this comparison could not be performed. However, previous published work indicates that many molecules presented in our studies have shown improvements in other CHO systems (stable and transient). Looking at the data available from our study, perhaps the most telling group was the chemical chaperones. Tested in a standard protein production system that is known to reach g L^{-1} titers (personal communication and **Section 5.3.15**), this protein molecule can be classed as relatively easy-to-express. We observed positive effects with a cohort of chemical chaperones that are known to target protein misfolding and liaise with molecular chaperones that alleviate ER stress. Since these abnormalities are likely to be present at low levels in our easy-to-express protein system, the effects of chemical chaperones observed could be amplified in DTE systems. There has been a steady increase in the number of published articles and reviews exploring post-transcriptional bottlenecks in CHO cells, indicative that engineering the secretory pathways for better production performance is of interest (Hansen et al., 2017; Zhou et al., 2018). An example of chemical chaperone utility can be represented by a study performed by Johari et al. (2015). Their DTE model system witnessed increases of 1.7 fold in short term transient expression. In a shaking fed-batch production culture, the addition of 2 chemical chaperones (4PBA and glycerol) and a molecular chaperone (cypB) led to ~3.5 fold improvements in total titer at the end of 12 days. Interestingly, 4PBA and glycerol were not the most effective chaperones in our production system, further providing evidence to the theory that effective enhancers and

their concentration are cell line and product dependent. This provides impetus for the creation of HT methods to isolate SMEs for different production processes, which is the overarching aim of this project.

The molecules selected for the study had varying targets. Metal ions and metabolic modulators targeted efficient cycling of nutrients for improvements in biomass accumulation. The remainder of the groups targeted the synthetic protein production process. For example, HDAC inhibitors boosted general transcriptional activity whereas chemical chaperones impacted protein folding and stability. To summarise, a multitude of different functions can be targeted and modulated intelligently for a desired production fingerprint.

Biphasic culture strategies also proved valuable in improving overall protein production. Enhancers like 4PBA and TSA did not provide titer improvements using a day 0 deployment strategy, but enhanced titer when deployed at mid-exponential phase. This was analogous to some of the more common biphasic strategies employed in the biopharmaceutical industry such as temperature shift from 37 to 32°C (Yoon et al., 2006). Combining small molecule supplementation with strategies like temperature shift can be used to create desired biphasic processes as demonstrated by Coronel et al. (2016).

Combinatorial designs further elevated enhancer effects on growth, titer and qP. Statistical analysis of the design model revealed multiple significant combinations that affected IVCD, titer or qP positively or negatively. However, from an engineering perspective, the design rules were simple, find the top producing or growing condition that did not negatively impact cell viability. The rationale behind adopting this strategy can be explained easily. A scenario where 2 factors produce the best IVCD, however their cumulative effect based on other “statistically identical” production runs is negative. Additionally, if their combination effect is lower that the sum of the individual factor effect, the interaction is classed as antagonistic. In our scenario, the most logical approach would be the selection of the best performing condition. Engineering firms use DOE design techniques for optimising factors that can’t be easily removed. Since our design operates on a plug and play concept, it is simple to remove factors and not all SMEs need to be employed. Thus, we adopted a simple strategy of just selecting the best performing condition. It is interesting to note

that some literature sources investigate more diverse cross-functional combinations. For example, butyrate and pentanoate while increasing protein yields were shown to initiate apoptotic pathways (Camire et al., 2017). Addition of an antioxidant molecule (N-acetyl cysteine) to the chemical treated cultures enhanced IVCD and lowered apoptotic cell abundance. This study thus demonstrates that combining small molecules intelligently could diminish any off-target negative effects of certain SME use. This would be particularly useful in protein glycosylation modulation, wherein if any molecule negatively impacts protein glycoform profiles (but is beneficial to growth/titer), addition of a small molecule modulator could “correct” protein glycosylation profiles to meet regulatory standards (Brühlmann et al., 2017b; Brühlmann et al., 2017a; Grainger and James, 2013; Gramer et al., 2011).

Trialling the predicted best combinations from DWP studies in a scaled-up, fed-batch culture mode, suggested that performance in DWPs depicted the same trends at scale-up, however the extent of improvement did not concur between the 2 scales. This conclusion is not definitive since only 1 feeding strategy was evaluated so follow-up experimentation would be required to confirm this conclusion. However, it was evident that cellular viability selection criteria would need to be re-evaluated. The best performing qP condition from DWP studies, (ABCD; A: TUDCA, B: NaBu, C: 3TAA and D: MS 275) revealed a gradual decrease in viability when added to shake flask fed-batch culture. Even cultures incubated with the DWP predicted most productive condition, ABD, faltered in viability in advance of the control cultures. DWP screens could not predict this phenomenon since the incubation time was short. The most straightforward approach to remedy this would be to incubate the plate for longer or to create a fed-batch modality in DWPs. However, to keep with the quick and easy incubation setup, we decided to slightly update the design space selection strategy. This is explained below.

The prospect of applying parsimony to the design space has always been discussed. Looking at our DWP qP combinatorial data, it was evident that combination AB had similar titer output to ABD and ABCD. However, growth inhibition was lower in comparison. It remains to be determined what its effect on viability would be when scaled-up to a larger culture volume. We predict that

since growth arrest was low in DWPs, cells would react more favourably to AB supplementation, with culture viability remaining high. Thus, with cultures potentially lasting longer, bigger gains due to addition of the combination could be harnessed, making it a better combination than ABD and ABCD. Parsimony is also beneficial from a regulatory point of view since the number of factors to consider is lower. It is obvious that these hypotheses would need to be thoroughly tested to examine validity.

The major limitation of our screening study was the lack of evaluation of product quality in the presence of SME molecules. Some small molecules can significantly alter the glycosylation state of the protein unfavourably (Hong et al., 2014). Additionally, some small molecule modulators have been shown to modulate product quality favourably to obtain a desired glycosylation profile (Brühlmann et al., 2017a; Grainger and James, 2013) (detailed in **Section 2.2.5**). Thus, addition of HT product quality assessment technologies to our HT analytics toolbox could assist in making more informed choices of SMEs with regards to product quality. Addition of small molecule glycosylation modulators would increase the diversity of the SME suite that we have already obtained.

Overall, we were able to demonstrate the use of our developed HT screening platform to isolate enhancers of CHO production culture. Chemicals could easily be titrated, in order to determine their effective concentration. Small combinatorial designs informed the predicted best culture supplementation strategy. Scale-up performance was not ideal however the HT screens did correctly indicate combinations that enhanced culture performance.

All the information presented in this chapter would assist in the creation of a commercial screening platform. We were able to assess the efficacy of a functionally diverse group of molecules. Ideally, singular enhancers or combinations of enhancers would be lyophilised on a 96 DWP. The contents of the plate would need to be determined through more cell line/product and basal media testing (resources that were not available for the purposes of this project). This would help determine chemicals and concentration ranges that are likely to be effective for a range of different cell types and production platforms. The user would add a pre-determined culture volume to the plate and incubate in shaking conditions for 5 days. Growth, titer and viability would be

determined on day 5 using the high-throughput assay techniques. Statistical modelling software would enable the creation of bespoke media environments tailored to the user's production process. Statistical computational modelling would be in the form of small DOE based combinatorial testing. Extra caution would need to be applied when selecting growth-arresting enhancers. Cell viability is potentially a critical determinant of scaled-up cell culture performance.

Chapter 6

A Mechanistic Understanding of Thiophene Molecule Facilitated Production Enhancement

ABSTRACT: We investigated the utility of novel thiophene carboxylic acid molecules in a CHO cell system stably producing a mAb product. 5 thiophene molecules were evaluated across a wide range of concentrations in our high-throughput screening platform. Growth and titer were measured on day 5 of batch deep well plate culture. 2 Thiopheneacetic acid (2TAA) and 3 Thiopheneacetic acid (3TAA) were shown to improve volumetric titer by 1.6 fold. Scaled-up studies in shake flasks confirmed that the enhancing efficiency of these molecules was conserved at a larger scale. 2TAA supplemented cultures produced a 2.4 increase whereas 3TAA supplemented cultures produced a 1.85 fold increase in volumetric titer. There is very little evidence in literature to elucidate mode of action of these 2 enhancer molecules. We investigated mode of action through iterative functional and mechanistic analyses. 2 and 3TAA were shown to arrest cells in the G1 phase of the cell cycle, a trait commonly observed with the use of HDAC inhibitors such as sodium butyrate. Interestingly, 2TAA was shown to induce early apoptosis in CHO cells upon treatment at its titer enhancing dose. Conversely, 3TAA did not have any impact on the apoptotic state of the cell. Product gene mRNA analysis revealed than both 2 and 3TAA acted partly at the mRNA level. Mass spectrometric analysis conducted showed increased abundances of acetylated lysine residues on histone tails. Acetylated histones are generally linked with increase in gene accessibility for transcription. It was concluded that both 2 and 3TAA acted epigenetically. Finally, glycosylation analysis revealed no major shifts in glycoforms due to the use of these molecules. The work presented in this chapter aims to provide a snapshot of the utility of thiophene molecules for improving CHO cell bioprocess and can be used to guide future studies on the topic.

Chapter Acknowledgements

The mass spectrometry methods and analysis were performed by Eleanor Hanson (The University of Sheffield). Glycan release and analysis of the purified protein product was performed by Dr. Roisin O'Flaherty and Dr. Karen P. Coss (NIBRT, Ireland).

6.1. Introduction

With g L^{-1} titer outputs becoming commonplace in the bioprocessing arena, it could be argued that focus should move towards downstream processing improvement. While improvements to downstream processes are crucial, upstream process improvement has consistently remained a core focal point for intense improvement. Chapter 5 focused on utilising the created HT screening platform to rapidly evaluate small molecule enhancer additives to improve cell growth and productivity. A by-product of this study was the ability to evaluate potential novel SME candidates.

Carboxylic acids have been found to be global enhancers of protein production in CHO. Molecules like sodium butyrate, valeric acid, sodium phenylbutyrate and valproic acid have been employed in multiple studies to improve protein production in CHO cells (Backliwal et al., 2008; Coronel et al., 2016; Jiang and Sharfstein, 2008; Johari et al., 2015; Park et al., 2016; Sung et al., 2004). Studies by Allen et al. (2008) and Bora-Tatar et al. (2009) performed large carboxylic acids screens (*in-vitro* and *in-silico* respectively) to evaluate potential carboxylic acid molecule efficacy. The former study revealed an interesting set of molecules that were able to boost stable production performance in CHO cells. We employed that study to form the basis of our in-house search into novel carboxylates for recombinant protein production.

We focused our efforts on thiophene carboxylate molecules (thiophenes: molecules that contain a sulphur group in the aromatic planar ring). There is hardly any evidence (apart from Allen et al. (2008) that employed 2 thiopheneacetic acid) of the use of these molecules as enhancers for bioprocess. They share their carboxylate structure with the established

carboxylate HDAC inhibitors. They have previously been employed in polymer and semiconductor nanoparticle manufacture (Narizzano et al., 2005).

The positive outcomes of various thiophene supplementations in our system motivated our efforts to investigate the molecular mode of action that is responsible for the protein production enhancement. Again, there is no literature evidence on mode of action (with the Allen paper failing to declare mechanism confidently). We consulted literature sources that contained detailed mechanistic analysis into the titer inducement prowess of SMEs to plan our mechanism exploratory strategy (detailed in Experimental approach) (Backliwal et al., 2008; Jiang and Sharfstein, 2008; Park et al., 2016).

Given that the thiophene molecules contained the same structural backbone as common HDAC inhibitors (such butyrate and valproate), i.e. a carboxylate structure, we hypothesised that the molecules could act epigenetically. Epigenetic modifications, such as histone acetylation play an important role in regulating gene expression (Dahodwala and Sharfstein, 2014). A balance between histone acetyltransferase (writers) and histone deacetylases (erasers) normally governs histone acetylation. Acetylation of lysine residues on the histone molecule imparts a negative charge on the histone molecule, causing a decrease in interaction with the negatively charged DNA (Kim and Bae, 2011). This prevents tight multiple nucleosome packing, improving gene accessibility to transcriptional machinery, thus upregulating transcriptional activity (Jiang and Sharfstein, 2008; Kim and Bae, 2011). Thus, investigating transcriptional activity and histone modification activity in response to the thiophenes was of interest. Cellular health and cell cycle analytics also played an important role in our analysis of the molecules. Chemical enhancer molecules can instigate off-target effects on cell viability (Lee and Lee, 2012). Additionally, initial screens depicted a repression in growth with the thiophene molecules, motivating efforts to investigate cell cycle arrest in greater detail. Lastly, it was important to evaluate product quality in the presence of the chemicals. It was necessary to determine any negative impacts on the protein product glycoform that could thwart product efficacy as a therapeutic. Protein glycosylation is often an underlying important parameter that is needed to ascertain SME suitability, as

incorrect glycosylation could hamper therapeutic efficacy and half-life (Hossler et al., 2009).

6.2. Experimental Approach

Our studies with the set of enhancer molecules listed in Allen et al. (2008) only yielded 2-Thiopheneacetic acid (or 2-Thienylacetic acid) (2TAA) (a molecule with a thiophene group) as an effective production stimulant. Since there is no mechanistic information regarding the molecule, we aimed to examine the molecule further. There are no studies in CHO cells elucidating the use of other thiophene molecules as production enhancers, so we took this as an opportunity to investigate mechanism and isolate novel enhancers for protein production.

Firstly, we sought to employ computational structural similarity assessment to isolate structurally similar molecules to 2TAA. We were able to identify 4 structurally similar molecules; these were subsequently tested in our HT system. Positive enhancers of productivity and/or qP were taken forward to test using delayed addition in our HT system (detailed in **Section 5.3.10**). Following the screens, we were able to identify 3TAA, a structural analogue to 2TAA as a protein production enhancer. Both these molecules were employed in scale-up batch culture shake flask studies to investigate their efficacy in a larger scale and over a longer incubation period. Only a single concentration per molecule (selected based on their HT day 0 addition screens) was tested in shake flasks, for ease of experimentation.

The batch culture shake flask studies were performed in a 30 mL culture volume. Cobra 38, a CHO-S derived cell line that stably expresses an IgG1 molecule was used in this study. The scale-up to 30 mL cultures allowed daily sampling for cell growth and titer analysis. Samples for other mechanistic studies (such as epigenetic, transcriptional and apoptosis analysis) were based on a single day sample collection for ease of experimentation. Most mechanistic and functional studies were performed on day 5 of a 9 to 10 day batch culture period. This time point (coinciding with late exponential/early stationary phase)

was chosen given that the largest increase in qP was observed at that time point. This was suggestive that cells were transitioning into peak production mode, wherein the effects of the SME on the protein production processes could be larger and more apparent. The chronology of experimentation was fluid. An iterative approach was employed, wherein results from previous experimentation was used to inform the next line of testing. Positive controls (in the form of well-known SME carboxylate molecule supplementation) were used to support some functional studies.

Overall, this chapter serves as a standalone study investigating the mode of action of 2 thiophene carboxylate molecules that can be employed as protein production enhancers in CHO cells. The HT platform (described in chapter 4) assisted in the screening and identification of novel carboxylate SMEs. These novel enhancers can be used and combined with existing SMEs for further enhancement.

6.3. Results

6.3.1. Identification and Assessment of 2TAA Analogs

Our SME screens indicated 2TAA as an effective protein enhancer molecule (detailed in **Section 5.3.9**). This is only the second study (first being: Allen et al. (2008)) to date that has reported the use of a thiophene carboxylic acid molecule as a cell culture process enhancer. We aimed to identify more thiophene molecules as enhancers for CHO bioprocess. *In-silico* molecular docking studies have often been employed to predict molecule efficacy based on structure and function (Bora-Tatar et al., 2009). Since we could not assess functional efficacy *in-silico* (molecule substrate was not established), we chose to employ structural similarity testing and subsequently assess functional efficacy experimentally. We employed ChemMine tools (Backman et al., 2011) in combination with PubChem similarity search (Kim et al., 2016b) to isolate potential enhancer molecules based on their Tanimoto similarity score. 4 unique molecules with a structural similarity >0.5 (maximum of 1) were isolated (**Figure 6.1**). 2-Thiophenepropionic acid (TPA), 2-Thiophenebutyric acid (TBA), 2-

Thiophenecarboxylic acid (2TCA) and 3-Thiopheneacetic acid (3TAA), all contained a thiophene group and a carboxylate group. The differences between the molecules stemmed from variation in hydrocarbon chain number.

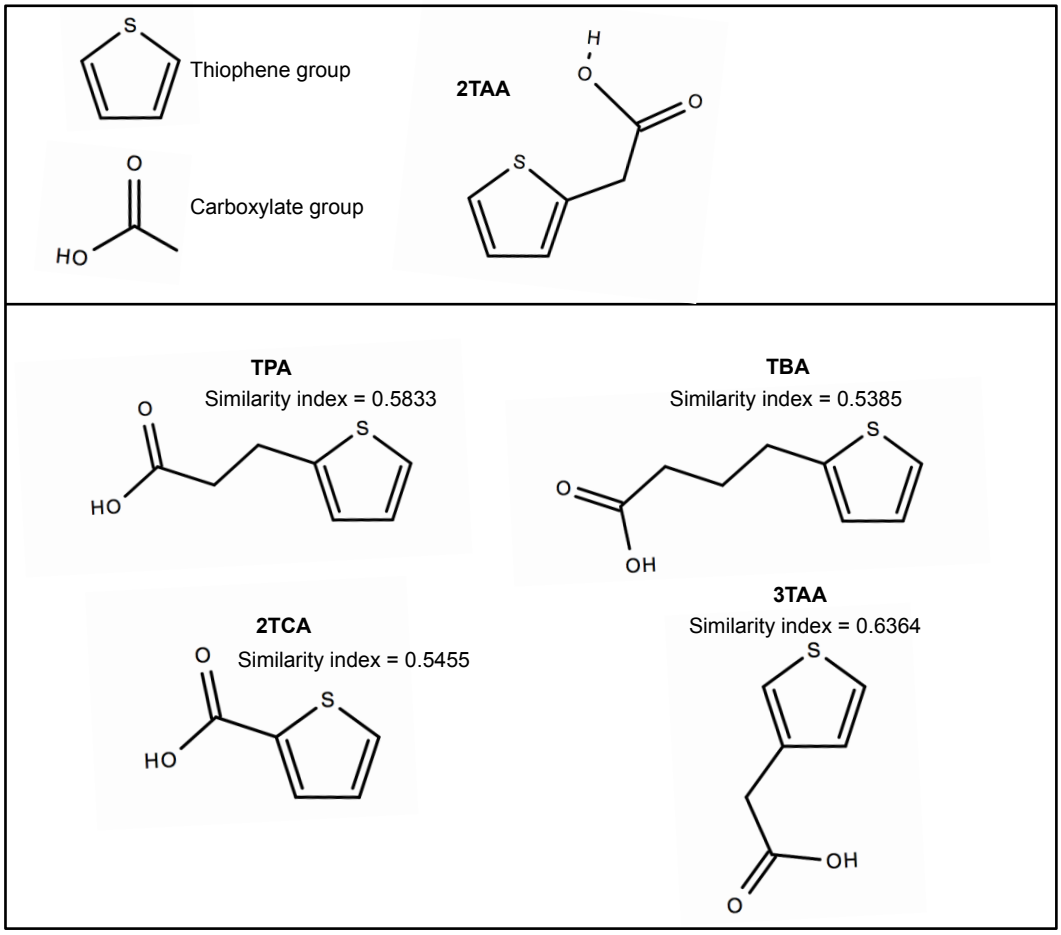

Figure 6.1 Structural Analogues of 2TAA. The molecules were selected based on their maximum common substructure (MCS) Tanimoto similarity (maximum similarity is 1; cut-off >0.5) scores against the parent molecule 2TAA. Similarity was computed using the PubChem similarity plugin on the ChemMine Web tool. Structures depicted here were drawn using Ketcher structure tool on ChemSpider (Karulin and Kozhevnikov, 2011).

These molecules were then tested in our HT platform to assess their efficacy as protein production enhancers in CHO cells. The results are displayed in **Figure 6.2**. The parent molecule 2TAA (tested from 0.2 to 2 mM) had recorded a maximum yield enhancement of 1.6 fold at 0.8 mM. The key culture characteristics of 2TAA supplementation were: (i) reduction in IVCD, (ii)

increase in qP and overall titer (concentration dependent) and (iii) no loss in viability at the highest titer yielding concentration. We aimed to investigate whether the analogues displayed similar performance in our HT screening platform. The same range of concentrations (as 2TAA) was initially tested for all analogue molecules.

TPA (**Figure 6.2B**) did not show any major titer improvements when tested from 0.2 to 2 mM. However, a gradual increase in qP with increasing concentrations was observed. This prompted us to further investigate a higher concentration range. Further enhancements in qP were observed with cell growth diminishing around the 4.8 mM concentration range, and viability dropping post 4 mM. TBA (**Figure 6.2C**) yielded the poorest performance amongst all the thiophene carboxylates tested. This was interesting since the molecule only had 1 extra carbon atom (1 hydrocarbon chain) in comparison to TPA. However, performance differed drastically, with cell growth diminishing and viability dropping at 0.8 mM. This molecule was thus excluded from any further experimentation. 2TCA (**Figure 6.2D**) displayed concentration dependent growth reduction, however, no positive effects to cellular qP were observed at any concentration. Testing higher concentrations did not yield any benefit either. Thus, this molecule was excluded from any further examination as well. Lastly, 3TAA (**Figure 6.2E**), recorded the best titer performance from the tested analogue molecules. The molecule is highly similar to 2TAA (the position of the aliphatic chain is displaced). Growth suppression was less severe compared to 2TAA, thus a large range of concentrations could be tested. The optimum concentration (1.6 fold titer increase at 2.5 mM) was also higher than 2TAA.

There is no literature evidence on the use of these molecules to improve biologics production. We decided to take forward 3TAA (as the best performing analogue for titer) along with the already reported 2TAA for scale-up batch studies in shake flasks. 3TAA, TPA along with 2TAA were also tested in our delayed addition setup to investigate whether titer could be further amplified when the qP enhancing thiophenes were added on day 3 (mid-exponential growth phase) instead of day 0 (detailed in **Section 5.3.10**).

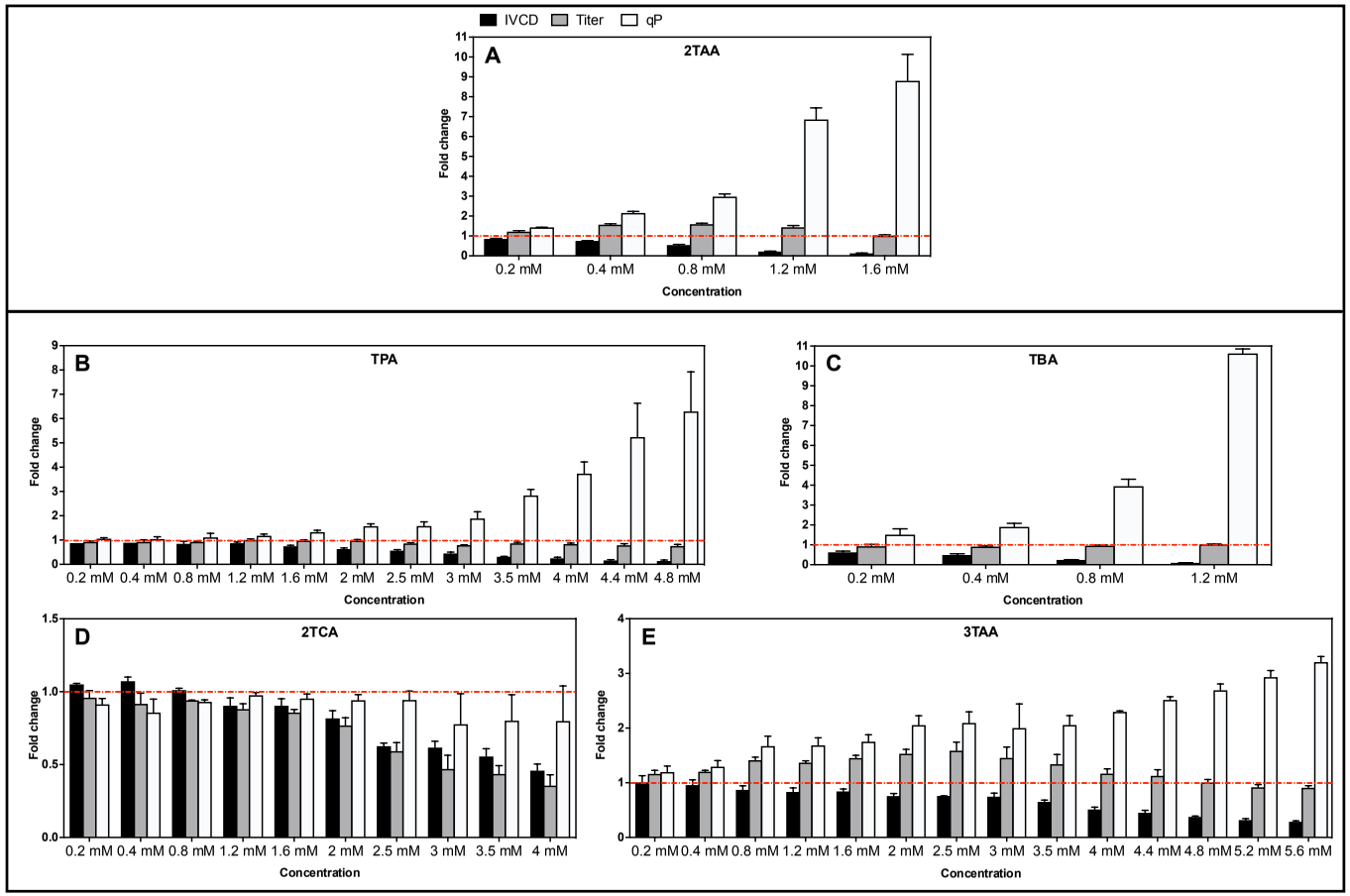

Figure 6.2 HT screens of the selected small molecules that were structurally similar to 2TAA. Cell growth (IVCD), Titer and qP displayed as a fold change over 0.2% v/v DMSO control. Cells were seeded at 0.2×10^6 cells mL^{-1} in 96 DWPs. Cell growth and titer were measured after 5 days using the PrestoBlue and Valita™TITER assay respectively. **(A)** 2TAA (original molecule) **(B-E)** structural analogues of 2TAA. **(B)** 2-Thiophenepropionic acid (TPA), **(C)** 2-Thiophenebutyric acid (TBA), **(D)** 2-Thiophenecarboxylic acid (2TCA) and **(E)** 3-Thiopheneacetic acid (3TAA). Data represents mean ± SEM of at least three experimental replicates with three technical replicates. Data for 2TCA and TBA represents mean ± SEM of two experimental replicates with three technical replicates.

6.3.2. Production Performance of 2TAA and 3TAA in Batch Shake Flask Culture

Our HT system allows for the discovery of novel chemical enhancer molecules as discussed in the previous section, however late stage culture performance and effect over a longer culture period cannot be elucidated. To ascertain that the culture elevating performance of 2TAA and its novel analogue enhancer 3TAA were maintained at a larger scale and over a longer time period, we trialled both molecules in 30 mL shake flask batch cultures. Culture conditions were monitored daily and the cultures terminated when the viability of all culture conditions fell below 30%.

Figure 6.3A depicts the growth profiles of the enhancer-supplemented cultures in comparison to the non-supplemented controls (no addition or 0.2% v/v DMSO (solubilisation vehicle for both 2 and 3TAA)). Cell growth was visibly reduced in both 2TAA and 3TAA supplemented cultures, however the cells remained viable (**Figure 6.3B**). The low number of cells in culture contributed towards the slow consumption of nutrients, resulting in the culture remaining viable for a longer period over the control cultures. Both the control conditions witnessed a drop in viability from day 7 onwards, with SME supplemented cultures remaining viable for at least an extra day. To compare the 2 molecules, 3TAA had a lower impact on cell growth arrest in comparison to 2TAA. Their mean peak cell densities (both achieved on day 7) were $6.1\pm0.137\times10^6$ cells mL^{-1} and $8.87\pm0.461\times10^6$ cells mL^{-1} for 2TAA and 3TAA respectively. In contrast, control cultures peaked at around 12×10^6 cells mL^{-1} on day 5 (no addition: $12.1\pm0.642\times10^6$ cells mL^{-1}; 0.2%v/v DSMO: 12.34 ± 0.625 cells mL^{-1}). The slower growing 2TAA cultures also recorded a slightly slower drop in viability in comparison to 3TAA cultures. IVCD is a measure of the accumulation of biomass throughout the culture period. Our studies showed that, unsurprisingly 2TAA and 3TAA cultures recorded lower IVCD than the control cultures. There was a 33% reduction in total IVCD for the 2TAA-supplemented cultures ($p<0.01$; one-way ANOVA, Dunnett's test), with a 13% drop (not significant) for the 3TAA-supplemented cultures in comparison to the DMSO control.

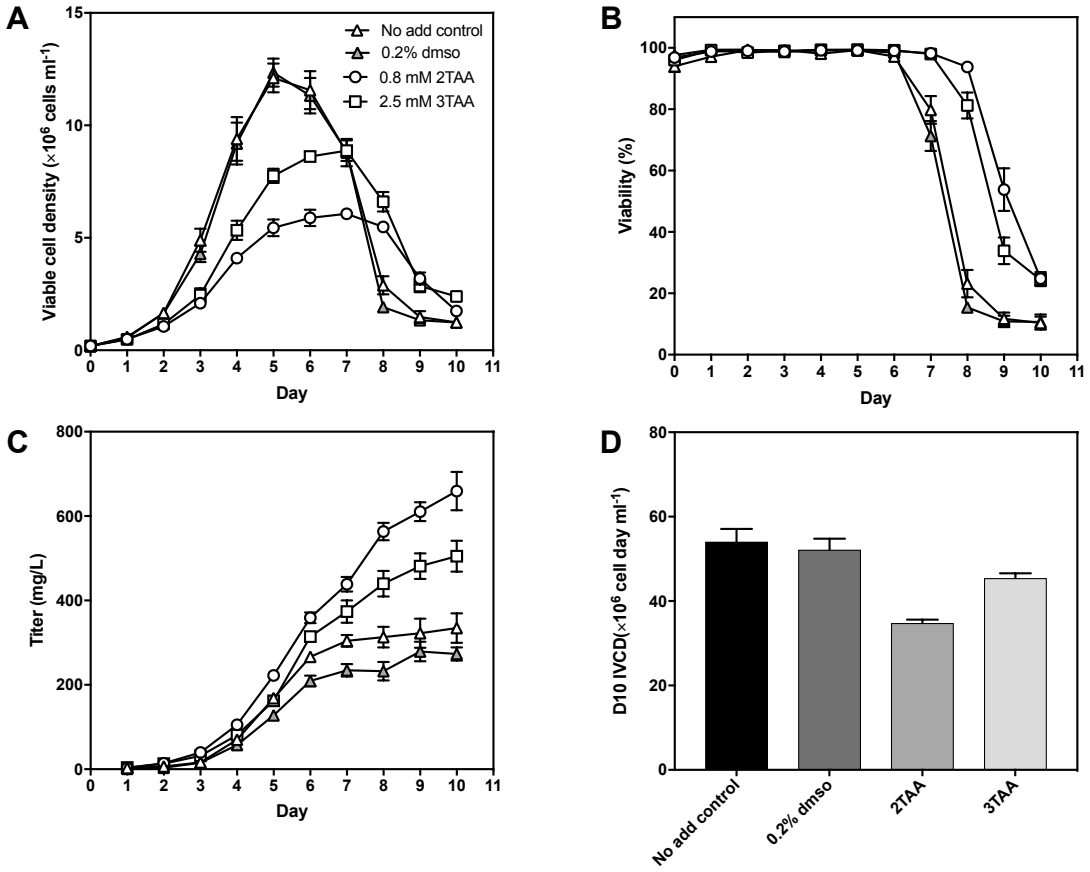

Figure 6.3 2TAA and 3TAA supplemented culture production performance in shake flask batch culture. Cobra 38 cells were seeded at 0.2×10^6 cell mL^{-1} in 30 mL shake flask cultures. The enhancer molecule was added on day 0 into the growth media (CD CHO). A 0.2% v/v DMSO control was included to account for any effects of the solvent on culture performance. Cell growth and viability readings were taken daily using the Vi-CELL XR and supernatant samples collected daily for analysis using the Valita™TITER assay. Cultures were maintained at 37°C for 10 days. **(A)** VCD, **(B)** Viability and **(C)** Titer shown for no addition control (-△-), 0.2% v/v DMSO control (-△-), 0.8 mM 2TAA (-○-) and 2.5 mM 3TAA (-□-). Total IVCD accumulated over the 10-day period is depicted in **(D)**. Data depicted is the mean and standard error of three experimental replicates each with two technical replicates.

Supernatant samples collected on each day were used to quantify the antibody levels in culture across all tested conditions. A shift in titer profiles with the SME supplemented cultures was evident from day 4 onwards for 2TAA. 2TAA supplemented culture titers consistently ranked over that of the control cultures until culture culmination. In comparison, 3TAA cultures recorded titer levels above the control from day 6 onwards. At the end of a 10-day batch culture period, 2TAA supplemented cultures were able to produce a 2.4 fold increase in

antibody titer ($p<0.001$) whereas 3TAA produced a 1.85 fold titer increase ($p<0.01$) over the DMSO control.

The concentration to test at the larger scale was informed through the HT screens. Thus, this study also embedded a secondary aim to understand scale-up batch performance. The growth arrests were comparable, i.e. 2TAA was predicted to be a stronger growth inhibitor than 3TAA in the HT screens. The HT screens predicted both enhancers to produce the same titer boost at their respective effective dose. However, batch culture shake flask studies showed that 2TAA outperformed 3TAA with respect to titer improvement spanning the culture period.

Overall, 2TAA was shown to be a stronger titer enhancer at the concentration tested. The major observation that decided the next line of experimentation was the growth arresting properties of both chemicals. Growth arrest is a common occurrence with many chemical enhancers such as butyrate and valproic acid (Chen et al., 2011; Park et al., 2016). G1 phase arrest is commonly linked to HDAC inhibition, as is the case with both butyrate and valproate (Yamaguchi et al., 2010). Since valproate and butyrate also contain a carboxylate structure, it was worth investigating the cell cycle state of the cells in 2 and 3TAA supplemented cultures.

6.3.3. Cell Cycle Analytics

2TAA and 3TAA supplemented cultures were analysed for their cell cycle distribution by PI based flow cytometry. As explained in the previous section, G1 arrest is often an accompaniment to carboxylate HDAC inhibitor SME main function. The results of cell cycle analysis performed on day 4 of batch culture (as shown in **Figure 6.3**) are displayed in **Figure 6.4**. The 3 main phases of cell cycle: G1, S and G2 were analysed. Both 2 and 3TAA recorded an increased accumulation in the G1 phase. There was an 18% increase ($p<0.001$) in G1 phase accumulation for 2TAA treated cells; while 3TAA cultures recorded a 13% increase ($p<0.01$) over the DMSO control. 2TAA was slightly more effective than 3TAA in arresting cells at G1, this is also evidenced by the lower

viable cell accumulation in **Figure 6.3A and D**. There were slight decreases in both S and G2 phase accumulation as a result of the G1 increase for the chemical supplemented cultures.

The results are in line with previous SME studies (of sodium butyrate and valeric acid) reporting an increase in G1 phase accumulation (Chen et al., 2011; Park et al., 2016). However, many SME led cell cycle arrest can culminate in apoptosis (Lee and Lee, 2012). Therefore, it was important to investigate the effect of 2 and 3TAA on cell health.

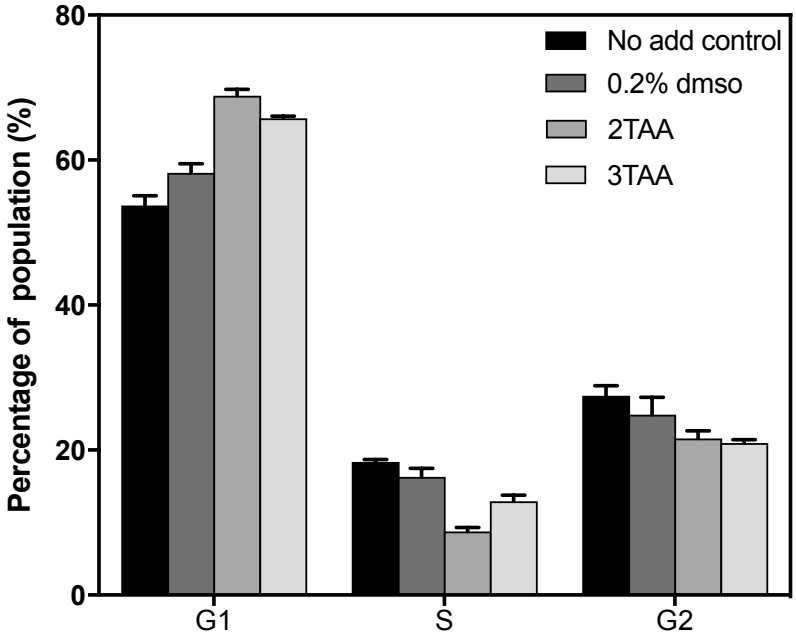

Figure 6.4 Cell cycle phase analysis of Cobra 38 cells in the presence of 2TAA and 3TAA. 1×10^6 cells were taken from the shake flask cultures on day 4 of batch culture (SME added on day 0) and fixed. Cell cycle phases were analysed using flow cytometry techniques using PI staining. Cell cycle distribution is depicted as a percentage of the total cell population analysed. Data represented as mean percentage and standard error of three experimental replicates each with two technical repeats. A one-way ANOVA was performed on the G1 phase data of all conditions tested, with a Dunnett's multiple corrections test.

6.3.4. Apoptosis Analysis

Cell cycle arrest can often come with one caveat, the induction of apoptosis. The increase in this type of programmed cell death can stunt viable cell culture

and result in lower product return (Kim and Lee, 2000). Cultures supplemented with NaBu have recorded an induction of apoptosis from as early as 24 hours (Lee and Lee, 2012). Other studies investigated apoptosis induction 4 days after chemical addition (Backliwal et al., 2008; Camire et al., 2017). Since both 2TAA and 3TAA were confirmed to be G1 phase inhibitors, it was vital to investigate if apoptotic induction accompanied it. The apoptotic profiles of the cells cultured with the chemical enhancers was analysed on day 5 post-addition using flow cytometry. The highest titer inducing concentrations for 2 and 3TAA (0.8 and 2.5 mM respectively) were analysed. A lower concentration of 2TAA (0.4 mM) was also included (one that grew around the same rate of 3TAA supplemented cultures) to more effectively compare apoptotic profiles with 3TAA. Additionally, NaBu was included as a comparative control; 2 concentrations with varying titer enhancement and growth suppression were chosen. The resultant early apoptotic profiles are displayed in **Figure 6.5 (A-B)**.

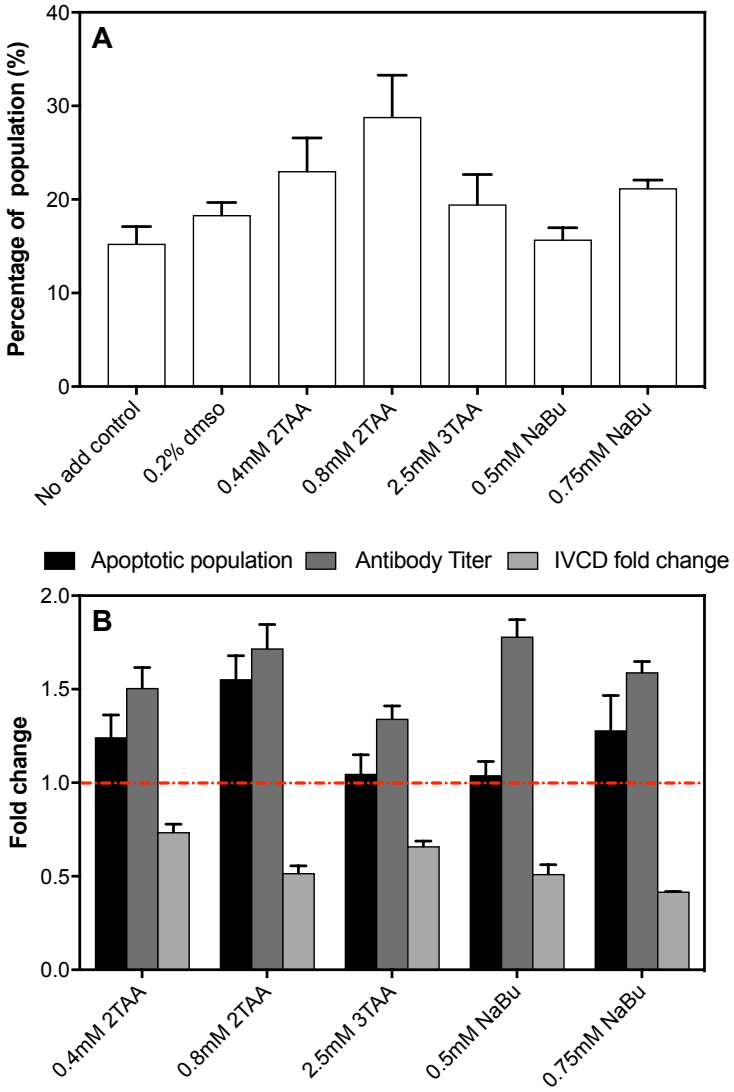

Figure 6.5 Apoptosis analysis of Cobra 38 cells in the presence of various concentrations of SMEs. Cobra 38 cells were seeded at 0.2×10^6 cells mL^{-1} in 10 mL TubeSpin disposable bioreactors for 5 days. Chemical added on day 0. 1×10^6 total cells were collected on day 5 of culture and analysed using Annexin V (apoptosis indicator) and 7AAD (dead cell indicator) staining on the Attune Acoustic Focusing Cytometer. 10,000 total events were analysed. Annexin V +ve but 7AAD −ve, cells were classed as early apoptotic cells with intact membranes. Cell growth and titer were also measured on day 5 using the Vi-CELL XR and Valita™TITER assay respectively. **(A)** depicts the percentage of cells that were Annexin V +ve and 7AAD −ve out of all cell events recorded. **(B)** shows the early apoptotic percentages as a fold change over the respective control percentages (0.2% v/v DMSO control for 2TAA and 3TAA cultures; no addition control for NaBu cultures). Titer and IVCD fold change on day 5 displayed for comparison. Data represented is the mean and standard error of three experimental replicates each with two technical replicates. No significant difference observed in comparison to respective controls (Dunnett's test).

Figure 6.5A shows the percentage of the culture population displaying early apoptotic traits. 28.8% of cells cultured in the presence of 0.8 mM 2TAA were recorded to be undergoing early apoptosis. The other SME conditions trialled did not display any major deviations from the apoptotic profiles of their respective controls. Interestingly, there was a very slight increase in apoptotic fractions in the DMSO control compared to the no addition control. There were also slight increases in apoptotic fractions with increasing concentrations of 2TAA and NaBu. This depicted the importance of titrating various concentrations to find the "sweet spot" in terms of titer enhancement and apoptosis onset. Interestingly, with our cell line and product, NaBu supplementation did not induce high levels of apoptosis or stunt cultures at its effective titer boosting concentration. This is in contrast with other studies on the topic (Backliwal et al., 2008; Lee and Lee, 2012).

Figure 6.5B compares the relative levels of apoptotic cell population increase with relative titer enhancement and growth suppression. 0.8 mM 2TAA and 0.5 mM NaBu supplemented cultures recorded similar growth reduction and titer enhancement over their respective controls. However, apoptotic induction for 0.8 mM 2TAA cultures was about 1.5 fold higher than 0.5mM NaBu. This suggested that 0.8 mM 2TAA supplementation did elevate apoptotic cell population levels. This observation was not picked up on the Vi-CELL XR, however this was not unexpected considering the need for membrane permeability for determination of percentage viability on the machine. It was interesting to note that while titer levels for both 0.8 mM 2TAA and 0.5 mM NaBu at the day 5 data collection point were similar, 2TAA was revealed to be a stronger titer enhancer overall, at the end of the culture period (2TAA: ~ 2.5 fold vs. NaBu: 2 fold; data not shown). Conversely, 3TAA was the lowest ranked titer enhancer at the day 5 data point, however recorded similar titer levels to 0.5 mM NaBu at the end of culture period. Both these observations were due to an extended culture period for 2 and 3TAA, caused by a slower crash in overall culture viability. This was surprising in the case of 2TAA since midpoint culture analysis revealed an onset of apoptosis.

6.3.5. Product Transcriptional Analysis

Transcription is the first step for recombinant protein expression. Monitoring transcriptional activity based on product mRNA levels can reveal 2 important attributes of SME activity. Firstly, does the molecule act at the transcriptional level at all, i.e. is there an increase in mRNA levels of the recombinant protein product? Secondly, if transcription is increased, is it solely responsible for the increases in protein production or do pathways downstream of transcription also have an impact? Simply put, is the transcriptional increase equivalent to the cellular productivity increase? The cell cycle arrest at G1 along with the carboxylate structure seen in many HDAC inhibitor molecules, led us to hypothesise that both 2 and 3TAA could act at the transcription level; a characteristic of HDAC inhibitor SMEs.

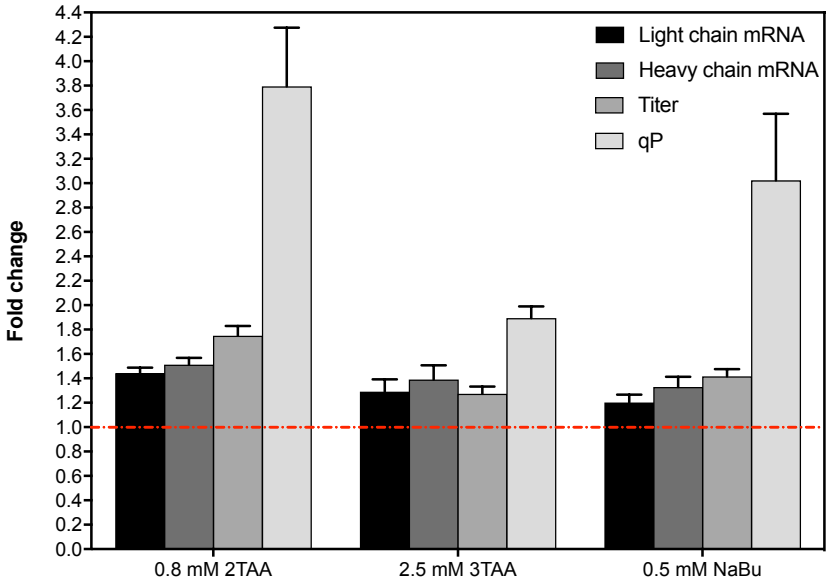

Figure 6.6 Heavy and light chain mRNA content analysis of cells cultured in the presence of 2TAA, 3TAA or NaBu. Total RNA was extracted on day 5 of shake flask batch culture, with the SME added on day 0. cDNA was created for each sample, which was in turn analysed using qPCR (SYBR green). Heavy and light chain primers were employed along with 2 reference gene primers. Fold change in mRNA expression was computed using the $2^{-\Delta\Delta Ct}$ method based on the Ct values recorded for each condition. Relative mRNA expression represented for each SME to its respective control (0.2% v/v DMSO control for 2 and 3TAA; no addition control for NaBu). Supernatant samples were also collected on the day 5 collection point to compute titer and qP. Titer and qP also depicted as a fold change to their respective controls. Red line depicts the control level, i.e. set to 1. Data represented is the mean and standard error of three experimental replicates each with two technical replicates.

We investigated transcriptional activity at day 5 of the batch cultures shown in **Figure 6.3**. mRNA levels of the heavy and light chain of the IgG1 product were determined using qPCR. 0.5 mM NaBu was included as a positive control due to its role as a transcription enhancer through HDAC inhibition. The results are shown in **Figure 6.6**. Since cell number was accounted for when taking samples for RNA extraction, comparison to cell specific productivity served as a more appropriate indicator of the extent of the role of transcription in increasing protein titer. All the SME supplementation conditions tested recorded an increase in both heavy and light chain mRNA levels. This was in accordance with our hypothesis that 2TAA and 3TAA acted at the transcription level.

Supplementation with 0.8 mM 2TAA recorded the largest increase in product mRNA levels. Given that those cultures recorded the highest qP, this was unsurprising. There was a 1.44 fold increase ($p<0.01$) in light chain mRNA and a 1.51 fold increase ($p<0.05$) in heavy chain mRNA. This observation was in discord with the previous study by Allen et al. (2008), which reported minimal increase in mRNA levels with 2TAA supplementation. However, the enhancement in mRNA levels was much lower in comparison to the increase in qP (3.8 fold), suggestive that post-transcription events could also play a role in increasing qP. 2.5 mM 3TAA supplementation induced a light chain mRNA enhancement of 1.29 fold ($p<0.05$), whereas heavy chain mRNA was increased by 1.39 fold ($p<0.05$). Again, there was no replication of the levels of increase obtained at the cellular qP level, however the gap between the levels was lower in comparison to 2TAA. However, it cannot be discounted that events downstream of transcription also assist in the 3TAA facilitated qP increase.

The positive control (0.5 mM NaBu), interestingly recorded a lower increase in mRNA levels in comparison to both 2 and 3TAA. There was a 1.2 fold increase in light chain mRNA levels and a 1.33 fold increase in heavy chain mRNA levels. Again, transcriptional activity increase did not account for all of the qP increase (3 fold).

Overall, this line of experimentation confirmed that both 2 and 3TAA at least in part on the mRNA level.

6.3.6. Histone Modification Analytics in Batch Culture Mode

The confirmation of increased transcriptionally activity, reminiscent of HDAC inhibitors, led us to hypothesise that 2 and 3TAA could indeed act at the epigenetic level. A HDAC inhibitory mechanism was proposed as the mode of action. This was due to the structural similarity to established HDAC inhibitors like sodium butyrate and valproate, along with the HDAC inhibitor behavioural characteristics observed (transcriptional enhancement, cell cycle block at G1). To test this hypothesis, histones were extracted from the cells on day 5. Histone modification analytics were performed using mass spectrometry methods. Mass spectrometry sample preparation, loading and analysis was performed by Eleanor Hanson at The University of Sheffield. Different peptide fragments of histones 3 and 4 were analysed for acetylation and methylation modifications. Different proteoforms (unique modified version of a peptide) were detected using the MS2 scan. The relative abundance of each identified proteoform was calculated based on the area under the curve of the proteoform peak on the MS1 scan relative to the summated proteoform peak areas.

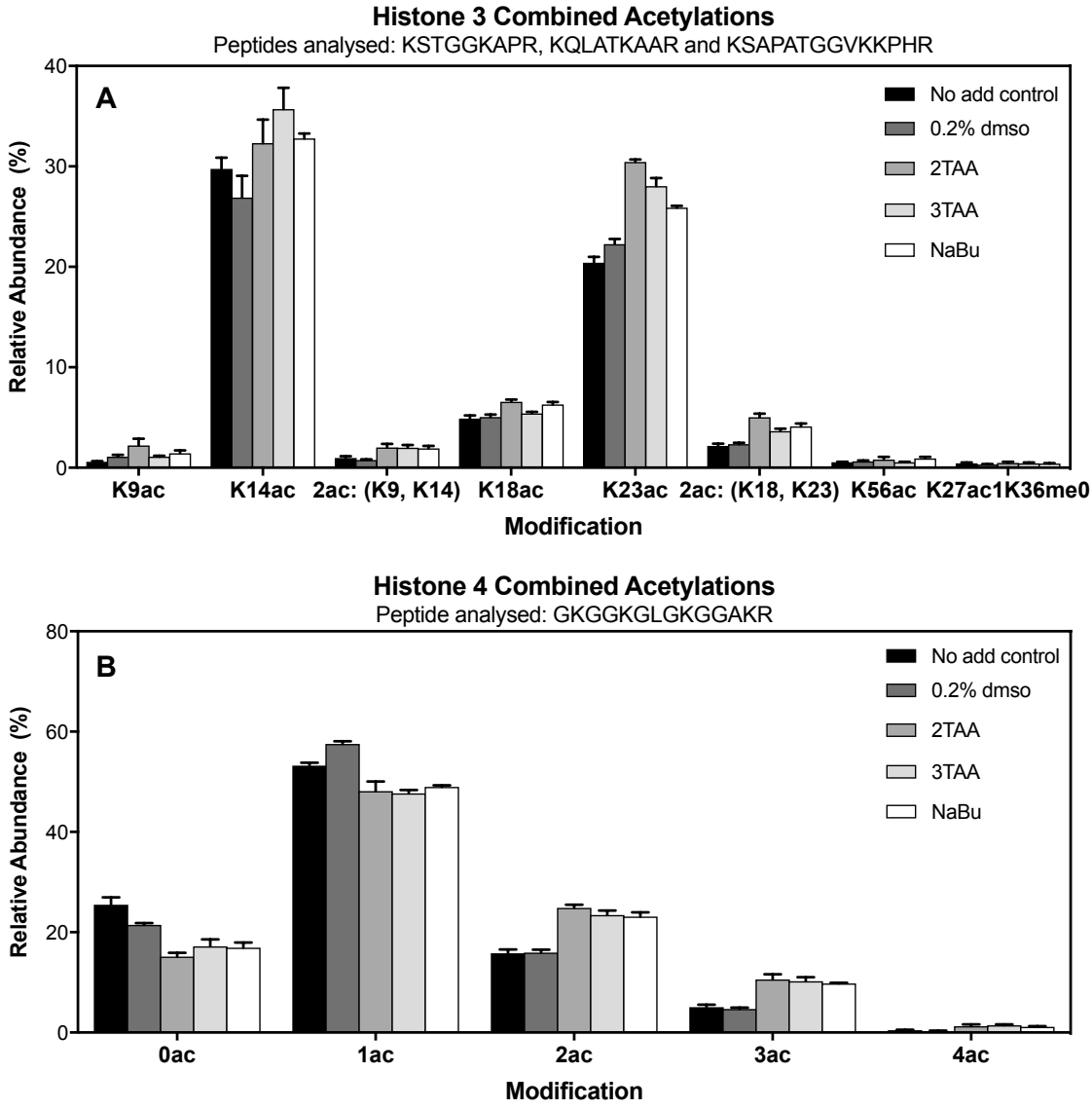

Figure 6.7 Acetylation modifications on histones 3 and 4 in the presence of thiophene SMEs. 10×10^6 cells were pelleted from shake flasks on day 5 of batch culture (SME was added on day 0). Histones were extracted, propionylated and analysed using the mass spectrometry techniques. MS1 spectra scans were labelled accordingly and area under each peak was calculated. Abundance was computed as a percentage for each proteoform relative to all proteoforms identified for that peptide. **(A)** Combined acetylation profiles for peptides analysed on histone 3. **(B)** Combined acetylation profiles for the single peptide analysed on histone 4. Relative abundances for proteoforms containing the same acetylation sites in each peptide were summated. Chemical concentrations used were: 0.8 mM 2TAA, 2.5 mM 3TAA and 0.5 mM NaBu. Glossary: K#: lysine at position #, ac: acetylation, me: methylation. Data represented is mean and standard error of three experimental replicates.

The acetylation state of histone 3 and 4 are depicted in **Figure 6.7**. 3 peptides were analysed on the histone 3 protein (**Figure 6.7A**): KSTGGKAPR (9^{th} to 17^{th}

amino acid from the N-terminus), KQLATKAAR (18^{th} to 26^{th} amino acid) and KSAPATGGVKKPHR (27^{th} to 40^{th} amino acid; letters represent one letter amino acid codes). All acetylated proteoforms tested recorded increased abundances for both 2 and 3TAA in comparison to the 0.2% v/v DMSO control. The level of enhancement varied between the 2 molecules, but generally 2TAA had higher abundance of acetylated lysine residues across histone 3. Double acetylated peptides, i.e. acetylated lysines at 2 positions on the peptide recorded the largest increase in abundance for both molecules. There was a 2.64 fold increase ($p<0.05$; Dunnett's test) in K9 and K14 double acetylation for 2TAA treated cultures. On the second peptide, K18 and K23 double acetylation abundance increased by 2.13 fold for 2TAA treated cells ($p\leq0.0001$). Similar trends were observed for 3TAA treated cultures. K9 and K14 double acetylation recorded a 2.61 fold increase ($p<0.05$) with K18 and K23 double acetylation also recording a 1.54 fold increase ($p<0.05$). The unmodified peptide relative abundances in the presence of both molecules were decreased (data not shown). This is not unexpected based on the method we employed to quantify abundances. Since relative abundance is based on the percentage of the total abundances of all proteoforms analysed, the rise in different acetylated versions of the peptide, resulted in a relative decrease of the unmodified peptide form.

NaBu treated cultures were included as positive controls for histone acetylation enhancement. On histone 3, consistent with the thiophene molecules, double acetylation recorded the highest enhancement in abundance compared to the no addition control (K18, K23: 1.88 fold ($p<0.01$) and K9, K14: 2.01 fold). Thus for histone 3, thiophene molecule supplementation followed the same trend as the established HDAC inhibitor molecule supplementation.

On histone 4, there were a number of co-eluting proteoforms with acetylation modifications on different lysine positions for the peptide (GKGGKGLGKGGAKR) tested. For ease of understanding, relative abundances were summated based on 4 categories: Unmodified (0ac), one lysine modified with acetylation (1ac), two lysines modified with acetylation (2ac), three lysines modified with acetylation (3ac), four lysines modified with acetylation (4ac). This data is displayed in **Figure 6.7B**. Expectedly, the unmodified proteoforms displayed lower relative abundance for all chemical supplementation conditions in comparison to the controls.

Interestingly, there was a shift towards multiple acetylation modifications rather than singular acetylation marks. All 3 chemicals recorded lower 1ac marks, however, all other multiple acetylation marks were enriched. The highest gains were observed for the 4ac proteoforms. Cells cultured in the presence of 2TAA yielded a 4.03 fold increase ($p<0.05$) in 4ac residues over the DMSO control. 3TAA supplementation resulted in a 4.6 fold 4ac ($p<0.01$) abundance enhancement over the DMSO control. 3ac for both chemicals was enhanced around 2.2 fold ($p<0.001$) and 2ac enhanced around 1.5 fold ($p<0.001$).

Similar trends were observed with the positive control, NaBu. Unmodified and 1ac abundances were lower than the no addition control. All other modifications witnessed increased abundances. 4ac modifications fold enhancement was slightly lower than the thiophene molecules (NaBu: 2.37 vs. 2TAA: 4.03 vs. 3TAA 4.6 fold) suggesting that 2 and 3TAA were more efficacious towards histone 4 HDACs in comparison, promoting acetylation on multiple lysine residues. Double and triple acetylation fold enhancements for NaBu were more comparable to the thiophene molecules (2ac: 1.47 ($p<0.001$) and 3ac: 1.94 fold ($p<0.01$)).

The data from this experimental study informed that both 2 and 3TAA increased abundance of acetylated histones (full significance testing and separate proteoform data is available in **Appendix D**). Histone acetylation opens up the chromatin, increasing the probability of binding of transcription factors to initiate transcription. Thus, it is safe to conclude that the gene expression enhancement obtained through the use of 2 and 3TAA stems from its role at the epigenetic level. Comparison to the histone state in the presence of NaBu, yielded similar trends, strengthening the validity of our hypothesis of the thiophene molecules acting as HDAC inhibitors.

6.3.7. *N*-Glycan Analytics

While investigating mechanism of action for titer enhancement was the main purpose for this study, evaluating any deleterious off-target effects on product quality was always imperative. It cannot be denied that SME use normally entails broad impacts; effects on product quality are not uncommon. Thus, IgG product glycosylation was analysed in the presence of 2TAA and 3TAA. Supernatant was collected from day 6 of batch culture and purified using protein A purification columns. Purified antibody samples (purity confirmed by SDS PAGE (see **Appendix D**)) were sent to NIBRT, Ireland and glycan release and subsequent analysis was performed by Dr. Roisin O'Flaherty and Dr. Karen P. Coss. 2-AB derivatised *N*-glycans were analysed by UPLC. 7 main *N*-glycan structures were analysed based on their chromatogram profiles depicted in **Figure 6.8**. The assignment of glycan peak (GP) to structure was performed in accordance with (Zhang et al., 2016). An additional control (human myeloma plasma derived IgG1 kappa) (IgG standard data **Appendix D**) was used for methods validation.

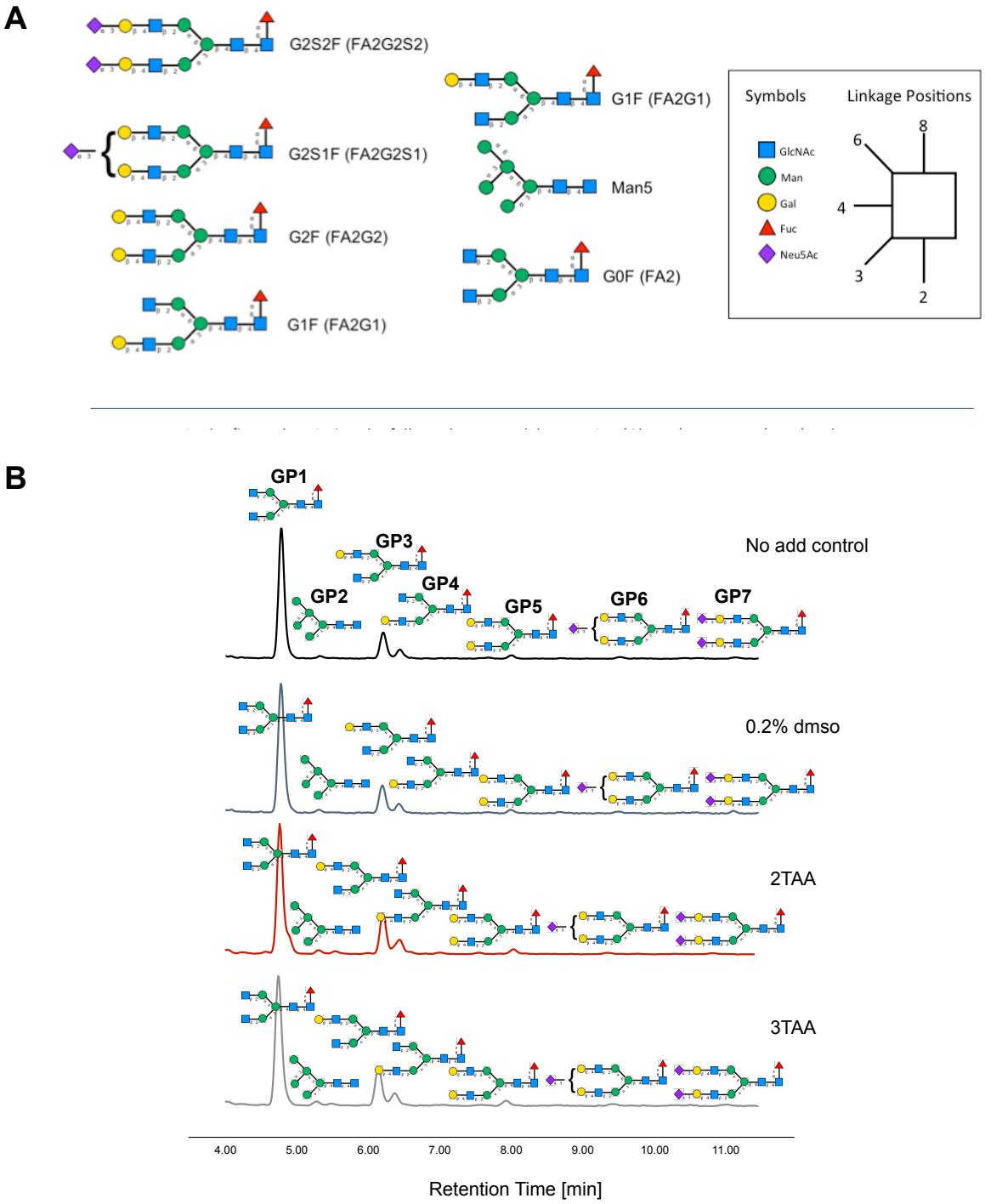

Figure 6.8 *N*-Glycans on the IgG1 molecule that were analysed using UPLC. (A) Predominant *N*-glycans present in CHO-S IgG1 kappa. **(B)** Representative chromatograms of CHO-S IgG1 kappa biological replicates, with predominant *N*-glycan structures indicated. GP refers to glycan peak. Chromatograms for culture conditions are as indicated.

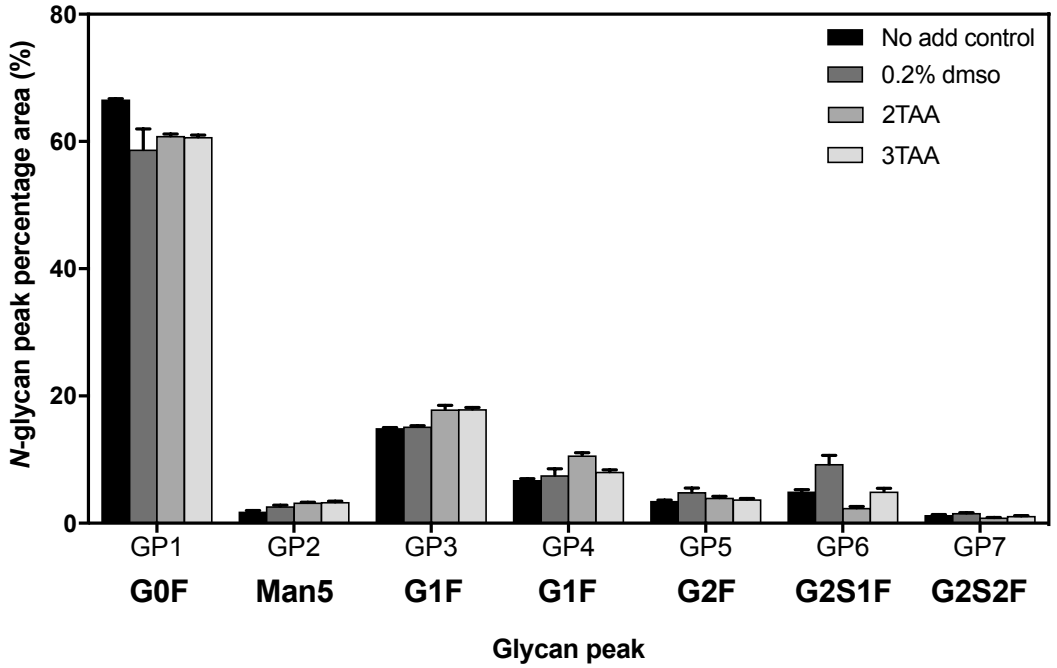

Figure 6.9 Average peak percentage areas of the different *N*-glycans analysed. Integrated chromatograms for each condition used to calculate peak area for each *N*-glycan. Peak area for each glycan peak is represented as a percentage of the total peak area. All replicate peaks recorded a percentage coefficient of variation of 20% or lower, within the biological variance acceptance limit. Data represented is the mean ± standard error of two biological replicates.

The released *N*-glycan structure profiles for each condition are summarised in **Figure 6.9**. The average peak percentage area is displayed for each glycan structure. On the whole, there were no major deviations of the protein product glycoprofiles of the chemical treated cultures from the control cultures. It could be concluded that 2 and 3TAA did not alter glycosylation majorly for it to be a cause for concern.

6.4. Discussion

The use of carboxylic acids is a common media engineering strategy when targeting improvements in recombinant product yield. Multiple studies have reported the use of these molecules, most notably sodium butyrate, sodium phenylbutyrate and valeric acid (Backliwal et al., 2008; Jiang and Sharfstein, 2008; Palermo et al., 1991; Park et al., 2016). These molecules mainly act by

inhibiting histone deacetylases, promoting a more open chromatin that can be easily transcribed, leading to re-activation of silenced genes. However, the deployment of these molecules can include deleterious off-target effects such as the induction of apoptosis (Backliwal et al., 2008; Lee and Lee, 2012) or variation in glycoform profiles such as decreased sialic acid content (Santell et al., 1999; Sung et al., 2004; Yin et al., 2018). However, these molecules normally provide vast increases in protein product titers, are cheap and easy to deploy, so prove difficult to completely ignore. Thus, the search for more suitable SME options is vital.

A large chemical library screening approach adopted by Allen et al. (2008), revealed novel carboxylate enhancers for protein production in CHO cells. This study revealed an effective thiophene carboxylate SME, 2TAA. However, mechanism of action was not clear from their experimentation. Screens with our in-house HT system and model CHO line and product confirmed its efficacy as a protein production enhancer. We investigated whether other thiophene molecules can be effective protein production enhancers. Instead of large cumbersome screening studies, we invested in small focused novel molecule screens based on structural similarity to 2TAA. Each analogue molecule had a unique culture performance profile; ranging from no impact (2TCA) and cytotoxic (TBA) to qP enhancing (TPA) to total titer improving (3TAA). It was interesting to note that similar structures resulted in drastically different phenotypic activity. It thus has to be noted that similar structure does not guarantee similar culture phenotype. It would be interesting to observe if each thiophene analogue has conserved activity when employed with different cell lines and products. The analogue screening revealed 3TAA as a previously unreported novel chemical enhancer molecule for improving CHO cell protein production. However, its mode of action as well as that of its parent molecule remained unknown. A series of carefully hypothesised experimentation enabled our understanding of the mode of action for both molecules.

Culture performance in shake flasks revealed 2TAA as a stronger growth suppressor and titer enhancer. This could be a concentration dependent observation and perhaps a higher concentration of 3TAA could push titer further (concentration was selected based on the best performing concentration at the

96 DWP level). Cell culture analysis also showed 2TAA to be a stronger G1 phase inhibitor. Interestingly, cells displaying apoptotic phenotypes also increased in the 2TAA cultures, while 3TAA did not appear to induce apoptosis. Halving the concentration of 2TAA still displayed apoptosis induction. Further experimentation and analytics would be required to confirm whether 2TAA induced apoptosis at every concentration that improved titer and what pathways were initiated to increase the apoptotic fraction. Interestingly, cell viability recorded on the Vi-CELL XR indicated no detriment to viability till about day 9, 4 days after the apoptotic analysis, which was detected on day 5. There could be 2 theories to support this observation: (i) the discrepancy between the flow cytometry and VI-CELL-XR, that latter is not sensitive to apoptotic cells and requires compromised membranes for dead cell classification and/or (ii) the cell had a slow rate of conversion from early apoptotic to dead state, this could also explain the lack of a drastic viability drop and steady increase in protein production observed between days 5 and 9. Perhaps more detailed analysis and replicates would help elucidate the differentiation effectively. The variation between apoptosis experimental replicates deterred us from making any strong concluding statements. Based on the apoptotic analysis we had available, 3TAA would outweigh 2TAA as the preferred enhancer despite the slightly lower titer return (2 vs 2.5 fold). Previous studies have shown the overexpression of bcl-2, addition of antioxidant chemicals or even reduction in culture temperature can combat carboxylic acid apoptotic activity while maintaining protein production enhancement activity (Camire et al., 2017; Chen et al., 2011; Kim and Lee, 2000). Perhaps the use of these strategies could be effective in controlling the supposed apoptosis induction by 2TAA. The inclusion of NaBu as a positive control for a G1 phase inhibiting carboxylic acid revealed no induction of apoptosis at its effective concentrations. This was interesting since this did not coincide with multiple studies that have reported on the induction of apoptosis in CHO and HEK293 in the presence of NaBu (Backliwal et al., 2008; Camire et al., 2017; Lee and Lee, 2012; Sung et al., 2004). Additionally, the lack of a sudden drop off in culture viability or production rates, suggests that NaBu indeed did not induce apoptosis at its effective concentration in our cell line. Then again, the effective dose for our cells was lower than many published studies like the ones mentioned above, so the

balance of apoptosis induction and production enhancement could vary between cell line and product.

Transcriptional analytics confirmed that both thiophene molecules acted at least in part at the transcriptional level. 2TAA unsurprisingly had the largest enhancement given that the molecules ranked the highest for titer and qP enhancement at the day 5 data collection point. 3TAA and NaBu also showed increased mRNA levels for both the light and heavy chain of the protein product. There were multiple interesting observations from the qPCR analysis. Firstly, in none of the conditions, were the increases at product mRNA level able to account for 100% of the increase in cellular specific productivity. This is not uncommon, wherein analysis revealed that similar discrepancies were observed in HDAC inhibitor studies by Allen et al. (2008) and Wulhfard et al. (2010). This suggests that while all 3 molecules tested in our study enhance transcription of the product gene of interest, they also directly or indirectly impact other pathways in the cell. Since the positive control used in this study, NaBu has been shown to differentially express multiple genes (Fomina-Yadlin et al., 2015), it would be logical to assume that the SMEs could impact processes downstream to transcription i.e. translation, folding and secretion.

Secondly, the cell cycle block induced by the thiophene molecules resulted in an increase in cell size (data not shown). This could indicate the availability of more cellular resources to potentiate protein-processing capacity. Additionally, the G1 phase is associated with increased ribosome biogenesis and upregulation of genes involved in translation (Kumar et al., 2007). Thus, an increased translational capacity could also be involved in the major qP enhancement associated with the use of 2 and 3TAA. This could constitute the basis of further experimentation in this area, perhaps proteomic analysis using mass spectrometry techniques could prove beneficial in understanding the translational capacity of the cell in the presence of the SMEs (Müller et al., 2017; Schwanhäusser et al., 2009).

Thirdly, heavy chain mRNA enhancement was slight stronger in comparison the light chain. It could be suggested that the opening up of the chromatin (suggestive from the histone acetylation data) indirectly alleviated transcriptional interference scenarios that normally burden the latter positioned

gene transcription (heavy chain gene in our vector). This could explain the larger gains for the heavy chain mRNA transcription.

As confirmed by our analysis using mass spectrometry, 2 and 3TAA both acted by promoting histone acetylation. This fits with the narrative of a HDAC inhibitor mode of action, with NaBu serving as a common exemplar. The abundance of acetylated lysine residues for majority of peptides analysed on histone 3 was increased in the presence of 2 and 3TAA. Interestingly, the thiophene molecules had no impact on the methylation state of the histone; this was consistent with the NaBu data as well. Thus, it could be concluded that both 2 and 3TAA (like NaBu) acted specifically on the acetylation state of the histone. On histone 4, unmodified and single acetylated proteoform abundance went down in favour of double, triple and quadruple acetylated proteoforms. It was evident that the molecules promoted addition of acetylation modifications on the lysine residues, thus opening up chromatin, increasing transcription factor accessibility (Bora-Tatar et al., 2009) for initiation of transcription. This, linked with the transcriptional enhancement results, confirmed the action of the molecules as relievers of epigenetic gene silencing. Interestingly, NaBu has previously also been shown to induce transcription factor expression directly, and thus helped upregulate CMV promoter driven expression (Fomina-Yadlin et al., 2015). Thus, it cannot be discounted that apart from epigenetic de-silencing to provide a more transcriptionally active chromosome physically, the thiophene molecules could also directly increase recombinant expression through induction of transcription factors. An RNA-seq based analysis would probably provide the most comprehensive view on the impact these molecules on a gene expression level.

Product quality is often a caveat that accompanies the use of SMEs. 2TAA and 3TAA use did not deviate the protein product from its standard product quality profile majorly, allaying fears of unwanted glycosylation patterns. This could make these molecules more attractive for use in comparison to already available HDAC inhibitors like NaBu. NaBu has been shown to negatively impact galactosylation (Hong et al., 2014) and has been shown in some cases to decrease α 2,3 sialylation (Oh et al., 2005; Sung et al., 2004). With 2TAA and 3TAA, such unacceptable shifts in glycoform profiles were not observed. More

replicates for glycosylation analytics and perhaps comparison to the protein glycoforms of cultures in the presence of NaBu, would elevate and cement the analysis presented here.

Given that these molecules act at the histone level, they could be used to inform novel chemotherapies for cancer. There is said to be a link between HDAC activity inhibition and tumour cell growth and survival (Kim and Bae, 2011). HDACs 1 and 2 were found to be overexpressed in various cancers (Kim and Bae, 2011). Multiple HDAC inhibitor molecules have been approved for use or are at the clinical trial stage (Biswas and Rao, 2017). The specific HDACs impacted by 2TAA and 3TAA could be ascertained using HDAC activity assays. Additionally, molecule potency could be evaluated against cancer lines. 2TAA has been shown to initiate slow apoptosis in our CHO cell line; it could be effective in initiating apoptotic activity in cancer cells. This could be a potential utility avenue to investigate.

To conclude, we were able to demonstrate the efficacy of our HT system in identifying previously untested SMEs for CHO cell bioprocess. We focused on thiophene carboxylic acid molecules and were able to isolate molecules with various degrees of impact on our stable bioproduction system. 2TAA and its structural analogue 3TAA maintained their enhancement activity in shake flask culture. We investigated the mechanism that mediated the titer improvement through various cell, product gene and epigenome specific pathways. We concluded that the molecules promoted gene transcription through their promotion of acetylated histone states. This associates them with an already growing repertoire of HDAC inhibitor molecules that are employed as inducers of protein expression. While some HDAC inhibitors aggravate apoptosis, while others struggle with correct glycosylation, 2 and 3TAA use can pose unique alternatives to battle these negative off-target impacts. Our studies indicate that 3TAA did not promote apoptotic pathway initiation, whereas neither molecule supplementation resulted in a change in a major shift in glycoform profile. We admit that it could be premature to deem these molecules as versatile enhancers without conducting a larger study that evaluates their efficacy in different production lines and products. However, the evidence presented here

is certainly promising and warrants increased interest in the investigation of thiophene molecules as enhancers for protein production.

Chapter 7

Conclusions and Future Directions

This chapter presents a summary and general discussion of the work presented in this thesis. As with any piece of research, there are a number of avenues that can be explored further. The recommendations for future work are also discussed in this chapter.

7.1. Summary and Conclusions

This thesis describes the development of a HT screening tool to establish culture performance enhancers for CHO cell based bioprocess. The work contained in this thesis would enable the creation of a commercial screening tool for users to fine-tune their production media and improve cell proliferation and/or production performance. While we were able to demonstrate the efficacy of a multitude of bioactive small molecules in a stable CHO cell producer system, it would be naïve to assume efficacy in a wider CHO processing arena. This understanding underpins the commercial opportunity of this research study. Molecule efficacy has repeatedly been shown to be cell type and product dependent (Backliwal et al., 2008; Johari et al., 2015; Yuk et al., 2015b). Thus, a simple to use, HT and informative media additive testing resource presents much promise. Counterparts such as genetic engineering, and directed evolution present cumbersome, costly and time intensive methodologies for CHO cell production enhancement. In comparison, bioactive molecules are incredibly easy to adopt and versatile.

The first step in creating a HT media additive screening tool was the development of HT culturing and analytical technologies (**Chapter 4**). The HT culturing platform developed was multi-well plate based. Shaken 96 DWP culturing allowed for better growth rates and longer culture duration in comparison to static cultures. Multiple studies reference the use of DWP technologies at various stages of cell line and process development (Hansen et al., 2015; Jordan and Stettler, 2014; Rouiller et al., 2016). This proves the popularity of the system in industry and academic circles. This was important since we want to present a commercial technology that can easily be adopted into the user's established cell line and process development workflow. The technology, based on the "System Duetz" (Duetz, 2007; Enzyscreen BV,) provided a flexible, HT, cost effective and scalable (to batch shake flask culture) culturing methodology. The addition of HT analytics completed the HT screening platform. Cell growth measured using the PrestoBlue assay and volumetric titer measured using the Valita™TITER assay allowed for cost effective and quick culture attribute determination. Again, flexibility to fit into the

user's available resources is key. Since both assays can be used on a single fluorescent plate reader, machinery costs are comparatively lower. However, if more sophisticated technologies such as the Iprasense Norma (Iprasense, Clapiers, France) or Guava® easyCyte (Merck, Darmstadt, Germany) are available for HT cell counting, these could be adopted into the platform. Overall, the HT screening platform developed allows for quick, simple and cost effective factor effect analysis. The ability to be easily adopted for robotic liquid handling and other automation methods is an added advantage of the platform. Additionally, the platform is robust and has shown adaptability to different cell lines and transient expression processes within our laboratory at The University of Sheffield.

In order to determine SME efficacy in CHO cell bioprocessing, a suite of 43 bioactive small molecules was evaluated in a stable CHO mAb producer system (**Chapter 5**). The screens were extensive in terms of functional targets and concentrations tested. A variety of molecules displayed improvements to the cell production process, enhancing cell growth, titer or both. Components that already formed part of the base media yielded improvements upon supplementation, suggestive of the potential of basal media component optimisation for cell growth and protein production benefit. The suite of molecules can be used for mainly 2 purposes: (i) maximising production and cell proliferation output in well established production systems and (ii) de-bottlenecking inefficient production systems. The second purpose would particularly find use in DTE production systems (Johari et al., 2015), or cell lines prone to toxic metabolite build-up (Yuk et al., 2015b). Additionally, molecule functionality and effective concentration were largely dependent upon timing of addition. Majority of the qP enhancers tested were more efficacious when added at the mid-exponential stage rather than at the start of culture. This was partly due to their negative impact on cell proliferation.

While singular addition of multiple molecules proved effective, combinatorial additions were able to elevate production levels further in our DWP culturing system. Strict criteria that governed design space suitability resulted in a small subset of molecules being tested for interactions with DOE techniques. The main advantage of factorial DOEs is the ability to screen for a large array of

factors in a short amount of time. However, we demonstrated its suitability in a relatively small design space, wherein we had an indication of significant singular factors in advance. Thus, the DOEs employed in this case were essentially for understanding the potential of interactions to improve cellular production performance. We were able to demonstrate the benefit of employing enhancer combinations wherein a best performing combination of 3 enhancers yielded a 4.3 fold titer improvement over the respective control population in our model production system. Given our production system records high titers in comparison to other systems (especially systems that require a DTE protein product to be produced (Johari et al., 2015)), the titer improvement achieved here bears the potential for further enhancement. The 7 factor DOE that utilised all the chemical modulators in the DOE design space served as an exemplar of the power of combinatorial designs in achieving varied production and proliferation phenotypes. The choice solely rests with the user to select which combination to employ. Generally combining more than 4 factors gave diminishing returns or negative interactions and thus employing parsimony is attractive.

Finally, our analysis on combinatorial treatment efficacy was trialled at a larger scale in shake flasks. The experimental model aimed to inform us on the scalability of our SME performance predictions. While the DWP platform was able to correctly predict enhancer combinations for improved production at scaled-up fed batch shake flask level, the extent of improvement did not concur. Our qP combinatorial strategy, while returning around a 60% improvement in titer in fed-batch shake flask studies did incur a loss in viability prematurely in comparison to the control cultures. Since DWP cultures only recorded culture attributes on a single day of short duration batch cultures, the loss in viability was not predicted at the smaller scale. This indicated that either a tweak in our DWP screening platform or our combination selection strategy was required. Perhaps adding feeds to the DWP system could provide us a more suitable, longer culture duration for testing enhancers that ultimately would be used in fed-batch production bioreactor studies. Alternatively, the guidelines on the extent of acceptable growth repression would need to be re-evaluated. Overall,

this chapter would form the foundation of a commercial screening tool. The envisioned screening tool is described in **Section 7.3**.

Finally, we employed our HT screening platform to test the efficacy of novel potential SME molecules (**Chapter 6**). We discovered that 2TAA, a thiophene carboxylic acid (Allen et al., 2008) was highly effective in our production system and give a 1.6 fold titer boost when added on day 0 of DWP culture, going up to 3.2 fold when added during the mid-exponential culture phase. Structural analogues of the molecule have never been previously investigated for the purposes of biotherapeutic production. 3TAA, a structural analogue of 2TAA, demonstrated production titer improvement in our screens and titer improvements were maintained for both molecules in shake flask batch cultures. Analysis of the epigenetic state of the cell revealed both molecules promoted acetylation modification on multiple sites on histones 3 and 4. This was in agreement with an established HDAC inhibitor, sodium butyrate. Transcriptional activation of the product gene was confirmed through qPCR. Transcriptional silencing due to the histone deacetylation is a common occurrence. The tightly packed chromosomal structure physically impairs transcription (Jiang and Sharfstein, 2008; Kim and Bae, 2011). Thus, both molecules played a pivotal role in improving product gene transcription. From a product quality perspective, no major shifts in glycoprofiles were observed instilling confidence in the use of these molecules. Overall, the chapter presented the potential of the combined use of *in-silico* structure analytics and HT screening to identify novel SMEs for bioprocess. This strategy could be applied to other established SMEs to isolate novel structural analogues that improve bioprocess.

7.2. Future Work Recommendations

Like previously mentioned, this research study presents the conceptualisation of a potential commercial media additive screening technology. It is imperative that a number of reduction to practice steps would be required to fully validate and develop this technology for commercial use. Recommendations for future and developmental work are presented here. While our recommendations

would focus mainly on the HT SME screening tool, future steps are also discussed to enhance the thiophene molecule mode of action analysis presented in **Chapter 6**.

The major limitation of our HT screening platform (described in **Chapter 4**) is the lack of product quality analytics. With the competitive era of biosimilars and biobetters upon us and with product quality playing a role in determining product safety and efficacy, HT product quality analytics would be a valuable addition to the screening tool. HT purification (Phytips; PhyNexus, San Jose, CA), HT sample preparation and glycan release technologies (Stöckmann et al., 2015) are increasingly being employed. Additionally, lectin microarrays (RayBiotech, Georgia, USA) or plate based lectin assays (GlycoImage; Galab Technologies, Hamburg, Germany) are available for HT analysis of glycan species. However, these are expensive, time intensive or low-throughput. Extensive research would be required to investigate commercial partners for glycoform analytics or development of a HT glycan assay in-house.

Another functionality that could elevate the HT screening technology would be the addition of fed-batch culturing modalities. Fed-batch microwell DWP culturing has been described previously (Rouiller et al., 2016). Addition of feeds, and thus extending the culture could provide better predictability of shake flask fed-batch performance. Again, this hypothesis would need to be thoroughly validated. However, it should be noted that fed-batch modality adds another variable into the system, the effect of feeds. Most companies have their bespoke feed and feeding strategies and flexibility could rest with the user whether testing in fed-batch modalities is desired. Some preliminary fed-batch studies with a candidate clone, media and feeds would be ideal in determining if scale-up fed-batch predictability is improved by screening in a fed-batch DWP mode.

The research contained in **Chapter 5** described the extensive processes undertaken to identify potential enhancers for CHO cell bioproduction. It cannot be assumed that functional efficacy will predictably transfer across other cell lines and products. This rationale underpins the commercial opportunity of a screening tool. However, testing in a single media and cell type cannot be used to define the product. Thus, validation studies performed with different cell lines

and basal media would be necessary. This would help gauge a better understanding of molecules and concentrations that would be functionally efficacious across a number of production platforms. This would help narrow down the molecules that would form part of the finalised commercial platform. Additionally, small DOE studies accompanying the SME assessment in different lines and media would be ideal. Herein, we would be informed of the DOE strategy moving forward. If certain combinations always bear some degree of enhanced efficacy over their respective singular factor effects, these combinations would form part of the coated DWP product along with the singular enhancers. If combinations are extremely production system specific, then combinatorial designs could be an add-on bespoke service to the product, informed by the initial singular molecule screening performed in the user's production process.

Our DWP platform correctly predicted enhancers that improved cellular IVCD and production at a larger scale (in fed-batch shake flask mode). However, the extent of improvement over the control was much lower than the DWP predictions. One aspect to explain this discrepancy would be the un-optimised nature of the experimentation; feeding regimes were not optimised to maximise potential. Optimisation experiments mainly focusing on the timing of addition of the qP enhancer molecules would be beneficial. Second, fed-batch modality was not adopted in DWPs. Addition of feeds, if required, could remedy that as explained in the section above. Thirdly, fed-batch mode itself might present a smaller margin for improvement. Finally, it was observed that the most productive condition produced a steady drop in viability post addition of enhancers. The loss in viability potentially shortened the productive culture duration. This was not visible in DWP cultures. Perhaps, fed batch modality in DWPs could solve this issue. However, it also pointed towards a change in enhancer selection stringency. The extent of growth suppression in the short DWP cultures could be an indication of viability issues that could be associated with scaled-up fed-batch shake flask culture. Thus, perhaps selecting combinations that do not highly suppress growth could be better suited for scaled-up fed-batch production runs. More experimentation exploring this hypothesis would be required. Ideally, all scale-up prediction studies would be

performed in an even larger scale such as bench top bioreactors. However, resource availability would play a major role in the realisation of such experimentation.

As stated previously, addition of a protein glycosylation analytical tool to the screening platform would help assess SME impact on product quality. Additionally, it could help expand the repertoire of molecules. Small molecule modulators of glycosylation could be impactful in fine-tuning glycoprofiles to the desired standard. Molecules like manganese, uridine and galactose are common supplements added to media to improve mAb galactosylation (as discussed in **Section 2.2.5**) (Grainger and James, 2013; Gramer et al., 2011). Additionally, other studies have revealed that several modulators can be intelligently employed to modulate protein quality towards a desired glycoform (Brühlmann et al., 2017a; Brühlmann et al., 2017b). Thus, if we are able to expand our screening platform to include protein analytics, then small molecule modulators for glycosylation could be an impactful addition to our chemical suite.

With regards to the thiophene study presented in **Chapter 6**, further analysis into their role in histone acetylation would be interesting. Kit-based HDAC activity assays are available to quantify impact on the different classes of HDACs. Additionally, a more sensitive detection of apoptosis induction through the use of the thiophenes would be beneficial. Due to equipment limitation at the time, that was not possible. As stated previously, an in-depth proteomic and transcriptomic analysis would provide most comprehensive analysis on impact of the molecules on cellular processes. Additionally, the discovery of thiophene molecules as novel enhancers for bioprocess could have a wider impact in other research circles. HDAC inhibitors find use in the treatment of various cancers (Kim and Bae, 2011), and the thiophene molecules could be re-purposed for cancer therapy use. Potency against cancer cell models would help inform upon the validity of this hypothesis.

7.3. Intended Product Use and Potential Impact

As mentioned previously, the lack of commercial, standardised, easy to use, HT, media additive screening and optimisation technologies presents a commercial opportunity. The envisioned screening tool is a simple-to-use DWP (or multiple DWPs) delivered with a single or combination of SMEs pre-coated on each well. The addition of a pre-determined cell culture volume would essentially re-constitute the chemical enhancers in culture allowing for a chemical supplemented culture. A secondary plate model would be included to test for mid-exponential phase chemical addition. Herein, cells would be grown on an uncoated DWP; the chemical suite would be pre-coated on wells of a microplate. Following reconstitution of the chemical, the microplate contents would be added to the respective wells of the DWP at the mid-exponential phase of culture. The multiple chemical supplemented cultures would be incubated in shaking conditions for a stipulated culture duration period, following which culture attributes (cell growth and titer in our current specification) would be assessed. Software to analyse the culture performance to inform recommendations for the next line of experimentation would accompany the plate-based tool. The potential product would find use in both cell line development and process development stages of upstream processing. It could be used to augment clone selection and screening. Selection of clones is their most productive environment can assist in a more dynamic ranking of clones in comparison to screening in standard conditions (Legmann et al., 2011). Clone selection under different media conditions, could inform of a highly productive clone that could have been eliminated in standard testing conditions (i.e. same production media). Our plate product could supplement the ambr 15 screening that normally occurs during the latter stages of cell line development. However, the main use of the product would be post clone selection stages wherein only a couple of clones remain. Herein, the screening plate would help inform the development and optimisation of bespoke media environments relative to the user's production system. Future experimental approaches can be gleaned from this quick and informative screening tool. Ultimately, the product would aid in obtaining desired growth and/or production profiles in CHO cell based bioprocessing.

References

Aggarwal S. 2014. What's fueling the biotech engine — 2012-2014. *Nat. Biotechnol.* **32**:32–39.

Allen MJ, Boyce JP, Trentalange MT, Treiber DL, Rasmussen B, Tillotson B, Davis R, Reddy P. 2008. Identification of novel small molecule enhancers of protein production by cultured mammalian cells. *Biotechnol. Bioeng.* **100**:1193–1204.

Allier C, Morel S, Vincent R, Ghenim L, Navarro F, Menneteau M, Bordy T, Hervé L, Cioni O, Gidrol X, Usson Y, Dinten JM. 2017. Imaging of dense cell cultures by multiwavelength lens-free video microscopy. *Cytom. Part A* **91**:433–442.

Allier C, Bordy T, Hervé L, Cioni O, Esteban G, Allier C, Bordy T, Hervé L, Cioni O, Esteban G, Pisaneschi M. 2018. Label-free cell viability assay using lens-free microscopy. *Proc. Spie* **10497**.

De Almeida SF, Picarote G, Fleming J V., Carmo-Fonseca M, Azevedo JE, De Sousa M. 2007. Chemical chaperones reduce endoplasmic reticulum stress and prevent mutant HFE aggregate formation. *J. Biol. Chem.* **282**:27905–27912.

Altamirano C, Cairó JJ, Gòdia F. 2001. Decoupling cell growth and product formation in Chinese hamster ovary cells through metabolic control. *Biotechnol. Bioeng.* **76**:351–360.

Amanullah A, Otero JM, Mikola M, Hsu A, Zhang J, Aunins J, Schreyer HB, Hope JA, Russo AP. 2010. Novel micro-bioreactor high throughput technology for cell culture process development: Reproducibility and scalability assessment of fed-batch CHO cultures. *Biotechnol. Bioeng.* **106**:57–67.

Anderson MJ, Whitcomb PJ. 2016. DOE simplified: practical tools for effective experimentation. Productivity press.

Backliwal G, Hildinger M, Kuettel I, Delegrange F, Hacker DL, Wurm FM. 2008. Valproic acid: A viable alternative to sodium butyrate for enhancing protein expression in mammalian cell cultures. *Biotechnol. Bioeng.* **101**:182–189.

Backman TWH, Cao Y, Girke T. 2011. ChemMine tools: An online service for analyzing and clustering small molecules. *Nucleic Acids Res.* **39**:486–491.

Bai Y, Wu C, Zhao J, Liu Y-H, Ding W, Ling WLW. 2010. Role of iron and sodium citrate in animal protein-free CHO cell culture medium on cell growth and monoclonal antibody production. *Biotechnol. Prog.* **27**:209–219.

Baldi L, Hacker DL, Adam M, Wurm FM. 2007. Recombinant protein production by large-scale transient gene expression in mammalian cells: State of the art and future perspectives. *Biotechnol. Lett.* **29**:677–684.

Bandaranayake AD, Almo SC. 2014. Recent advances in mammalian protein production. *FEBS Lett.* **588**:253–260. http://dx.doi.org/10.1016/j.febslet.2013.11.035.

Barrett TA, Wu A, Zhang H, Levy MS, Lye GJ. 2010. Microwell engineering characterization for mammalian cell culture process development. *Biotechnol. Bioeng.* **105**:260–275.

Berlec A, Štrukelj B. 2013. Current state and recent advances in biopharmaceutical production in Escherichia coli, yeasts and mammalian cells. *J. Ind. Microbiol. Biotechnol.* **40**:257–274.

Bhambure R, Kumar K, Rathore AS. 2011. High-throughput process development for biopharmaceutical drug substances. *Trends Biotechnol.* **29**:127–135. http://dx.doi.org/10.1016/j.tibtech.2010.12.001.

Biolog. 2013. Phenotype MicroArrays for Mammalian Cells. https://cdn.shopify.com/s/files/1/0902/6558/files/PM_for_Mammalian_Cells.pdf?12601105330837845125.

Biswas S, Rao CM. 2017. Epigenetics in cancer: Fundamentals and Beyond. *Pharmacol. Ther.* **173**:118–134. http://dx.doi.org/10.1016/j.pharmthera.2017.02.011.

Blondeel EJM, Aucoin MG. 2018. Supplementing glycosylation: A review of applying nucleotide-sugar precursors to growth medium to affect therapeutic recombinant protein glycoform distributions. *Biotechnol. Adv.* **36**:1505–1523. http://www.ncbi.nlm.nih.gov/pubmed/29913209%0Ahttps://linkinghub.elsevier.com/retrieve/pii/S0734975018301071.

Blondeel EJM, Braasch K, McGill T, Chang D, Engel C, Spearman M, Butler M, Aucoin MG. 2015. Tuning a MAb glycan profile in cell culture: Supplementing N-acetylglucosamine to favour G0 glycans without compromising productivity and cell growth. *J. Biotechnol.* **214**:105–112. http://dx.doi.org/10.1016/j.jbiotec.2015.09.014.

Bora-Tatar G, Dayangaç-Erden D, Demir AS, Dalkara S, Yelekçi K, Erdem-Yurter H. 2009. Molecular modifications on carboxylic acid derivatives as potent histone deacetylase

inhibitors: Activity and docking studies. *Bioorganic Med. Chem.* **17**:5219–5228. http://dx.doi.org/10.1016/j.bmc.2009.05.042.

Borys MC, Dalal NG, Abu-Absi NR, Khattak SF, Jing Y, Xing Z, Li ZJ. 2010. Effects of culture conditions on N-glycolylneuraminic acid (Neu5Gc) content of a recombinant fusion protein produced in CHO cells. *Biotechnol. Bioeng.* **105**:1048–1057.

Bradford JA, Buller GM. 2009. Dead cell stains in flow cytometry: A comprehensive analysis.

Brown AJ, Sweeney B, Mainwaring DO, James DC. 2014. Synthetic promoters for CHO cell engineering. *Biotechnol. Bioeng.* **111**:1638–1647.

Brown AJ, Kalsi D, Fernandez-Martell A, Cartwright J, Barber NOW, Patel YD, Turner R, Bryant CL, Johari YB, James DC. 2017. Expression Systems for Recombinant Biopharmaceutical Production by Mammalian Cells in Culture. In: . *Protein Ther.* Wiley-Blackwell, pp. 423–467. https://onlinelibrary.wiley.com/doi/abs/10.1002/9783527699124.ch13.

Brown A, Gibson S, Hatton D, James D. 2018. Transcriptome-Based Identification of the Optimal Reference CHO Genes for Normalisation of qPCR Data. *Biotechnol J.* **13**.

Brühlmann D, Jordan M, Hemberger J, Sauer M, Stettler M, Broly H. 2015. Tailoring recombinant protein quality by rational media design. *Biotechnol. Prog.* **31**:615–629.

Brühlmann D, Muhr A, Parker R, Vuillemin T, Bucsella B, Kalman F, Torre S, La Neve F, Lembo A, Haas T, Sauer M, Souquet J, Broly H, Hemberger J, Jordan M. 2017a. Cell culture media supplemented with raffinose reproducibly enhances high mannose glycan formation. *J. Biotechnol.* **252**:32–42. http://dx.doi.org/10.1016/j.jbiotec.2017.04.026.

Brühlmann D, Sokolov M, Butté A, Sauer M, Hemberger J, Souquet J, Broly H, Jordan M. 2017b. Parallel experimental design and multivariate analysis provides efficient screening of cell culture media supplements to improve biosimilar product quality. *Biotechnol. Bioeng.* **114**:1448–1458.

Buchsteiner M, Quek L-E, Gray P, Nielsen LK. 2018. Improving culture performance and antibody production in CHO cell culture processes by reducing the Warburg effect. *Biotechnol. Bioeng.* http://www.ncbi.nlm.nih.gov/pubmed/29704441%0Ahttp://doi.wiley.com/10.1002/bit.26724.

Butler M, Huzel N. 1995. The effect of fatty acids on hybridoma cell growth and antibody productivity in serum-free cultures. *J. Biotechnol.* **39**:165–173.

Butler M, Huzel N, Barnabe N, Gray T, Bajno L. 1999. Linoleic acid improves the robustness of cells in agitated cultures. *Cytotechnology* **30**:27–36. http://www.ncbi.nlm.nih.gov/pmc/articles/PMC3449933/pdf/10616_2004_Article_201185.pdf.

Butler M. 2005. Animal cell cultures: Recent achievements and perspectives in the production of biopharmaceuticals. *Appl. Microbiol. Biotechnol.* **68**:283–291.

Butler M, Spearman M. 2014. The choice of mammalian cell host and possibilities for glycosylation engineering. *Curr. Opin. Biotechnol.* **30**:107–112. http://dx.doi.org/10.1016/j.copbio.2014.06.010.

Camire J, Kim D, Kwon S. 2017. Enhanced production of recombinant proteins by a small molecule protein synthesis enhancer in combination with an antioxidant in recombinant Chinese hamster ovary cells. *Bioprocess Biosyst. Eng.* **40**:1049–1056.

Carter PJ. 2011. Introduction to current and future protein therapeutics: A protein engineering perspective. *Exp. Cell Res.* **317**:1261–1269. http://dx.doi.org/10.1016/j.yexcr.2011.02.013.

Carvalhal A V., Marcelino I, Carrondo MJT. 2003. Metabolic changes during cell growth inhibition by p27 overexpression. *Appl. Microbiol. Biotechnol.* **63**:164–173.

Celik E, Calık P. 2012. Production of recombinant proteins by yeast cells. *Biotechnol. Adv.* **30**:1108–18. http://www.ncbi.nlm.nih.gov/pubmed/21964262.

Chang C-C, Hung C-M, Yang Y-R, Lee M-J, Hsu Y-C. 2013. Sulforaphane induced cell cycle arrest in the G2/M phase via the blockade of cyclin B1/CDC2 in human ovarian cancer cells. *J. Ovarian Res.* **6**:41. http://www.pubmedcentral.nih.gov/articlerender.fcgi?artid=3733945&tool=pmcentrez&rendertype=abstract.

Chaturvedi K, Sun SY, O'Brien T, Liu YJ, Brooks JW. 2014. Comparison of the behavior of CHO cells during cultivation in 24-square deep well microplates and conventional shake flask systems. *Biotechnol. Reports* **1**–**2**:22–26. http://dx.doi.org/10.1016/j.btre.2014.04.001.

Chen F, Kou T, Fan L, Zhou Y, Ye Z, Zhao L, Tan WS. 2011. The combined effect of sodium butyrate and low culture temperature on the production, sialylation, and biological activity of an antibody produced in CHO cells. *Biotechnol. Bioprocess Eng.* **16**:1157–1165.

Chiu SJ, Lee MY, Chen HW, Chou WG, Lin LY. 2002. Germanium oxide inhibits the transition

from G2 to M phase of CHO cells. *Chem. Biol. Interact.* **141**:211–228.
Chollet ME, Skarpen E, Iversen N, Sandset PM, Skretting G. 2015. The chemical chaperone sodium 4-phenylbutyrate improves the secretion of the protein CA267T mutant in CHO-K1 cells trough the GRASP55 pathway. *Cell Biosci.* **5**:1–4.
Chong WPK, Reddy SG, Yusufi FNK, Lee DY, Wong NSC, Heng CK, Yap MGS, Ho YS. 2010. Metabolomics-driven approach for the improvement of Chinese hamster ovary cell growth: Overexpression of malate dehydrogenase II. *J. Biotechnol.* **147**:116–121. http://dx.doi.org/10.1016/j.jbiotec.2010.03.018.
Christensen M. 2016. Modulation of Mammalian Cell Behavior for Enhancing Polymer-mediated Transgene Expression; Arizona State University.
Christman JK. 2002. 5-Azacytidine and 5-aza-2′-deoxycytidine as inhibitors of DNA methylation: Mechanistic studies and their implications for cancer therapy. *Oncogene* **21**:5483–5495.
Chung CY, Wang Q, Yang S, Yin B, Zhang H, Betenbaugh M. 2017. Integrated genome and protein editing swaps α-2, 6 sialylation for α-2, 3 sialic acid on recombinant antibodies from CHO. *Biotechnol. J.* **12**.
Chung JY, Lim SW, Hong YJ, Hwang SO, Lee GM. 2004. Effect of Doxycycline-Regulated Calnexin and Calreticulin Expression on Specific Thrombopoietin Productivity of Recombinant Chinese Hamster Ovary Cells. *Biotechnol. Bioeng.* **85**:539–546.
Collen D, Lijnen HR. 2004. Tissue-type plasminogen activator: a historical perspective and personal account. *J. Thromb. Haemost.* **2**:541–546. http://doi.wiley.com/10.1111/j.1538-7933.2004.00645.x.
Collen D, Stassen JM, Marafino BJ, Builder S, De Cock F, Ogez J, Tajiri D, Pennica D, Bennett WF, Salwa J. 1984. Biological properties of human tissue-type plasminogen activator obtained by expression of recombinant DNA in mammalian cells. *J. Pharmacol. Exp. Ther.* **231**:146 LP-152. http://jpet.aspetjournals.org/content/231/1/146.abstract.
Comley J. 2009. Design Of Experiments: useful statistical tool in assay development or vendor disconnect! *Drug Discov. World*. https://www.ddw-online.com/drug-discovery/p146741-design-of-experiments:useful-statistical-tool-in-assay-development-or-vendor-disconnect!winter-09.html.
Coronel J, Klausing S, Heinrich C, Noll T, Figueredo-Cardero A, Castilho LR. 2016. Valeric acid supplementation combined to mild hypothermia increases productivity in CHO cell cultivations. *Biochem. Eng. J.* **114**:101–109. http://dx.doi.org/10.1016/j.bej.2016.06.031.
Cortez L, Sim V. 2014. The therapeutic potential of chemical chaperones in protein folding diseases. *Prion* **8**:197–202.
Crowell CK, Grampp GE, Rogers GN, Miller J, Scheinman RI. 2007. Amino Acid and Manganese Supplementation Modulates the Glycosylation State of Erythropoietin in a CHO Culture System. *Biotechnol. Bioeng.* **96**:538–549.
Curry E, Green I, Chapman-Rothe N, Shamsaei E, Kandil S, Cherblanc FL, Payne L, Bell E, Ganesh T, Srimongkolpithak N, Caron J, Li F, Uren AG, Snyder JP, Vedadi M, Fuchter MJ, Brown R. 2015. Dual EZH2 and EHMT2 histone methyltransferase inhibition increases biological efficacy in breast cancer cells. *Clin. Epigenetics* **7**:1–12. http://dx.doi.org/10.1186/s13148-015-0118-9.
Dahodwala H, Sharfstein ST. 2014. Role of epigenetics in expression of recombinant proteins from mammalian cells. *Pharm. Bioprocess.* **2**:403–419. http://www.future-science.com/doi/abs/10.4155/pbp.14.47.
Daramola O, Stevenson J, Dean G, Hatton D, Pettman G, Holmes W, Field R. 2014. A high-yielding CHO transient system: Coexpression of genes encoding EBNA-1 and GS enhances transient protein expression. *Biotechnol. Prog.* **30**:132–141.
Davies SL, Lovelady CS, Grainger RK, Racher AJ, Young RJ, James DC. 2013. Functional heterogeneity and heritability in CHO cell populations. *Biotechnol. Bioeng.* **110**:260–274.
Dean J, Reddy P. 2013. Metabolic analysis of antibody producing CHO cells in fed-batch production. *Biotechnol. Bioeng.* **110**:1735–1747.
Defrancesco L. 2018. Drug pipeline: 1Q18. *Nat. Biotechnol.* **36**:386. http://dx.doi.org/10.1038/nbt.4142.
Deloitte. 2016. Global life sciences outlook: Moving forward with cautious optimism 1-28 p. https://www2.deloitte.com/content/dam/Deloitte/global/Documents/Life-Sciences-Health-Care/gx-lshc-2016-life-sciences-outlook.pdf.
Demain AL, Vaishnav P. 2009. Production of recombinant proteins by microbes and higher organisms. *Biotechnol. Adv.* **27**:297–306. http://dx.doi.org/10.1016/j.biotechadv.2009.01.008.

Derouazi M, Martinet D, Besuchet Schmutz N, Flaction R, Wicht M, Bertschinger M, Hacker DL, Beckmann JS, Wurm FM. 2006. Genetic characterization of CHO production host DG44 and derivative recombinant cell lines. *Biochem. Biophys. Res. Commun.* **340**:1069–1077.

Dez C, Tollervey D. 2004. Ribosome synthesis meets the cell cycle. *Curr. Opin. Microbiol.* **7**:631–637.

Doerflinger M, Glab J, Nedeva C, Jose I, Lin A, O'Reilly L, Allison C, Pellegrini M, Hotchkiss RS, Puthalakath H. 2016. Chemical chaperone TUDCA prevents apoptosis and improves survival during polymicrobial sepsis in mice. *Sci. Rep.* **6**:1–10. http://dx.doi.org/10.1038/srep34702.

Drugmand JC, Schneider YJ, Agathos SN. 2012. Insect cells as factories for biomanufacturing. *Biotechnol. Adv.* **30**:1140–1157. http://dx.doi.org/10.1016/j.biotechadv.2011.09.014.

Du Z, Treiber D, Mccarter JD, Fomina-Yadlin D, Saleem RA, Mccoy RE, Zhang Y, Tharmalingam T, Leith M, Follstad BD, Dell B, Grisim B, Zupke C, Heath C, Morris AE, Reddy P. 2015. Use of a small molecule cell cycle inhibitor to control cell growth and improve specific productivity and product quality of recombinant proteins in CHO cell cultures. *Biotechnol. Bioeng.* **112**:141–155.

Duetz W a. 2007. Microtiter plates as mini-bioreactors: miniaturization of fermentation methods. *Trends Microbiol.* **15**:469–475.

Duetz WA, Witholt B. 2001. Effectiveness of orbital shaking for the aeration of suspended bacterial cultures in square-deepwell microtiter plates. *Biochem. Eng. J.* **7**:113–115.

Duetz WA, Witholt B. 2004. Oxygen transfer by orbital shaking of square vessels and deepwell microtiter plates of various dimensions. *Biochem. Eng. J.* **17**:181–185.

Duetz WA, Rüedi L, Hermann R, Connor O, Büchs J, Witholt B, Connor KO, Ru L. 2000. Methods for Intense Aeration , Growth , Storage , and Replication of Bacterial Strains in Microtiter Plates Methods for Intense Aeration , Growth , Storage , and Replication of Bacterial Strains in Microtiter Plates **66**:2641–2646.

Dumont J, Euwart D, Mei B, Estes S, Kshirsagar R. 2015. Human cell lines for biopharmaceutical manufacturing : history, status, and future perspectives and future perspectives. *Crit. Rev. Biotechnol.* **1–13**.

Dutton RL, Scharer J, Moo-Young M. 2006. Cell cycle phase dependent productivity of a recombinant Chinese hamster ovary cell line. *Cytotechnology* **52**:55–69.

Enzyscreen BV. Clamps for deepwell MTPs + covers. http://www.enzyscreen.com/clamps_for_deepwell_mtps.htm.

Escher G, Hoang A, Georges S, Tchoua U, El-Osta A, Krozowski Z, Sviridov D. 2005. Demethylation using the epigenetic modifier, 5-azacytidine, increases the efficiency of transient transfection of macrophages. *J. Lipid Res.* **46**:356–365. http://www.jlr.org/lookup/doi/10.1194/jlr.D400014-JLR200.

Estes S, Melville M. 2014. Mammalian cell line developments in speed and efficiency. *Adv Biochem Eng Biotechnol.* **139**:11–33.

Fischer S, Handrick R, Otte K. 2015. The art of CHO cell engineering: A comprehensive retrospect and future perspectives. *Biotechnol. Adv.* **33**:1878–1896. http://dx.doi.org/10.1016/j.biotechadv.2015.10.015.

Fomina-Yadlin D, Mujacic M, Maggiora K, Quesnell G, Saleem R, McGrew JT. 2015. Transcriptome analysis of a CHO cell line expressing a recombinant therapeutic protein treated with inducers of protein expression. *J. Biotechnol.* **212**:106–115. http://dx.doi.org/10.1016/j.jbiotec.2015.08.025.

Le Fourn V, Girod PA, Buceta M, Regamey A, Mermod N. 2014. CHO cell engineering to prevent polypeptide aggregation and improve therapeutic protein secretion. *Metab. Eng.* **21**:91–102.

Franceschini G, Macchietto S. 2008. Model-based design of experiments for parameter precision: State of the art. *Chem. Eng. Sci.* **63**:4846–4872.

Fussenegger M, Schlatter S, Dätwyler D, Mazur X, Bailey JE. 1998. Controlled proliferation by multigene metabolic engineering enhances the productivity of Chinese hamster ovary cells. *Nat. Biotechnol.* **16**:468–472.

Galbraith DJ, Brown CJ, Birch JR, Racher AJ, James DC. Germanium dioxide improves specific Mab production by CHO cells in transient ans stable production formats.

Galvao J, Davis B, Tilley M, Normando E, Duchen MR, Cordeiro MF. 2014. Unexpected low-dose toxicity of the universal solvent DMSO. *FASEB J.* **28**:1317–1330.

Garcia BA, Mollah S, Ueberheide BM, Busby SA, Shabanowitz J, Hunt DF. 2007. Chemical derivatization of histones for facilitated analysis by mass spectrometry. *Nat. Protoc.* **2**:933–

938.
Gawron K, Jensen DA, Steplewski A, Fertala A. 2010. Reducing the effects of intracellular accumulation of thermolabile collagen II mutants by increasing their thermostability in cell culture conditions. *Biochem. Biophys. Res. Commun.* **396**:213–218.
GE Healthcare. 2014. HiTrap MabSelect SuRe - Data File 1-20 p.
Girod PA, Nguyen DQ, Calabrese D, Puttini S, Grandjean M, Martinet D, Regamey A, Saugy D, Beckmann JS, Bucher P, Mermod N. 2007. Genome-wide prediction of matrix attachment regions that increase gene expression in mammalian cells. *Nat. Methods* **4**:747–753.
González-Leal IJ, Carrillo-Cocom LM, Ramírez-Medrano A, López-Pacheco F, Bulnes-Abundis D, Webb-Vargas Y, Alvarez MM. 2011. Use of a plackett-burman statistical design to determine the effect of selected amino acids on monoclonal antibody production in CHO cells. *Biotechnol. Prog.* **27**:1709–1717.
Grainger RK, James DC. 2013. CHO cell line specific prediction and control of recombinant monoclonal antibody n-glycosylation. *Biotechnol. Bioeng.* **110**:2970–2983.
Gramer MJ, Eckblad JJ, Donahue R, Brown J, Shultz C, Vickerman K, Priem P, van den Bremer ETJ, Gerritsen J, van Berkel PHC. 2011. Modulation of antibody galactosylation through feeding of uridine, manganese chloride, and galactose. *Biotechnol. Bioeng.* **108**:1591–1602.
Gross A, Schoendube J, Zimmermann S, Steeb M, Zengerle R, Koltay P. 2015. Technologies for single-cell isolation. *Int. J. Mol. Sci.* **16**:16897–16919.
Gupta SK, Srivastava SK, Sharma A, Nalage VHH, Salvi D, Kushwaha H, Chitnis NB, Shukla P. 2017. Metabolic engineering of CHO cells for the development of a robust protein production platform. *PLoS One* **12**:e0181455. http://dx.plos.org/10.1371/journal.pone.0181455.
Ha TK, Kim Y-G, Lee GM. 2014. Effect of lithium chloride on the production and sialylation of Fc-fusion protein in Chinese hamster ovary cell culture. *Appl Microbiol Biotechnol* **98**:9239–9248.
Ha TK, Lee GM. 2014. Effect of glutamine substitution by TCA cycle intermediates on the production and sialylation of Fc-fusion protein in Chinese hamster ovary cell culture. *J. Biotechnol.* **180**:23–29. http://dx.doi.org/10.1016/j.jbiotec.2014.04.002.
Hansen HG, Nilsson CN, Lund AM, Kol S, Grav LM, Lundqvist M, Rockberg J, Lee GM, Andersen MR, Kildegaard HF. 2015. Versatile microscale screening platform for improving recombinant protein productivity in Chinese hamster ovary cells. *Sci. Rep.* **5**:1–12. http://dx.doi.org/10.1038/srep18016.
Hansen HG, Pristovšek N, Kildegaard HF, Lee GM. 2017. Improving the secretory capacity of Chinese hamster ovary cells by ectopic expression of effector genes: Lessons learned and future directions. *Biotechnol. Adv.* **35**:64–76.
Hansmannel F, Mordier S, Iynedjian PB. 2006. Insulin induction of glucokinase and fatty acid synthase in hepatocytes: analysis of the roles of sterol-regulatory-element-binding protein-1c and liver X receptor. *Biochem. J.* **399**:275–283. http://biochemj.org/lookup/doi/10.1042/BJ20060811.
Hemmerich J, Noack S, Wiechert W, Oldiges M. 2018. Microbioreactor Systems for Accelerated Bioprocess Development. *Biotechnol. J.* **13**:1–9.
Hermann R, Lehmann M, Büchs J. 2003. Characterization of gas-liquid mass transfer phenomena in microtiter plates. *Biotechnol. Bioeng.* **81**:178–186.
Hill EJ, Martin SJ, Weikart CM. 2018. Characterization of Extractable Species from Polypropylene Microplates. *SLAS Technol.*
Hills AE, Patel A, Boyd P, James DC. 2001. Metabolic control of recombinant monoclonal antibody N-glycosylation in GS-NS0 cells. *Biotechnol. Bioeng.* **75**:239–251.
Hong JK, Cho SM, Yoon SK. 2010. Substitution of glutamine by glutamate enhances production and galactosylation of recombinant IgG in Chinese hamster ovary cells. *Appl. Microbiol. Biotechnol.* **88**:869–876.
Hong JK, Lee GM, Yoon SK. 2011. Growth factor withdrawal in combination with sodium butyrate addition extends culture longevity and enhances antibody production in CHO cells. *J. Biotechnol.* **155**:225–231. http://dx.doi.org/10.1016/j.jbiotec.2011.06.020.
Hong JK, Lee SM, Kim KY, Lee GM. 2014. Effect of sodium butyrate on the assembly, charge variants, and galactosylation of antibody produced in recombinant Chinese hamster ovary cells. *Appl. Microbiol. Biotechnol.* **98**:5417–5425.
Hossler P, Khattak SF, Li ZJ. 2009. Optimal and consistent protein glycosylation in mammalian cell culture. *Glycobiology* **19**:936–949.

Hsu WT, Aulakh RPS, Traul DL, Yuk IH. 2012. Advanced microscale bioreactor system: A representative scale-down model for bench-top bioreactors. *Cytotechnology* **64**:667–678.

Huang C-J, Lin H, Yang X. 2012. Industrial production of recombinant therapeutics in Escherichia coli and its recent advancements. *J. Ind. Microbiol. Biotechnol.* **39**:383–399.

Huang Y-M, Hu W, Rustandi E, Chang K, Yusuf-Makagiansar H, Ryll T. 2010. Maximizing productivity of CHO cell-based fed-batch culture using chemically defined media conditions and typical manufacturing equipment. *Biotechnol. Prog.* **26**:1400–1410.

Hwang SJ, Jeon CJ, Cho SM, Lee GM, Yoon SK. 2011. Effect of chemical chaperone addition on production and aggregation of recombinant flag-tagged COMP-angiopoietin 1 in chinese hamster ovary cells. *Biotechnol. Prog.* **27**:587–591.

Jaffe SR, Benjamin S, Zdenko L, Pandhal J, Wright PC. 2014. Escherichia coli as a glycoprotein production host: Recent developments and challenges. *Curr. Opin. Biotechnol.* **30**:205–210.

Jayapal K, Wlaschin K, Hu W, Yap G. 2007. Recombinant protein therapeutics from CHO cells-20 years and counting. *Chem. Eng. Prog.* **103**:40–47. http://www.aiche.org/sites/default/files/docs/pages/CHO.pdf.

Jeong D won, Kim TS, Lee JW, Kim KT, Kim HJ, Kim IH, Kim IY. 2001. Blocking of acidosis-mediated apoptosis by a reduction of lactate dehydrogenase activity through antisense mRNA expression. *Biochem. Biophys. Res. Commun.* **289**:1141–1149.

Jerums M, Yang X. 2005. Optimization of Cell Culture Media. *Bioprocess Int.* **3**:38–44. http://cat.inist.fr/?aModele=afficheN&cpsidt=20038850.

De Jesus M, Wurm FM. 2011. Manufacturing recombinant proteins in kg-ton quantities using animal cells in bioreactors. *Eur. J. Pharm. Biopharm.* **78**:184–188. http://dx.doi.org/10.1016/j.ejpb.2011.01.005.

Jiang Z, Sharfstein ST. 2008. Sodium butyrate stimulates monoclonal antibody over-expression in CHO cells by improving gene accessibility. *Biotechnol. Bioeng.* **100**:189–194.

Johari YB, Estes SD, Alves CS, Sinacore MS, James DC. 2015. Integrated cell and process engineering for improved transient production of a “difficult-to-express” fusion protein by CHO cells. *Biotechnol. Bioeng.* **112**:2527–2542.

Johari YB. 2015. Cell Line and Process Development for Improved Transient Production of a " Difficult-to-Express " Fusion Protein by CHO Cells.

Jordan M, Stettler M. 2014. Tools for high-throughput process and medium optimization. *Anim. Cell Biotechnol. Methods Protoc. Methods Mol. Biol.*:77–88.

Karulin B, Kozhevnikov M. 2011. Ketcher: Web-based chemical structure editor. *J. Cheminform.* **3**:2011.

Kelley B. 2009. Industrialization of mAb production technology: The bioprocessing industry at a crossroads. *MAbs* **1**:440–449.

Kesik-Brodacka M. 2018. Progress in biopharmaceutical development. *Biotechnol. Appl. Biochem.* **65**:306–322.

Kildegaard HF, Fan Y, Sen JW, Larsen B, Andersen MR. 2015. Glycoprofiling effects of media additives on IgG produced by CHO cells in fed-batch bioreactors. *Biotechnol. Bioeng.* **113**:359–366.

Kim BG, Park HW. 2016. High zinc ion supplementation of more than 30 μM can increase monoclonal antibody production in recombinant Chinese hamster ovary DG44 cell culture. *Appl. Microbiol. Biotechnol.* **100**:2163–2170.

Kim CL, Ha TK, Lee GM. 2016a. Combinatorial treatment with lithium chloride enhances recombinant antibody production in transiently transfected CHO and HEK293E cells. *Biotechnol. Bioprocess Eng.* **21**:667–675.

Kim HJ, Bae SC. 2011. Histone deacetylase inhibitors: molecular mechanisms of action and clinical trials as anti-cancer drugs. *Am J Transl Res* **3**:166–179. http://www.ncbi.nlm.nih.gov/pubmed/21416059.

Kim JY, Kim YG, Lee GM. 2012. CHO cells in biotechnology for production of recombinant proteins: Current state and further potential. *Appl. Microbiol. Biotechnol.* **93**:917–930.

Kim KH, Song MJ, Yoo EJ, Choe SS, Park SD, Kim JB. 2004. Regulatory Role of Glycogen Synthase Kinase 3 for Transcriptional Activity of ADD1/SREBP1c. *J. Biol. Chem.* **279**:51999–52006. http://www.jbc.org/lookup/doi/10.1074/jbc.M405522200.

Kim NS, Lee GM. 2000. Overexpression of bcl-2 inhibits sodium butyrate-induced apoptosis in Chinese hamster ovary cells resulting in enhanced humanized antibody production.

Kim SH, Lee GM. 2007. Down-regulation of lactate dehydrogenase-A by siRNAs for reduced lactic acid formation of Chinese hamster ovary cells producing thrombopoietin. *Appl.*

Microbiol. Biotechnol. **74**:152–159.
Kim S, Thiessen PA, Bolton EE, Chen J, Fu G, Gindulyte A, Han L, He J, He S, Shoemaker BA, Wang J, Yu B, Zhang J, Bryant SH. 2016b. PubChem substance and compound databases. *Nucleic Acids Res.* **44**:D1202–D1213.
Kim WH, Kim YJ, Lee GM. 2014. Gadd45-induced cell cycle G2/M arrest for improved transient gene expression in Chinese hamster ovary cells. *Biotechnol. Bioprocess Eng.* **19**:386–393.
Kishishita S, Katayama S, Kodaira K, Takagi Y, Matsuda H, Okamoto H, Takuma S, Hirashima C, Aoyagi H. 2015. Optimization of chemically defined feed media for monoclonal antibody production in Chinese hamster ovary cells. *J. Biosci. Bioeng.* **120**:78–84. http://dx.doi.org/10.1016/j.jbiosc.2014.11.022.
Kolb PS, Ayaub EA, Zhou W, Yum V, Dickhout JG, Ask K. 2015. The therapeutic effects of 4-phenylbutyric acid in maintaining proteostasis. *Int. J. Biochem. Cell Biol.* **61**:45–52. http://dx.doi.org/10.1016/j.biocel.2015.01.015.
Krishnan N, Dickman MB, Becker DF. 2008. Proline modulates the intracellular redox environment and protects mammalian cells against oxidative stress. *Free Radic Biol Med.* **44**:671–81.
Ku SCY, Ng DTW, Yap MGS, Chao S-H. 2008. Effects of Overexpression of X-Box Binding Protein 1 on Recombinant Protein Production in Chinese Hamster Ovary and NS0 Myeloma Cells. *Biotechnol. Bioeng.* **99**:155–164.
Kumar N, Gammell P, Clynes M. 2007. Proliferation control strategies to improve productivity and survival during CHO based production culture: A summary of recent methods employed and the effects of proliferation control in product secreting CHO cell lines. *Cytotechnology* **53**:33–46.
Kwaks THJ, Otte AP. 2006. Employing epigenetics to augment the expression of therapeutic proteins in mammalian cells. *Trends Biotechnol.* **24**:137–142.
De La Torre BG, Albericio F. 2018. The pharmaceutical industry in 2017. An analysis of FDA drug approvals from the perspective of molecules. *Molecules* **23**.
Lai T, Yang Y, Ng SK. 2013. Advances in mammalian cell line development technologies for recombinant protein production. *Pharmaceuticals* **6**:579–603.
Lalonde ME, Durocher Y. 2017. Therapeutic glycoprotein production in mammalian cells. *J. Biotechnol.* **251**:128–140. http://dx.doi.org/10.1016/j.jbiotec.2017.04.028.
Landauer K. 2014. Designing Media for Animal Cell Culture: CHO Cells, the Industrial Standard. In: Pörtner, R, editor. *Anim. Cell Biotechnol. Methods Protoc. Methods Mol. Biol.* Totowa, NJ: Humana Press, pp. 89–103. https://doi.org/10.1007/978-1-62703-733-4_7.
Le H, Vishwanathan N, Jacob NM, Gadgil M, Hu WS. 2015. Cell line development for biomanufacturing processes: recent advances and an outlook. *Biotechnol. Lett.* **37**:1553–1564.
Le K, Tan C, Gupta S, Guhan T, Barkhordarian H, Lull J, Stevens J, Munro T. 2018. A Novel Mammalian Cell Line Development Platform utilizing Nanofluidics and OptoElectro Positioning (OEP) technology. *Biotechnol. Prog.* http://doi.wiley.com/10.1002/btpr.2690.
Lee EU, Roth J, Paulson JC. 1989. Alteration of terminal glycosylation sequences on N-linked oligosaccharides of Chinese hamster ovary cells by expression of beta-galactoside alpha 2,6-sialyltransferase. *J. Biol. Chem.* **264**:13848–13855. http://www.jbc.org/content/264/23/13848.abstract.
Lee EJ, Lee B Bin, Kim S-J, Park Y-D, Park J, Kim D-H. 2008. Histone deacetylase inhibitor scriptaid induces cell cycle arrest and epigenetic change in colon cancer cells. *Int. J. Oncol.* **33**:767–776.
Lee JS, Lee GM. 2012. Effect of Sodium Butyrate on Autophagy and Apoptosis in Chinese Hamster Ovary Cells. *Biotechnol. Prog.*:349–357.
Lee JH, Reier J, Heffner KM, Barton C, Spencer D, Schmelzer AE, Venkat R. 2017. Production and characterization of active recombinant human factor II with consistent sialylation. *Biotechnol. Bioeng.* **114**:1991–2000.
Legmann R, Benoit B, Fedechko RW, Deppeler CL, Srinivasan S, Robins RH, Mccormick EL, Ferrick D a., Rodgers ST, Russo a. P. 2011. A Strategy for clone selection under different production conditions. *Biotechnol. Prog.* **27**:757–765.
Legmann R, Schreyer HB, Combs RG, McCormick EL, Russo AP, Rodgers ST. 2009. A predictive high-throughput scale-down model of monoclonal antibody production in CHO cells. *Biotechnol. Bioeng.* **104**:1107–1120.
Lewis G, Lugg R, Lee K, Wales R. 2010. Novel Automated Micro-Scale Bioreactor Technology:

A Qualitative and Quantitative Mimic for Early Process Development. *Bioprocess. J.* **9**:23–26. http://www.tapbiosystems.com/tap/news/media/media2007/Bioprocessing Article - Novel Automated.pdf#search='Novel+automated+microscale+bioreactor+technology:+a+qualitative+and+quantitative+mimic+for+early+process+development'.

Li F, Vijayasankaran N, Shen A, Kiss R, Amanullah A. 2010. Cell culture processes for monoclonal antibody production. *MAbs* **2**:466–479.

Ling WLW, Deng L, Lepore J, Cutler C, Cannon-Carlson S, Wang Y, Voloch M. 2003. Improvement of Monoclonal Antibody Production in Hybridoma Cells by Dimethyl Sulfoxide. *Biotechnol. Prog.*:158–162.

Liu C, Chu I, Hwang S. 2001. Pentanoic acid, a novel protein synthesis stimulant for Chinese Hamster Ovary (CHO) cells. *J. Biosci. Bioeng.* **91**:71–75.

Liu CH, Chen LH. 2007. Enhanced recombinant M-CSF production in CHO cells by glycerol addition: Model and validation. *Cytotechnology* **54**:89–96.

Liu J, Wang J, Fan L, Chen X, Hu D, Deng X, Fai Poon H, Wang H, Liu X, Tan WS. 2015a. Galactose supplementation enhance sialylation of recombinant Fc-fusion protein in CHO cell: an insight into the role of galactosylation in sialylation. *World J. Microbiol. Biotechnol.* **31**:1147–1156.

Liu Y, Zhang W, Deng X, Poon HF, Liu X, Tan WS, Zhou Y, Fan L. 2015b. Chinese hamster ovary cell performance enhanced by a rational divide-and-conquer strategy for chemically defined medium development. *J. Biosci. Bioeng.* **120**:690–696. http://dx.doi.org/10.1016/j.jbiosc.2015.04.016.

Livak KJ, Schmittgen TD. 2001. Analysis of relative gene expression data using real-time quantitative PCR and the 2-ΔΔCT method. *Methods* **25**:402–408.

Lloyd DR, Holmes P, Jackson LP, Emery AN, Al-Rubeai M. 2000. Relationship between cell size, cell cycle and specific recombinant protein productivity. *Cytotechnology* **34**:59–70.

Long Q, Liu X, Yang Y, Li L, Harvey L, McNeil B, Bai Z. 2014. The development and application of high throughput cultivation technology in bioprocess development. *J. Biotechnol.* **192**:323–338.

Lu S, Archer MC. 2010. Sp1 coordinately regulates de novo lipogenesis and proliferation in cancer cells. *Int. J. Cancer* **126**:416–425.

Lundholt BK, Scudder KM, Pagliaro L. 2003. A simple technique for reducing edge effect in cell-based assays. *J. Biomol. Screen.* **8**:566–570.

Luo J, Vijayasankaran N, Autsen J, Santuray R, Hudson T, Amanullah A, Li F. 2012. Comparative metabolite analysis to understand lactate metabolism shift in Chinese hamster ovary cell culture process. *Biotechnol. Bioeng.* **109**:146–156.

Lyko F, Brown R. 2005. DNA methyltransferase inhibitors and the development of epigenetic cancer therapies. *J. Natl. Cancer Inst.* **97**:1498–1506.

m2p-labs GmbH. 2018. Biolector® I:1–6. www.m2p-labs.com.

MacLean B, Tomazela DM, Shulman N, Chambers M, Finney GL, Frewen B, Kern R, Tabb DL, Liebler DC, MacCoss MJ. 2010. Skyline: An open source document editor for creating and analyzing targeted proteomics experiments. *Bioinformatics* **26**:966–968.

Malhotra JD, Miao H, Zhang K, Wolfson A, Pennathur S, Pipe SW, Kaufman RJ. 2008. Antioxidants reduce endoplasmic reticulum stress and improve protein secretion. *Proc. Natl. Acad. Sci. U. S. A.* **105**:18525–18530.

Malphettes L, Freyvert Y, Chang J, Liu PQ, Chan E, Miller JC, Zhou Z, Nguyen T, Tsai C, Snowden AW, Collingwood TN, Gregory PD, Cost GJ. 2010. Highly efficient deletion of FUT8 in CHO cell lines using zinc-finger nucleases yields cells that produce completely nonfucosylated antibodies. *Biotechnol. Bioeng.* **106**:774–783.

Mandenius C-F, Brundin A. 2008. Bioprocess Methodology, Using Design-of-experiments. *Biotechnol. Prog.* **24**:1191–1203.

Matsuhashi T, Hishiki T, Zhou H, Ono T, Kaneda R, Iso T, Yamaguchi A, Endo J, Katsumata Y, Atsushi A, Yamamoto T, Shirakawa K, Yan X, Shinmura K, Suematsu M, Fukuda K, Sano M. 2015. Activation of pyruvate dehydrogenase by dichloroacetate has the potential to induce epigenetic remodeling in the heart. *J. Mol. Cell. Cardiol.* **82**:116–124. http://dx.doi.org/10.1016/j.yjmcc.2015.02.021.

Mazur X, Fussenegger M, Renner WA, Bailey JE. 1998. Higher Productivity of Growth-Arrested Chinese Hamster Ovary Cells Expressing the Cyclin-Dependent Kinase Inhibitor p27. *Biotechnol. Prog.* **14**:705–713.

McGrew JT. 2005. Cell Culture Performance with Vanadate. United States US 6,974,681 B1.

Meyer H-J, Turincio R, Ng S, Li J, Wilson B, Chan P, Zak M, Reilly D, Beresini MH, Wong AW. 2017. High throughput screening identifies novel, cell cycle-arresting small molecule enhancers of transient protein expression. *Biotechnol. Prog.*:1579–1588. http://doi.wiley.com/10.1002/btpr.2517.

Mimori S, Ohtaka H, Koshikawa Y, Kawada K, Kaneko M, Okuma Y, Nomura Y, Murakami Y, Hamana H. 2013. 4-Phenylbutyric acid protects against neuronal cell death by primarily acting as a chemical chaperone rather than histone deacetylase inhibitor. *Bioorganic Med. Chem. Lett.* **23**:6015–6018. http://dx.doi.org/10.1016/j.bmcl.2013.08.001.

Mimori S, Okuma Y, Kaneko M, Kawada K, Hosoi T, Ozawa K, Nomura Y, Hamana H. 2012. Protective Effects of 4-Phenylbutyrate Derivatives on the Neuronal Cell Death and Endoplasmic Reticulum Stress. *Biol. Pharm. Bull.* **35**:84–90. http://joi.jlc.jst.go.jp/JST.JSTAGE/bpb/35.84?from=CrossRef.

Moerke NJ. 2009. Fluorescence Polarization (FP) Assays for Monitoring Peptide-Protein or Nucleic Acid–Protein Binding. *Curr. Protoc. Chem. Biol.* **1**:1–15.

Moussaieff A, Rouleau M, Kitsberg D, Cohen M, Levy G, Barasch D, Nemirovski A, Shen-Orr S, Laevsky I, Amit M, Bomze D, Elena-Herrmann B, Scherf T, Nissim-Rafinia M, Kempa S, Itskovitz-Eldor J, Meshorer E, Aberdam D, Nahmias Y. 2015. Glycolysis-mediated changes in acetyl-CoA and histone acetylation control the early differentiation of embryonic stem cells. *Cell Metab.* **21**:392–402.

Mukherjee A, Wu J, Barbour S, Fang X. 2012. Lysophosphatidic acid activates lipogenic pathways and de novo lipid synthesis in ovarian cancer cells. *J. Biol. Chem.* **287**:24990–25000.

Müller B, Heinrich C, Jabs W, Kaspar-Schönefeld S, Schmidt A, Rodrigues de Carvalho N, Albaum SP, Baessmann C, Noll T, Hoffrogge R. 2017. Label-free protein quantification of sodium butyrate treated CHO cells by ESI-UHR-TOF-MS. *J. Biotechnol.* **257**:87–98.

Nan X, Hyndman L, Agbi N, Porteous DJ, Boyd AC. 2004. Potent stimulation of gene expression by histone deacetylase inhibitors on transiently transfected DNA. *Biochem. Biophys. Res. Commun.* **324**:348–354.

Narizzano R, Erokhin V, Nicolini C. 2005. A heterostructure composed of conjugated polymer and copper sulfide nanoparticles. *J. Phys. Chem. B* **109**:15798–15802.

Nishihara M, Kanda GN, Suzuki T, Yamakado S, Harashima H, Kamiya H. 2017. Enhanced transgene expression by plasmid-specific recruitment of histone acetyltransferase. *J. Biosci. Bioeng.* **123**:277–280. http://dx.doi.org/10.1016/j.jbiosc.2016.09.008.

Noh SM, Sathyamurthy M, Lee GM. 2013. Development of recombinant Chinese hamster ovary cell lines for therapeutic protein production. *Curr. Opin. Chem. Eng.* **2**:391–397. http://dx.doi.org/10.1016/j.coche.2013.08.002.

Oh HK, So MK, Yang J, Yoon HC, Ahn JS, Lee JM, Kim JT, Yoo JU, Byun TH. 2005. Effect of N-Acetylcystein on butyrate-treated Chinese hamster ovary cells to improve the production of recombinant human interferon-beta-1a. *Biotechnol. Prog.* **21**:1154–1164. http://www.ncbi.nlm.nih.gov/pubmed/16080696.

Onitsuka M, Tatsuzawa M, Asano R, Kumagai I, Shirai A, Maseda H, Omasa T. 2014. Trehalose suppresses antibody aggregation during the culture of Chinese hamster ovary cells. *J. Biosci. Bioeng.* **117**:632–638. http://dx.doi.org/10.1016/j.jbiosc.2013.10.022.

Palermo DP, DeGraaf ME, Marotti KR, Rehberg E, Post LE. 1991. Production of analytical quantities of recombinant proteins in Chinese hamster ovary cells using sodium butyrate to elevate gene expression. *J. Biotechnol.* **19**:35–47.

Parampalli A, Eskridge K, Smith L, Meagher MM, Mowry MC, Subramanian A. 2007. Developement of serum-free media in CHO-DG44 cells using a central composite statistical design. *Cytotechnology* **54**:57–68.

Park H-S, Kim I-H, Kim I-Y, Kim K-H, Kim H-J. 2000. Expression of carbamoyl phosphate synthetase I and ornithine transcarbamoylase genes in Chinese hamster ovary dhfr -cells decreases accumulation of ammonium ion in culture media. *J. Biotechnol.* **81**:129–140. http://linkinghub.elsevier.com/retrieve/pii/S0168165600002820.

Park JH, Noh SM, Woo JR, Kim JW, Lee GM. 2016. Valeric acid induces cell cycle arrest at G1 phase in CHO cell cultures and improves recombinant antibody productivity. *Biotechnol. J.* **11**:487–496.

Patel KA, Sethi R, Dhara AR, Roy I. 2017. Challenges with osmolytes as inhibitors of protein aggregation: Can nucleic acid aptamers provide an answer? *Int. J. Biol. Macromol.* **100**:75–88. http://dx.doi.org/10.1016/j.ijbiomac.2016.05.014.

Priola JJ, Calzadilla N, Baumann M, Borth N, Tate CG, Betenbaugh MJ. 2016. High-throughput

screening and selection of mammalian cells for enhanced protein production. *Biotechnol. J.* **11**:853–865.

Pybus LP, Dean G, West NR, Smith A, Daramola O, Field R, Wilkinson SJ, James DC. 2014. Model-directed engineering of “difficult-to-express” monoclonal antibody production by Chinese hamster ovary cells. *Biotechnol. Bioeng.* **111**:372–385.

Qian Y, Khattak SF, Xing Z, He A, Kayne PS, Qian NX, Pan SH, Li ZJ. 2011. Cell culture and gene transcription effects of copper sulfate on Chinese hamster ovary cells. *Biotechnol. Prog.* **27**:1190–1194.

R.S. R, K. T, M. T, H. T, Y. K. 2011. Chemical and pharmacological chaperones: Application for recombinant protein production and protein folding diseases. *Curr. Med. Chem.* **18**:1–15. http://ovidsp.ovid.com/ovidweb.cgi?T=JS&PAGE=reference&D=emed13&NEWS=N&AN=361137274.

Rabbani G, Choi I. 2018. Roles of osmolytes in protein folding and aggregation in cells and their biotechnological applications. *Int. J. Biol. Macromol.* **109**:483–491. http://dx.doi.org/10.1016/j.ijbiomac.2017.12.100.

Rameez S, Mostafa SS, Miller C, Shukla AA. 2014. High-throughput miniaturized bioreactors for cell culture process development: Reproducibility, scalability, and control. *Biotechnol. Prog.* **30**:718–727.

Reinhart D, Damjanovic L, Kaisermayer C, Kunert R. 2015. Benchmarking of commercially available CHO cell culture media for antibody production. *Appl. Microbiol. Biotechnol.* **99**:4645–4657.

Rita Costa A, Elisa Rodrigues M, Henriques M, Azeredo J, Oliveira R. 2010. Guidelines to cell engineering for monoclonal antibody production. *Eur. J. Pharm. Biopharm.* **74**:127–138. http://dx.doi.org/10.1016/j.ejpb.2009.10.002.

Rita Costa A, Rodrigues ME, Henriques M, Oliveira R, Azeredo J. 2014. Glycosylation : impact , control and improvement during therapeutic protein production. *Crit. Rev. Biotechnol.* **34**:281–299.

Rodrigues ME, Costa AR, Henriques M, Azeredo J, Oliveira R. 2012. Comparison of commercial serum-free media for CHO-K1 cell growth and monoclonal antibody production. *Int. J. Pharm.* **437**:303–305. http://dx.doi.org/10.1016/j.ijpharm.2012.08.002.

Rodriguez J, Spearman M, Huzel N, Butler M. 2005. Enhanced production of monomeric interferon-β by CHO cells through the control of culture conditions. *Biotechnol. Prog.* **21**:22–30.

Ropero S, Esteller M. 2007. The role of histone deacetylases (HDACs) in human cancer. *Mol. Oncol.* **1**:19–25.

Roth SD, Schüttrumpf J, Milanov P, Abriss D, Ungerer C, Quade-Lyssy P, Simpson JC, Pepperkok R, Seifried E, Tonn T. 2012. Chemical Chaperones Improve Protein Secretion and Rescue Mutant Factor VIII in Mice with Hemophilia A. *PLoS One* **7**.

Rouiller Y, Bielser JM, Brühlmann D, Jordan M, Broly H, Stettler M. 2016. Screening and assessment of performance and molecule quality attributes of industrial cell lines across different fed-batch systems. *Biotechnol. Prog.* **32**:160–170.

Rouiller Y, Périlleux A, Collet N, Jordan M, Stettler M, Broly H. 2013. A high-throughput media design approach for high performance mammalian fed-batch cultures. *MAbs* **5**:501–511.

Royle L, Campbell MP, Radcliffe CM, White DM, Harvey DJ, Abrahams JL, Kim YG, Henry GW, Shadick NA, Weinblatt ME, Lee DM, Rudd PM, Dwek RA. 2008. HPLC-based analysis of serum N-glycans on a 96-well plate platform with dedicated database software. *Anal. Biochem.* **376**:1–12.

Sanchez-Garcia L, Martín L, Mangues R, Ferrer-Miralles N, Vázquez E, Villaverde A. 2016. Recombinant pharmaceuticals from microbial cells: a 2015 update. *Microb. Cell Fact.* **15**:33. http://www.microbialcellfactories.com/content/15/1/33.

Sandadi S, Ensari S, Kearns B. 2006. Application of fractional factorial designs to screen active factors for antibody production by Chinese hamster ovary cells. *Biotechnol. Prog.* **22**:595–600.

Santell L, Ryll T, Etcheverry T, Santoris M, Dutina G, Wang a, Gunson J, Warner TG. 1999. Aberrant metabolic sialylation of recombinant proteins expressed in Chinese hamster ovary cells in high productivity cultures. *Biochem. Biophys. Res. Commun.* **258**:132–137.

Santos CR, Schulze A. 2012. Lipid metabolism in cancer. *FEBS J.* **279**:2610–2623.

Santos RB, Pires AS, Abranches R. 2017. Addition of a histone deacetylase inhibitor increases recombinant protein expression in Medicago truncatula cell cultures. *Sci. Rep.* **7**:1–9. http://dx.doi.org/10.1038/s41598-017-17006-9.

Sartorius Stedium biotech. Ambr15 cell culture-system overview. https://www.tapbiosystems.com/tap/cell_culture/ambr.htm.

Schmid G, Zilg H, Eberhard U, Johannsen R. 1991. Effect of free fatty acids and phospholipids on growth of and product formation by recombinant baby hamster kidney (rBHK) and Chinese hamster ovary (rCHO) cells in culture. *J. Biotechnol.* **17**:155–167.

Schwanhäusser B, Gossen M, Dittmar G, Selbach M. 2009. Global analysis of cellular protein translation by pulsed SILAC. *Proteomics* **9**:205–209.

Selleck Chemicals. 2013. Screening Libraries. http://www.selleckchem.com/screening-libraries.html.

Shechter D, Dormann HL, Allis CD, Hake SB. 2007. Extraction, purification and analysis of histones. *Nat. Protoc.* **2**:1445–1457.

Shukla AA, Thömmes J. 2010. Recent advances in large-scale production of monoclonal antibodies and related proteins. *Trends Biotechnol.* **28**:253–261.

Sigma-Aldrich. Zinc in Cell Culture. https://www.sigmaaldrich.com/life-science/cell-culture/learning-center/media-expert/zinc.html.

Sigma-Aldrich. Iron in Cell Culture. https://www.sigmaaldrich.com/life-science/cell-culture/learning-center/media-expert/iron.html#Products_.

Sigma-Aldrich. 2018. LOPAC®1280; Library of Pharmacologically Active Compounds. https://www.sigmaaldrich.com/catalog/product/SIGMA/LO3300?lang=en&region=GB.

Skelton D, Goodyear A, Ni D, Walton WJ, Rolle M, Hare JT, Logan TM. 2010. Enhanced production and isotope enrichment of recombinant glycoproteins produced in cultured mammalian cells. *J. Biomol. NMR* **48**:93–102.

Srivastava AK, Mehdi MZ. 2005. Insulino-mimetic and anti-diabetic effects of vanadium compounds. *Diabet. Med.* **22**:2–13.

Stöckmann H, O'Flaherty R, Adamczyk B, Saldova R, Rudd PM. 2015. Automated, high-throughput serum glycoprofiling platform. *Integr. Biol. (United Kingdom)* **7**:1026–1032.

Strohl WR. 2018. Current progress in innovative engineered antibodies. *Protein Cell* **9**:86–120.

Su GH, Sohn TA, Ryu B, Kern SE. 2000. A novel histone deacetylase inhibitor identified by high-throughput transcriptional screening of a compound library. *Cancer Res.* **60**:3137–3142.

Sung YH, Song YJ, Lim SW, Chung JY, Lee GM. 2004. Effect of sodium butyrate on the production, heterogeneity and biological activity of human thrombopoietin by recombinant Chinese hamster ovary cells. *J. Biotechnol.* **112**:323–335.

Sunley K, Butler M. 2010. Strategies for the enhancement of recombinant protein production from mammalian cells by growth arrest. *Biotechnol. Adv.* **28**:385–394. http://dx.doi.org/10.1016/j.biotechadv.2010.02.003.

Surve T, Gadgil M. 2015. Manganese increases high mannose glycoform on monoclonal antibody expressed in CHO when glucose is absent or limiting: Implications for use of alternate sugars. *Biotechnol. Prog.* **31**:460–467.

Swiech K, Picanço-Castro V, Covas DT. 2012. Human cells: New platform for recombinant therapeutic protein production. *Protein Expr. Purif.* **84**:147–153. http://dx.doi.org/10.1016/j.pep.2012.04.023.

Tabuchi H, Sugiyama T. 2013. Cooverexpression of alanine aminotransferase 1 in Chinese hamster ovary cells overexpressing taurine transporter further stimulates metabolism and enhances product yield. *Biotechnol. Bioeng.* **110**:2208–2215.

Tait AS, Brown CJ, Galbraith DJ, Hines MJ, Hoare M, Birch JR, James DC. 2004. Transient production of recombinant proteins by Chinese hamster ovary cells using polyethyleneimine/DNA complexes in combination with microtubule disrupting anti-mitotic agents. *Biotechnol. Bioeng.* **88**:707–721.

Takagi M, Hayashi H, Yoshida T. 2000. The effect of osmolarity on metabolism and morphology in adhesion and suspension chinese hamster ovary cells producing tissue plasminogen activator. *Cytotechnology* **32**:171–179.

Tanigawa T, Hikida M, Takai T, Yasuda T, Ohmori H. 1993. Enhancement of expression of an introduced gene by 5-azacytidine in mammalian cell lines. *J. Ferment. Bioeng.* **75**:254–258.

Tejwani V, Andersen MR, Nam JH, Sharfstein ST. 2018. Glycoengineering in CHO Cells: Advances in Systems Biology. *Biotechnol. J.* **13**:1–16.

Templeton N, Dean J, Reddy P, Young JD. 2013. Peak antibody production is associated with increased oxidative metabolism in an industrially relevant fed-batch CHO cell culture. *Biotechnol. Bioeng.* **110**:2013–2024.

Templeton N, Lewis A, Dorai H, Qian EA, Campbell MP, Smith KD, Lang SE, Betenbaugh MJ, Young JD. 2014. The impact of anti-apoptotic gene Bcl-2Δ expression on CHO central metabolism. *Metab. Eng.* **25**:92–102. http://dx.doi.org/10.1016/j.ymben.2014.06.010.

Thermo Fisher Scientific. Microplate Assays for Cell Viability. https://www.thermofisher.com/uk/en/home/life-science/cell-analysis/fluorescence-microplate-assays/microplate-assays-cell-viability.html.

Thermo Fisher Scientific. 2012. PrestoBlue ™ reagent Product Overview. *Tech. Inf.*:1–13. https://tools.thermofisher.com/content/sfs/manuals/PrestoBlueFAQ.pdf.

Thompson BC, Segarra CRJ, Mozley OL, Daramola O, Field R, Levison PR, James DC. 2012. Cell line specific control of polyethylenimine-mediated transient transfection optimized with "Design of experiments" methodology. *Biotechnol. Prog.* **28**:179–187.

Thompson B, Clifford J, Jenns M, Smith A, Field R, Nayyar K, James DC. 2017. High-throughput quantitation of Fc-containing recombinant proteins in cell culture supernatant by fluorescence polarization spectroscopy. *Anal. Biochem.* **534**:49–55. http://dx.doi.org/10.1016/j.ab.2017.07.013.

Tjio JH, Puck TT. 1958. Genetics of somatic mammalian cells. II. Chromosomal constitution of cells in tissue culture. *J. Exp. Med.* **108**:259–68. http://www.pubmedcentral.nih.gov/articlerender.fcgi?artid=2136870&tool=pmcentrez&rendertype=abstract.

Uppala JK, Gani AR, Ramaiah KVA. 2017. Chemical chaperone, TUDCA unlike PBA, mitigates protein aggregation efficiently and resists ER and non-ER stress induced HepG2 cell death. *Sci. Rep.* **7**:1–13.

Vassilev LT, Tovar C, Chen S, Knezevic D, Zhao X, Sun H, Heimbrook DC, Chen L. 2006. Selective small-molecule inhibitor reveals critical mitotic functions of human CDK1. *Proc. Natl. Acad. Sci.* **103**:10660–10665. http://www.pnas.org/cgi/doi/10.1073/pnas.0600447103.

Vassilev LT. 2006. Cell cycle synchronization at the G2/M phase border by reversible inhibition of CDK1. *Cell Cycle* **5**:2555–2556.

Velugula-Yellela SR, Williams A, Trunfio N, Hsu C-J, Chavez B, Yoon S, Agarabi C. 2017. Impact of media and antifoam selection on monoclonal antibody production and quality using a high throughput micro-bioreactor system. *Biotechnol. Prog.*:262–270. http://doi.wiley.com/10.1002/btpr.2575.

Wagener J, Plennevaux C. 2014. Eppendorf 96-Well Tissue Culture Plate : A simple method of minimizing the edge effect in cell-based assays.

Walsh G. 2014. Biopharmaceutical benchmarks 2014 **32**.

Wang Z, Patel DJ. 2013. Small molecule epigenetic inhibitors targeted to histone lysine methyltransferases and demethylases Zhanxin. *Q Rev Biophys.* **46**:349–373.

Warburg O. 1956. On the Origin of Cancer Cells. *Science (80-.).* **123**:309–314. http://www.jstor.org/stable/1750066%5Cnhttp://www.jstor.org/stable/1750066?seq=1&cid=pdf-reference#references_tab_contents%5Cnhttp://about.jstor.org/terms.

Welch WJ, Brown CR. 1996. Influence of molecular and chemical chaperones on protein folding. *Cell Stress Chaperones*.

Wong VVT, Ho KW, Yap MGS. 2004. Evaluation of insulin-mimetic trace metals as insulin replacements in mammalian cell cultures. *Cytotechnology* **45**:107–115.

Wulhfard S, Baldi L, Hacker DL, Wurm F. 2010. Valproic acid enhances recombinant mRNA and protein levels in transiently transfected Chinese hamster ovary cells. *J. Biotechnol.* **148**:128–132.

Wurm F. 2013. CHO Quasispecies—Implications for Manufacturing Processes. *Processes* **1**:296–311. http://www.mdpi.com/2227-9717/1/3/296/htm.

Wurm FM. 2004. Production of recombinant protein therapeutics in cultivated mammalian cells. *Nat. Biotechnol.* **22**:1393–1398.

Xing Z, Kenty B, Koyrakh I, Borys M, Pan SH, Li ZJ. 2011. Optimizing amino acid composition of CHO cell culture media for a fusion protein production. *Process Biochem.* **46**:1423–1429. http://dx.doi.org/10.1016/j.procbio.2011.03.014.

Xu M, McCanna DJ, Sivak JG. 2015. Use of the viability reagent PrestoBlue in comparison with alamarBlue and MTT to assess the viability of human corneal epithelial cells. *J. Pharmacol. Toxicol. Methods* **71**:1–7. http://dx.doi.org/10.1016/j.vascn.2014.11.003.

Xu W, Li Z, Yu B, He X, Shi J, Zhou R, Liu D, Wu Z. 2013. Effects of DNMT1 and HDAC Inhibitors on Gene-Specific Methylation Reprogramming during Porcine Somatic Cell Nuclear Transfer. *PLoS One* **8**:1–13.

Yam GHF, Gaplovska-Kysela K, Zuber C, Roth J. 2007. Sodium 4-phenylbutyrate acts as a chemical chaperone on misfolded myocilin to rescue cells from endoplasmic reticulum stress and apoptosis. *Investig. Ophthalmol. Vis. Sci.* **48**:1683–1690.

Yamaguchi T, Cubizolles F, Zhang Y, Reichert N, Kohler H, Seiser C, Matthias P. 2010. Histone deacetylases 1 and 2 act in concert to promote the G1-to-S progression. *Genes Dev.* **24**:455–469.

Yamamoto K, Niwa A. 1993. Amino Acid and Vitamin requirements in mammalian cultured cells. *Amino Acids*:1–16.

Yamane-Ohnuki N, Kinoshita S, Inoue-Urakubo M, Kusunoki M, Iida S, Nakano R, Wakitani M, Niwa R, Sakurada M, Uchida K, Shitara K, Satoh M. 2004. Establishment of FUT8 knockout Chinese hamster ovary cells: An ideal host cell line for producing completely defucosylated antibodies with enhanced antibody-dependent cellular cytotoxicity. *Biotechnol. Bioeng.* **87**:614–622.

Yang M, Butler M. 2002. Effects of ammonia and glucosamine on the heterogeneity of erythropoietin glycoforms. *Biotechnol. Prog.* **18**:129–138.

Yang M, Butler M. 2000. Effects of Ammonia on CHO Cell Growth, Erythropoietin Production, and Glycosylation. *Biotechnol Bioeng* **68**:370–380.

Yang WC, Lu J, Nguyen NB, Zhang A, Healy N V., Kshirsagar R, Ryll T, Huang YM. 2014. Addition of Valproic Acid to CHO Cell Fed-Batch Cultures Improves Monoclonal Antibody Titers. *Mol. Biotechnol.* **56**:421–428.

Yang X, Kim SM, Ruzanski R, Chen Y, Moses S, Ling WL, Li X, Wang SC, Li H, Ambrogelly A, Richardson D, Shameem M. 2016. Ultrafast and high-throughput N-glycan analysis for monoclonal antibodies. *MAbs* **8**:706–717. http://dx.doi.org/10.1080/19420862.2016.1156828.

Yang Y, Mariati, Chusainow J, Yap MGS. 2010. DNA methylation contributes to loss in productivity of monoclonal antibody-producing CHO cell lines. *J. Biotechnol.* **147**:180–185. http://dx.doi.org/10.1016/j.jbiotec.2010.04.004.

Yin B, Wang Q, Chung CY, Ren X, Bhattacharya R, Yarema KJ, Betenbaugh MJ. 2018. Butyrated ManNAc analog improves protein expression in Chinese hamster ovary cells. *Biotechnol. Bioeng.* **115**:1531–1541.

Yokota M, Tanji Y. 2008. Analysis of cell-cycle-dependent production of tissue plasminogen activator analogue (pamiteplase) by CHO cells. *Biochem. Eng. J.* **39**:297–304.

Yoon SK, Kim SH, Song JY, Lee GM. 2006. Biphasic culture strategy for enhancing volumetric erythropoietin productivity of Chinese hamster ovary cells **39**:362–365.

Yuk IH, Nishihara J, Walker D, Huang E, Gunawan F, Subramanian J, Pynn AFJ, Yu XC, Zhu-Shimoni J, Vanderlaan M, Krawitz DC. 2015a. More similar than different: Host cell protein production using three null CHO cell lines. *Biotechnol. Bioeng.* **112**:2068–2083.

Yuk IH, Russell S, Tang Y, Hsu W-T, Mauger JB, Aulakh RPS, Luo J, Gawlitzek M, Joly JC. 2015b. Effects of copper on CHO cells: Cellular requirements and product quality considerations. *Biotechnol. Prog.* **31**:226–238. http://doi.wiley.com/10.1002/btpr.2004.

Yuk IH, Zhang JD, Ebeling M, Berrera M, Gomez N, Werz S, Meiringer C, Shao Z, Swanberg JC, Lee KH, Luo J, Szperalski B. 2014. Effects of copper on CHO cells: Insights from gene expression analyses. *Biotechnol. Prog.* **30**:429–442.

Zhang H, Lamping SR, Pickering SCR, Lye GJ, Shamlou PA. 2008. Engineering characterisation of a single well from 24-well and 96-well microtitre plates. *Biochem. Eng. J.* **40**:138–149.

Zhang J. 2010. Mammalian Cell Culture for Biopharmaceutical Production. *Man. Ind. Microbiol. Biotechnol.*:157–178.

Zhang J, Robinson D, Salmon P. 2006. A Novel Function for Selenium in Biological System: Selenite as a Highly Effective Iron Carrier for Chinese Hamster Ovary Cell Growth and Monoclonal Antibody Production. *Biotechnol. Bioeng.*:1188–1197.

Zhang P, Woen S, Wang T, Liau B, Zhao S, Chen C, Yang Y, Song Z, Wormald MR, Yu C, Rudd PM. 2016. Challenges of glycosylation analysis and control: An integrated approach to producing optimal and consistent therapeutic drugs. *Drug Discov. Today* **21**:740–765. http://dx.doi.org/10.1016/j.drudis.2016.01.006.

Zhang Y, Reinberg D. 2001. Transcription regulation by histone methylation: Interplay between different covalent modifications of the core histone tails. *Genes Dev.* **15**:2343–2360.

Zhou M, Crawford Y, Ng D, Tung J, Pynn AFJ, Meier A, Yuk IH, Vijayasankaran N, Leach K, Joly J, Snedecor B, Shen A. 2011. Decreasing lactate level and increasing antibody production in Chinese Hamster Ovary cells (CHO) by reducing the expression of lactate

dehydrogenase and pyruvate dehydrogenase kinases. *J. Biotechnol.* **153**:27–34.

Zhou Y, Raju R, Alves C, Gilbert A. 2018. Debottlenecking protein secretion and reducing protein aggregation in the cellular host. *Curr. Opin. Biotechnol.* **53**:151–157. http://dx.doi.org/10.1016/j.copbio.2018.01.007.

Zhu J. 2012. Mammalian cell protein expression for biopharmaceutical production. *Biotechnol. Adv.* **30**:1158–1170. http://dx.doi.org/10.1016/j.biotechadv.2011.08.022.

Appendix A.

Appendix Table A.1 Primer efficiencies for all primers utilised in the qPCR study. A slope of -3.322 equates to 100% efficiency. Primer efficiencies between 95 and 105% were deemed acceptable.

Primer	Slope	Efficiency	Amplicon size
Heavy chain (Primer 7)	-3.31	100.56	198
Light chain (Primer 1)	-3.30	100.92	88
Fkbp1a	-3.34	99.09	95
Mmadhc	-3.38	97.63	145

A.1 Detailed Description Of Histone Extraction Methodology:

Acid Extraction:

The cell pellet was re-suspended in 950 µL of a hypotonic lysis buffer (10 mM Tris-HCl pH 8, 1 mM KCl, 1.5 mM $MgCl_2$ and 1mM DTT) and 5 µL of Protease Halt Cocktail (Thermo Fisher Scientific). After shaking the mix on ice for 30 minutes, the extracted nucleus was pelleted. The nucleus was dissolved in 0.2 M H_2SO_4 for 4 hours (on ice, shaken). Any nuclear debris was removed by centrifugation and histones precipitated overnight in a tube containing 132 µL of 6.1 N Trichloroacetic acid. The histones were then washed twice in ice cold acetone and dissolved in 100 µL HPLC grade water.

Propionylation:

7 µg-10 µg of histones were mixed 1:1 with 100 mM ABC. A propionylation mix was created using propionic anhydride and isopropanol in a 1:3 ratio. 10 µL of the mix was added to the histone+ABC mix. pH was adjusted to 8 using ammonium hydroxide. The mix was incubated at 37°C for 15 minutes and dried down using a SpeedVac (Thermo Fisher Scientific). 10 µL of ABC was added and the process repeated once. 40 µL of 100 mM ABC containing 1.5 µg of Trypsin was added to the derivatised histones and left to incubate at 37°C overnight before quenching the reaction with 4 µL glacial acetic acid, on ice for an hour. The mix was dried down and propionylation performed twice.

Gradient:

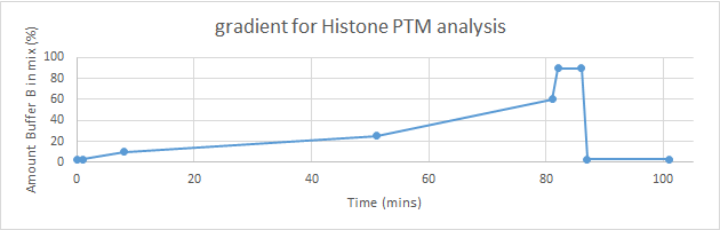

Appendix Figure A.1 Gradient employed for histone modification analytics.

Resolution:

m/z range was between 300-1100. MS1 resolution was set at 60,000; automatic gain control (ACG) target was 3×10^6 with a maximum fill time of 55 ms. A MS1 scan was performed once every 10 MS2 scans. MS2 resolution was set at 30,000 with an ACG target of 1×10^6. m/z isolation window set at 20 m/z.

Appendix B.

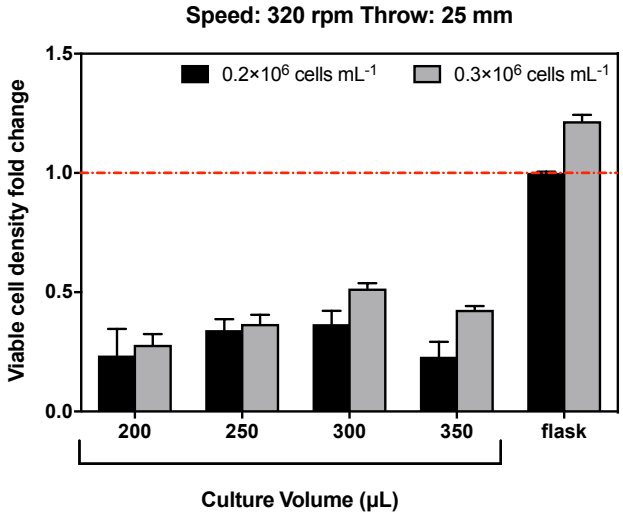

Appendix Figure B.1 Viable cell density on day 3 of a batch culture in a round well DWP. Different culture volumes and seeding densities trialed in a NUNC™ 96-well polypropylene DeepWell™ plate (Thermo Fisher Scientific). Incubator speed: 320 rpm, throw: 25 mm. VCD measured using the Vi-CELL XR. Data is mean and standard error of three technical replicates.

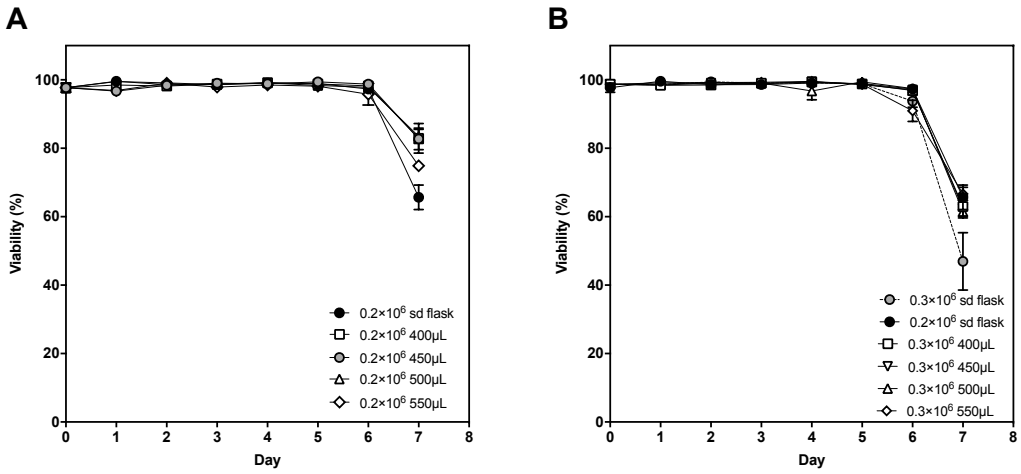

Appendix Figure B.2 Viability profiles of the DWP batch cultures varied for seeding density and culture volume. (A) 0.2×10^6 cells mL^{-1} and **(B)** 0.3×10^6 cells mL^{-1} seeded DWP cultures. Data shown is the mean and standard deviation of three experimental repeats.

Appendix C.

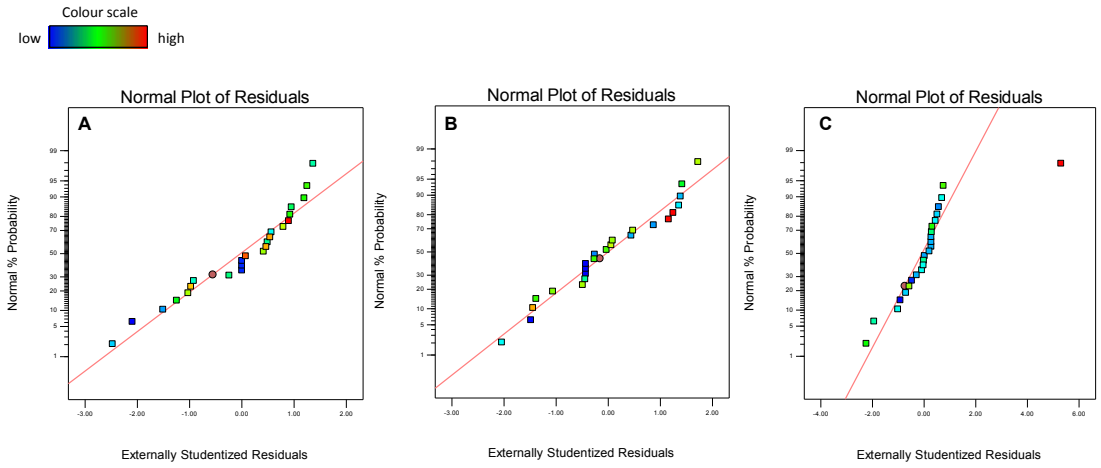

Appendix Figure C.1 Growth DOE: Normal plot of residuals to validate statistical assumptions. Residual normal plot for **(A)** IVCD, **(B)** Titer and **(C)** qP depicted. If the residuals fall roughly in a straight line, then the normality of residuals is confirmed and no power transform is required. No power transforms were deemed necessary for A, B or C. The colours of the residual dots indicate the actual output relative to the group i.e. the lowest ranking is blue while the highest ranking is red. Three replicate experimental datasets used to create this normality plot.

Appendix Table C.1 Growth DOE: ANOVA table. Culture attributes modeled for: IVCD, Titer, qP. Significance of model and its terms presented. Model predictability seen as reasonable if difference between Pred R^2 and Adj R^2 is less than 0.2. Adeq precision presents signal-to-noise ratio, ratio of 4 or more is desirable. Lack of fit: Titer: F value: 0.98, p value: 0.4269, not significant. qP: F value: 0.60, p value: 0.5620, not significant.

Response	Factor	Sum of squares	P value	Model Predictability (Pred/Adj R^2)	Adeq Precision
IVCD	Model	2.87	< 0.0001	0.7096/0.8145	11.693
	A-Cu	0.42	0.0011		
	B-Zn	0.59	0.0002		
	C-FAC	1.12	< 0.0001		
	AB	0.19	0.0164		
	AC	0.17	0.0234		
	BC	0.30	0.0038		
	ABC	0.077	0.1078		
Titer	Model	8.30	< 0.0001	0.9307/0.9474	27.083
	A-Cu	0.92	< 0.0001		
	B-Zn	0.50	< 0.0001		
	C-FAC	6.73	< 0.0001		
	AB	0.14	0.0148		
qP	Model	2.72	< 0.0001	0.6721/0.7643	11.538
	A-Cu	0.072	0.1650		
	B-Zn	1.16	< 0.0001		

	C-FAC	0.96	< 0.0001		
	AB	0.31	0.0078		
	BC	0.22	0.0210		

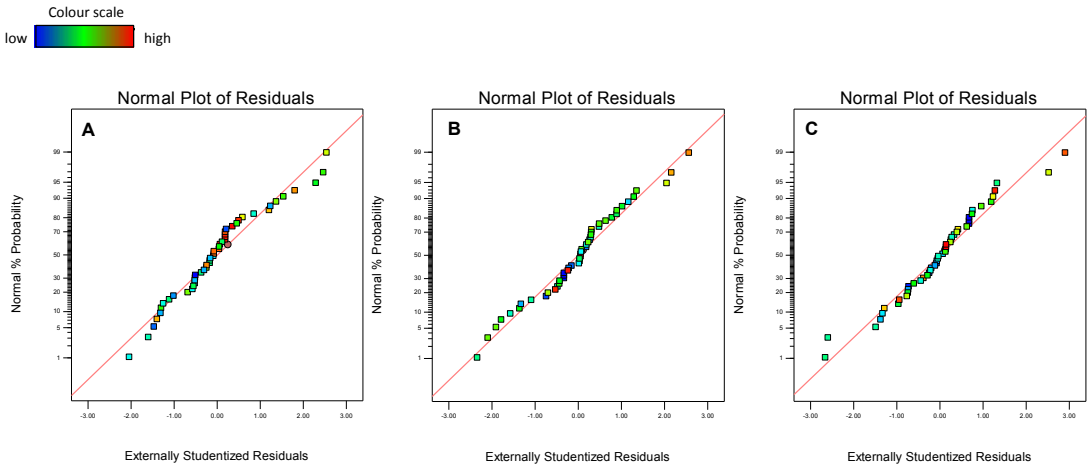

Appendix Figure C.2 qP/Titer DOE: Normal plot of residuals to validate statistical assumptions. (A) IVCD, **(B)** Titer and **(C)** qP.

Appendix Table C.2 qP/Titer DOE: ANOVA table. Model lack of fit : IVCD: F value: 0.24, p value 0.9808, not significant. Titer: F value: 1.03, p value 0.3910, not significant. qP: F value: 0.82, p value: 0.5890, not significant.

Response	Factor	Sum of squares	P value	Model Predictability (Pred/Adj R^2)	Adeq Precision
IVCD	Model	1.75	< 0.0001	0.8342/0.8647	20.103
	A-TUDCA	0.029	0.0310		
	B-NaBu	0.31	< 0.0001		
	C-3TAA	1.20	< 0.0001		
	D-MS 275	0.088	0.0003		
	AC	0.039	0.0124		
	BC	0.062	0.0020		
	BD	0.025	0.0437		
Titer	Model	33.28	< 0.0001	0.8944/0.9246	26.755
	A-TUDCA	6.62	< 0.0001		
	B-NaBu	18.00	< 0.0001		
	C-3TAA	5.002E-003	0.7679		
	D-MS 275	2.34	< 0.0001		
	AB	0.19	0.0726		
	AC	0.75	0.0009		
	AD	0.14	0.1277		
	BC	0.42	0.0103		
	BD	0.96	0.0002		
	CD	2.61	< 0.0001		

	ABC	0.77	0.0007		
	ACD	0.48	0.0061		
qP	Model	170.91	< 0.0001	0.9192/0.9341	34.453
	A-TUDCA	29.69	< 0.0001		
	B-NaBu	84.67	< 0.0001		
	C-3TAA	36.80	< 0.0001		
	D-MS 275	14.69	< 0.0001		
	AB	1.52	0.0188		
	AC	1.71	0.0131		
	CD	1.83	0.0105		

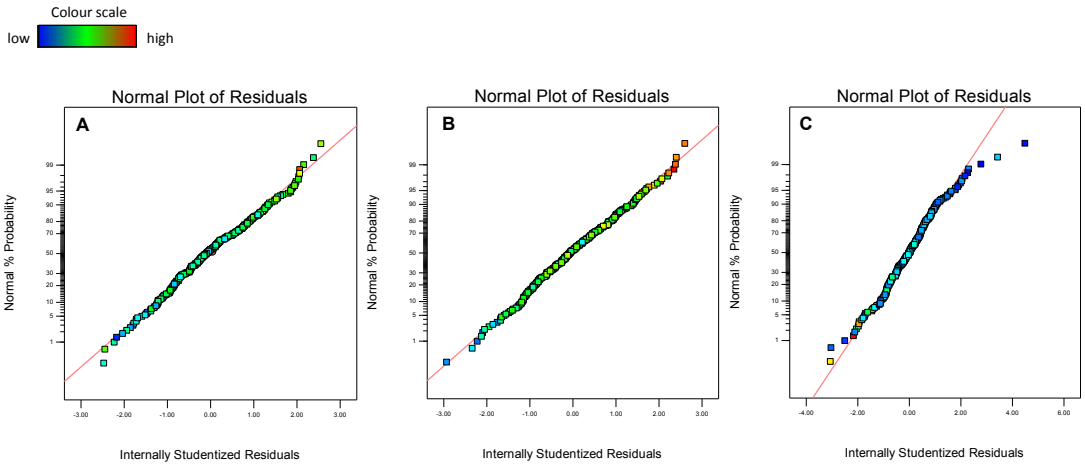

Appendix Figure C.3 Seven factor titer DOE: Normal plot of residuals to validate statistical assumptions. (A) IVCD, **(B)** $\log_{10}$(Titer) and **(C)** 1/√qP.

Appendix Table C.3 Seven factor titer DOE: ANOVA table. Model lack of fit: IVCD: F value: 0.94, p value: 0.6245, not significant. $\log_{10}$(Titer): F value: 1.08, p value: 0.3309, not significant. 1/√qP: F value: 1.13, p value: 0.2602, not significant.

Response	Factor	Sum of squares	P value	Model Predictability (Pred/Adj R^2)	Adeq Precision	Final Equation in Coded Terms
IVCD						IVCD=
	Model	34.32	< 0.0001	0.7939/ 0.8228	31.408	+0.90
	A-TUDCA	1.06	< 0.0001			-0.064×A
	B-NaBu	5.43	< 0.0001			-0.15×B
	C-3TAA	9.68	< 0.0001			-0.19×C
	D-MS 275	0.80	< 0.0001			-0.056×D
	E-Cu	0.69	< 0.0001			+0.052×E
	F-Zn	0.66	< 0.0001			-0.051×F
	G-FAC	8.81	< 0.0001			+0.19×G

	AB	0.21	0.0066			+0.029×AB
	AC	0.17	0.0146			-0.026×AC
	AD	0.096	0.0667			-0.019×AD
	AG	0.026	0.3344			-0.010×AG
	BC	3.25	< 0.0001			+0.11×BC
	BD	0.54	< 0.0001			+0.046×BD
	BE	0.25	0.0034			-0.031×BE
	BF	0.051	0.1798			+0.014×BF
	BG	8.972E-003	0.5739			-5.933E-003×BG
	CD	0.048	0.1923			-0.014×CD
	CF	0.26	0.0025			+0.032×CF
	CG	9.647E-004	0.8537			-1.946E-003×CG
	DF	0.024	0.3599			+9.666E-003×DF
	DG	3.755E-003	0.7159			+3.839E-003×DG
	EF	0.29	0.0017			-0.033×EF
	FG	0.61	< 0.0001			-0.049×FG
	ACD	4.409E-003	0.6934			-4.159E-003×ACD
	ACG	4.946E-003	0.6762			+4.405E-003×ACG
	ADG	0.061	0.1424			-0.016×ADG
	BCF	0.10	0.0598			-0.020×BCF
	BCG	0.038	0.2473			-0.012×BCG
	BEF	0.22	0.0059			+0.029×BEF
	BFG	0.31	0.0011			+0.035×BFG
	CDG	1.450E-004	0.9430			-7.543E-004×CDG
	CFG	0.11	0.0486			+0.021×CFG
	DFG	0.26	0.0027			+0.032×DFG
	ACDG	0.27	0.0024			-0.032×ACDG
Titer	Model	3.66	< 0.0001	0.7718/ 0.7942	30.996	$Log_{10(Titer)}$= +0.40
	A-TUDCA	0.18	< 0.0001			+0.027×A
	B-NaBu	1.00	< 0.0001			+0.063×B
	C-3TAA	0.060	< 0.0001			+0.015×C
	D-MS 275	0.64	< 0.0001			+0.050×D
	E-Cu	0.080	< 0.0001			+0.018×E
	F-Zn	0.050	0.0003			-0.014×F
	G-FAC	0.97	< 0.0001			+0.062×G
	AC	0.090	< 0.0001			-0.019×AC
	AD	0.048	0.0004			-0.014×AD
	AG	0.047	0.0004			-0.014×AG
	BC	0.018	0.0293			-8.302E-003×BC
	BD	0.035	0.0021			-0.012×BD
	BF	0.098	< 0.0001			-0.020×BF
	BG	0.018	0.0277			-8.387E-003×BG
	CD	0.050	0.0003			-0.014×CD

	CF	0.054	0.0002			-0.015×CF
	CG	0.025	0.0097			-9.872E-003×CG
	DG	2.744E-003	0.3868			-3.281E-003×DG
	FG	0.041	0.0010			+0.013×FG
	ADG	0.037	0.0016			-0.012×ADG
	BCD	0.037	0.0017			+0.012×BCD
	BCF	0.030	0.0045			+0.011×BCF
	BFG	0.047	0.0004			+0.014×BFG
qP	Model	6.82	< 0.0001	0.8946/ 0.9078	43.204	1/Sqrt(qP)= +0.59
	A-TUDCA	0.53	< 0.0001			-0.046×A
	B-NaBu	2.07	< 0.0001			-0.090×B
	C-3TAA	1.66	< 0.0001			-0.081×C
	D-MS 275	0.86	< 0.0001			-0.058×D
	E-Cu	0.013	0.0299			+7.104E-003×E
	F-Zn	0.016	0.0148			-7.982E-003×F
	G-FAC	0.10	< 0.0001			+0.020×G
	AB	0.053	< 0.0001			+0.014×AB
	AG	0.029	0.0011			+0.011×AG
	BC	0.65	< 0.0001			+0.050×BC
	BD	0.21	< 0.0001			+0.029×BD
	BF	0.055	< 0.0001			+0.015×BF
	BG	0.023	0.0041			+9.428E-003×BG
	CD	0.018	0.0107			+8.365E-003×CD
	CF	0.11	< 0.0001			+0.021×CF
	CG	0.075	< 0.0001			+0.017×CG
	DE	1.997E-006	0.9783			-8.852E-005×DE
	DF	7.952E-003	0.0871			+5.586E-003×DF
	DG	0.012	0.0328			+6.981E-003×DG
	EF	0.013	0.0321			-7.012E-003×EF

Appendix D.

Appendix Table D.1 Histone 3 peptide proteoform significance testing.

K9ac								
Dunnett's multiple comparisons test	Significant?	Summary	Adjusted P Value		Dunnett's multiple comparisons test	Significant?	Summary	Adjusted P Value
0.2% dmso vs. 2TAA	No	ns	0.1201		No add control vs. 2TAA	Yes	*	0.0209
0.2% dmso vs. 3TAA	No	ns	0.9999		No add control vs. 3TAA	No	ns	0.6789
0.2% dmso vs. No add control	No	ns	0.669		No add control vs. 0.2% dmso	No	ns	0.669
0.2% dmso vs. NaBu	No	ns	0.8824		No add control vs. NaBu	No	ns	0.2792
K14ac								
Dunnett's multiple comparisons test	Significant?	Summary	Adjusted P Value		Dunnett's multiple comparisons test	Significant?	Summary	Adjusted P Value
0.2% dmso vs. 2TAA	No	ns	0.1668		No add control vs. 2TAA	No	ns	0.7078
0.2% dmso vs. 3TAA	Yes	*	0.0193		No add control vs. 3TAA	No	ns	0.1189
0.2% dmso vs. No add control	No	ns	0.6419		No add control vs. 0.2% dmso	No	ns	0.6419
0.2% dmso vs. NaBu	No	ns	0.1248		No add control vs. NaBu	No	ns	0.5891
2ac: (K9, K14)								
Dunnett's multiple comparisons test	Significant?	Summary	Adjusted P Value		Dunnett's multiple comparisons test	Significant?	Summary	Adjusted P Value
0.2% dmso vs. 2TAA	Yes	*	0.0158		No add control vs. 2TAA	Yes	*	0.0406
0.2% dmso vs. 3TAA	Yes	*	0.0173		No add control vs. 3TAA	Yes	*	0.0446
0.2% dmso vs. No add control	No	ns	0.9374		No add control vs. 0.2% dmso	No	ns	0.9374
0.2% dmso vs. NaBu	Yes	*	0.0223		No add control vs. NaBu	No	ns	0.0573
K18ac								
Dunnett's multiple comparisons test	Significant?	Summary	Adjusted P Value		Dunnett's multiple comparisons test	Significant?	Summary	Adjusted P Value
0.2% dmso vs. 2TAA	Yes	**	0.0045		No add control vs. 2TAA	Yes	**	0.0024
0.2% dmso vs. 3TAA	No	ns	0.7115		No add control vs. 3TAA	No	ns	0.4555
0.2% dmso vs. No add control	No	ns	0.98		No add control vs. 0.2% dmso	No	ns	0.98
0.2% dmso vs. NaBu	Yes	*	0.0159		No add control vs. NaBu	Yes	**	0.0082
K23ac								

Dunnett's multiple comparisons test	Significant?	Summary	Adjusted P Value		Dunnett's multiple comparisons test	Significant?	Summary	Adjusted P Value
0.2% dmso vs. 2TAA	Yes	****	0.0001		No add control vs. 2TAA	Yes	****	0.0001
0.2% dmso vs. 3TAA	Yes	****	0.0001		No add control vs. 3TAA	Yes	****	0.0001
0.2% dmso vs. No add control	No	ns	0.0863		No add control vs. 0.2% dmso	No	ns	0.0863
0.2% dmso vs. NaBu	Yes	**	0.0019		No add control vs. NaBu	Yes	****	0.0001
2ac: (K18, K23)								
Dunnett's multiple comparisons test	Significant?	Summary	Adjusted P Value		Dunnett's multiple comparisons test	Significant?	Summary	Adjusted P Value
0.2% dmso vs. 2TAA	Yes	****	0.0001		No add control vs. 2TAA	Yes	****	0.0001
0.2% dmso vs. 3TAA	Yes	*	0.0178		No add control vs. 3TAA	Yes	**	0.0082
0.2% dmso vs. No add control	No	ns	0.9659		No add control vs. 0.2% dmso	No	ns	0.9659
0.2% dmso vs. NaBu	Yes	**	0.0024		No add control vs. NaBu	Yes	**	0.0012
K56ac								
Dunnett's multiple comparisons test	Significant?	Summary	Adjusted P Value		Dunnett's multiple comparisons test	Significant?	Summary	Adjusted P Value
0.2% dmso vs. 2TAA	No	ns	0.764		No add control vs. 2TAA	No	ns	0.4883
0.2% dmso vs. 3TAA	No	ns	0.9708		No add control vs. 3TAA	No	ns	0.9999
0.2% dmso vs. No add control	No	ns	0.9749		No add control vs. 0.2% dmso	No	ns	0.9749
0.2% dmso vs. NaBu	No	ns	0.4287		No add control vs. NaBu	No	ns	0.2332
K27ac1K36me0								
Dunnett's multiple comparisons test	Significant?	Summary	Adjusted P Value		Dunnett's multiple comparisons test	Significant?	Summary	Adjusted P Value
0.2% dmso vs. 2TAA	No	ns	0.3319		No add control vs. 2TAA	No	ns	0.9738
0.2% dmso vs. 3TAA	No	ns	0.6203		No add control vs. 3TAA	No	ns	0.9999
0.2% dmso vs. No add control	No	ns	0.578		No add control vs. 0.2% dmso	No	ns	0.578
0.2% dmso vs. NaBu	No	ns	0.7922		No add control vs. NaBu	No	ns	0.9901

Appendix Table D.2 Histone 4 peptide proteoform significance testing.

0ac								
Dunnett's multiple comparisons test	Signifi cant?	Sum mary	Adjusted P Value		Dunnett's multiple comparisons test	Signifi cant?	Sum mary	Adjusted P Value
0.2% dmso vs. 2TAA	Yes	**	0.0064		No add control vs. 2TAA	Yes	***	0.0002
0.2% dmso vs. 3TAA	No	ns	0.0557		No add control vs. 3TAA	Yes	***	0.001
0.2% dmso vs. No add control	No	ns	0.0769		No add control vs. 0.2% dmso	No	ns	0.0769
0.2% dmso vs. NaBu	Yes	*	0.042		No add control vs. NaBu	Yes	***	0.0008
1ac								
Dunnett's multiple comparisons test	Signifi cant?	Sum mary	Adjusted P Value		Dunnett's multiple comparisons test	Signifi cant?	Sum mary	Adjusted P Value
0.2% dmso vs. 2TAA	Yes	***	0.0002		No add control vs. 2TAA	Yes	*	0.0146
0.2% dmso vs. 3TAA	Yes	***	0.0001		No add control vs. 3TAA	Yes	**	0.0087
0.2% dmso vs. No add control	Yes	*	0.0342		No add control vs. 0.2% dmso	Yes	*	0.0342
0.2% dmso vs. NaBu	Yes	***	0.0004		No add control vs. NaBu	Yes	*	0.0398
2ac								
Dunnett's multiple comparisons test	Signifi cant?	Sum mary	Adjusted P Value		Dunnett's multiple comparisons test	Signifi cant?	Sum mary	Adjusted P Value
0.2% dmso vs. 2TAA	Yes	****	0.0001		No add control vs. 2TAA	Yes	****	0.0001
0.2% dmso vs. 3TAA	Yes	***	0.0001		No add control vs. 3TAA	Yes	***	0.0001
0.2% dmso vs. No add control	No	ns	0.9993		No add control vs. 0.2% dmso	No	ns	0.9993
0.2% dmso vs. NaBu	Yes	***	0.0002		No add control vs. NaBu	Yes	***	0.0002
3ac								
Dunnett's multiple comparisons test	Signifi cant?	Sum mary	Adjusted P Value		Dunnett's multiple comparisons test	Signifi cant?	Sum mary	Adjusted P Value
0.2% dmso vs. 2TAA	Yes	***	0.0003		No add control vs. 2TAA	Yes	***	0.0004
0.2% dmso vs. 3TAA	Yes	***	0.0004		No add control vs. 3TAA	Yes	***	0.0007
0.2% dmso vs. No add control	No	ns	0.9846		No add control vs. 0.2% dmso	No	ns	0.9846
0.2% dmso vs. NaBu	Yes	***	0.0008		No add control vs. NaBu	Yes	**	0.0014
4ac								
Dunnett's multiple comparisons test	Signifi cant?	Sum mary	Adjusted P Value		Dunnett's multiple comparisons test	Signifi cant?	Sum mary	Adjusted P Value

0.2% dmso vs. 2TAA	Yes	*	0.022		No add control vs. 2TAA	No	ns	0.0616
0.2% dmso vs. 3TAA	Yes	**	0.0078		No add control vs. 3TAA	Yes	*	0.0214
0.2% dmso vs. No add control	No	ns	0.9183		No add control vs. 0.2% dmso	No	ns	0.9183
0.2% dmso vs. NaBu	Yes	*	0.0395		No add control vs. NaBu	No	ns	0.1099

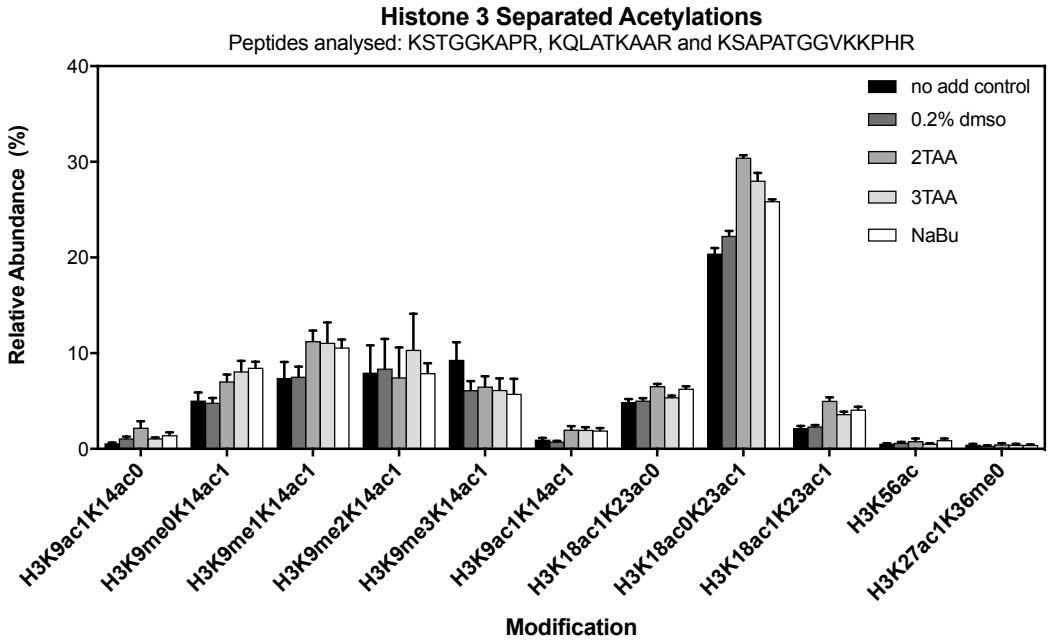

Appendix Figure D.1 Histone 3 separated acetylated proteoforms for all peptides analysed. Glossary: H: histone, K: lysine, me: methylation, ac:acetylation.

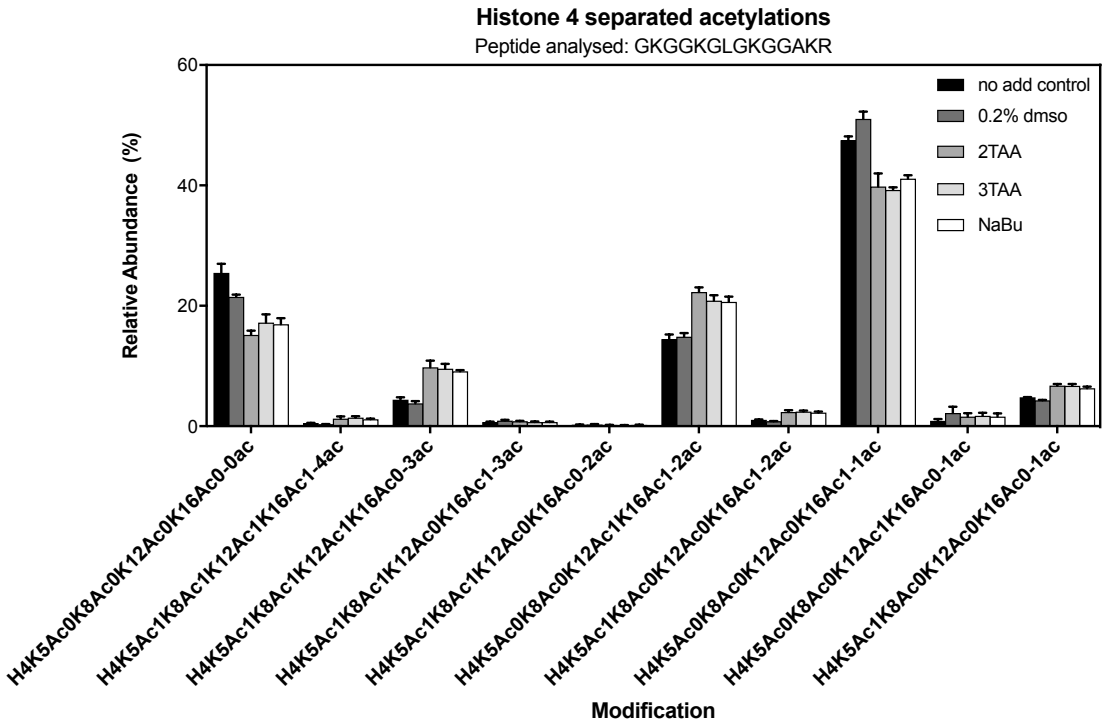

Appendix Figure D.2 Histone 4 separated acetylated proteoforms for all peptides analysed.

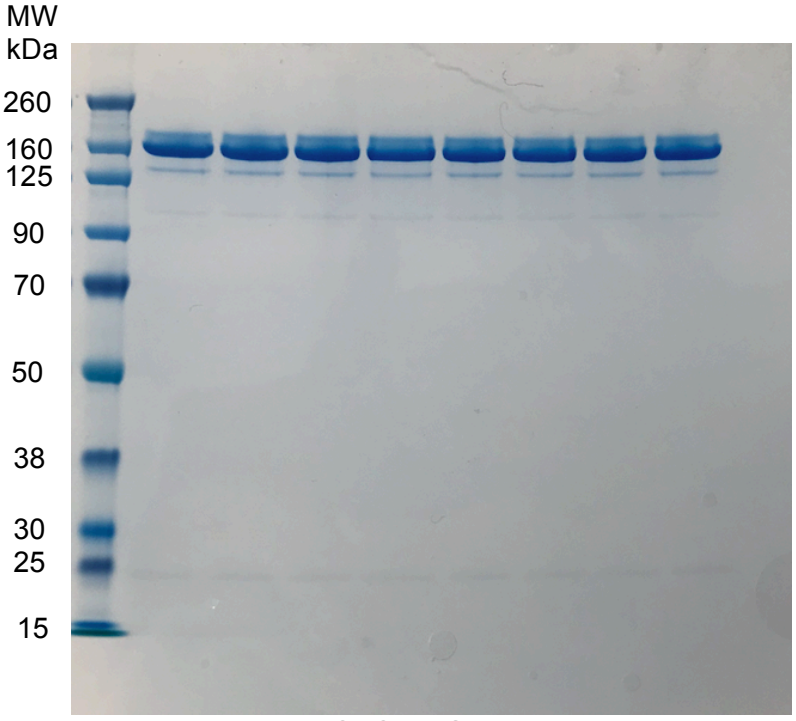

Appendix Figure D.3 Non-reduced SDS-PAGE gel depicting the purified IgG1 samples. Prominent band seen at ~150 kDa (H2L2: complete antibody). Faint bands seen at ~125, ~100 and ~25 kDa, indicating slight degradation of the antibody in the storage solution. This gel was run ~2.5 weeks after purification and glycan analysis was completed so degradation is expected however was considered acceptable since the glycan analysis had already been performed. Lane 1-8: Control 1, 0.2% DMSO 1, 2TAA 1, 3TAA 1, control 2, 0.2% DMSO 2, 2TAA 2, 3TAA 2.

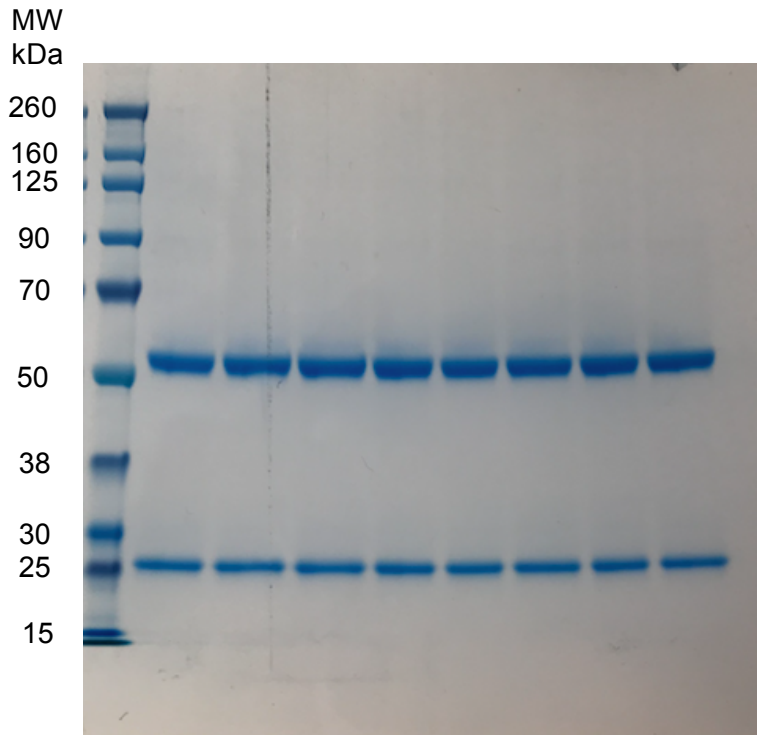

Appendix Figure D.4 Reduced SDS-PAGE gel depicting the purified IgG1 samples. Prominent bands seen at ~50 kDa (Heavy chain) and ~25 kDa (Light chain). Lane 1-8: Control 1, 0.2% DMSO 1, 2TAA 1, 3TAA 1, control 2, 0.2% DMSO 2, 2TAA 2, 3TAA 2.

Appendix Table D.3 *N*-glycan peak percentage areas from CHO-S IgG1 kappa integrated chromatograms. Peak percentage areas of glycan peaks (GP) of biological replicates, standard deviations (SD±) and percentage coefficient of variance (CV*100) are indicated. CV*100 below 20% is indicative of an acceptable level of biological variance. GP6 from 0.2% DMSO controls is 20%; the rest of the samples are below this value.

	GP1	GP2	GP3	GP4	GP5	GP6	GP7
Untreated control_1	66.75	1.99	15.02	7.00	3.35	4.66	1.21
Untreated control_2	66.46	1.71	14.92	6.62	3.64	5.28	1.37
Untreated control_Ave	66.61	1.85	14.97	6.81	3.50	4.97	1.29
SD±	0.21	0.20	0.07	0.27	0.21	0.44	0.11
CV*100	0.31	10.70	0.47	3.95	5.87	8.82	8.77
0.2% DMSO control_1	61.98	2.51	15.05	6.57	4.26	7.95	1.68
0.2% DMSO control_2	55.48	2.83	15.32	8.54	5.55	10.68	1.60
0.2% DMSO control_Ave	58.73	2.67	15.19	7.56	4.91	9.32	1.64
SD±	4.60	0.23	0.19	1.39	0.91	1.93	0.06
CV*100	7.83	8.47	1.26	18.44	18.60	20.72	3.45
2TAA treated_1	61.19	3.19	18.51	10.28	3.78	2.18	0.88
2TAA treated_2	60.58	3.29	17.29	11.08	4.24	2.63	0.89
2TAA treated_Ave	60.89	3.24	17.90	10.68	4.01	2.41	0.89

SD±	0.43	0.07	0.86	0.57	0.33	0.32	0.01
CV*100	0.71	2.18	4.82	5.30	8.11	13.23	0.80
3TAA treated_1	60.44	3.46	18.20	8.41	3.90	4.47	1.12
3TAA treated_2	61.02	3.21	17.66	7.76	3.66	5.50	1.20
3TAA treated_Ave	60.73	3.34	17.93	8.09	3.78	4.99	1.16
SD±	0.41	0.18	0.38	0.46	0.17	0.73	0.06
CV*100	0.68	5.30	2.13	5.68	4.49	14.61	4.88

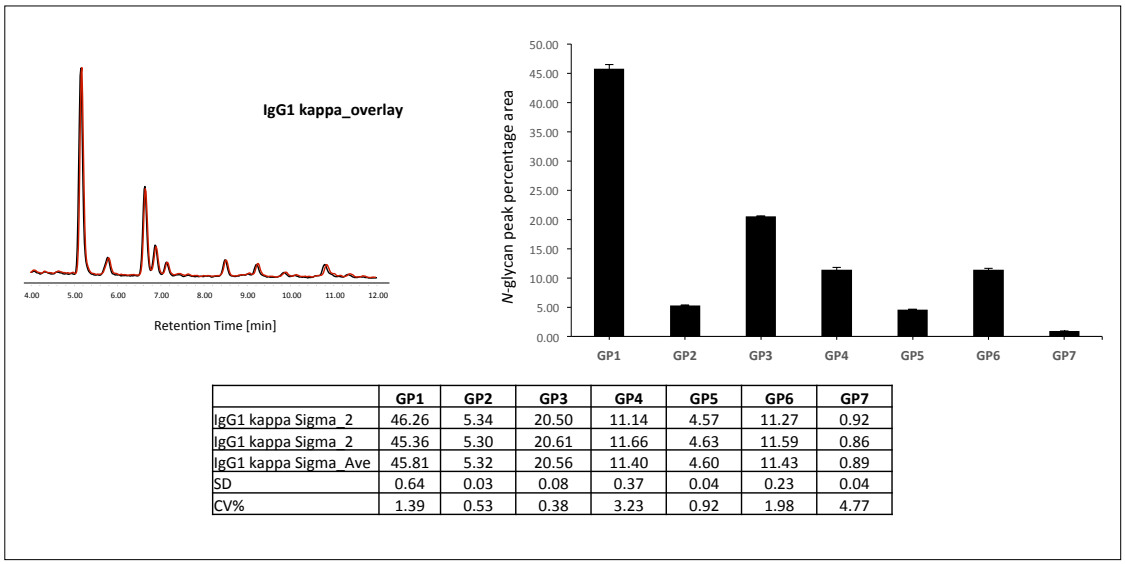

	GP1	GP2	GP3	GP4	GP5	GP6	GP7
IgG1 kappa Sigma_2	46.26	5.34	20.50	11.14	4.57	11.27	0.92
IgG1 kappa Sigma_2	45.36	5.30	20.61	11.66	4.63	11.59	0.86
IgG1 kappa Sigma_Ave	45.81	5.32	20.56	11.40	4.60	11.43	0.89
SD	0.64	0.03	0.08	0.37	0.04	0.23	0.04
CV%	1.39	0.53	0.38	3.23	0.92	1.98	4.77

Appendix Figure D.5 Technical replicates of IgG1 kappa standard. Chromatogram overlay of replicates for reproducibility; graph of average peak percentage areas of biological with SD, and CV*100. All CV% are under 20%.

Appendix Table D.4 Glycan peak significance testing for cultures in the presence of 2 or 3TAA.

G0F								
Dunnett's multiple comparisons test	Signifi cant?	Sum mary	Adjusted P Value		Dunnett's multiple comparisons test	Signifi cant?	Sum mary	Adjusted P Value
0.2% dmso vs. No add control	No	ns	0.0608		No add control vs. 0.2% dmso	No	ns	0.0608
0.2% dmso vs. 2TAA	No	ns	0.7002		No add control vs. 2TAA	No	ns	0.1485
0.2% dmso vs. 3TAA	No	ns	0.7384		No add control vs. 3TAA	No	ns	0.1387
Man5								
Dunnett's multiple comparisons test	Signifi cant?	Sum mary	Adjusted P Value		Dunnett's multiple comparisons test	Signifi cant?	Sum mary	Adjusted P Value
0.2% dmso vs. No add control	Yes	*	0.0226		No add control vs. 0.2% dmso	Yes	*	0.0226
0.2% dmso vs. 2TAA	No	ns	0.0724		No add control vs. 2TAA	Yes	**	0.0033

0.2% dmso vs. 3TAA	Yes	*	0.0451		No add control vs. 3TAA	Yes	**	0.0026
G1F (GP3)								
Dunnett's multiple comparisons test	Significant?	Summary	Adjusted P Value		Dunnett's multiple comparisons test	Significant?	Summary	Adjusted P Value
0.2% dmso vs. No add control	No	ns	0.9411		No add control vs. 0.2% dmso	No	ns	0.9411
0.2% dmso vs. 2TAA	Yes	*	0.0112		No add control vs. 2TAA	Yes	**	0.0085
0.2% dmso vs. 3TAA	Yes	*	0.0108		No add control vs. 3TAA	Yes	**	0.0082
G1F (GP4)								
Dunnett's multiple comparisons test	Significant?	Summary	Adjusted P Value		Dunnett's multiple comparisons test	Significant?	Summary	Adjusted P Value
0.2% dmso vs. No add control	No	ns	0.6972		No add control vs. 0.2% dmso	No	ns	0.6972
0.2% dmso vs. 2TAA	Yes	*	0.0388		No add control vs. 2TAA	Yes	*	0.0189
0.2% dmso vs. 3TAA	No	ns	0.8462		No add control vs. 3TAA	No	ns	0.3681
G2F								
Dunnett's multiple comparisons test	Significant?	Summary	Adjusted P Value		Dunnett's multiple comparisons test	Significant?	Summary	Adjusted P Value
0.2% dmso vs. No add control	No	ns	0.1055		No add control vs. 0.2% dmso	No	ns	0.1055
0.2% dmso vs. 2TAA	No	ns	0.3036		No add control vs. 2TAA	No	ns	0.6452
0.2% dmso vs. 3TAA	No	ns	0.1874		No add control vs. 3TAA	No	ns	0.8928
G2S1F								
Dunnett's multiple comparisons test	Significant?	Summary	Adjusted P Value		Dunnett's multiple comparisons test	Significant?	Summary	Adjusted P Value
0.2% dmso vs. No add control	Yes	*	0.0342		No add control vs. 0.2% dmso	Yes	*	0.0342
0.2% dmso vs. 2TAA	Yes	**	0.0067		No add control vs. 2TAA	No	ns	0.1581
0.2% dmso vs. 3TAA	Yes	*	0.0345		No add control vs. 3TAA	No	ns	0.9999
G2S2F								
Dunnett's multiple comparisons test	Significant?	Summary	Adjusted P Value		Dunnett's multiple comparisons test	Significant?	Summary	Adjusted P Value
0.2% dmso vs. No add control	Yes	*	0.0165		No add control vs. 0.2% dmso	Yes	*	0.0165
0.2% dmso vs. 2TAA	Yes	***	0.0009		No add control vs. 2TAA	Yes	**	0.0098
0.2% dmso vs. 3TAA	Yes	**	0.0053		No add control vs. 3TAA	No	ns	0.2756